ETH DISS. NO.: 20017

Electrochemical Redox Characterization of Humic Substances

A dissertation submitted to
ETH Zurich
for the degree of
Doctor of Sciences

Presented by

Michael Aeschbacher

Master of Science, ETH Zurich
Born January 30th, 1982
Citizen of Radelfingen BE

Accepted on the recommendation of
Prof. Dr. René Schwarzenbach, examiner
Prof. Dr. Andreas Kappler, co-examiner
Dr. Michael Sander, co-examiner

2011

Dank

Table of Contents

Summary

Humic substances are redox active organic macromolecules and have been shown to play an important role in biogeochemical and pollutant redox reactions, both under oxic and anoxic conditions. Some key redox properties of HS remain incompletely characterized, including the reversibility of electron transfer to and from HS, the electron and proton transfer equilibria of the reducible moieties in HS, the electron donating properties of HS under oxic conditions.

The overall objective of this work was to characterize the electron accepting and electron donating properties of a diverse set of HS using electrochemical approaches. In order to meet this objective and to investigate the key redox properties specified above, a novel electrochemical approach was developed. This approach comprised the following methods: *Direct electrochemical reduction* (DER) of HS at carbon working electrodes can be used to generate large quantities of reduced HS. DER allows for continuous monitoring of electron and proton transfer to HS by chronocoulometry and automated acid titration, respectively. *Mediated electrochemical reduction and oxidation* (MEO and MER) directly quantify the number of electrons transferred to and from small HS samples at a given applied redox potential E_h and pH. *Mediated potentiometry*. In this methods electron transfer mediators are used to facilitate attainment of equilibria between redox electrodes and the electron accepting moieties in HS. These methods were applied to the redox characterization of HS.

The electron transfer to a model HS was largely reversible over three cycles of electrochemical reduction and O_2 reoxidation. A large fraction of the reduced moieties was reoxidized within minutes. These results support that HS can act as electron acceptors for microorganisms under anoxic conditions and donate these electrons to O_2 upon reaeration. The electron accepting capacities (EACs) of a chemically diverse set of HS, quantified by MER, showed a linear correlation with the aromaticities of the HS. This correlation was consistent with quinones as the major electron accepting moieties in HS.

Acid titration coupled DER showed that electron transfer to humic acids (HA) was coupled to proton uptake by HA. Consistently, mediated potentiometry showed that the E_h of the tested HA decreased with increasing solution pH. Reduction of selected HA resulted in a gradual decrease in reduction potential E_h over a wide potential range. Modeling of the decrease in E_h with the number of electrons

transferred to the HA revealed a wide distributions in the apparent standard reduction potentials of the reducible moieties in the HA. These findings are consistent with the multitude of environmental redox reactions involving HS. Moreover these results allow assessing the thermodynamics of electron transfer reactions to and from HS under reducing conditions.

Electrochemical oxidation of three model HAs was largely irreversible. The EDCs of the same HAs, quantified by MEO, continuously increased with increasing E_h and pH. These findings suggested that these HAs contain moieties that donate electrons over a wide potential range and that oxidation of these moieties is coupled to the release of protons. The EDCs of a diverse set of HS were linearly correlated with their titrated phenol contents. These findings are consistent with phenols as major electron donating moieties in HS. The EDCs of 15 HS were compared to their respective EACs. Aquatic HS had higher EDCs but lower EACs than terrestrial HS. Relating EDCs and EACs to HS aromaticities indicated that electron donating phenol moieties are depleted relative to the electron accepting quinone moieties during transformation of HS in the environment.

DER was used to reduce a model HA, which was subsequently used in sorption experiments to assess whether HS reduction affects its sorbent properties for apolar naphthalene, the monopolar acetophenone and quinoline, the bipolar 2-naphthol and the organocation paraquat. The redox states of both the unreduced and the reduced HAs did not change during the sorption experiments as demonstrated by a spectrophotometric assay based on the reductive decolorization of 2,6-dichlorophenol indophenol. There were no significant differences in sorption to reduced and unreduced HA for all organic pollutants tested. This implies that HA reduction did not result in detectable changes in its cohesive energy, its H-donor and H-acceptor properties, and its number of anionic binding sites. The work suggests that models describing organic pollutant sorption to oxidized natural organic matter are also valid for sorption to reduced organic matter.

This work contributes to a better understanding of the redox properties of HS and the reactions they are involved in. Beyond the redox characterization of HS these methods are also applicable to other redox active organic and mineral phases.

Zusammenfassung

Huminstoffe sind redox-aktive organische Makromoleküle, die sowohl unter oxischen als auch unter anoxischen Bedingungen eine wichtige Rolle in biogeochemischen Redoxprozessen und in Redoxreaktionen von Schadstoffen spielen. Einige der wichtigsten Redoxeigenschaften von Huminstoffen sind bisher unzureichend charakterisiert. Diese Eigenschaften beinhalten die Reversibilität des Elektronentransfers auf und von Huminstoffen, die Protonen- und Elektronentransfergleichgewichte der reduzierbaren Gruppen in Huminstoffen und die Elektrondonorkapazitäten von Huminstoffen unter oxischen Bedingungen.

Das übergeordnete Ziel dieser Arbeit war eine Charakterisierung der Elektronakzeptor- und Elektronendonoreigenschaften einer Auswahl von chemisch diversen Huminstoffen. Um dieses Ziel zu erreichen und um die oben genannten Redoxeigenschaften genauer zu charakterisieren wurde ein neuartiger elektrochemischer Ansatz entwickelt. Dieser Ansatz umfasst die folgenden Methoden: *Direkte elektrochemische Reduktion* (DER) von Huminstoffen an Glascarbonelektroden erlaubt es, grosse Mengen von Huminstoffen sauber zu reduzieren. Die bei der Reduktion übertragenen Elektronen und Protonen können durch Chronocoulometrie beziehungsweise automatische Säuretitration bestimmt werden. *Mediierte elektrochemische Oxidation und Reduktion* (MEO und MER) erlauben es, die Anzahl an Elektronen zu quantifizieren, die bei einem gegebenen Potential und pH Wert von beziehungsweise auf Huminstoffe transferiert werden. In der *mediierten Potentiometrie* werden organische Elektronentransfermediatoren verwendet, um das Einstellen von Gleichgewichten zwischen Redoxelektroden und elektronenakzeptierenden Gruppen in den Huminstoffen zu beschleunigen. Diese Methoden wurden im Weiteren für die Redoxcharakterisierung von Huminstoffen angewendet.

Das Übertragen von Elektronen auf eine Modellhuminsäure war grösstenteils reversibel über drei aufeinanderfolgende elektrochemische Reduktions- und O_2 Reoxidationsschritte. Ein grosser Anteil der reduzierten Gruppen wurde innerhalb weniger Minuten rückoxidiert. Diese Ergebnisse bestätigen, dass Huminstoffe unter anoxischen Bedingungen als Elektronenakzeptoren für Mikroorganismen fungieren können und dass die

reduzierten Huminstoffe diese Elektronen bei Wiederbelüftung auf O_2 übertragen können. die mittels MER quantifizierten Elektronenakzeptorkapazitäten (EAKs) einer Auswahl chemisch unterschiedlicher Huminstoffe waren linear mit der Aromatizität der Huminstoffe korreliert. Diese Korrelation weist auf Quinone als prädominante elektronenakzeptierende Gruppen in Huminstoffen hin.

DER mit gekoppelter automatischer Säuretitration zeigte, dass der Elektronentransfer auf Huminsäuren auch zu einer Aufnahme von Protonen führt. Diese Beobachtung war im Einklang mit mediierten Potentiometriemessungen, die eine Abnahme des Reduktionspotentials der getesteten Huminsäuren mit zunehmenden pH Werten zeigten. Die Reduktion ausgewählter Huminstoffen führte zu einer graduellen Abnahme des Reduktionspotentials über einen weiten Potentialbereich. Das Modellieren der Potentialabnahme mit zunehmender Anzahl übertragener Elektronen verdeutlichte, dass die reduzierbaren Gruppen in den Huminsäuren einen weiten Bereich an Standardreduktionspotentialen abdecken. Diese Resultate sind im Einklang mit der grossen Anzahl von Redoxreaktionen in der Umwelt, an denen Huminstoffe beteiligt sind. Diese Ergebnisse ermöglichen zudem die Thermodynamik von Elektrontransferreaktionen auf und von Huminstoffen unter reduzierenden Bedingungen abzuschätzen.

Es konnte gezeigt werden, dass die elektrochemische Oxidation von drei Huminsäuren, im Gegensatz zu deren Reduktion, grösstenteils irreversibel war. Die mittels MEO quantifizierte Elektronendonorkapazitäten (EDKs) der gleichen Huminsäuren nahmen kontinuierlich zu mit zunehmendem Reduktionspotential und mit zunehmendem pH Wert. Diese Ergebnisse weisen auf funktionelle Gruppen hin, die über einen weiten Potentialbereich Elektronen abgeben. Die Oxidation dieser Gruppen ist an eine Protonenübertragung gekoppelt. Die EDKs einer grossen Anzahl chemisch diverser Huminstoffe war linear mit deren titrierten Phenolgehalten korreliert. Diese Ergebnisse weisen auf Phenole als prädominante elektronabgebende Gruppen in Huminstoffen hin. Die EDKs von 15 Huminstoffen wurde mit ihren jeweiligen EAKs verglichen. Aquatische Huminstoffe zeigten grössere EDKs aber kleinere EAKs als terrestrische Huminstoffe. Werden diese EDCs und EAKs mit den Aromatizitäten der jeweiligen Huminstoffe in Verbindung gesetzt, so deutet

sich an, dass die elektonenabgebenden Gruppen während der Umwandlung der Huminstoffe in der Umwelt präferentiell abgereichert werden.

Mittels DER wurde eine Modellhuminsäure reduziert. Diese reduzierte Huminsäure wurde anschliessend verwendet, um in Sorptionsexperimenten den Einfluss des Redoxstatus der Huminsäure auf deren Eigenschaften als Sorbens für organische Schadstoffe zu untersuchen. Die ausgewählten Schadstoffe umfassten die apolare Substanz Naphthalene, die monopolaren Verbindungen Acetophenone und Quinoline, die bipolare Substanz 2-Naphthol sowie das organische Kation Paraquat. Ein spektroskopischer Test, der auf der reduktiven Entfärbung von 2,6-Dichlorophenol Indophenol beruht, zeigte, dass sich der Redoxstatus sowohl der unreduzierten als auch der reduzierten Huminsäure über den Verlauf des Sorptionsexperimentes nicht änderte. Keiner der getesteten Schadstoffe zeigte einen erkennbaren Unterschied in ihrer Sorption an die unreduzierte und an die reduzierte Huminsäure. Dieses Ergebnis bedeutet, dass die Reduktion von Huminsäure zu keiner nachweisbaren Änderung der kohäsiven Energie, der H-Donor-und Akzeptoreigenschaften und der Anzahl an Kationenbindungsplätzen führte. Diese Studie deutet darauf hin, dass Modelle, die basierend auf der Schadstoffsorption an oxidierte natürliche organisch Substanz entwickelt worden sind, auch zur Beschreibung der Sorption an reduzierte organische Substanz angewendet werden können.

Diese Arbeit trägt unmittelbar zu einem besseren Verständnis der Redoxeigenschaften von Huminstoffen und ihrer Reaktionen in der Umwelt bei. Darüber hinaus leistet diese Arbeit auch einen Beitrag dazu, weitere redoxaktive organische und mineralische Umweltphasen mittels der entwickelten elektrochemischen Methoden zu charakterisieren.

Chapter 1

General Introduction

1.1. Background

Humic substances (HS) are a heterogeneous mixture of refractory organic macromolecules originating mainly from higher plant and microbial precursors [1, 2]. HS are a major fraction of natural organic matter in the environment and exhibit key functions in terrestrial and aquatic ecosystems. This work focuses on the redox properties of HS under both reducing and oxidizing conditions.

Electron accepting properties. Under reducing conditions HS may both accept and donate electrons, which largely affects numerous biogeochemical electron transfer reactions as well as reactions involving redox-active organic and inorganic pollutants [3, 4]. In temporarily anoxic systems such as bogs, sediments, and capillary fringes of soils, HS may accept electrons directly from microorganisms [5] or from microbially reduced species (e.g. Fe^{2+}, HS^-) during anoxic phases. Upon aeration, reduced HS may donate electrons to oxygen, resulting in a regeneration of the pool of electron accepting moieties in HS. These redox buffer properties of HS may reduce the flow of electrons to other electron acceptors [6]. In peat bogs, and potentially also in other wetlands electron transfer to HS is hypothesized to result in a significant decrease of methanogenesis [7]. Since 20-39% of the global methane emission stems from wetlands, electron transfer to HS likely is relevant for global methane budgets [8].

HS also act as redox mediators under reducing conditions. For instance, HS may facilitate the electron transfer from microorganisms to solid iron oxides and hydroxides, which leads to an enhanced reductive dissolution of these phases [5, 9]. Furthermore, HS can mediate electron transfer from microorganisms and inorganic electron donors to organic and inorganic pollutants [3]. Given the numerous redox reactions in which HS participate under reducing conditions, the electron accepting properties of HS have received considerable research interest. The electron accepting properties of humic substances has been ascribed primarily to quinone moieties [3, 10-13] although it has been argued that other HS components, including complexed metals (e.g. ferric iron), may also be involved [14]. Quinones are present in HS, as shown by spectroscopy, including HS analysis by ^{15}N NMR after derivatization with ^{15}N-labeled

3

hydroxylamine [15] and by 2D NMR techniques [16]. Evidence supportive of quinones as major electron accepting moieties includes largely reversible electron transfer to HS [13, 17], linear correlation of the number of electrons transferrable to different HS with the aromaticities of the HS [10, 13], the presence of organic radicals (presumably semiquinones) in HS [18, 19], which increase in concentration upon HS reduction [10, 11, 20]. Furthermore similar electron transfer mediation of HS and of model quinones have been observed in organic pollutant reduction experiments [3, 21]. Many studies have focused on quantifying the number of electron accepting moieties in different HS, which has been termed electron carrying capacity [13], microbial and chemical reducing capacity [22], or electron accepting capacity [10, 23]. In this work, the term electron accepting capacity (EAC) is used. The EAC is operationally defined as it depends on the used quantification method.

In most previous studies, the EAC of a HS was quantified in a two-step approach. The HS was first reduced, commonly by H_2 and catalysts, microorganisms such as *Geobacter metallireducens*, H_2S, or reducing metals (e.g. Zn) [10, 13]. In a subsequent step, the reduced HS was reoxidized, typically with complexed Fe^{3+}-species such as iron citrate or ferricyanide.
The EAC of the HS was thereby inferred from the moles of chemical oxidant reduced by the HS (i.e., the moles of Fe^{2+} formed) [10, 13, 23]. Fewer studies determined the EAC by quantifying the oxidation of the added chemical reductants (i.e., Zn^0 to Zn^{2+} and H_2S to $S_2O_3^{2-}$) [24, 25].

Electron donating properties under oxic conditions Compared to the redox properties of HS under reducing conditions, the electron donating properties of HS under oxic conditions have received less attention. The presence of electron donating moieties in HS stored under oxic conditions has been demonstrated by reduction of chemical oxidants such as iron complexes or iodine [14, 22, 23, 26]. Because of their electron donating properties, HS may act as antioxidants in the environment. For example HS may donate electrons to free radicals (such as peroxy radicals) and interrupt oxidative radical chain reactions [27-30]. It has been hypothesized that the antioxidant properties of soil organic matter slow down its oxidative breakdown and increase its recalcitrance in the environment [31-33]. In aquatic systems, the antioxidant properties of HS have been invoked to rationalize the inhibitory effect of HS on the indirect phototransformation

rates of organic pollutants. Inhibition is hypothesized to result from HS donating electrons to radical pollutant oxidation intermediates, which are reduced back to the parent compounds [34, 35]. The electron donating properties of HS are also relevant in oxidative water treatment processes. Electron donation by HS is expected to determine the oxidant doses required for the disinfection and the decoloration of water and for the removal of pollutants from the water. Furthermore, the antioxidant properties of HS may be linked to their potential to form disinfection byproducts [36-38].

Previous work suggested that polyphenolic moieties are the major electron donating moieties in HS [39] and that these moieties are derived from higher plant precursors, such as lignin and tannins. The presence of phenolic moieties in HS can be inferred from their pronounced acid/base buffering capacities in the pH range from 8 to 10, which corresponds to the typical pK_a range for phenols [40, 41]. Furthermore, the presence of lignin-derived residues in HS was demonstrated by Fourier transform-ion cyclotron resonance mass spectrometry, NMR spectroscopy, and Pyrolysis-GC-MS techniques [42-44]. Phenols as major electron donating moieties were suggested by similar redox titration curves of HS and of mixtures of synthetic, low molecular weight phenols [39]. Evidence for proton coupled electron transfer (including proton release during HS oxidation) further supported phenolic electron donating moieties in HS [14, 39, 45]. As for the electron accepting moieties, the number of electron donating moieties in HS is operationally defined because it varies depending on the used oxidant and the pH). In this work, the term electron donating capacity (EDC) is used. It refers to the moles of electrons which are donated from a given mass of HS under well-defined experimental conditions [23]. In previous work, EDCs have primarily been determined by reacting HS with chemical oxidants, either in batch experiments or by potentiometric redox titrations. The most commonly oxidants used were the iron complexes ferricyanide and Fe^{3+} citrate, and iodine [14, 22, 23, 39, 45]. In a different approach, Rimmer et al. [31] recently determined the EDCs of soil extracts using the organic radical oxidant 2,2'-azino-bis(3-ethylbenzothiazoline-sulfonic acid) (ABTS). This radical is widely used in antioxidant assays in the food science and in medical research [28, 46].

Critical evaluation of previous approaches to the redox characterization of HS. Previously used methods to determine the EACs and EDCs of HS were indirect in that they relied primarily on quantifying electron transfer reactions between HS added chemical reducants and oxidants. The electron transfer kinetics between HS and some of the chemical reductants and oxidants are, however, rather slow [23], which raises the question whether some of the reported EACs and EDCs are true equilibrium values. In addition, many of the used chemical oxidants and reductants have pH dependent reduction potentials [23] which makes it difficult to compare EACs and EDCs that were determined at different pH values. Finally, many of the previously used reduction methods do not allow determining the moles of electrons transferred to HS. In these cases, it is, strictly speaking, impossible to assess the reversibility of electron transfer to and from HS.

In addition to chemical reduction and oxidation methods, a number of spectroscopic techniques have been used to characterize the redox properties of HS. It was proposed that the analysis of fluorescence excitation emission matrices of HS provides insight into the redox state of the HS [47]. However, the fluorescence spectra largely vary between HS and are strongly pH dependent. Also, the deconvolution of excitation emission matrices into several distinct components some of which were assigned to quinone species has been questioned both on theoretical and experimental grounds [48, 49].

Electron paramagnetic resonance (EPR) spectroscopy was used to show that the number of organic radicals, presumably semiquinones, in HS increased upon HS reduction [11, 20]. However, EPR cannot be used to quantify the moles of electrons transferred to the HS, due to the fact that the semiquinone species is not expected to be the predominant quinone species at circumneutral pH [50] (i.e., the quinone is directly reduced to the hydroquinone). Consistently, the increase in the number of radicals during reduction at circumneutral pH accounted for only a few percent of the electrons transferred to the HS [10, 14].

Other spectroscopic techniques, including Nuclear Magnetic Resonance (NMR) and Fourier-Transform-Infrared (FTIR) spectroscopy, were successfully applied in a general characterization of the chemical structures of HS [15, 16, 51]. These techniques have, however, limited selectivity for the reducible moieties in HS. High resolution methods such as Fourier Transform Cyclotron Resonance Mass Spectrometry (FTCR-MS) [51] have not yet been applied to

study the redox properties of HS. It is questionable whether this technique is applicable as the intrinsic redox state of HS samples is likely lost in the ionization unit of the MS.

Research needs. While previous work on the redox properties of HS has greatly contributed to a better understanding of the role of HS in biogeochemical and pollutant redox reactions, methodological constraints have impaired addressing some fundamental redox properties of HS.

Electron transfer reversibility. Previous work showed that electron transfer to HS is at least partially reversible upon re-aeration of reduced HS with O_2 [10, 13, 17]. These studies did not quantify the numbers of electrons transferred to HS during reduction. Reversibility can however only be unambiguously established by balancing the moles of electrons transferred to and from the HS during both reduction and oxidation, respectively.

Thermodynamics of redox reactions involving HS. While the electron accepting and donating capacities of HS are well studied [10, 13, 23], the thermodynamics of the electron transfer reactions to and from HS have received considerably less attention. Research is warranted on the redox potential distribution of the electron accepting and donating moieties in HS and on the effect of pH on the redox potentials of HS.

Integrated assessment of the electron donating and accepting properties of HS. While the diversity of HS from different source material has been addressed in studies on the electron accepting properties of HS [10, 13], studies on the electron donating properties of HS have focused on few HS [14, 23, 45]. An integrated assessment of both electron donating and accepting properties of a large and diverse set of HS is required to identify the environmental factors and the structural properties of HS that affect their redox properties. This set of HS has to include aquatic, terrestrial, and synthetic HS.

These research questions can only be addressed if new approaches to characterize the redox properties of HS are developed. These new approaches need to be selective for the electron accepting or electron donating moieties in HS and have to fulfill several requirements including a direct quantification of electron transfer to and from HS, independent control of E_h and pH during HS reduction and oxidation, and accurate E_h measurement in HS solutions.

In principle, electrochemical methods are selective for the reducible or oxidizable moieties in HS and promise to fulfill the above requirements. In several studies, electrochemical methods, including bulk electrolysis, open circuit potential measurements, and cyclic voltammetry have been applied to characterize the redox properties of HS [12, 39, 52-54].

For instance, bulk electrolysis with a platinum working electrode was used to generate reduced HA that was subsequently used as reductant for chlorinated hydrocarbons [52]. However, proton reduction at the Pt electrode resulted in high background currents, which impeded direct chronocoulometric quantification of the electron transfer to the HA [55]. Furthermore the production of H_2 on the Pt surface may have resulted in chemical modifications of the HA, including the hydrogenation of double bonds. Therefore, other inert electrode materials that have a higher overpotential for proton reduction than Pt are required. In this regard, carbon may be a suitable working electrode material [55].

In addition to bulk electrolysis at a constant redox potential, potential sweep methods have also been applied. These methods include linear sweep voltammetry [53] and cyclic voltammetry [12, 39, 56]. Linear sweep and cyclic voltammograms a of HS in aqueous solutions were, however, devoid of clear features, presumable due to slow direct electron transfer between the electrode and HS [12, 39, 56]. Conversely, discrete reduction and oxidation current peaks were obtained in the cyclic voltammograms of HS dissolved in an aprotic solvent [12]. The half peak potentials were comparable to those of model quinones dissolved in the same solvent. While these studies provided insight into the redox potentials distribution of the redox-active moieties in HS in aprotic organic solvents, these results are not directly transferrable to HS in aqueous solutions. Electron transfer to and from HS in aqueous solutions may result in the uptake and release of protons, which are, however, absent in the aprotic organic solvent. Furthermore, HS likely adapts very different conformations in the aprotic organic solvent and in water, which is expected to affect HS redox properties.

A few studies have quantified the pH dependence of the reduction potentials of HS by potentiometric redox potential measurements [54, 57]. These measurements were, however, conducted only for unreduced HS, over a rather narrow pH range, and showed clear signs of redox nonequilibria between

the HS and the redox electrode [54]. Attainment of redox equilibria between HS and the redox electrodes may be facilitated by the use of small amounts of organic redox mediator molecules [58, 59].

1.2. Objectives of this work

The overall goal of this work was to characterize the electron accepting and donating properties of a diverse set of humic substances, using electrochemical approaches.

Five specific objectives were defined to operationalize this overall goal:
1) To advance and validate an electrochemical approach that allows for (i) selective reduction of electron accepting moieties in HS, (ii) the direct quantification of the electron donating and accepting capacities of HS at different E_h and pH, and (iii) accurate potentiometric E_h measurement in HS solutions.
2) To establish the extent of reversibility of HS reduction and oxidation
3) To determining the redox potential distribution of the electron accepting and electron donating moieties in HS and to assess the pH dependence of HS redox potentials
4) To determine the relationship between electron donating and accepting properties of HS and their origin and chemical structure
5) To elucidate whether reduction of HS affects its properties as sorbent for apolar, polar, and ionic organic pollutants.

1.3. Thesis organization

Chapter 2. In this chapter a novel electrochemical approach to characterize the redox properties of HS is presented and evaluated. This approach comprises two methods. The first is direct electrochemical reduction (DER) of HS in a bulk electrolysis setup at glassy carbon working electrodes. This method allows generating large quantities of reduced HS. The moles of electrons transferred to the HS are determined by chronocoulometry. DER in bulk electrolysis cells can be coupled to automated pH stat titration to quantify the number of protons transferred to HS during the reduction. The second method comprises mediated electrochemical reduction (MER) and oxidation (MEO) in which small amounts of HS are spiked to an electrochemical cell containing electron transfer mediators. The organic radicals 2,2'-azino-bis(3-ethylbenzthiazoline-6-sulfonic acid) (ABTS•+) and 1,1'-Ethylene-2,2'-bipyridyldiylium dibromide (DQ•+) served as mediators to fascilitate electron transfer between electrodes and HS. The reductive and oxidative current responses in MER and MEO resulting from the HS spikes are integrated to give the EACs and EDCs, respectively, of the spiked HS samples. The two methods were combined to assess (i) whether MER and MEO quantitatively detected electrons transferred to an HA by DER, (ii) the reversibility of electron transfer to and from a model HA over successive electrochemical reduction and O_2-reoxdation cycles, and (iii) the kinetics of O_2-reoxidation of a reduced HA. Finally, MER was used to quantify the EACs of a diverse set of 13 terrestrial and aquatic HS. The EACs were related to the chemical composition of the HS and compared to previously published EAC values for the same HS.

Chapter 3. This chapter focuses on elucidating the electron and proton transfer equilibria of the reducible moieties in an aquatic, a terrestrial, and a lignite-derived HA. Cyclic voltammetry experiments served to assess electron transfer mediation between HS and electrodes by the redox-active organic radicals DQ•+, 1,1′-Diethyl-4,4′-bipyridinium dibromide (EV•+) and 1,1'-Bis(cyanomethyl)-4,4'-bipyridinium (CV•+). It was further tested whether these radicals facilitate attainment of redox equilibrium in potentiometric E_h measurements in HS solutions. The pH dependencies of the E_h of the electron accepting moieties in HAs were determined by quantifying the molar ratios of

protons to electrons transferred to the HAs during electrochemical reduction and by potentiometric E_h-pH titrations of HAs pre-reduced by DER to different extents. Finally, the decrease in E_h with increasing moles of electrons transferred to the tested HAs during electrochemical reduction was quantified and modeled to assess the distribution of apparent standard reduction potentials of the reducible moieties.

Chapter 4. This chapter presents the results of a systematic study of the effects of E_h and pH on the antioxidant properties of a diverse set of terrestrial and aquatic humic substances and natural organic matter samples. Similar to chapter 3, cyclic voltammetry experiments were conducted to assess mediated electron transfer from HS to the working electrode by the organic radical ABTS•+. Model antioxidants with known EDCs were analyzed using MEO with ABTS•+ as mediator to test whether this technique allows for a quantitative detection of EDCs. The results from a number of electrochemical experiments are presented that were conducted to determine the reversibility of HS oxidation and the dependence of the EDCs on the redox potential and on solution pH. Furthermore MEO was used to quantify the EDCs of a diverse set of terrestrial, aquatic, microbial, and artificial HS. These EDCs were correlated to the titrated phenol content and the aromaticities of the HS. Finally the EDC and EACs of the different HS were used to assess the relationship between HS redox properties on their origin and chemical structure.

Chapter 5. The work presented in this chapter assesses whether the reduction of HS alters their sorbent properties for organic pollutants. Leonardite humic acid (LHA), a well characterized HA with a relatively high EAC, was reduced by bulk electrolysis at different pH. The redox state of LHA was determined prior to and after each sorption experiment by a novel spectrophotometric assay that relies on the decolorization of the blue redox dye 2,6-dichlorophenol indophenol upon its reduction by LHA. The unreduced and reduced LHA were subsequently used in sorption experiments at pH 7, 9, and 11. The set of organic pollutants included apolar napththalene, the H-bond accepting acteophenone and quinoline, the H-bond donating and accepting 2-naphthol, and the organocation 1,1'-Dimethyl-4,4'-bipyridinium (paraquat). This set of probe molecules was chosen to test whether HA redox state changes the H-bond

interactions between the HA and the organic pollutants, the cohesive energy of the HA phase, and/or the number of anionic sites in HA for cation binding.

Chapter 6 provides a general conclusion and an outlook.

1.4. References

1.   Sutton, R.; Sposito, G., Molecular structure in soil humic substances: The new view. *Environ Sci Technol* **2005,** *39*, (23), 9009-9015.

2.   Cooper, W. T.; Stenson, A. C.; Marshall, A. G., Exact masses and chemical formulas of individual Suwannee River fulvic acids from ultrahigh resolution electrospray ionization Fourier transform ion cyclotron resonance mass spectra. *Anal Chem* **2003,** *75*, (6), 1275-1284.

3.   Dunnivant, F. M.; Schwarzenbach, R. P.; Macalady, D. L., Reduction of substituted nitrobenzenes in aqueous solutions containing natural organic matter *Environ. Sci. Technol.* **1992,** *26*, (11), 2133-2141.

4.   Alberts, J. J.; Schindle.Je; Miller, R. W.; Nutter, D. E., Elemental Mercury Evolution Mediated by Humic Acid *Science* **1974,** *184*, (4139), 895-896.

5.   Lovley, D. R.; Coates, J. D.; Blunt-Harris, E. L.; Phillips, E. J. P.; Woodward, J. C., Humic substances as electron acceptors for microbial respiration. *Nature* **1996,** *382*, (6590), 445-448.

6.   Cervantes, F. J.; van der Velde, S.; Lettinga, G.; Field, J. A., Competition between methanogenesis and quinone respiration for ecologically important substrates in anaerobic consortia. *Fems Microbiol Ecol* **2000,** *34*, (2), 161-171.

7.   Blodau, C.; Heitmann, T.; Goldhammer, T.; Beer, J., Electron transfer of dissolved organic matter and its potential significance for anaerobic respiration in a northern bog. *Global Change Biol* **2007,** *13*, (8), 1771-1785.

8.   Denman, K. L., G. Brasseur, A. Chidthaisong, P. Ciais, P.M. Cox, R.E. Dickinson, D. Hauglustaine, C. Heinze, E. Holland, D. Jacob, U. Lohmann, S Ramachandran, P.L. da Silva Dias, S.C. Wofsy and X. Zhang, 2007, *Couplings Between Changes in the Climate System and Biogeochemistry. In: Climate Change 2007: The Physical Science Basis. Contribution of Working Group I to the Fourth Assessment Report of the Intergovernmental Panel on Climate Change [Solomon, S., D. Qin, M. Manning, Z. Chen, M. Marquis, K.B. Averyt, M.Tignor and H.L. Miller (eds.)]. Cambridge University Press, Cambridge, United Kingdom and New York, NY, USA.*

9.   Kappler, A.; Benz, M.; Schink, B.; Brune, A., Electron shuttling via humic acids in microbial iron(III) reduction in a freshwater sediment. *Fems Microbiol Ecol* **2004,** *47*, (1), 85-92.

10.   Scott, D. T.; McKnight, D. M.; Blunt-Harris, E. L.; Kolesar, S. E.; Lovley, D. R., Quinone moieties act as electron acceptors in the reduction of humic substances by humics-reducing microorganisms. *Environ. Sci. Technol.* **1998,** *32*, (19), 2984-2989.

11.   Senesi, N.; Chen, Y.; Schnitzer, M., Role of free radicals in oxidation and reduction of fulvic acid. *Soil. Biol. Biochem.* **1977,** *9*, (6), 397-403.

12.   Nurmi, J. T.; Tratnyek, P. G., Electrochemical properties of natural organic matter (NOM), fractions of NOM, and model biogeochemical electron shuttles. *Environ. Sci. Technol.* **2002,** *36*, (4), 617-624.

13.   Ratasuk, N.; Nanny, M. A., Characterization and quantification of reversible redox sites in humic substances. *Environ. Sci. Technol.* **2007,** *41*, 7844-7850.

14.   Sposito, G.; Struyk, Z., Redox properties of standard humic acids. *Geoderma* **2001,** *102*, (3-4), 329-346.

15.   Thorn, K. A.; Arterburn, J. B.; Mikita, M. A., N-15 and C-13 Nmr Investigation of Hydroxylamine-Derivatized Humic Substances. *Environ Sci Technol* **1992,** *26*, (1), 107-116.

16.   Mao, J. D.; Xing, B.; Schmidt-Rohr, K., New Structural Information on a Humic Acid from Two-Dimensional 1H-13C Correlation Solid-State Nuclear Magnetic Resonance. *Environ Sci Technol* **2001,** *35*, (10), 1928-1934.

17.   Bauer, I.; Kappler, A., Rates and extent of reduction of Fe(III) compounds and O_2 by humic substances. *Environ. Sci. Technol.* **2009,** *43*, (13), 4902-4908.

18.   Paul, A.; Stosser, R.; Zehl, A.; Zwirnmann, E.; Vogt, R. D.; Steinberg, C. E. W., Nature and abundance of organic radicals in natural organic matter: Effect of pH and irradiation. *Environ Sci Technol* **2006,** *40*, (19), 5897-5903.

19.   Rex, R. W., Electron Paramagnetic Resonance Studies of Stable Free Radicals in Lignins and Humic Acids. *Nature* **1960,** *188*, (4757), 1185-1186.

20. Senesi, N.; Schnitzer, M., Effects of Ph, Reaction-Time, Chemical Reduction and Irradiation on Esr-Spectra of Fulvic-Acid. *Soil Sci* **1977,** *123*, (4), 224-234.

21. Schwarzenbach, R. P.; Stierli, R.; Lanz, K.; Zeyer, J., Quinone and iron porphyrin mediated reduction of nitroaromatic compounds in homogeneous aqueous solution. *Environ. Sci. Technol.* **1990,** *24*, (10), 1566-1574.

22. Peretyazhko, T.; Sposito, G., Reducing capacity of terrestrial humic acids. *Geoderma* **2006,** *137*, (1-2), 140-146.

23. Bauer, M.; Heitmann, T.; Macalady, D. L.; Blodau, C., Electron transfer capacities and reaction kinetics of peat dissolved organic matter. *Environ. Sci. Technol.* **2007,** *41*, 139-145.

24. Blodau, C.; Bauer, M.; Regenspurg, S.; Macalady, D., Electron accepting capacity of dissolved organic matter as determined by reaction with metallic zinc. *Chem Geol* **2009,** *260*, (3-4), 186-195.

25. Blodau, C.; Heitmann, T., Oxidation and incorporation of hydrogen sulfide by dissolved organic matter. *Chem Geol* **2006,** *235*, (1-2), 12-20.

26. Helburn, R. S.; Maccarthy, P., Determination of Some Redox Properties of Humic-Acid by Alkaline Ferricyanide Titration. *Anal Chim Acta* **1994,** *295*, (3), 263-272.

27. Jovanovic, S. V.; Jankovic, I.; Josimovic, L., Electron-Transfer Reactions of Alkyl Peroxy-Radicals. *J Am Chem Soc* **1992,** *114*, (23), 9018-9021.

28. Huang, D. J.; Ou, B. X.; Prior, R. L., The chemistry behind antioxidant capacity assays. *J Agr Food Chem* **2005,** *53*, (6), 1841-1856.

29. Ingold, K. U., Inhibition of the Autoxidation of Organic Substances in the Liquid Phase. *Chem Rev* **1961,** *61*, (6), 563-589.

30. Ingold, K. U., Inhibition of Autoxidation. *Adv Chem Ser* **1968**, (75), 296-&.

31. Rimmer, D. L.; Smith, A. M., Antioxidants in soil organic matter and in associated plant materials. *Eur J Soil Sci* **2009,** *60*, (2), 170-175.

32. Rimmer, D. L., Free radicals, antioxidants, and soil organic matter recalcitrance. *Eur J Soil Sci* **2006,** *57*, (2), 91-94.

33. Rimmer, D. L.; Abbott, G. D., Phenolic compounds in NaOH extracts of UK soils and their contribution to antioxidant capacity. *Eur J Soil Sci* **2011,** *62*, (2), 285-294.

34. Canonica, S.; Laubscher, H. U., Inhibitory effect of dissolved organic matter on triplet-induced oxidation of aquatic contaminants. *Photochemical & Photobiological Sciences* **2008,** *7*, (5), 547-551.

35. Wenk, J.; von Gunten, U.; Canonica, S., Effect of Dissolved Organic Matter on the Transformation of Contaminants Induced by Excited Triplet States and the Hydroxyl Radical. *Environ Sci Technol* **2011,** *45*, (4), 1334-1340.

36. von Gunten, U., Ozonation of drinking water: Part I. Oxidation kinetics and product formation. *Water Res* **2003,** *37*, (7), 1443-1467.

37. von Gunten, U., Ozonation of drinking water: Part II. Disinfection and by-product formation in presence of bromide, iodide or chlorine. *Water Res* **2003,** *37*, (7), 1469-1487.

38. Norwood, D. L.; Christman, R. F.; Hatcher, P. G., Structural Characterization of Aquatic Humic Material .2. Phenolic Content and Its Relationship to Chlorination Mechanism in an Isolated Aquatic Fulvic-Acid. *Environ Sci Technol* **1987,** *21*, (8), 791-798.

39. Helburn, R. S.; Maccarthy, P., Determination of some redox properties of humic acid by alkaline ferricyanide titration. *Anal. Chim. Acta.* **1994,** *295*, (3), 263-272.

40. Ritchie, J. D.; Perdue, E. M., Proton-binding study of standard and reference fulvic acids, humic acids, and natural organic matter. *Geochim. Cosmochim. Acta.* **2003,** *67*, (1), 85-96.

41. Milne, C. J.; Kinniburgh, D. G.; Tipping, E., Generic NICA-Donnan model parameters for proton binding by humic substances. *Environ Sci Technol* **2001,** *35*, (10), 2049-2059.

42. Lu, X. Q.; Hanna, J. V.; Johnson, W. D., Source indicators of humic substances: an elemental composition, solid state C-13 CP/MAS NMR and Py-GC/MS study. *Appl Geochem* **2000,** *15*, (7), 1019-1033.

43. Cooper, W. T.; Stenson, A. C.; Landing, W. M.; Marshall, A. G., Ionization and fragmentation of humic substances in electrospray ionization Fourier transform-ion cyclotron resonance mass spectrometry. *Anal Chem* **2002,** *74*, (17), 4397-4409.

44. Schmidt-Rohr, K.; Mao, J. D.; Xing, B. S., New structural information on a humic acid from two-dimensional H-1-C-13 correlation solid-state

nuclear magnetic resonance. *Environ Sci Technol* **2001,** *35*, (10), 1928-1934.

45. Matthiessen, A., *Determining the redox capacity of humic substances as a function of pH*. VCH: Weinheim, ALLEMAGNE, 1995; Vol. 84.

46. Rice-Evans, C.; Re, R.; Pellegrini, N.; Proteggente, A.; Pannala, A.; Yang, M., Antioxidant activity applying an improved ABTS radical cation decolorization assay. *Free Radical Bio Med* **1999,** *26*, (9-10), 1231-1237.

47. Cory, R. M.; McKnight, D. M., Fluorescence spectroscopy reveals ubiquitous presence of oxidized and reduced quinones in dissolved organic matter. *Environ Sci Technol* **2005,** *39*, (21), 8142-8149.

48. Macalady, D. L.; Walton-Day, K., New light on a dark subject: On the use of fluorescence data to deduce redox states of natural organic matter (NOM). *Aquat Sci* **2009,** *71*, (2), 135-143.

49. Boyle, E. S.; Guerriero, N.; Thiallet, A.; Vecchio, R. D.; Blough, N. V., Optical Properties of Humic Substances and CDOM: Relation to Structure. *Environ Sci Technol* **2009,** *43*, (7), 2262-2268.

50. Gamage, R.; McQuillan, A. J.; Peake, B. M., Ultraviolet visibile and electron paramagnetic resonance spectroelectrochemical studies of the reduction products of some anthraquinone sulfonates in aqueous solutions *J. Chem. Soc. Faraday. T.* **1991,** *87*, (22), 3653-3660.

51. Kujawinski, E. B.; Hatcher, P. G.; Freitas, M. A., High-resolution Fourier transform ion cyclotron resonance mass spectrometry of humic and fulvic acids: Improvements and comparisons. *Anal. Chem.* **2002,** *74*, (2), 413-419.

52. Kappler, A.; Haderlein, S. B., Natural organic matter as reductant for chlorinated aliphatic pollutants. *Environ Sci Technol* **2003,** *37*, (12), 2714-2719.

53. Fimmen, R. L.; Cory, R. M.; Chin, Y. P.; Trouts, T. D.; McKnight, D. M., Probing the oxidation-reduction properties of terrestrially and microbially derived dissolved organic matter. *Geochim. Cosmochim. Acta.* **2007,** *71*, (12), 3003-3015.

54. Osterberg, R.; Shirshova, L., Oscillating, nonequilibrium redox properties of humic acids. *Geochim. Cosmochim. Acta.* **1997,** *61*, (21), 4599-4604.

55.	Bard, A. J.; Faulkner, L. R., *Electrochemical methods : fundamentals and applications*. 2nd ed.; Wiley: New York, 2001; p xxi, 833 p.

56.	Motheo, A. J.; Pinhedo, L., Electrochemical degradation of humic acid. *Sci Total Environ* **2000,** *256*, (1), 67-76.

57.	Sachs, S.; Bernhard, G., Humic acid model substances with pronounced redox functionality for the study of environmentally relevant interaction processes of metal ions in the presence of humic acid. *Geoderma* **2011,** *162*, (1-2), 132-140.

58.	Clark, W., *Oxidation-Reduction Potentials of Organic Systems*. Baltimore, 1960.

59.	Tratnyek, P. G.; Wolfe, N. L., Characterization of the reducing properties of anaerobic sediment slurries using redox indicators. *Environ. Toxicol. Chem.* **1990,** *9*, (3), 289-295.

Chapter 2

Novel electrochemical approach to assess the redox properties of humic substances

Abstract

Two electrochemical methods to assess the redox properties of humic substances (HS) are presented: Direct electrochemical reduction (DER) on glassy carbon working electrodes (WE) and mediated electrochemical reduction (MER) and oxidation (MEO) using organic radicals to facilitate electron transfer between HS and the WE. DER allows for continuous monitoring of electron and proton transfer to HS by chronocoulometry and automated acid titration, respectively, and of changes in bulk HS redox potential E_h. Leonardite humic acid (LHA) showed an H^+/e^- ratio of unity and a decrease in potential from E_h= +0.18 to -0.23 V upon transfer of 822 μmol_{e^-} g_{LHA}^{-1} at pH 7, consistent with quinones as major redox-active functional moieties in LHA. MER and MEO quantitatively detected electrons in LHA samples that were pre-reduced by DER to different extents. MER and MEO therefore accurately quantify the redox state of HS. Cyclic DER and O_2-reoxidation revealed that electron transfer to LHA was largely reversible. However, LHA contained a small pool of moieties that were not re-oxidized, likely due to endergonic first electron transfer to O_2. Electron accepting capacities of 13 different HS, determined by MER, strongly correlated with their C/H ratios and aromaticities and with previously published values, which, however, were a factor of three smaller due to methodological limitations

2.1. Introduction

Humic substances (HS), including humic and fulvic acids, are redox-active natural organic macromolecules that are ubiquitous in soils and sediments and predominate in the subsurface of peatlands and bogs. The redox-activity of HS has been primarily ascribed to quinone-hydroquinone moieties (1-5), although complexed metals, in particular iron, may also play a role. In environments with changing redox conditions, such as capillary fringes of soils, HS may act as redox buffers by accepting electrons from microbial respiration under anoxic condition (6-8), and, upon re-aeration, by donating electrons to oxygen. In peatlands and bogs, this process is believed to significantly decrease methanogenesis (8, 9). In addition to acting as redox buffers, HS mediate biogeochemical redox reactions, including the transfer of electrons from microorganisms to poorly accessible mineral phases, such as Fe^{3+}-oxides (6, 7, 10). HS also mediate electron transfer from abiotic reductants (e.g., H_2S) to organic pollutants (e.g., halogenated hydrocarbons and nitroaromatics) (11-13). The role of HS as redox buffers and mediators has drawn considerable interest in their redox properties, including the reversibility of electron transfer to and from HS and their electron acceptor (EAC) and donor (EDC) capacities (i.e., the moles of electrons that can be transferred or withdrawn, respectively, from HS at a given potential E_h).

Some previous methods to determine EAC have used H_2S and Zn^0 as reductants (14, 15). Following HS reduction, the oxidation products $S_2O_3^{2-}$ and Zn^{2+} were quantified and set equal to EAC. Other studies determined the EAC indirectly by measuring the difference in EDCs of a pre-reduced and a non-treated HS. Pre-reduction was achieved either microbially (*Geobacter metallireducens*), chemically (H_2 in the presence of Pt or Pd, H_2S, Zn^0), or electrochemically (bulk electrolysis at a Pt working electrode) (2, 12, 16, 17). The EDCs were determined by quantifying the amount of Fe^{2+} formed by the reduction of added Fe^{3+} complexes (most often Fe^{3+}-citrate or hexacyanoferrate) by HS. This experimental approach has also been used to determine changes in the redox states of HS samples, for instance along environmental redox-gradients (8).

Although widely used, the above methods have some limitations: First, the amount of electrons transferred to and withdrawn from HS was determined

only indirectly by quantifying the oxidation or reduction of added chemicals. A direct measurement of transferred electrons is, however, required to improve accuracy and reduce analysis time. Second, electron transfer to and from added chemical oxidants and reductants is often coupled to proton exchange, which resulted in a pH-dependent reduction potential E_h and hence driving force for HS oxidation and reduction. This impedes direct comparisons of the redox properties of HS (e.g. EAC and EDC) if determined at different pH. Ideally, both EAC and EDC should be determined relative to reference states with pH-independent E_h. Third, EDC quantification by re-oxidation with Fe^{3+} is slow, requiring hours to days to attain apparent reaction equilibrium (17). Yet, reaction times were often not more than 15 min to one hour (2, 16), such that determined values underestimated true equilibrium EDCs. Clearly, methods with faster electron transfer kinetics to and from HS are required. Fourth, the use of chemical reductants may result in side reactions, including complexation of added Fe and Zn by HS or covalent modification of HS (e.g., nucleophilic addition of reduced sulfur species) (14, 15).

In this paper, we present a novel electrochemical approach to study the redox properties of HS, which overcomes the limitations of previously used methods. The approach combines two electrochemical methods. The first is constant-potential direct electrochemical reduction (DER) of HS at a glassy carbon (GC) working electrode (WE). The use of GC allowed for a continuous chronocoulometric quantification of the amount of electrons transferred to HS, since background currents from H^+ reduction were negligible. DER served to generate clean HS samples with known redox states, to quantify the ratio of protons to electrons transferred during reduction, and to monitor the resulting decrease in redox potential E_h during the reduction. The second method, mediated electrochemical reduction (MER) and oxidation (MEO), quantified differences in the electron contents between small HS samples by chronocoulometry. Organic radicals mediated the electron transfer between the HS and carbon electrode and established stable, pH-independent redox potentials in the electrochemical cell.

The versatility of this novel approach is demonstrated by evaluation of the reversibility of electron transfer to Leonardite humic acid (LHA) in successive DER and O_2 re-oxidation cycles, and by the quantification of the EACs of a broad set of terrestrial and aquatic humic and fulvic acids.

2.2. Materials and Methods

Chemicals. Diquat dibromide monohydrate (99.5%, Supelco) (DQ), 2,2'-azino-bis(3-ethylbenzthiazoline-6-sulfonic acid) diammonium salt (>99%) (ABTS), 2,6–dichlorophenol indophenol sodium salt hydrate (purum.p.a) (DCPIP), starch from wheat, potassium chloride (>99.5 %), sodium hydroxide (puriss. p.a.), and hydrochloric acid (puriss. p.a.) were purchased from Fluka (St. Louis, MO, USA). Ethyl viologen dibromide (>99%), 9,10-anthraquinone-2,6-disulfonic acid disodium salt (>98%), and 2-hydroxy-1,4-naphthoquinone (Lawsone) (>97%) were from Sigma-Aldrich (St. Louis, MO, USA), disodium hydrogen phosphate dihydrate (p.a.) was from Merck (Darmstadt, Germany).

All aqueous solutions were prepared with nanopure water (Barnstead NANOpure Diamond Water Purification System).

Humic substances (HS) were used as received. Aldrich humic acid was obtained from Sigma-Aldrich (St Louis, MO). All other HS (i.e., Suwannee River Humic Acid Standard II, Suwannee River Fulvic Acid Standard II, Elliott Soil Humic Acid Standard, Eliott Soil Fulvic Acid Standard III, Leonardite Humic Acid Standard, Pahokee Peat Humic Acid Standard, Pahokee Peat Humic Acid Reference, Pahokee Peat Fulvic Acid Standard II, Waskish Peat Humic Acid Reference, Nordic Aquatic Humic Acid Reference, Nordic Aquatic Fulvic Acid Reference, Pony Lake (Antarctica) Fulvic Acid Reference) were from the International Humic Substances Society (IHSS, St. Paul, MN, USA).

Electrochemical experiments. All electrochemical measurements were conducted in an anoxic glovebox (N_2 atmosphere at 25±1 °C, O_2< 0.1 ppm). Aqueous solutions were made anoxic by purging with argon for one hour at 150°C and for one hour at room temperature. All solutions used for electrochemical experiments contained 0.1 M KCl as supporting electrolyte. Potentials were measured vs. Ag/AgCl but are reported vs. SHE.

Direct electrochemical reduction (DER) of Leonardite humic acid (LHA). Dissolved LHA (2 g_{LHA} L^{-1}) was reduced in a ~0.1 L bulk electrolysis cell. The cell consisted of a glass vessel closed with a Teflon® cover, a GC WE (Sigradur G®, HTW, Tierhaupten, Germany), an Ag/AgCl reference electrode,

and a coiled platinum wire auxiliary electrode (both from Bioanalytical Systems Inc., West Lafayette, IN, USA). The auxiliary electrode was placed in an anodic compartment separated from the cathodic compartment by a glass frit to minimize re-oxidation of reduced HA. A CHInstruments 630C instrument (Austin, TX, USA) and an Autolab PG 302 instrument (EcoChemieB.V, Utrecht, The Netherlands) were used to measure currents I (A) and to control potentials at the WE. Unless stated otherwise, DER were carried out at E_h= -0.59 V. The transferred amount of electrons, Q_{DER} (μmol_{e-}), was obtained by chronocoulometry (i.e., integration of the reductive and oxidative currents I over time t (s)).

Two different setups were used to ensure constant pH 7 throughout DER. In the first, HS solutions contained 0.1 M phosphate. In the second setup, the HS solution (75 ml, 2 g_{LHA} L^{-1}) was continuously circulated through the electrochemical cell and two flow-through cells (Figure **1a**). Increase in solution pH by proton consumption was monitored by a pH electrode in the first flow through cell and compensated by titration of diluted HCl (18.5 mM) to the electrochemical cell using an automated titrator (751 GPD Titrino, Metrohm, Zofingen, Switzerland). The redox potential E_h was measured by a platinum-ring redox electrode (Metrohm, Zofingen, Switzerland) placed in the second flow through cell.

Mediated electrochemical reduction (MER) and oxidation (MEO) of HS samples was conducted with the electrochemical equipment described above. However, instead of GC, reticulated vitreous carbon (RVC, Bioanalytical Systems Inc., West Lafayette, IN, USA) was used as WE material to increase the surface area and hence to facilitate electron transfer to and from the mediator. The electrochemical cell was filled with 80 mL buffer (0.1 M KCl, 0.1 M phosphate, pH 7) and the electrode was equilibrated to the desired potentials (i.e. E_h= -0.49 V in MER and E_h= +0.61 V in MEO, which were below respectively above the potential range reported for quinones (see Figure **S1**)). Subsequently the mediators DQ for MER and ABTS for MEO were spiked, resulting in reductive and oxidative currents, respectively. Structural formula and standard potentials of these mediators are given in Figure **1d**. After re-attainment of constant background currents, small amounts (< 1 mg) of HS

samples were spiked to the cells and the transferred amount of electrons was measured by chronocoulometry.

Reversibility of electron transfer to HS using O_2 as oxidant. DER-reduced LHA was transferred to a gas tight serum flask, and re-oxidized with excess O_2 by purging the flask with synthetic air for 1h, followed by 24h incubation. Subsequently, un-reacted O_2 was removed by Ar-purging for 1h. This reduction-re-oxidation cycle was carried out three times, with incubation periods of LHA after purging with synthetic air of 24 h (cycle 1 and 2) and 8 d (cycle 3). After each reduction and oxidation step, an aliquot of the LHA was withdrawn and the EAC was determined by MER. To determine the re-oxidation kinetics of LHA by O_2, 9 mL aliquots of DER-reduced LHA were transferred into stoppered, gas tight serum flasks. Using a gas-tight syringe, 25 mL of the flasks headspace were withdrawn and replaced with oxygen. The flasks were incubated for different time spans. Oxidation of LHA was quenched by purging the flasks with argon for >1 hour to remove un-reacted O_2. Changes in EACs of the samples were quantified by MER.

Electron-accepting capacities (EAC) of HS. Solutions of a diverse set of HS listed above were prepared in buffer (0.5 g_{HS} L^{-1}; 0.1 M KCl, 0.1 M phosphate, pH 7). The EACs were quantified by MER.

2.3. Results and Discussion

2.3.1. Description and Evaluation of Electrochemical Methods

Electron transfer, proton consumption and change in redox potential in DER of LHA. Figure **1b** shows the reductive current *I* during DER of LHA (red line) using acid titration to maintain constant pH 7 (black line). High initial $I > 300$ µA decreased to (but did not level off at) ~ 30 µA after 50 h at which DER was stopped. Negligible background currents were measured in the absence of LHA (< 1 µA; grey line). This shows that the redox-active moieties in LHA can be directly reduced at GC and that no significant H_2 generation by proton reduction occurred. Hence the electrons transferred during DER could be quantified directly by integration of the LHA reduction current and was $Q_{DER} = 822$ µmol$_{e^-}$ g$_{LHA}^{-1}$ after 50 h. In contrast, the platinum electrode used in (12, 17), resulted in extensive H_2 production (and potentially catalytic hydrogenation reactions by H_2/Pt), which impaired accurate quantification of the transferred amount of electrons.
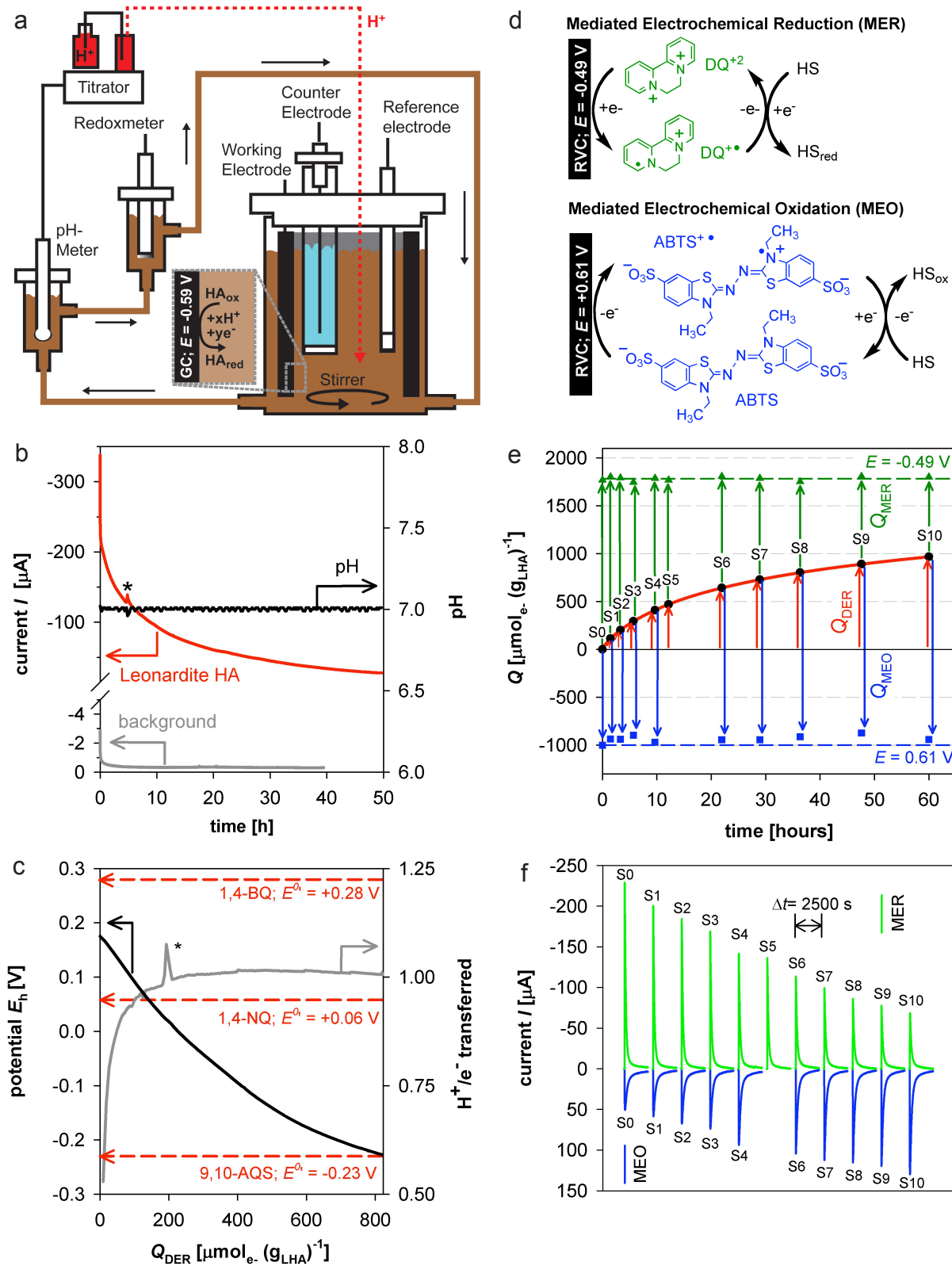
Figure 1. **a**. Direct electrochemical reduction (DER) of humic acid (HA). The electrochemical cell consisted of a cylindrical glassy carbon (GC) working electrode (applied potential E_h vs. SHE), an Ag/AgCl reference electrode, and a platinum-wire counter electrode

separated from the main compartment by a glass frit to avoid re-oxidation of reduced HA. The HA solution was continuously circulated through two small volume flow-through cells containing a pH electrode and a Pt-ring redox electrode. A constant experimental pH was maintained by automated addition of diluted acid to the electrochemical cell by a titration unit connected to the pH electrode. **b**. Reductive current (red trace) and solution pH (black trace) during DER of Leonardie humic acid (LHA) at E_h= -0.59V for 50 h. The background current (grey trace) was measured at the same E_h in the absence of LHA. **c**. Decrease in solution potential E_h (V vs. SHE) (black trace) and ratio of protons to electrons, H^+/e^-, transferred to LHA (grey trace) as a function of the amount of electrons transferred to LHA by DER, Q_{DER}, at pH 7. The standard redox potentials E_h^0 of 1,4-benzoquinone (1,4-BQ), 1,4-naphthoquinone (1,4-NQ), and 9,10-anthraquione-2-sulfonate (9,10-AQS) at pH 7 are given as references. The peaks in I, pH, and H^+/e^- (indicated by asterisk *) in panels b and c resulted from short time malfunctioning of the pH electrode. **d**. Schematic of mediated electrochemical reduction (MER) at E_h= -0.49 V and oxidation (MEO) at E_h= 0.61 V using the organic radicals diquat (DQ) and 2,2'-Azino-bis(3-ethylbenzthiazoline-6-sulfonic acid) (ABTS), respectively, to facilitate electron transfer between the reticulated vitreous carbon (RVC) working electrode to humic substances (HS). **e**. Electrons transferred to LHA in DER, Q_{DER} (red trace and arrows) and MEO, Q_{MEO} (green arrows), and electrons withdrawn from LHA in MEO, Q_{MEO} (blue arrows). Samples S0 to S10 were withdrawn from the electrochemical cell during DER and represented LHA standards with known Q_{DER}. **f.** Reductive and oxidative current responses in MER (green peaks) and MEO (blue peaks), respectively, for LHA samples S0 to S10. Current peaks were integrated to give transferred charge equivalents, Q_{MER} and Q_{MEO}, represented by arrows in panel e. Sample S5 could only be analyzed in MER.

The transfer of electrons to LHA during DER resulted in a gradual decrease in solution redox potential from E_h= +0.18 to -0.23 V (black line; Figure **1c**). E_h decreased only slightly when the same potential was applied to buffer in the absence of LHA (data not shown). The gradual decrease in E_h in combination with the absence of inflexion point(s) supports that LHA contains redox-active functional moieties with a wide distribution in redox potentials, falling into the potential range covered by benzo-, naphtha-, and anthraquinones (Figure **1c** and Figure **S1**). This is consistent with the hypothesis that quinones are the predominant redox active moieties in HS. A similar wide range of HS redox potentials was reported in (7). Note that the wide potential distribution of redox-active moieties in LHA and slow electron transfer kinetics at GC provide plausible explanations for the absence of distinct reduction and oxidation waves in cyclic voltammetry measurements of HA (4, 19).

The solution potential after 50 h of DER, E_h= -0.23 V, was significantly higher than the potential at the WE, E_h= -0.59 V. Therefore, LHA had not come to equilibrium with the WE over the course of DER. Plausible explanations for non-equilibrium (i.e., sluggish electron transfer) include passivation of the GC electrode surface due to HA adsorption (20) and the macromolecular nature of HA (e.g. slow reduction of redox-sites in the interior of HA colloids) (21). The non-equilibrium led to increasing Q_{DER} with increasing reduction time and with decreasing applied potential (shown for LHA in Figure **S3a** for applied potentials of E_h= -0.39, -0.59, and -0.79 V). Slow DER reduction kinetics were linked to HA since the same setup resulted in much faster and quantitative reduction of the model quinone lawsone (Figure **S3b**). The chosen E_h= -0.59 V allowed for DER also at pH< 7 without significant H_2 generation (data not shown).

The molar ratio of titrated protons to transferred electrons increased from 0.6 to 1.0 within the first ~250 μmol_{e^-} g_{LHA}^{-1} transferred after which it remained constant (Figure **1c**, grey trace). The final H^+ to e^- ratio was 1.01. Proton titration was negligible when the potential E_h= -0.59 V was applied to buffer in the absence of LHA (data not shown). The H^+ to e^- ratio of unity implies that one H^+ was taken up per e^- transferred to redox-active functional moieties in LHA. This again supports the hypothesis that quinones are the major redox active groups in HS, because most hydroquinones have acidity constants pK_a> 7 (22). The smaller initial H^+ to e^- ratio likely resulted from internal proton

buffering by LHA and/or by the transient formation of semiquinone radical anions, which is not coupled to H^+ uptake (2, 22). A detailed analysis of the pH-dependency of the ratio of H^+ to e^- transferred during DER will be presented in a forthcoming paper. DER of LHA solutions in which the pH was buffered by phosphate resulted in very similar current responses (Figure **S3a)**.

In summary, the results show that DER at GC has several advantages over previously employed reduction methods: DER allows for (i) a direct quantification of transferred electrons during reduction, (ii) simultaneous monitoring of electron and proton transfers, pH, and E_h during reduction, (iii) reduction at different E_h, (Figure S3) and pH (data not shown), and (iv) generation of bulk (mg to g) amounts of 'clean' reduced HA samples (devoid of chemical reducing agents such as complexed metal cations or covalently bonded H_2S species) with defined redox states that can be directly used in follow up experiments.

Mediated electrochemical reduction and oxidation (MER and MEO). Spiking of small volumes of pre-reduced and non-treated LHA samples into electrochemical cells with the WE pre-polarized to E_h= -0.49 V and +0.61 V, but in the absence of organic electron transfer mediators, resulted in poorly defined reductive and oxidative current responses, respectively (Figure **S4**), reflecting sluggish direct electron transfer between LHA and the WE. The peaks could not be exactly integrated. Hence, in order to facilitate the electron transfer, organic electron transfer mediators were employed. The radicals diquat (DQ, first electron reduction potential E_h^1= -0.36 V) and ethylviologen (EV, E_h^1= -0.48 V) (data not shown) were used for MER and ABTS (second electron reduction potential E_h^2= +0.68 V) for MEO (Figure **S2**) (23, 24), because these chemicals fulfilled the following requirements (25, 26): (i) fast and reversible heterogeneous electron transfer at the electrode and homogenous electron transfer with LHA in solution, (ii) pH-independent redox potentials E_h (i.e., organic radicals), (iii) stability at potentials sufficiently low (mediator in MER) respectively high (mediator in MEO) to cover the E_h-range of the redox-active moieties in LHA (Figure **S1**), and (iv) sufficiently high water solubility. Spiking of DQ to the electrochemical cell with the WE pre-polarized to E_h= -0.49 V resulted in reductive current peaks due to one-electron reduction of DQ^{2+} to the radical $DQ^{\bullet+}$ (Figures **S2** and **S4a**). The transferred amount of electrons

obtained from peak integration was 100±5% of the amount expected for an equimolar electron transfer to DQ^{2+}, demonstrating accurate chronocoulometric quantification. Analogously, spiking of ABTS to the electrochemical cell with the WE pre-polarized to E_h= +0.61 V resulted in oxidative currents due to one-electron oxidation of ABTS to $ABTS^{\bullet+}$ (Figures **S2** and **S4b**). Subsequent spiking of LHA samples to both systems resulted in very sharp, well-defined current peaks (Figure **S4**), demonstrating that DQ and ABTS facilitated the electron transfer between LHA and the WE (Figure **1d**).

A series of eleven LHA samples (S0 to S10) with increasing Q_{DER} from 0 $\mu mol_{e^-} \ g_{LHA}^{-1}$ (S0) to 966 $\mu mol_{e^-} \ g_{LHA}^{-1}$ (S10) were obtained by DER (Figure **1e**). These samples served as standards with known differences in electron contents to test the recovery of DER-transferred electrons by MER and MEO. Figure **1f** shows the current responses of samples S0 to S10 in MER (green peaks) and MEO (blue peaks). The height of the current peaks decreased in MER and increased in MEO with increasing pre-reduction of LHA by DER (i.e., from S0 to S10, Figure **1f**). No reductive and oxidative current peaks were detected when background buffer without LHA was spiked. The results of a number of additional control experiments, including MER and MEO of two model quinones, lawsone and AQDS, and of starch, a non redox-active organic polymer, are summarized in Table **S1**.

The amount of electrons transferred to and from LHA in sample SX (X= 0 to 10) during MER, $Q_{MER}(SX)$, and MEO, $Q_{MEO}(SX)$, were obtained by integration of the respective reductive and oxidative current peaks in Figure **1f**. Figure **1e** shows that Q_{MER} (green arrows), decreased, while Q_{MEO} (blue arrows) increased with increasing amounts of electrons transferred to LHA during pre-reduction by DER, Q_{DER} (red arrows). Notably, the same total amount of electrons, $Q_{DER}(SX) + Q_{MER}(SX)$, was transferred to each of the samples. Moreover, the amount of electrons withdrawn by MEO from sample SX, $Q_{MEO}(SX)$, was equal to $Q_{DER}(SX) + Q_{MEO}(S0)$, where sample S0 contained LHA that was not pre-reduced by DER (Figure **1e**). The recovery of Q_{DER} was 104 (± 3) % by MER and 90 (± 4) % by MEO (determined by regression analysis, see Figure **S5** for details). MER and MEO therefore quantitatively detected the electrons that had been transferred to LHA during DER.

These findings have the following implications: (i) Redox-active moieties in HS that were reducible by DER in the absence of mediator were also reduced by DQ in MER. Furthermore, electron transfer to LHA by DER was largely reversible when ABTS was used as oxidant. Re-oxidation by ABTS was therefore both kinetically fast and thermodynamically favorable. (ii) Non-treated LHA (sample S0) contained reduced moieties that were oxidized by ABTS. The E_h-data in Figures **1c** and **S1** suggests that some of these moieties might have been hydroquinones with E_h^0 > +0.18 V at pH 7, the potential of un-treated LHA inside the glovebox. Note that Q_{MEO} increased with increasing E_h applied to the WE (data not shown). This was likely due to oxidation of phenolic and other oxidizable moieties in LHA, as suggested by MEO of model quinones lawsone and AQDS (Table **S1**). (iii) Electron transfer to LHA in MER was much faster and more extensive than in DER, even though the potentials of the WE were lower in DER (E_h= -0.59 V) than in MER (E_h= -0.49 V), thus confirming non-equilibrium conditions of LHA and the WE during DER. (iv) The quantitative recovery confirmed that reductive currents during DER were due to electron transfer to redox-active moieties in LHA and not due to reduction of solution protons (i.e., H_2 generation). (v) MER and MEO are perfectly suited to determine the redox states (i.e., the degree of reduction and oxidation with regard to the reference states of MER and MEO) of HS from small environmental samples. Other redox-active species (e.g. iron) in the sample will also be detected.

2.3.2. Method applications

Reversibility of electron transfer to and from LHA Redox buffering and electron transfer mediation by HS requires that they contain functional moieties that reversibly accept and donate electrons. Reversibility in successive reduction and O_2-oxidation cycles is of particular interest to studies of redox-dynamics in temporarily anoxic environments. In previous work it was shown for a set of eight HS, that the difference in the EDCs of Pd/H_2-reduced and O_2 re-oxidized HS to Fe^{3+}-citrate remained more or less constant over five successive reduction and oxidation cycles. This demonstrated that within the range of E_h values considered, each of the tested HS contained a constant pool of functional moieties with reversible electron transfer (16). However, because the size of this pool could not be related to the unknown amount of electrons transferred to HS

during Pd/H$_2$ reduction, the degree of electron transfer reversibility in one and over all cycles remained unknown. As demonstrated in the following example, electron transfer reversibility in reduction-oxidation cycles can be accurately determined by combining DER with MEO and MER.

Figure **2a** shows the excess amount of electrons, Q, on LHA samples relative to non-treated LHA during three DER-reduction (red traces) and O$_2$-reoxidation (black dashed arrows) cycles. Within each cycle Q increased by DER of LHA and decreased by exposure of LHA to excess O$_2$. Each reduction and re-oxidation step therefore regenerated a large fraction of the capacity of LHA to donate and accept electrons, respectively. This reversible fraction underpins that HS act as redox buffers in temporarily anoxic environments. A smaller fraction of DER-transferred electrons was not re-oxidized by O$_2$ over 1d in cycles 1 and 2 and 8d in cycle 3. The size of this recalcitrant fraction was consistently quantified both by MER and MEO and accounted for 28%, 38%, and 32% of Q in LHA prior to exposure to O$_2$ in cycles 1, 2, and 3, respectively.

Quantitative recovery of DER-transferred electrons by ABTS in MEO at E_h= +0.61 V implies that the recalcitrant fraction did not result from truly irreversible electron transfer during LHA reduction. The reduction potential for the half reaction of O$_2$ + 4e$^-$ + 4H$^+$ $\Leftrightarrow$ 2 H$_2$O, E_h^0= +0.77 V at pH 7 (27), is much higher than the E_h in MEO and the measured E_h for extensively reduced LHA (Figures **1c** and **S1**), indicating that re-oxidation of LHA by O$_2$ to form water was thermodynamically favorable. In contrast, the first electron reduction potential of O$_2$ at pH 7, E_h^1= –0.16 V, to form superoxide lies at the lower end of measured E_h for LHA. Notably, the recalcitrant fraction was largely formed during the first DER step and increased only slightly to the second DER step (Figure **2a**). This suggests that the oxidation-recalcitrant fraction was composed of (benzo-)quinones with first electron reduction potentials above the potential applied at the working electrode (i.e., moieties that were readily reduced in the first DER step), yet with second electron reduction potentials much higher than the E_h^1 of O$_2$, resulting in endergonic and hence slow first electron transfer to O$_2$. This is supported by a highly endergonic free energy of one electron transfer from 1,4-hydroquinone, a model for benzoquinone moieties in LHA, to molecular oxygen of ΔG^1= +64.5 kJ mol^{-1} at pH 7 (calculations in SI).
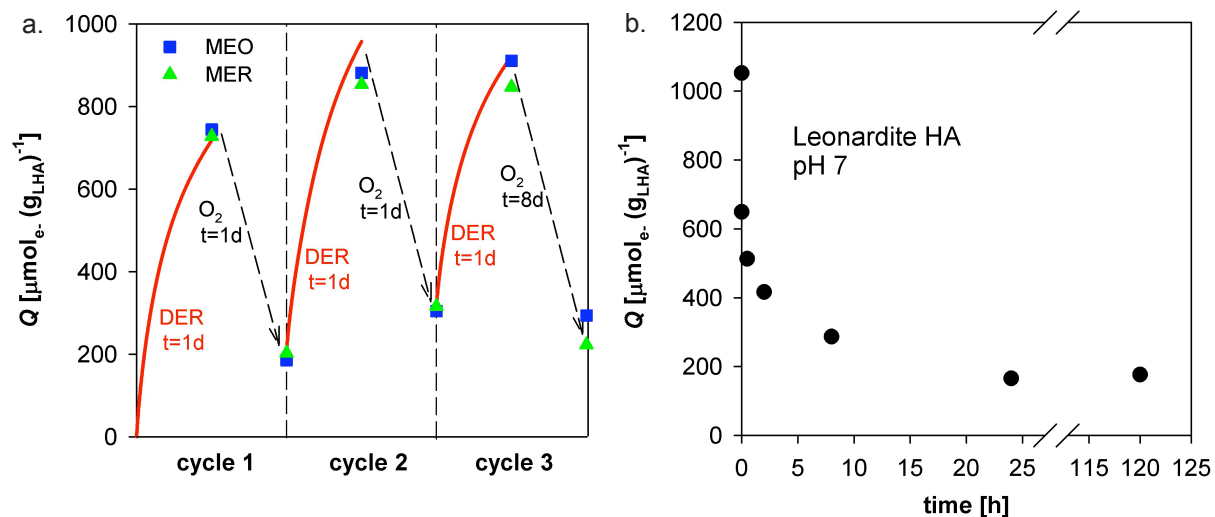
Figure 2. **a.** Change in the amount of electrons on Leonardite humic acid (LHA), Q, relative to non-treated LHA during three successive cycles of direct electrochemical reduction (DER) and re-oxidation by O_2. Electrons transferred to LHA were directly quantified in DER (red traces). Mediated electrochemical reduction (MER; green triangles) and oxidation (MEO; blue squares) were used to quantify Q following DER and O_2 re-oxidation and were generally very good agreement. **b.** Re-oxidation kinetics of DER-reduced LHA by excess O_2. The amount of electrons on LHA, Q, relative to non-treated LHA was quantified by MER.

Slow and incomplete re-oxidation was verified by oxidizing reduced LHA (Q_{DER}= 1053 μmol_{e^-} g_{LHA}^{-1}) with excess O_2 (Figure **2b**). About 50% of Q_{DER} was transferred to O_2 within less than 1 min, consistent with similar findings in (10). This fast initial re-oxidation was followed by slower re-oxidation (up to 24 h), during which an additional ~35% of Q_{DER} was transferred to O_2. Beyond 24 h, no further re-oxidation was detected up to 5 d. The amounts of DER-transferred electrons recalcitrant to O_2-reoxidation in Figure **2a** and **2b** were very similar (i.e., 200-300 μmol_{e^-} g_{LHA}^{-1}), albeit the total Q_{DER} was higher in the second than the first experiment. This indicates a constant pool of readily reducible quinones in LHA that form hydroquinones with low first electron oxidation potentials. The size of this pool in LHA corresponds well to the size recently reported for a peat humic acid (~220 μmol_{e^-} g^{-1}) (10).

Electron accepting capacities (EACs) of a broad spectrum of terrestrial and aquatic HS. The EACs of eight HA and five FA was determined by MER. The EACs ranged from 493±10 μmol_{e^-} g^{-1} for Pony Lake Fulvic Acid Standard to 1961±15 μmol_{e^-} g^{-1} for Eliott Soil Humic Acid Standard (Figure **3a** and Table **S2**). There are two clear trends among the tested HS. First, HA had higher EACs than FA (i.e., 920 to 1960 μmol_{e^-} g^{-1} compared to 490 to 1050 μmol_{e^-} g^{-1}, respectively). This is particularly evident when comparing HA and FA extracted from the same source material (No. 2 and 5 or 8 and 11 in Figure **2a**). Second, terrestrial HA had higher EACs than aquatic HA. The EACs therefore decreased in the order terrestrial HA> aquatic HA, aquatic FA, terrestrial FA > Pony Lake FA. The latter is of microbial origin (28) and therefore devoid of lignin-derived moieties.
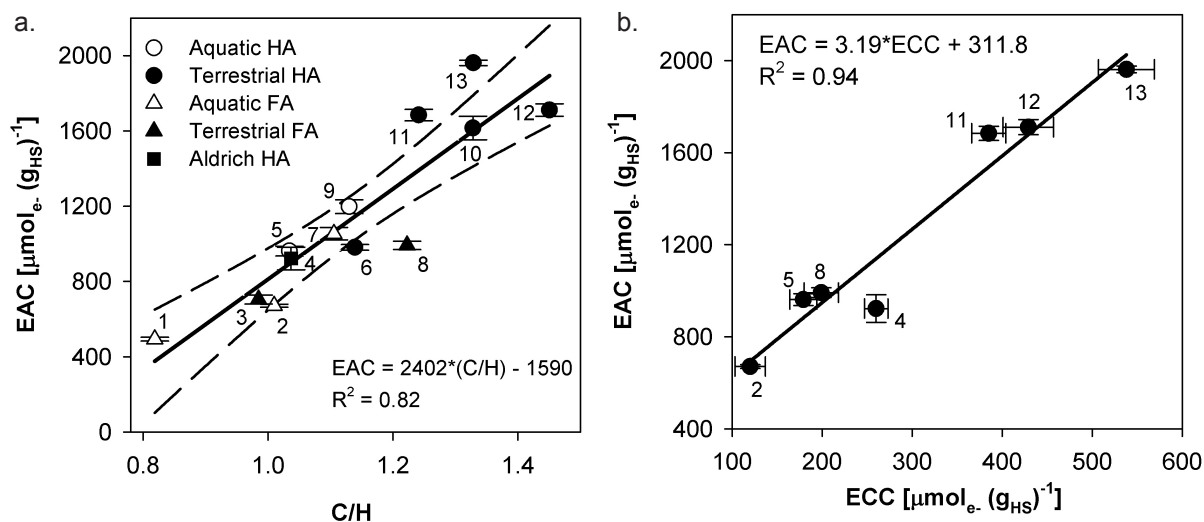
Figure 3. **a.** Linear correlation of electron accepting capacity (EACs) versus the carbon to hydrogen ratio (C/H) of 13 tested humic substances. The EACs were determined by mediated electrochemical reduction (MER) at an electrode potentials E_h=-0.49 V vs. SHE using diquat as mediator. C/H were determined by the International Humic Substances Society (IHSS; http://ihss.gatech.edu/ihss2/). The solid line represents the best fit of experimental data and dashed lines correspond to the 95% confidence intervals of the experimental fit. 1: Pony lake fulvic acid reference; 2 Suwannee River Fulvic acid Standard; 3: Elliott Soil Fulvic acid Standard; 4: Aldrich humic acid; 5 Suwannee River humic acid Standard; 6: Waskish Peat Humic acid Reference; 7: Nordic Lake Fulvic acid Reference; 8: Pahokee Peat Fulvic Acid Standard; 9: Nordic Lake Humic acid Reference; 10: Pahokee Peat Humic Acid Reference; 11: Pahokee Peat Humic Acid Standard; 12: Leonardite Humic acid Standard; 13: Elliot Soil Humic acid Standard. **b.** Linear correlation of EACs of a subset of tested HS versus the electron carrying capacities (ECC) of the same HS taken from (16). The numbers in panel b correspond to numbers in panel a.

The EACs correlated linearly with the C/H elemental ratios of all thirteen tested HS (R^2= 0.82; Figure **3a**) and with aromaticity for eleven of the tested HS, for which experimental aromaticity data from ^{13}C-NMR was available (R^2= 0.82; Figure **S6**). The correlation with aromaticity was stronger than a previously published correlation based on nine HS (R^2= 0.66) in (2), in which EACs were determined indirectly by oxidation of non-treated and microbially reduced HS using Fe^{3+}. The good correlations presented herein provide additional evidence that aromatic systems, likely quinone moieties, dominate the redox characteristics of HS. This is supported by calculations showing that the molar concentrations of non-carboxylic and non-phenolic oxygen ($\mu mol_O \ g_{HS}^{-1}$) of the

tested HS, which include oxygen in quinone moieties, were much larger than their respective EAC (Table **S2**). The high EAC of terrestrial HA and the low EAC of aquatic FA, particularly of Pony lake FA, suggests that such quinone groups most likely originate from phenolic moieties in lignin (2).

Comparison of different methods for determining EACs. The EACs of seven of the tested HS linearly correlated (R^2= 0.94) with their electron carrying capacities (ECC) reported in (16) (Figure **3b**), where the ECC was defined as the difference in the amounts of electrons transferred to Fe^{3+}-citrate within 15 min of reaction between non-treated and from Pd/H_2 pre-reduced HS. However, since the electron transfer from HS to Fe^{3+}-citrate requires >24 hours to reach equilibrium (17), reported ECCs likely underestimated equilibrium values. This explains why ECCs were about a factor of three smaller than EACs determined by MER (Figure **3b**). The linear correlation of EAC and ECC, however, implies that the HS in Figure **3b** had similar relative amounts of their EACs that were readily re-oxidized by Fe^{3+}-citrate. Thus, even though short time oxidation of extensively reduced HS by Fe^{3+}-citrate resulted in incomplete recovery of reductively transferred electrons, the assay may be used to determine the relative differences in the EACs among HS and to detect changes in the redox states of partially reduced HS.

Similar to re-oxidation by Fe^{3+}, the non-radical organic mediator dichlorophenol-indophenol (DCPIP) (Figure **S2**), when used in MEO at E_h= +0.61 V, recovered 50% of the electrons that had been transferred to LHA samples by DER (samples B0 to B4 in Figure **S5**). Incomplete recovery by DCPIP yet close to complete recovery by ABTS, despite the same electrode potential in MEO, show that DER-reduced LHA contained moieties that were only slowly oxidized by DCPIP, likely due to slow first electron transfer kinetics. The amount of electrons recovered by DCPIP, however, correlated linearly with the amount of electrons that had been transferred to LHA during DER (Figure **S5**). DCPIP therefore accurately detected changes in the redox states of partially reduced HA.

Oxidized DCPIP is blue (λ_{max}= 603 nm), while reduced $DCPIPH_2$ is colorless. The reductive decolorization of DCPIP can therefore be used in a spectrophotometric assay to quantify redox changes in HS (method details in

SI), extending on an earlier approach using DCPIP to determine sediment redox states (18).

Addition of DER-reduced LHA (Q_{DER}= 999 μmol_{e-} g_{LHA}^{-1}) to DCPIP resulted in a decrease in the absorption at λ_{max}= 603 nm (due to reduction of DCPIP), which was proportional to the amount of LHA added (Figure **S7**). In contrast, addition of non-treated LHA resulted in little reduction of DCPIP (Figure **S7**). The calculated amounts of electrons transferred from pre-reduced and non-treated LHA to DCPIP were 612 and 42 μmol_{e-} g_{LHA}^{-1}, respectively. This corresponds to a recovery of 57% of Q_{DER}, which agreed well with the recovery in MEO using DCPIP as mediator. Higher recoveries were obtained when the reoxidation was conducted over longer time periods (data not shown). Quantification of HS redox status is faster and more direct by this DCPIP assay than by currently used Fe^{3+}-assays in which complexation of the reduction product Fe^{2+} with ferrozin is required prior to its spectroscopic analysis (17). The DCPIP assay is therefore suited for high-throughput analysis of changes in the redox states of large sets of HS samples. Yet, for accurate balancing (i.e., complete recovery) of electrons transferred to and from HS, the use of organic radical mediators in MER and MEO is recommended.

Brief. The electrochemical approach allows for direct quantification of electrons and protons transferred to and from humic substances under controlled potential and pH conditions.

2.4. References

1.   Klapper, L.; McKnight, D. M.; Fulton, J. R.; Blunt-Harris, E. L.; Nevin, K. P.; Lovley, D. R.; Hatcher, P. G., Fulvic acid oxidation state detection using fluorescence spectroscopy. *Environ. Sci. & Technol.* **2002**, *36*, (14), 3170-3175.

2.   Scott, D. T.; McKnight, D. M.; Blunt-Harris, E. L.; Kolesar, S. E.; Lovley, D. R., Quinone moieties act as electron acceptors in the reduction of humic substances by humics-reducing microorganisms. *Environ. Sci. & Technol.* **1998**, *32*, (19), 2984-2989.

3.   Struyk, Z.; Sposito, G., Redox properties of standard humic acids. *Geoderma* **2001**, *102*, (3-4), 329-346.

4.   Nurmi, J. T.; Tratnyek, P. G., Electrochemical properties of natural organic matter (NOM), fractions of NOM, and model biogeochemical electron shuttles. *Environ. Sci. & Technol.* **2002**, *36*, (4), 617-624.

5.   Fimmen, R. L.; Cory, R. M.; Chin, Y. P.; Trouts, T. D.; McKnight, D. M., Probing the oxidation-reduction properties of terrestrially and microbially derived dissolved organic matter. *Geochimica Et Cosmochimica Acta* **2007**, *71*, (12), 3003-3015.

6.   Lovley, D. R.; Coates, J. D.; BluntHarris, E. L.; Phillips, E. J. P.; Woodward, J. C., Humic substances as electron acceptors for microbial respiration. *Nature* **1996**, *382*, (6590), 445-448.

7.   Kappler, A.; Benz, M.; Schink, B.; Brune, A., Electron shuttling via humic acids in microbial iron(III) reduction in a freshwater sediment. *Fems Microbiology Ecology* **2004**, *47*, (1), 85-92.

8.   Heitmann, T.; Goldhammer, T.; Beer, J.; Blodau, C., Electron transfer of dissolved organic matter and its potential significance for anaerobic respiration in a northern bog. *Global Change Biology* **2007**, *13*, (8), 1771-1785.

9.   Cervantes, F. J.; van der Velde, S.; Lettinga, G.; Field, J. A., Competition between methanogenesis and quinone respiration for ecologically important substrates in anaerobic consortia. . *FEMS Microbiology Ecology* **2000**, *34*, (2), 161-171.

10.   Bauer, I.; Kappler, A., Rates and Extent of Reduction of Fe(III) Compounds and O2 by Humic Substances. *Environ. Sci. & Technol.* **2009**, *43*, (13), 4902-4908.

11.   Collins, R.; Picardal, F., Enhanced anaerobic transformations of carbon tetrachloride by soil organic matter. *Environmental Toxicology and Chemistry* **1999**, *18*, (12), 2703-2710.

12.   Kappler, A.; Haderlein, S. B., Natural organic matter as reductant for chlorinated aliphatic pollutants. *Environ. Sci. & Technol.* **2003**, *37*, (12), 2714-2719.

13.   Dunnivant, F. M.; Schwarzenbach, R. P.; Macalady, D. L., Reduction of substituted nitrobenzenes in aqueous solutions containing natural organic matter *Environ. Sci. & Technol.* **1992**, *26*, (11), 2133-2141.

14.   Blodau, C.; Bauer, M.; Regenspurg, S.; Macalady, D., Electron accepting capacity of dissolved organic matter as determined by reaction with metallic zinc. *Chemical Geology* **2009**, *260*, (3-4), 186-195.

15.   Heitmann, T.; Blodau, C., Oxidation and incorporation of hydrogen sulfide by dissolved organic matter. *Chemical Geology* **2006**, *235*, (1-2), 12-20.

16.   Ratasuk, N.; Nanny, M. A., Characterization and quantification of reversible redox sites in humic substances. *Environ. Sci. & Technol.* **2007**, *41*, 7844-7850.

17.   Bauer, M.; Heitmann, T.; Macalady, D. L.; Blodau, C., Electron transfer capacities and reaction kinetics of peat dissolved organic matter. *Environ. Sci. & Technol.* **2007**, *41*, 139-145.

18.   Tratnyek, P. G.; Wolfe, N. L., Characterization of the reducing properties of anaerobic sediment slurries using redox indicators *Environmental Toxicology and Chemistry* **1990**, *9*, (3), 289-295.

19.   Helburn, R. S.; Maccarthy, P., Determination of some redox properties of humic acid by alkaline ferricyanide titration. *Analytica Chimica Acta* **1994**, *295*, (3), 263-272.

20.   Xu, J. S.; Chen, Q. Y.; Swain, G. M., Anthraquinonedisulfonate electrochemistry: A comparison of glassy carbon, hydrogenated glassy carbon, highly oriented pyrolytic graphite, and diamond electrodes. *Analytical Chemistry* **1998**, *70*, (15), 3146-3154.

21. Osterberg, R.; Shirshova, L., Oscillating, nonequilibrium redox properties of humic acids. *Geochimica Et Cosmochimica Acta* **1997**, *61*, (21), 4599-4604.

22. Uchimiya, M.; Stone, A. T., Redox reactions between iron and quinones: Thermodynamic constraints. *Geochimica Et Cosmochimica Acta* **2006**, *70*, (6), 1388-1401.

23. Bourbonnais, R.; Leech, D.; Paice, M. G., Electrochemical analysis of the interactions of laccase mediators with lignin model compounds. *Biochimica Et Biophysica Acta-General Subjects* **1998**, *1379*, (3), 381-390.

24. Watt, G. D., Electrochemical method for measuring redox potentials of low potential proteins by microcoulometry at controlled potentials. *Analytical Biochemistry* **1979**, *99*, (2), 399-407.

25. Fultz, M. L.; Durst, R. A., Mediator compounds for the electrochemical study of biological redox systems - a compilation. *Analytica Chimica Acta* **1982**, *140*, (1), 1-18.

26. Clark, W., *Oxidation-Reduction Potentials of Organic Systems*. Baltimore, 1960.

27. Schwarzenbach, R. P., Gschwend, P.M, Imboden, D. M, *Environmental Organic Chemistry*. 2nd ed.; John Wiley & Sons Hoboken, NJ, 2003.

28. McKnight, D. M. A., E. D.; Spaulding, S. A.; Aiken, G. R., , Aquatic fulvic acids in algal-rich antarctic ponds *Limnology and Oceanography* **1994**, *39*, (8), 1972-1979.

2.5. Supporting information Chapter 2

All potentials E_h are reported versus the standard hydrogen electrode (SHE)

Section 1. Decrease in potential E_h of Leonardite Humic Acid during direct electrochemical reduction (DER) in comparison to the standard reduction potentials (pH 7) $E_h^{0'}$ of electron transfer mediators, selected model quinones, and selected chemical oxidants, and to electrode potentials applied in DER, mediated electrochemical reduction (MER) and oxidation (MEO).
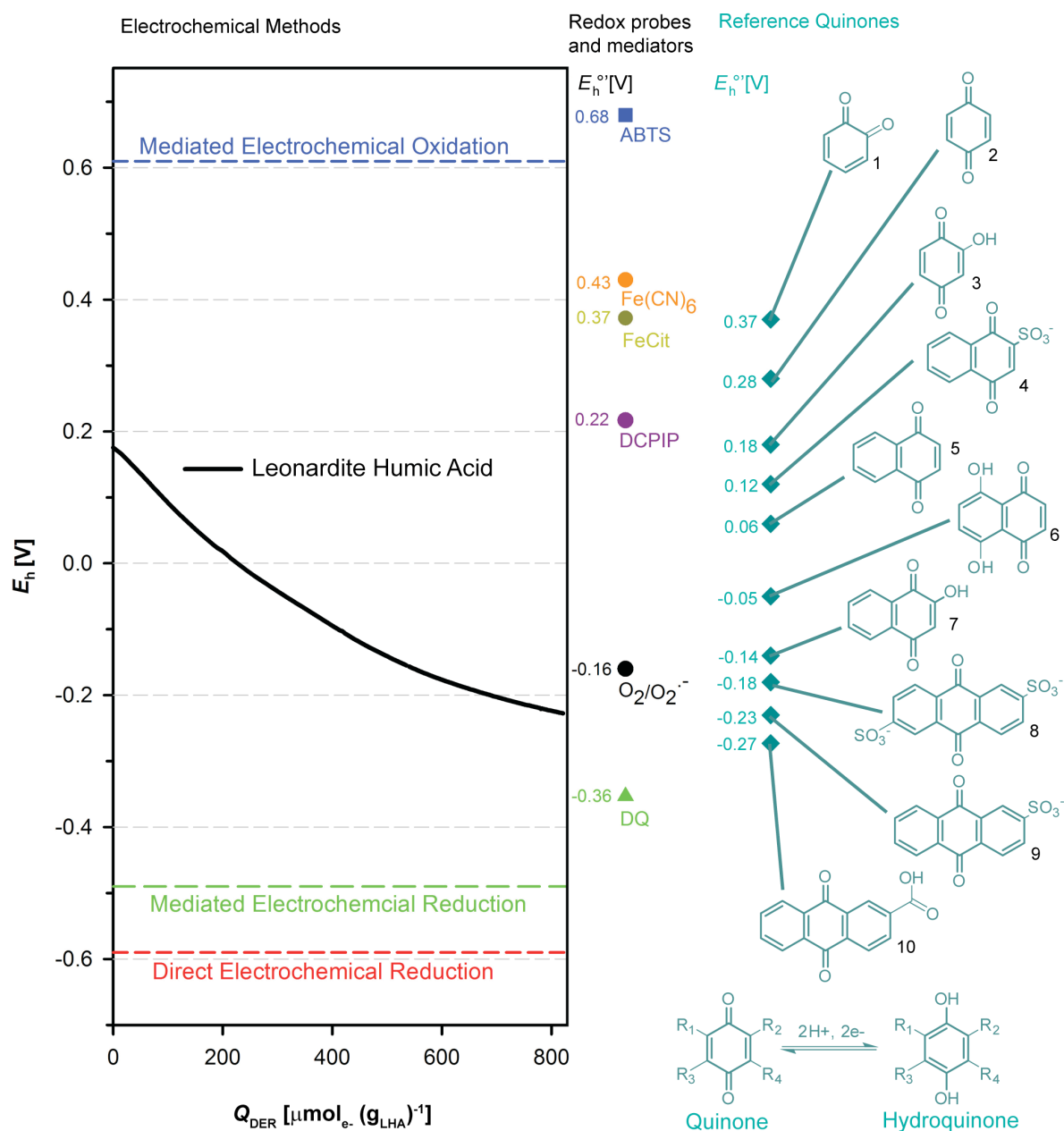
Figure S1. Decrease in solution potential E_h during direct electrochemical reduction (DER) of Leonardite Humic Acid (LHA) at pH 7 as a function of DER-transferred amount of

electrons, Q_{DER} (μmol_{e^-} g_{LHA}^{-1}). Dashed horizontal lines indicate potentials E_h at which DER (red dashed line), mediated electrochemical reduction (MER) using the mediator 1-1'-ethylene-2-2'bipyridyl (diquat, DQ, green dashed line), and mediated electrochemical oxidation (MEO) using the mediator 2,2'azino-bis(3-ethylbenzthiazoline-6-sulfonic acid) (ABTS, blue dashed line) were conducted. The colored symbols to the right of the experimental data represent standard reduction potentials (pH 7) $E_h^{0'}$ of the radical mediators ABTS (blue square) and DQ (green triangle), of the mediator 2,6-dichlorophenol indophenol (DCPIP) (purple circle), molecular oxygen O_2 to superoxide radical anion $O_2\bullet^-$ (black circle), Fe^{3+}-citrate (olive-colored circle) (1), hexacyanoferrate (orange circle) (2), and of several model benzo-, naphtho-, and anthraquinones (cyan diamonds; from top to bottom: 1. 1,2-benzoquinone (3); 2. 1,4-benzoquinone (2); 3. 2-hydroxy-1,4-benzoquinone (4); 4. 1,4-naphthoquinone-2-sulfonate (3); 5. 1,4-naphthoquinone (2); 6. 5,8-dihydroxy-1,4-naphthoquione (2); 7. 2-hydroxy-1,4-naphthoquione (2); 8. 9,10-anthraquinone-2,6-disulfonate (2); 9. 9,10-anthraquinone-2-sulfonate (2); 10. 9,10-anthraquinone-2-carboxylic acid (5)).

Section 2. Direct electrochemical reduction (DER) of Leonardite Humic Acid (LHA) and the model quinone Lawsone at different electrode potentials E_h.
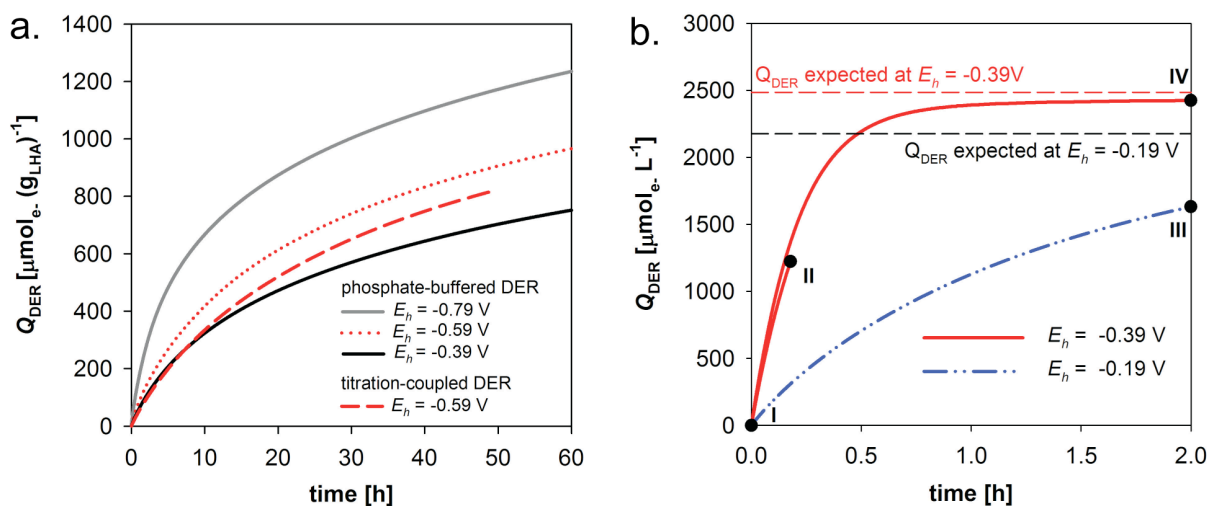
Figure S2. a. Amount of electrons transferred to Leonardite Humic Acid Standard (LHA; 2 g L^{-1}; pH 7) during direct electrochemical reduction (DER), Q_{DER} (μmol_{e-} g_{LHA}^{-1}) at electrode potentials E_h= -0.79 V (grey curve), E_h=-0.59 V (red dotted curve), and E_h=-0.39 V (black curve), using phosphate as buffer to maintain constant pH 7. Similar reduction curves at E_h= -0.59 V were obtained when coupling DER to proton titration to maintain constant pH 7 (red dashed curve). **b.** Amount of electrons transferred to the model quinone lawsone (2-hydroxy-1,4-naphthoquinone) during DER, Q_{DER}, at electrode potentials E_h= -0.39 V (red curve) and E_h= -0.19V (blue curve). Numbers I, II, III, and IV represent Lawsone samples with known Q_{DER} used to validate mediated electrochemical reduction (MER) and oxidation (MEO) (see Table S1). The red and the grey dashed horizontal lines represent expected Q_{DER} (calculated by Nernst equation) upon attainment of reduction equilibrium at E_h= -0.39 V and E_h= -0.19 V, respectively.

Section 3. Facilitation of electron transfer between Leonardite Humic Acid (LHA) and the reticulated vitreous carbon (RVC) working electrode by the radical mediators diquat (DQ) and 2,2'Azino-bis(3-ethylbenzthiazoline-6-sulfonic acid (ABTS).
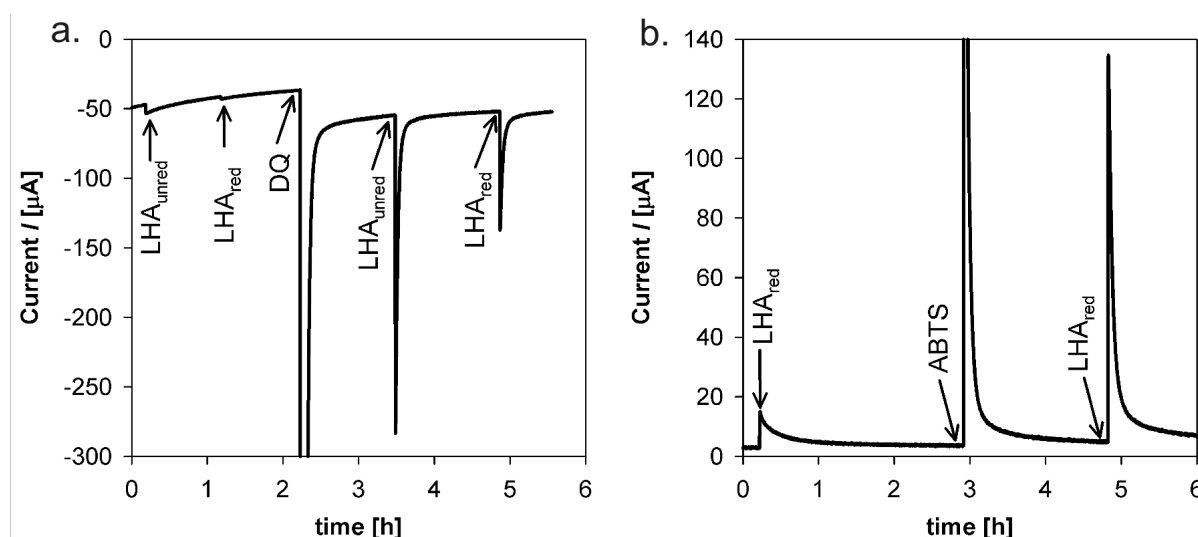
Figure S3. a. Reductive current peaks obtained upon spiking (i) non-treated (i.e., 'unreduced') LHA (LHA$_{unred}$; 100 μL of 2 g$_{LHA}$ L^{-1}; peak #1), (ii) LHA prereduced by direct electrochemical reduction (DER) (LHA$_{red}$; 100 μL of 2 g$_{LHA}$ L^{-1} with 962 μmol$_{e-}$ g$_{LHA}$$^{-1}$ transferred by DER; peak #2), (iii) the mediator diquat (DQ; 2 mL of 5 mmol L^{-1}; peak #3), followed by re-spiking (i) 'unreduced' LHA (peak #4) and (ii) prereduced LHA (peak #5), on RVC electrode pre-polarized to E_h= -0.49 V. Peaks #1 and #2 could not be accurately integrated due to small peak maxima and broad peak shapes. Conversely, in the presence of the mediator DQ, the same LHA spikes resulted in sharp, well defined peaks #4 and #5, which could be accurately integrated. The difference in the areas of current peaks #4 and #5 corresponds to the amount of electrons transferred to LHA$_{red}$ in DER. **b**. Oxidative current peaks obtained upon spiking (i) LHA prereduced by direct electrochemical reduction (DER) (LHA$_{red}$ 100 μL of 2 g$_{LHA}$ L^{-1} with 966 μmol$_{e-}$ g$_{LHA}$$^{-1}$ transferred by DER; peak #1), (ii) the mediator 2,2'azino-bis(3-ethylbenzthiazoline-6-sulfonic acid) (ABTS; 4 mL of 2.3 mmol L^{-1}; peak #2), followed by re-spiking (i) prereduced LHA (peak #3) on RVC electrode pre-polarized to E_h= +0.61 V. Peak #1 could not be accurately integrated due to small peak maximum and broad peak shape. Conversely, in the presence of the mediator ABTS, the same LHA spike resulted in a sharp, well-defined peak #3, which could be accurately integrated.

Section 4. Chemical structures of radical and non-radical organic electron transfer mediators used in mediated electrochemical reduction (MER) and oxidation (MER) of humic substances.

Mediators for Mediated Electrochemical Reduction (MER)
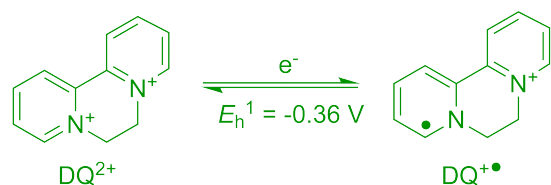
diquat (1,1'-ethylene-2,2'-bipyridyl)
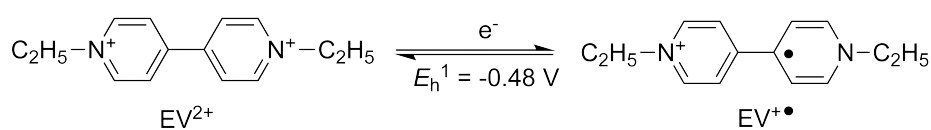
ethyl viologen (1,1'-diethyl-4,4'-bipyridyl)

Mediators for Mediated Electrochemical Oxidation (MEO)
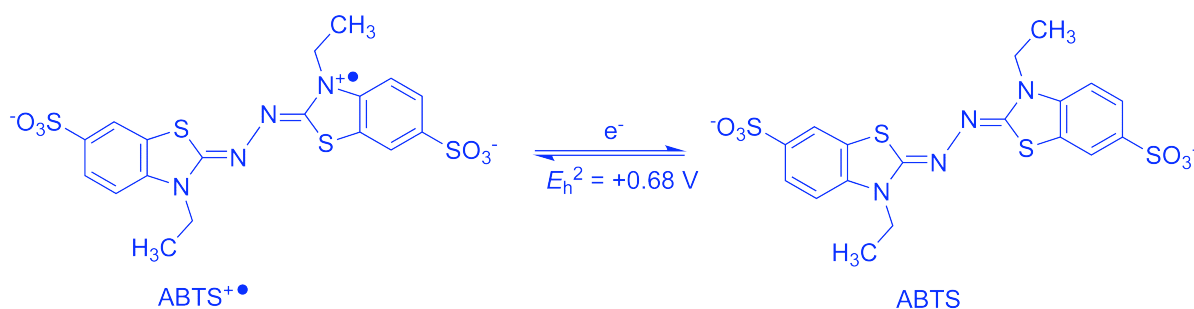
ABTS (2,2'-azino-bis(3-ethylbenzthiazoline-6-sulfonic acid))
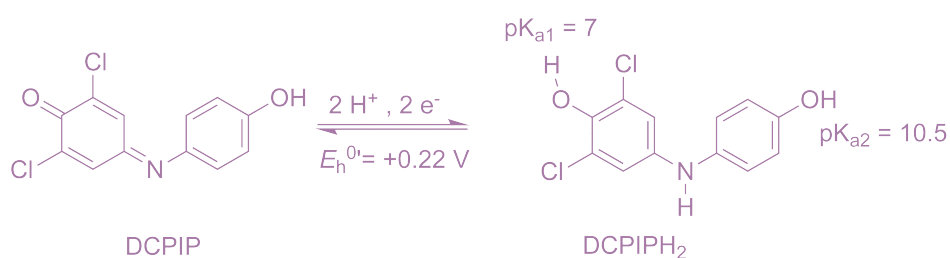
DCPIP (2,6-dichlorophenol indophenol)

Figure S4. Chemical structures and standard reduction potentials E_h^0 of organic radical mediators 1-1'-ethylene-2-2'bipyridyl (diquat, DQ (2)), 1,1'-diethyl-4,4'-bipyridyl (ethylviologen, EV (2)), 2,2'Azino-bis(3-ethylbenzthiazoline-6-sulfonic acid) (ABTS (6)), and standard reduction potentials (pH 7) $E_h^{0'}$ of 2,6-dichlorophenol indophenol (DCPIP (2)). Mediators used for mediated electrochemical reduction (MER) were DQ and EV (no data

shown in the paper) and mediators used for mediated electrochemical oxidation (MEO) were ABTS and DCPIP. One electron reduction and oxidation of $DQ^{2+}/DQ^{\bullet+}$, $EV^{2+}/EV^{\bullet+}$, and $ABTS^{2-}/ABTS^{\bullet-}$ were not coupled to proton uptake and release, whereas two electron reduction and oxidation of $DCPIP/DCPIPH_2$ at pH 7 was coupled to uptake and release of 2 protons (i.e., pK_{a1} of $DCPIPH_2 = 7.0$ and $pK_{a2} = 10.5$ (7)).

Section 5. Recovery of electrons transferred to Leonardite Humic Acid (LHA) in mediated electrochemical reduction (MER) and oxidation (MEO).
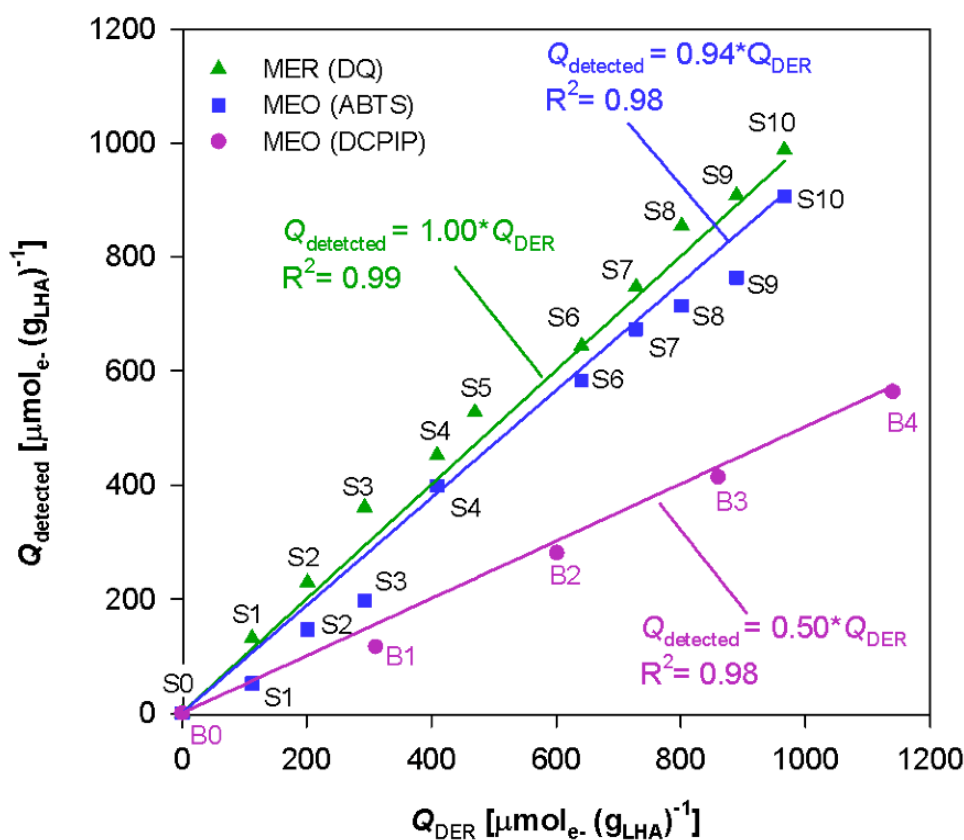
Figure S5. Regression analysis of charge equivalents $Q_{detected}$ (μmol_{e-} g_{LHA}^{-1}) on Leonardite Humic Acid samples S0 to S10 and samples B0 to B4 detected by mediated electrochemical reduction (MER; mediator 1-1'-ethylene-2-2'bipyridyl (diquat, DQ) (samples S0 to S10; green line), and by mediated electrochemical oxidation (MEO; mediators 2,2'azino-bis(3-ethylbenzthiazoline-6-sulfonic acid) (ABTS) (samples S0 to S10; blue line) and 2,6-dichlorophenol indophenol (DCPIP) (samples B0 to B4; purple line)) versus the known amount of electrons transferred to LHA in samples S0 to S10 and B0 to B4 by direct electrochemical reduction (DER). MER and MEO were conducted at electrode potentials E_h= -0.49 V and E_h = +0.61 V, respectively. $Q_{detected}$ for sample SX in MER corresponds to the difference in the amount of electrons transferred to sample S0 (i.e., LHA not prereduced by DER), Q_{MER}(S0), and to sample SX, Q_{MER}(SX) in MER. $Q_{detected}$ for samples SX and BX in MEO corresponds to the difference in the amount of electrons withdrawn from sample SX (i.e., LHA prereduced by DER), Q_{MEO}(SX), and from sample S0 (i.e., LHA not prereduced by DER), Q_{MEO}(S0) in MEO. Regression analysis yielded slopes of 1.00 (± 0.03) for MER (R^2= 1.00), 0.94 (± 0.04) (R^2= 0.98) for MEO with ABTS as mediator, and 0.50 (±0.03) (R^2=

0.98) for MEO with DCPIP as mediator, corresponding to recoveries of DER transferred electrons of 100%, 94%, and 50%, respectively.

Section S6. Linear correlation of electron accepting capacities (EACs) determined by mediated electrochemical reduction (MER) of humic substances with their aromaticities.
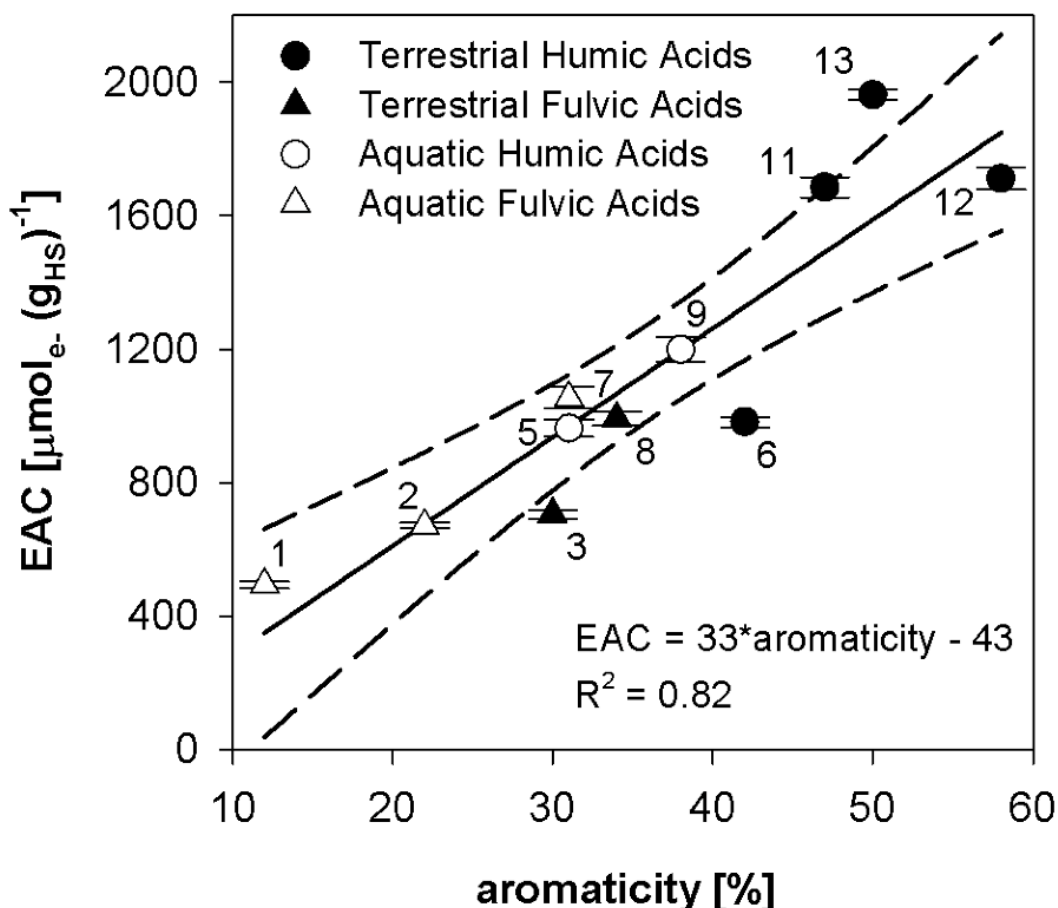
Figure S6. Linear correlation of electron accepting capacities (EACs) (μmol_{e^-} g_{HS}^{-1}) with the aromaticities (%) of tested humic substances. The EACs were determined by mediated electrochemical reduction (MER) at E_h= -0.49 V using diquat as mediator. Aromaticities determined by ^{13}C-Nuclear magnetic resonance are provided by the International Humic Substances Society (IHSS; http://ihss.gatech.edu/ihss2/). The solid line represents the linear fit and dashed lines correspond to the 95% confidence intervals of the fitted line. The humic substances are: #1: Pony Lake Fulvic Acid Reference; #2 Suwannee River Fulvic Acid Standard; #3: Elliott Soil Fulvic Acid Standard; #4: Aldrich Humic Acid; #5 Suwannee River Humic Acid Standard; #6: Waskish Peat Humic Acid Reference; #7: Nordic Lake Fulvic Acid Reference; #8: Pahokee Peat Fulvic Acid Standard; #9: Nordic Lake Humic Acid

Reference; #10: Pahokee Peat Humic Acid Reference; #11: Pahokee Peat Humic Acid Standard; #12: Leonardite Humic Acid Standard; #13: Elliot Soil Humic Acid Standard.

Section S7. Spectrophotometric assay to determine the redox states of HS samples based on the reductive decolorization of the redox-dye dichlorophenol-indophenol (DCPIP).

The spectrophotometric assay involves the following steps:

(i) Aliquots of 20 μL, 40 μL and 80 μL of the reduced HS sample are spiked into plastic cuvettes (Brand GMBH, Wertheim, Germany) containing 2 mL of an anoxic 50 μM solution of oxidized DCPIP (buffered at pH 7). Cuvettes are capped, thoroughly mixed and transferred to the spectrophotometer outside the glovebox. Reduction of DCPIP by reduced HS is followed by measuring the decrease in absorption of DCPIP from λ=400 to 800 nm (λ $_{max}$ at 603 nm).

Figure **S7a** shows the decrease in absorbance of DCPIP with increasing amounts of added LHA to which 999 μmol$_{e-}$ $(g_{LHA})^{-1}$ had been transferred by direct electrochemical reduction. The spectra were taken after 15 min of reaction.

(ii) Aliquots of 0 μL, 40 μL, 80 μL and 150 μL of the non-treated (i.e., not prereduced by DER) HS sample are spiked into plastic cuvettes (Brand GMBH, Wertheim, Germany) containing two mL of an anoxic 50 μM solution of oxidized DCPIP (in buffer pH 7). Cuvettes are capped, thoroughly mixed and transferred to the spectrophotometer outside the glovebox. Reduction of DCPIP by reduced HS is followed by measuring the decrease in absorption of DCPIP from λ=400 to 800 nm (λ $_{max}$ at 603 nm).

Figure **S7b** shows the decrease in absorbance of DCPIP with increasing amount of added LHA that had not been prereduced in DER. The spectra were taken after 15 min of reaction.

(iii) The same volumes of reduced HS (20 μL, 40 μL and 80 μL) and non-treated (i.e., not prereduced) HS (40 μL, 80 μL and 150 μL) are spiked into reference cuvettes containing 2 mL of buffer. Absorbance measurements in (i) and (ii) are corrected for the absorbance of HS at 603 nm.

(iv) The amounts of electrons transferred from HS to DCPIP in both (i) and (ii) are calculated (using a linear, four point DCPIP calibration curve collected at λ_{max}= 603 nm) from the decrease in DCPIP absorbance and plotted versus the added masses of reduced and non-treated (i.e., not prereduced) HS. The slope of

the linear regression lines corresponds to the amount of electrons that can be withdrawn by DCPIP per mass of HS.

As an example, Figure **S7c** shows the linear correlations of detected amounts of electrons on reduced and non-treated (i.e., not prereduced) LHA (R^2= 1.00 and 0.99, respectively). The reduced LHA was obtained by DER in which 999 μmol_{e-} $(g_{LHA})^{-1}$ had been transferred. The assay detected 612 and 42 μmol_{e-} $(g_{LHA})^{-1}$ on the reduced and non-treated LHA, respectively. This corresponds to a recovery of DER-transferred electrons of 57% [i.e., (612 μmol_{e-} $(g_{LHA})^{-1}$ - 42 μmol_{e-} $(g_{LHA})^{-1}$) / (999μmol_{e-} $(g_{LHA})^{-1}$)*100].
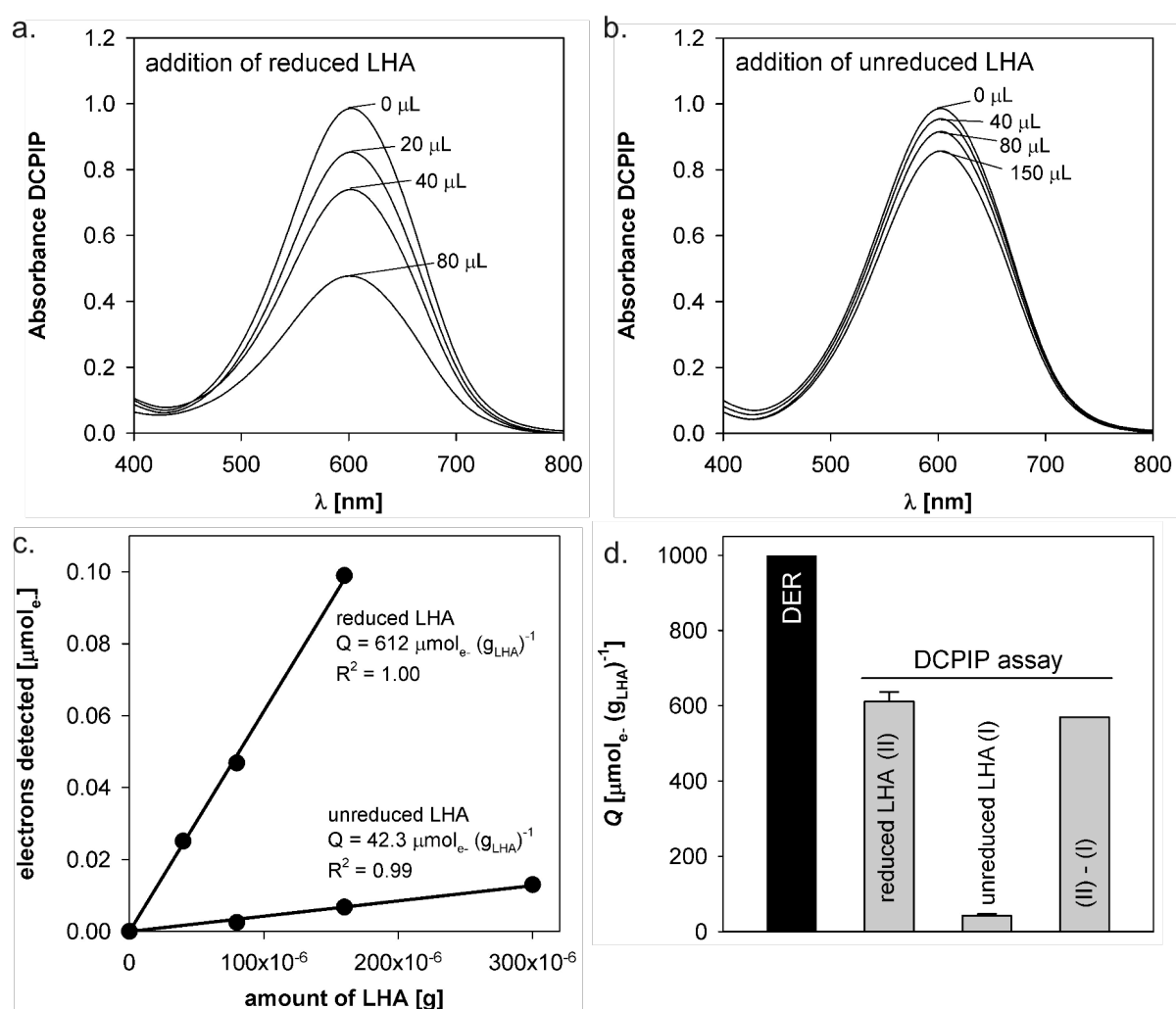
Figure S7. Quantification of the redox states of prereduced (by direct electrochemical reduction (DER)) and non-treated (i.e., not prereduced by DER) Leonardite Humic Acid (LHA) samples by spectrophotometric analysis of the reduction of the dye 2,6-dichlorophenol indophenol (DCPIP). **a, b.** Decrease in absorbance of DCPIP (wavelengths measured from

λ= 400 to 800 nm with λ_{max} at 603 nm) upon addition of small volumes of prereduced (panel a) and non-treated (panel b) LHA (concentration: 0.5 g_{LHA} L^{-1}), respectively. The reaction time was 15 minutes. **c**. Linear correlation of the amount of electrons withdrawn from LHA by DCPIP versus the added amount of prereduced (top) and non-treated (bottom) LHA. The slopes of the regression lines correspond the amount of electrons detected per mass of added LHA. **d.** Comparison of charge transferred to LHA during direct electrochemical reduction (DER), Q_{DER}= 999 μmol_{e^-} g_{LHA}^{-1}, and the amount of electrons withdrawn from DER prereduced LHA (612 μmol_{e^-} g_{LHA}^{-1}) and non-treated LHA (42 μmol_{e^-} g_{LHA}^{-1}) by DCPIP. The recovery was 57%, which is in good agreement with the recovery obtained for mediated electrochemical oxidation (MEO) using DCPIP as mediator (see Figure **S5**).

Section S8. Free energy of the one electron transfer from 1,4-benzohydroquinone to molecular oxygen.

(I) $\quad O_2 + e^- \rightleftharpoons O_2^{\bullet -} \qquad\qquad E_h^1 = -0.16$ V (pH 7)[a]

superoxide

(II)

$+ e^- + 2H^+ \rightleftharpoons$

$E_h^{1'} = -0.509$ V (pH 7)[b]

1,4 - benzosemiquinone
(SQ)

1,4 - benzohydroquinone
(H$_2$Q)

(I) - (II)

$+ O_2 \rightleftharpoons$

$+ O_2^{\bullet -} + 2H^+$

$\Delta E_h^{1'} = -0.669$ V

$\Delta G^{1'} = -1 * F * \Delta E_h^{1'}$

$= +64.5$ kJ mol^{-1}

Figure S8. Calculation of the standard free energy for the one electron transfer from 1,4-benzohydroquinone to molecular oxygen O$_2$ at pH 7, $\Delta G^{1'}$. Reaction (I): one electron reduction of O$_2$ to form superoxide; (II): one electron reduction of 1,4-benzo-semiquinone (SQ) to form 1,4-benzohydroquinone (H$_2$Q). (III) One electron reduction of O$_2$ by H$_2$Q to form superoxide and SQ. [a, b] One electron reduction potentials, $E_h^{1'}$ (pH 7) from (8) and (9), respectively.

Table S1. Control experiments using the model quinones Lawsone and anthraquinone 2,6-disulfonate to evaluate the accuracy of mediated electrochemical reduction (MER) and oxidation (MEO) for electron balancing. Q_{MAX} ($\mu mol_{e^-}\ L^{-1}$) is the maximum possible amount of electrons for complete reduction of the model quinones. Q_{DER}, Q_{MER}, and Q_{MEO} (all $\mu mol_{e^-}\ L^{-1}$) are the amounts of electrons transferred in direct electrochemical reduction (DER), MEO and MER, respectively. Q ($\mu mol_{e^-}\ L^{-1}$) is the amount of electrons detected by MER and MEO.

Direct electrochemical reduction (DER)				Mediated electrochemical reduction (MER; mediator: diquat; E_h=-0.49V)			Mediated electrochemical oxidation (MEO, mediator: ABTS; E_h=+0.71V)			Mediated electrochemical oxidation (MEO; mediator: DCPIP; E_h=+0.61V)		
DER conditions	aqueous concentration -(μmol L⁻¹)-	Q_{MAX} -(μmol_e- L⁻¹)-	Q_{DER} -(μmol_e- L⁻¹)-	Q_{MER} ---- (μmol_e- L⁻¹) ----	Q	recovery Q/Q_{DER} -- (%) --	Q_{MEO} ---- (μmol_e- L⁻¹) ----	Q	recovery Q/Q_{DER} -- (%) --	Q_{MEO} ---- (μmol_e- L⁻¹) ----	Q	recovery Q/Q_{DER} -- (%) --
Lawsone												
(I)[a] E_h= -0.39 V; 2h	1243	2485	2425	61	2403 (=2464-61)	**99**	3517	2223 (=3517-1294)	**92**	2231	2231	**92**
(II)[a] E_h= -0.39V; 11min	1243	2485	1224	1151	1313 (=2464-1151)	**107**	2500	1206 (=2500-1294)	**99**	1159	1159	**95**
(III)[a] E_h= -0.19 V; 2h	1243	2485	1632	796	1668 (=2464-796)	**102**	2856	1562 (=2856-1294)	**96**	1523	1523	**93**
(IV)[a] Non reduced	1243	2485	0	2464	0	-	1294	0	-	0	0	-
anthraquinone 2,6-disulfonate (AQDS)												
~100% reduced	1249	2499	2406	54	2392 (=2446-54)	**99**						
~50% reduced	1249	2499	1226	1182	1264 (=2446-1182)	**103**						
0% reduced	1249	2499	0	2446	0	-						
wheat starch												
nontreated	-	-	-	0	-	-						

a. Numbers I to IV refer to data points I to IV in Figure **S2b** in the Supporting Information.

Table S2. Electron accepting capacities (EACs) and elemental compositions of the tested humic and fulvic acids determined by mediated electrochemical reduction (MER)[a].

	order number	EAC (x) μmol_{e^-} g_{HS}^{-1}	**Elemental composition and chemical characteristics**									non-carboxylic & non phenolic O (y)	(x)/(y)
			C	H	O	N	S	C/H ratio[d]	aromaticity	carboxylic O	phenolic O		%
			------------- mmol g_{HS}^{-1} [d] -------------						% of C	------------- mmol g_{HS}^{-1} -------------			
IHSS Standard HA[b]													
Suwannee River II	2S101H	962 ± 26	43.8	42.4	26.3	0.835	0.168	1.03	31	4.81	1.96	14.7	6
Elliott Soil	1S102H	1962 ± 15	48.4	36.4	21.3	2.955	0.137	1.33	50	4.81	1.09	10.6	19
Pahokee Peat	1S103H	1684 ± 30	46.9	37.8	23.3	2.634	0.221	1.24	47	5.08	1.08	12.1	14
Leonardite	1S104H	1711 ± 33	53.1	36.6	19.5	0.878	0.237	1.45	58	4.76	1.47	8.5	20
IHSS Standard FA[b]													
Suwannee River II	2S101F	671 ± 8	43.6	43.2	26.9	0.478	0.143	1.01	22	5.85	1.49	13.7	5
Elliott Soil III	3S102F	704 ± 15	41.5	42.3	27.7	2.320	0.384	0.98	30	6.64*	1.14*	12.2*	6
Pahokee Peat II	2S103F	992 ± 21	42.7	35.0	27.1	1.670	0.237	1.22	34	6.73*	1.17*	13.8*	7
IHSS Reference HA[b]													
Pahokee Peat	1R103H	1616 ± 63	47.3	35.6	22.9	2.670	0.218	1.33	n.a.	5.04	1.17	11.6	14
Nordic Lake	1R105H	1197 ± 37	44.4	39.3	26.9	0.828	0.181	1.13	38	4.83	1.72	15.5	8
Waskish Peat	1R107H	981 ± 15	45.6	40.0	24.1	1.049	0.112	1.14	42	n.a	n.a	n.a	
IHSS Reference FA[b]													
Nordic Lake	1R105F	1053 ± 33	43.6	39.4	28.2	0.485	0.143	1.11	31	5.84	1.66	14.9	7
Pony Lake	1R109F	493 ± 10	43.7	53.4	19.6	4.647	0.945	0.82	12	n.a	n.a	n.a	
Other HA													
Aldrich	H16752	923 ± 60	46.0	44.4	23.5	0.228	0.727	1.04	n.a.	n.a	n.a	n.a	

[a] Experimental setup as described in the manuscript at electrode potential E_h= -0.49 V using diquat as mediator. [b] from IHSS= International Humic Substances Society. [c] Average ± standard deviation (triplicate measurements). [d] from IHSS (http://ihss.gatech.edu/ihss2/)

References

1.   Straub, K. L.; Benz, M.; Schink, B., Iron metabolism in anoxic environments at near neutral pH. *Fems Microbiology Ecology* **2001**, *34*, (3), 181-186.

2.   Fultz, M. L.; Durst, R. A., Mediator compounds for the electrochemical study of biological redox systems - a compilation. *Analytica Chimica Acta* **1982**, *140*, (1), 1-18.

3.   Clark, W., *Reduction Potentials of Organic Systems*. The Williams & Wilkins Company: Baltimore, 1960.

4.   Bailey, S. I.; Ritchie, I. M., A cyclic voltammetric study of the aqueous electrochemistry of some quinones *Electrochimica Acta* **1985**, *30*, (1), 3-12.

5.   Mogharrab, N.; Ghourchian, H., Anthraquinone 2-carboxylic acid as an electron shuttling mediator and attached electron relay for horseradish peroxidase. *Electrochemistry Communications* **2005**, *7*, (5), 466-471.

6.   Bourbonnais, R.; Leech, D.; Paice, M. G., Electrochemical analysis of the interactions of laccase mediators with lignin model compounds. *Biochimica Et Biophysica Acta-General Subjects* **1998**, *1379*, (3), 381-390.

7.   Tratnyek, P. G.; Wolfe, N. L., Characterization of the reducing properties of anaerobic sediment slurries using redox indicators *Environmental Toxicology and Chemistry* **1990**, *9*, (3), 289-295.

8.   Schwarzenbach, R. P., Gschwend, P.M, Imboden, D. M, *Environmental Organic Chemistry*. 2nd ed.; John Wiley & Sons Hoboken, NJ, 2003.

9.   Uchimiya, M.; Stone, A. T., Redox reactions between iron and quinones: Thermodynamic constraints. *Geochimica Et Cosmochimica Acta* **2006**, *70*, (6), 1388-1401.

Chapter 3

Electrochemical analysis of proton and electron transfer equilibria of the reducible moieties in humic acids

Abstract

Humic substances play a key role in biogeochemical and pollutant redox reactions. The objective of this work was to characterize the proton and electron transfer equilibria of the reducible moieties in different humic acids (HA). Cyclic voltammetry experiments demonstrated electron transfer mediation between electrodes and HA by diquat or ethylviologen present at low concentrations. These compounds were used to facilitate attainment of redox equilibria between redox electrodes and HA in potentiometric E_h measurements. Bulk electrolysis of HA combined with pH-stat acid titration demonstrated that electron transfer to the reducible moieties in HA also resulted in proton uptake, suggesting decreasing reduction potentials E_h of HA with increasing pH. This was confirmed by potentiometric E_h-pH titrations of HA at different redox states. E_h measurements of HA samples pre-reduced to different redox states by bulk electrolysis revealed reducible moieties in HA that cover a wide range of apparent standard reduction potentials at pH 7 from $E_h^{0*} = +0.15$ to -0.3 V. Modeling revealed an overall increase in the relative abundance of reducible moieties with decreasing E_h. The wide range of HA is consistent with its involvement in numerous environmental electron transfer reactions under various redox conditions.

3.1. Introduction

Humic substances (HS) play a key role in many biogeochemical redox reactions with natural and anthropogenic chemicals (1-7). As a consequence, the redox properties of HS have received considerable interest. Previous work suggested quinones as major reducible moieties in HS. Experimental evidence supportive of quinones includes largely reversible electron transfer to HS (8-10), increases in organic radical contents upon HS reduction (presumably due to semiquinone formation) (2, 11), comparable features in cyclic voltammograms of HS and model quinones in non-aqueous solvents (12), and positive correlations of HS electron-accepting capacities (EAC) with HS aromaticity (2, 8, 9). HS and model quinones also showed similar reactivities as electron transfer mediators in the reductive transformation of organic pollutants (6, 13).

The distribution of standard reduction potentials, E_h^0, and the protonation equilibria of reducible moieties in HS remain, however, poorly characterized, although they are of key importance for assessing the role of HS in environmental redox reactions. First, the E_h distribution determines the thermodynamics of electron transfer reactions involving HS (14) as well as the extent of redox buffering by HS at a given reduction potential. Second, the protonation equilibria of reducible moieties define the extent to which E_h is pH dependent. Furthermore protonation equilibra provide insight into the chemical nature of the redox-active moieties. For instance, quinone moieties exist in three oxidation states, the quinone (Q), semiquinone (QH•), and hydroquinone (QH$_2$), which interconvert via reversible single electron transfer reactions coupled to pH-dependent proton transfers (15-17) (see section **S1**, Supporting Information (SI)). Third, the transfer of unequal numbers of protons and electrons to HS alters its charge. This, in turn, may affect other environmentally relevant processes such as pH buffering and metal binding by HS (18).

Previous information on protonation equilibria of the reducible moieties in HS was primarily derived from the effect of pH on HS reduction potentials (19, 20). The E_h-pH dependencies suggested coupled proton and electron transfers with molar ratios between 0.75 and 1.1. However, the E_h-pH dependencies were only determined for unreduced HA and only at pH≤ 6. Furthermore, accurate E_h measurements were hindered by the lack of redox equilibria between redox electrodes and the redox active moieties in the HS

(19). More systematic studies on the E_h-pH dependencies need to investigate wider pH ranges, include HA at different redox states, and find means to facilitate attainment of redox equilibria in E_h measurements.

In a recent publication we demonstrated that analytical electrochemistry, namely mediated and direct electrochemical reduction (MER and DER), can be used to study HS redox properties. MER allowed for accurate and direct quantification of electron accepting capacities and redox states of HS (8). This was achieved by spiking small amounts of HS into an electrochemical cell containing high concentrations of pre-reduced redox mediator. Added HS oxidized the mediator, which was readily re-reduced at the working electrode, resulting in a current peak. Integration of this peak yielded the moles of electrons transferred per added mass of HS. Diquat and ethylviologen, both radicals in their reduced form, were used as mediators. Compared to mediators with coupled proton and electron transfers, these radicals are advantageous in that pH does not affect their speciation and, hence, E_h at a given extent of reduction. DER of HS at carbon working electrodes in bulk electrolysis cells was used to generate bulk amounts of HS with defined reduction states. When coupled to automated acid titration, bulk electrolysis allowed quantifying the moles of both electrons, n_{e^-} (mol$_{e^-}$ g$_{HA}^{-1}$), and protons, n_{H+} (mol$_{H+}$ g$_{HA}^{-1}$) transferred to a given mass of HA during the reduction. Using this approach, molar ratios of protons to electrons $n_{H+}(n_{e^-})^{-1}$ close to unity were reported for two humic acids at pH 7 (8, 18).

The objective of this work was a systematic characterization of the proton and electron transfer equilibria of the reducible moieties in selected terrestrial and mixed aquatic-terrestrial humic acids (HA). To this end, we further advanced the analytical electrochemistry of HA. First, we used cyclic voltammetry to test whether small concentrations of diquat and ethylviologen facilitated electron transfer between working electrodes and HA. We further assessed whether these compounds mediated the attainment of redox equilibria in potentiometric E_h measurements of HA. Such E_h measurements of HA require low mediator concentrations to ensure that the redox active moieties in the HA and not the mediator dominate the measured E_h. While the concept of redox mediation is not new (21-23), this is the first time it is used to determine the E_h characteristics of HA. Second, we used bulk electrolysis coupled to automated acid titration to determine $n_{H+}(n_{e^-})^{-1}$ during the reduction of HA over

a wide pH range and to prepare HA at different redox states for subsequent potentiometric E_h-pH titrations. Complementary experiments were conducted for selected model quinones. These experiments provide information on the protonation equilibria of reducible moieties in the HA and on the pH dependencies of E_h. Third, we conducted potentiometric E_h measurements in HA samples pre-reduced at pH 7 and 9 to different redox states by bulk electrolysis. The dependence of E_h on HA redox state was modeled to derive the distribution of apparent standard reduction potentials, E_h^0*, of the reducible moieties in the HA. The term 'apparent' standard reduction potentials reflects that the activities of the oxidized and reduced species in the HA were unknown.

3.2. Materials and Methods

Chemicals. 1,1'-Ethylene-2,2'-bipyridyldiylium dibromide monohydrate (= diquat, DQ; 99.5%) was from Supelco. Sodium hydroxide (puriss. p.a.), hydrochloric acid (puriss. p.a.), potassium chloride (KCl, puriss. p.a.), boric acid (puriss. p.a.), and 2,6-dichlorophenol indophenol sodium salt hydrate (DCPIP; >97%) were purchased from Fluka. 1,1′-Diethyl-4,4′-bipyridinium dibromide (= ethylviologen, EV; >99%), disodium hydrogen phosphate dihydrate (p.a.), 9,10-anthraquinone-2,6-disulfonic acid disodium salt (AQ26DS, >98%), 2-hydroxy-1,4-naphthoquinone (NQOH, >97%), 9,10-anthraquinone-1,5-disulfonic acid (AQ15DS, 95%), 1,2-naphthoquinone-4-sulfonic acid (NQSA, 97%) were from Sigma-Aldrich. Titration experiments were conducted with 0.5 mol L^{-1} hydrochloric acid and 0.5 mol L^{-1} sodium hydroxide solutions prepared from Titrisol® ampoules (Merck, Darmstadt, Germany). All aqueous solutions were prepared with nanopure water (Barnstead NANOpure Water System). 1,1'-Bis(cyanomethyl)-4,4'-bipyridinium dibromide (= cyaonoviologen, CyV) was synthesized and purified according to (24). The identity of CyV was confirmed by ^{13}C-NMR, ^{1}H-NMR, and high-resolution mass spectrometry (data not shown).

Humic acid (HA) standards of Suwannee River (Nr. II, SRHA), Elliott Soil (ESHA), and Leonardite (LHA) and the HA reference of Pahokee Peat (PPHA) were purchased from the International Humic Substances Society (IHSS, St. Paul, MN, USA) and were used as received. The concentrations of Fe, Mn, and Cu in the HA were determined by ICP-OES (Varian Vista-MPX)

(Table **S1**, SI). The metal concentrations in all three HA were much smaller than the respective electron accepting capacities of the HA reported in (8), demonstrating that electrons were predominantly transferred to organic moieties in the HA during reductions.

Experimental setup. All experiments sensitive to oxygen were conducted in an anoxic glovebox (N_2 atmosphere at 25±1 °C, O_2 < 0.1 ppm). Water, KCl solutions, buffer solutions, and diluted acids and bases were made anoxic by purging with argon for two hours at 150°C and for one hour at room temperature prior to transfer to the glovebox. All other solutions were prepared directly in the glovebox by dissolving the respective chemicals or HAs in anoxic water or buffer. Solutions used in electrochemical experiments contained 0.1 M KCl as background electrolyte. Electrochemical experiments were conducted either with an Autolab PG 302 (EcoChemie B.V., Netherlands) or a CHInstruments 630C (Austin, TX) electrochemical analyzer. Potentials were measured vs. Ag/AgCl but are reported vs. SHE. The reduction states of HAs or model quinones are reported as the moles of electrons, n_{e^-}, transferred to a unit mass of HA [$mmol_{e^-}(g_{HA})^{-1}$] or model quinone [$mmol_{e^-}(g_{quinone})^{-1}$]. The pH adjusted, apparent standard reduction potentials for the HA and the standard reduction potentials for the quinones are denoted as $E_h^0*(pH)$ and E_h^0 (pH), respectively.

Bulk electrolysis of HA and model quinones was carried out by DER as described in (8). In brief, bulk electrolysis was conducted in an ~0.1 L electrochemical cell containing a glassy carbon working electrode (Sigradur G®, HTW, Tierhaupten, Germany), a coiled platinum wire auxiliary electrode, which was placed in an anode compartment separated from the cathodic compartment by a porous frit, and an Ag/AgCl reference electrode (both from Bioanalytical Systems Inc., West Lafayette, IN, USA). The anode compartment was constantly flushed with background electrolyte solution (0.1 M KCl) to remove O_2 and H^+ formed by water oxidation at the Pt counter electrode. Reductions were carried out at applied potentials of E_h= -0.59 V for > 48 h for HA and of E_h= -0.14 to -0.69 V for 2 to 4 hours for the quinones and diquat. The moles of electrons transferred during the reduction were determined by chronocoulometry. The pH of HA and quinone solutions was kept constant

during electrolysis either by the use of pH buffers (i.e., phosphate and borate at pH 7 and 9) or by automated acid titration (see below).

The pH dependence of $n_{H+}(n_{e-})^{-1}$ during HA and quinone reduction was determined by bulk electrolysis coupled to automated acid titration. HA or quinone solutions were circulated from the electrolysis cell through a flow through system containing a pH electrode connected to a titration unit (Titrino 751 GPD, Metrohm) operated in pH-stat mode. In reductions that consumed protons, a constant pH was maintained by addition of known volumes of 0.01 M HCl (prepared from a 0.5 M Titrisol ® solution) to the solutions in the bulk electrolysis cell. This setup allows quantifying the moles of both electrons, n_{e-} (mmol$_{e-}$ g$_{HA}^{-1}$ or mmol$_{e-}$ g$_{quinone}^{-1}$), and protons, n_{H+} (mmol$_{H+}$ g$_{HA}^{-1}$ or mmol$_{H+}$ g$_{quinone}^{-1}$), transferred to a unit mass of HA and quinone during electrolysis. $n_{H+}(n_{e-})^{-1}$ were determined for LHA, PPHA, ESHA at pH 6 to 10.5, for the model quinones AQ26DS, AQ15DS, NQOH and NQSA at pH 3.5 to 11, and for diquat at pH 7 and 9.

Cyclic voltammetry experiments were conducted in 4-5 mL solutions using a 3 mm diameter glassy carbon disk working electrode (WE), a platinum wire counter electrode (both Radiometer Analytical SAS, France), and an Ag/AgCl reference electrode (Bioanalytical Systems Inc., USA). The WE was polished and cleaned before each series of scans, as described in section **S2**, SI. Cyclic voltammograms (CVs) were collected for solutions (i) containing neither mediator nor LHA (background), (ii) containing unreduced LHA at various concentrations (0.25 – 5 g$_{LHA}$L^{-1}), (iii) containing either DQ, EV, or CyV (*C*= 30 µM) but no LHA, and (iv) containing unreduced LHA and either DQ, EV, or CyV (*C*= 30 µM). In addition we tested how HA pre-reduction and solution pH affected electron transfer mediation by DQ to HA: we recorded CVs of LHA solutions (2 gL^{-1}) that were pre-reduced by bulk electrolysis to different n_{e-}, and of unreduced LHA solutions (2 gL^{-1}) titrated from pH 6.3 to 11.7 and from pH 11.7 to 5.7, respectively.

Reoxidation of LHA. We further assessed whether the electrochemically-reduced moieties in HA could be re-oxidized by O_2. To this end, we collected CVs of unreduced LHA, of LHA pre-reduced by bulk electrolysis, and of pre-reduced LHA after O_2 re-oxidation. Re-oxidation was achieved by transferring 10-12 mL of reduced HA into 20 mL gas tight serum flasks, which were then purged with synthetic air for 15 min. The flasks were agitated for ~5 days and

then purged with argon (> 1h) to remove unreacted O_2. Prior to CV measurements, the reduction states of unreduced, reduced, and re-oxidized LHA were quantified by MER according to (8). We further assessed re-oxidation of LHA by running CV of LHA (C_{LHA}= 2 gL^{-1}) experiments in the presence of both DQ (C_{DQ}= 30 μM) and DCPIP (C_{DCPIP}= 16 μM). Further details on the CV measurements are provided in section **S3**, SI.

Potentiometric E_h-pH titrations were conducted for HA and selected quinones pre-reduced to different extents by bulk electrolysis (i.e., n_{e-}= 0, 0.54, and 1.15 mmol$_{e-}$(g$_{LHA}$)$^{-1}$ for LHA; n_{e-}= 0 and 0.38 mmol$_{e-}$(g$_{SRHA}$)$^{-1}$ for SRHA; n_{e-}= 0 and 0.6 mmol$_{e-}$(g$_{PPHA}$)$^{-1}$ for PPHA; and n_{e-}= 0 mmol$_{e-}$(g$_{ESHA}$)$^{-1}$ for ESHA, all n_{e-} were quantified by MER (8); and for AQ26DS, NQOH, NQSA, and DQ brought to 50% reduction by bulk electrolysis). For the E_h-pH titrations, 30 to 40 mL of HA (0.4 -2 gL^{-1}) or quinone (~ 1 mM) were transferred into a 0.1 L glass vessel covered by Parafilm® (Pechiney Plastic Packaging, USA), followed by acid and base titrations (2.5-10 mM HCl and 2.5-20 mM NaOH, all containing 0.1 M KCl) using an automated titrator (751 GPD Titrino, Metrohm, Switzerland). The E_h was monitored using a Metrohm Pt-ring redox electrode connected to a Metrohm 827 pH lab instrument.

E_h^{0*} *distribution of reducible moieties in HA*. The E_h-n_{e-} dependencies were determined for LHA at pH 7 and 9, and for ESHA, SRHA, and AQ26DS at pH 7. The reductions were carried out by bulk electrolysis (applied E_h= -0.59 V) in the presence of 0.1 M phosphate (pH 7) or borate (pH 9) that served as pH buffers and in the presence of DQ and EV at low concentrations (i.e., <2% of the EAC of the HA in the electrochemical cell). During the reduction, aliquots were withdrawn from the bulk electrolysis cell and stored for >12 hours to allow for intra-HA redox equilibration. MER and potentiometry with a Pt ring redox electrode were used to quantify n_{e-} and the E_h of each sample, respectively. For ESHA, E_h of the aliquots were also measured with a combined Au ring electrode (Metrohm, Zofingen, Switzerland) and with the GC working electrode and the reference electrode used for bulk electrolysis. The reported E_h values were measured after equilibration times of at least 50 min and when the drifts in measured E_h had decreased to less than 0.005 V per h.

The E_h-n_{e-} data was described by a model assuming *i* types of redox-active sites with different pH-adjusted apparent standard reduction potentials $E_{h,i}^{0*}$(pH). At redox equilibrium, n_{e-} is given by equation 1 which was derived

from the Nernst equation (section **S3**, SI):

$$n_{e^-} = \sum_i \frac{10^{\frac{E_{h,i}^{0*}(pH)}{a}} C_i}{10^{\frac{E_h}{a}} + 10^{\frac{E_{h,i}^{0*}(pH)}{a}}}$$ (1)

, where C_i is the total moles of sites i per unit HA mass, a $= \ln(10) \cdot RT \cdot (F)^{-1}$, where R, T, and F are the universal gas constant, the absolute temperature, and the Faraday constant, respectively.

The fitting was performed with i=16 and $E_{h,i}^{0*}(pH)$ that were equally distributed over the experimentally relevant potential range from E_h = +0.2 to - 0.4 V (Figure **S1**). Following interpolation of the experimental data as described in section **S3**, SI, equation 1 was fitted to the E_h-n_{e^-} dependencies using the FindFit function in Mathematica® 7.0.1.0 (Wolfram Research, IL, USA) with C_i as fitting parameters. Two boundary conditions were implemented: the total moles of reducible moieties per mass of HA, $C_{tot} = \sum_{i=1}^{16} C_i$, was set equal to the electron accepting capacity (EAC) as published in (8), and each C_i was larger than 0 and smaller than the EAC (0< C_i< EAC).

3.3. Results and Discussion

Electron transfer mediation by diquat and ethylviologen. Relative to the background, CVs of LHA solutions showed higher reductive currents I_c during cathodic scanning (Figure **1a**), which increased with increasing concentration of LHA, C_{LHA} (Figure **S2a**, section **S4**, SI). LHA was therefore directly reduced at the glassy carbon working electrode. The CVs of LHA were featureless at all tested scan rates (v= 0.01 to 0.1 V s^{-1}), likely due to electrode passivation by surface-active fractions of LHA and/or due to slow electron transfer from the electrode to LHA relative to the applied scan rates. Featureless CVs of HS in aqueous solutions were also reported in previous studies (12, 25, 26). The CV of DQ-containing solutions showed reversible one-electron cathodic and anodic waves centered at E_h= -0.37 V (Figure **1a**), which is close to the literature E_h^0 =

-0.361 V of DQ (22). A detailed analysis of CVs of DQ is provided in Figure **S3**, SI.

At all tested scan rates, the CVs of LHA in the presence of low DQ concentrations showed much higher I_c than the CVs of either only DQ or only LHA (Figure **1a**). While the cathodic peak currents, $I_{p,c}$, were linearly correlated with C_{LHA} (inset Figure **1a** and Figure **S2b**, SI), the peak current potentials, $E_h(I_{p,c})$, did not change with C_{LHA}. These results demonstrate that small DQ concentrations facilitated electron transfer from the working electrode to LHA. Chronocoulometric analysis suggests that each DQ molecule shuttled up to 17 electrons from the working electrode to LHA during one cathodic scan ($C_{LHA} =$ 2 gL^{-1}; $C_{DQ} =$ 30 μM; $v =$ 0.01 V/s; Figure **S2c**, SI). The onset of the cathodic wave in the DQ-LHA system was at $E_h =$ -0.15 V. This implies that LHA contains a significant number of moieties that can be reduced at or above $E_h =$ -0.15 V and that DQ effectively mediated electron transfer to LHA at potentials much higher than its $E_h^0 =$ -0.361 V. This suggests that DQ can also be used as a mediator in potentiometric E_h-pH titrations over a wide E_h range. Results similar to those for DQ were found for ethylviologen (Figure **S2d**, SI), indicating that other bipyridinium compounds may also facilitate electron transfer from electrodes to HA.

DQ-facilitated electron transfer from the working electrode to HA is expected to decrease with increasing depletion of the pool of reducible moieties in LHA. Consistently, cathodic peak currents, $I_{p,c}$, decreased with increasing extent of LHA pre-reduction by bulk electrolysis from samples S$_0$ (unreduced LHA) to sample S$_5$ (pre-reduced to $n_{e-} =$ 1.00 mmol$_{e-}$ g$_{LHA}^{-1}$) (Figures **1b** and **S4**, SI). The cathodic wave of CVs of extensively pre-reduced LHA (sample S_{DQ}; n_{e-} = 1.40 mmol$_{e-}$ g$_{LHA}^{-1}$, corresponding to 82% of the EAC of LHA (8)) approached that of only DQ. The linear correlation of $I_{p,c}$ with n_{e-} (inset Figure **1b**), shows that CVs in the presence of mediators may be used to quantify the redox state of HA.
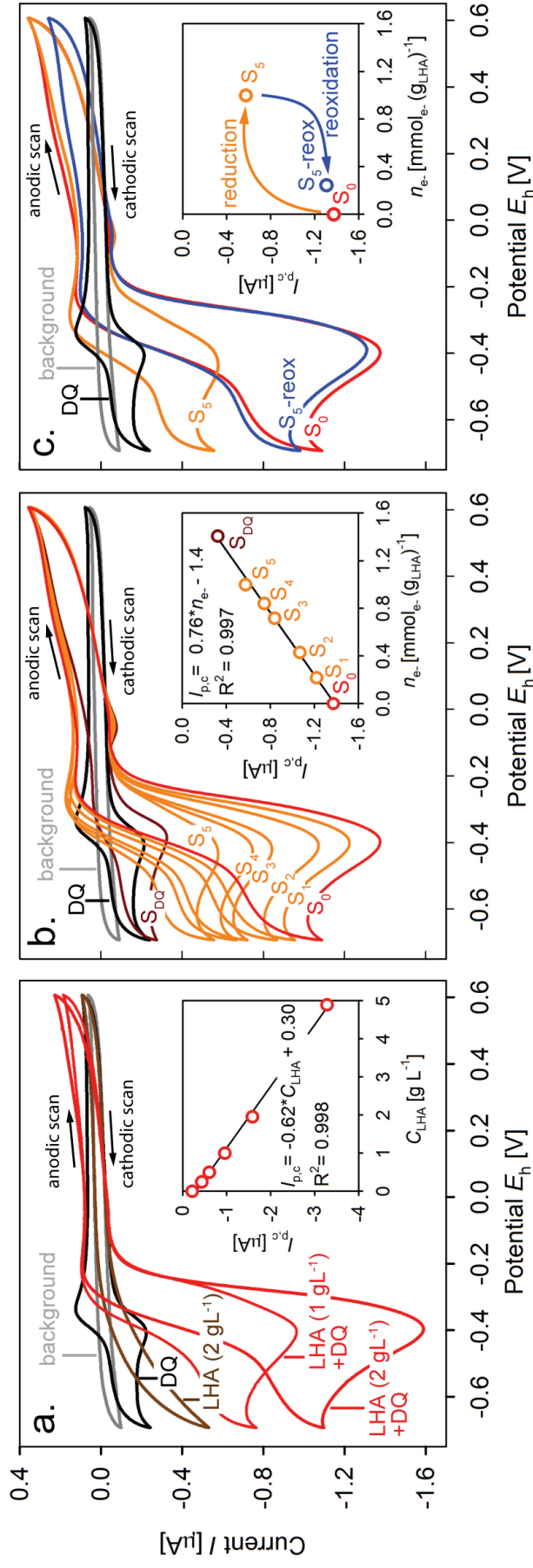
Figure 1 a. Cyclic voltammograms (CVs) of background buffer (grey trace), the redox mediator diquat (DQ) (black trace; concentration $C_{DQ}=$ 30 μM), Leonardite humic acid standard (LHA) (brown trace; $C_{LHA}= 2$ gL^{-1}), and LHA and DQ (red traces; $C_{LHA}= 1$ and 2 gL^{-1}; $C_{DQ}= 30$ μM). Inset: Linear correlation of cathodic peak currents, $I_{p,c}$, with C_{LHA}. **b.** Effect of LHA redox state on catalytic currents ($C_{LHA}= 2$ gL^{-1}; $C_{DQ}= 30$ μM). Sample S_0 contained unreduced LHA. Samples S_1 to S_5 contained LHA pre-reduced to different extents by bulk electrolysis (i.e., moles of electrons transferred per mass of LHA ranged from $n_{e^-}= 0$ to 1.00 mmol$_{e^-}$ g^{-1} for S_1 to S_5, respectively). Sample S_{DQ} contained LHA extensively pre-reduced by bulk electrolysis in the presence of DQ (i.e., $n_{e^-}= 1.40$ mmol$_{e^-}$ g^{-1}). Inset: Linear correlation of $I_{p,c}$ with increasing n_{e^-}. **c.** Regeneration of the pool of reducible moieties in LHA upon O$_2$-oxidation of sample S_5 to S_{5-reox}. Inset: Corresponding changes in $I_{p,c}$. All CVs were collected at pH 7 (0.1 M KCl and 0.1 M potassium phosphate) and at scan rates of $v= 0.01$ V s^{-1} .

Figure **1b** shows that $I_{p,c}$ decreased and that the onset potential of the cathodic wave shifted towards more negative E_h with increasing extent of LHA pre-reduction from samples S_0 to S_5. Such shifts were not observed when changing the concentration of unreduced LHA (Figures **1a** and **S2b**). The shifts suggest that bulk electrolysis resulted in preferential electron transfer to moieties in the LHA with the highest reduction potentials.

Re-oxidation of LHA. Figure **1c** shows that O_2 re-oxidation of the reduced LHA re-increased $I_{p,c}$ and shifted the onset potential of the cathodic wave to more positive values (sample S_5 to $S_{5\text{-reox}}$). The cathodic wave of the re-oxidized LHA was almost identical to that of LHA prior to reduction by bulk electrolysis (sample S_0), demonstrating reversible electron transfer to LHA over a reduction-O_2 re-oxidation cycle, consistent with (8, 10, 18). Oxidation of the extensively reduced S_{DQ} by O_2 had similar effects on the CVs (Figure **S5**, SI).

Reversible electron transfer to LHA over a reduction, O_2 re-oxidation cycle does not stand in contrast to the absence of oxidative current peaks during anodic scanning in the CVs of LHA in the presence of DQ (Figure **1**). The absence of oxidative peak currents merely showed that DQ was not a suitable mediator to effectively shuttle electrons from the LHA to the working electrode. Inefficient mediation resulted from the fact that the E_h^0 of DQ was much lower that the potentials at which re-oxidation of LHA became thermodynamically feasible. In this context, it is important to note that the cathodic peak currents resulted from electron transfer to moieties in the LHA with reduction potentials that were likely much higher than the potentials applied to the working electrode. Consistently, the onset potential of the cathodic wave shifted towards higher E_h when using CyV ($E_h^0 = -0.18$ V) as mediator instead of DQ (Figure **S6**). The onset potentials of the cathodic waves were therefore defined by the 'availability' of sufficient amounts of reduced mediator and not by the E_h of the reducible moieties in the LHA. Yet, direct electrochemical oxidation occurred, as demonstrated by increasing anodic currents with increasing extents of LHA pre-reduction by bulk electrolysis (Figure **S4**). Direct electrochemical oxidation was, however, slow and resulted in only small oxidative currents.

We used DCPIP, a two-electron transfer mediator with $E_h^0(\text{pH } 7) = +0.217$ V (21), to demonstrate electron transfer reversibility to LHA also directly by cyclic voltammetry. Compared to other mediators with high E_h^0, DCPIP did not significantly oxidize non pre-reduced LHA (8), a pre-requisite

for our experiments. In the absence of LHA, both DQ and LHA showed reductive and oxidative waves during cathodic and anodic scanning, respectively. In Figure **2a**, the scanning direction was inverted from cathodic to anodic at potentials larger than those required for significant LHA reduction by DQ. As LHA was not reduced during cathodic scanning, it was also not oxidized by DCPIP during anodic scanning, such that anodic scans showed no catalytic oxidative peak currents. Lowering the vertex potential resulted in increasing extent of LHA reduction during cathodic scanning and increasing LHA oxidation by DCPIP during subsequent anodic scanning. Overall smaller catalytic DCPIP than DQ peaks are consistent with slower electron transfer between LHA and DCPIP than between LHA and DQ (8).
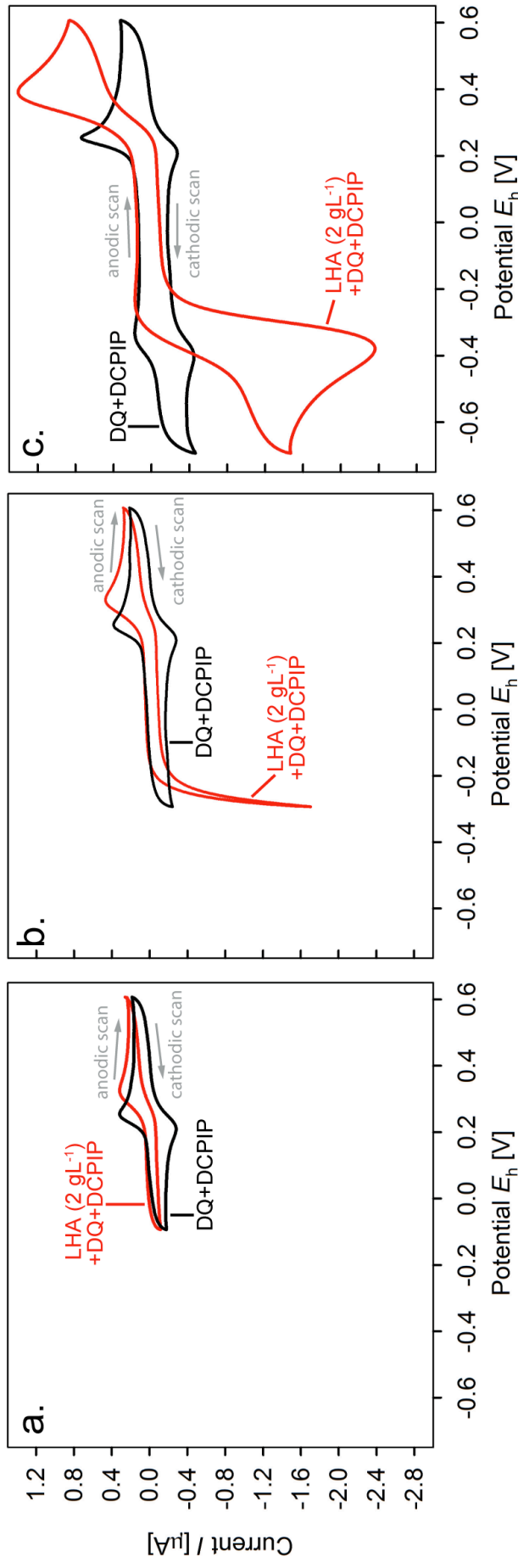
Figure 2. Cyclic voltammograms (CVs) collected in solutions containing the mediators diquat (DQ; concentration C_{DQ}= 30 μM) and dichlorophenol indophenol (DCPIP; C_{DCPIP}= 16 μM), either in the absence (black trace) or in the presence of Leonardite humic acid (LHA; 2 g_{LHA} L⁻¹) (red trace). The scan rate was v= 0.025 V s⁻¹, and the cathodic vertex potentials were at **a.** E_h= −0.09 V, **b.** E_h= −0.29 V, and **c.** E_h= −0.69 V.

Similar to the effects of LHA pre-reduction on the catalytic cathodic waves, increasing the solution pH decreased the $I_{p,c}$ and shifted the onset potential of the cathodic wave towards lower E_h (Figure **S5a**, SI). These pH effects were largely reversible (Figures **S5b**, SI). Electron transfer to reducible moieties in LHA therefore decreased with increasing pH, consistent with decreasing E_h^0(pH) of the reducible moieties in LHA with increasing pH.

The CV data demonstrate that small concentrations of DQ or EV mediate the electron transfer between electrodes and LHA. DQ also facilitated bulk electrolysis of LHA (Figure **3a**): the addition of small amounts of DQ largely facilitated electron transfer from the working electrode to LHA, while it did not affect $n_{H+}(n_{e-})^{-1}$. In addition, DQ may be used as redox mediator in potentiometric E_h measurements, as shown in Figure **3b** for LHA. While the E_h values measured by a Pt-ring redox electrode slowly drifted in the absence of DQ, E_h readings rapidly stabilized after addition of DQ. Constant E_h readings strongly suggest attainment of redox equilibrium between the mediator and the LHA. DQ therefore allowed for fast and reliable quantification of E_h as a function of pH and n_{e-}, as shown below.
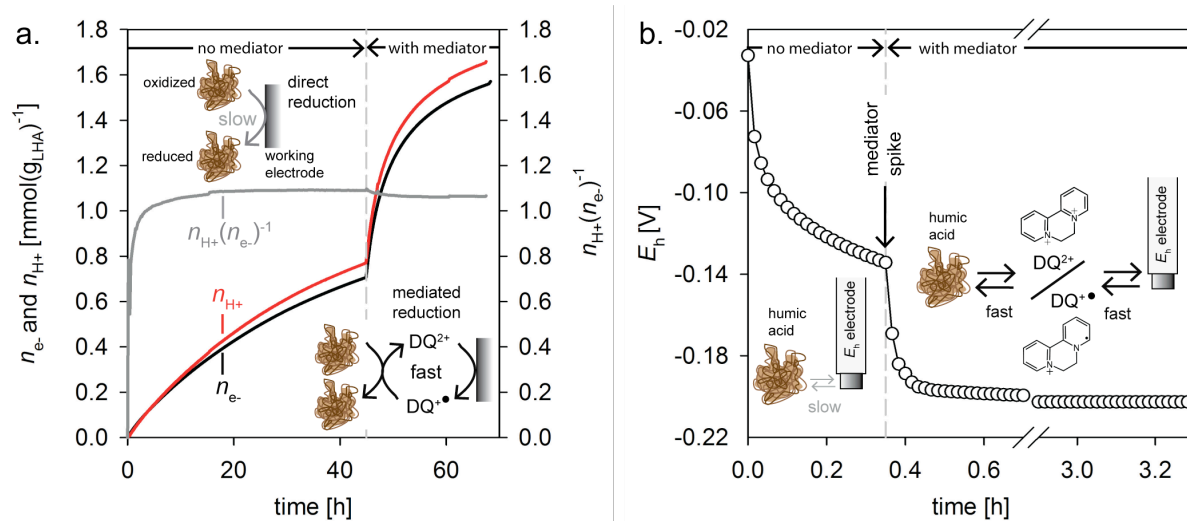
Figure 3. Redox mediation between Leonardite humic acid (LHA) and electrodes by diquat (DQ). **a.** The moles of electrons and protons, n_{e-} and n_{H+}, and their ratio, $n_{e-}(n_{H+})^{-1}$, transferred to a unit mass of LHA during bulk electrolysis prior to and after the addition of DQ (final concentration C_{DQ} ~23 μM). **b.** Change in the reduction potential E_h of LHA measured with a Pt ring redox electrode over time prior to and after the addition of DQ (final C_{DQ} = 18.6 μM).

pH dependencies of $n_{H+}(n_{e-})^{-1}$ and E_h. This section provides a systematic assessment of the protonation equilibria of the reducible moieties in selected HAs by acid-titration coupled bulk electrolysis at different pH and by potentiometric E_h-pH titrations of HA at different redox states. Prior to analyzing HA, we validated the experimental setups with model quinones that have known redox properties.

Figure **4a** shows the pH-dependence of the molar ratio of protons to electrons, $n_{H+}(n_{e-})^{-1}$, transferred to four quinones during bulk electrolysis coupled to automated acid titration. The experimental $n_{H+}(n_{e-})^{-1}$ values at the end of the reduction (symbols) were in good agreement with the curves calculated from literature E_h^0 and pK_a values (solid lines) (15, 16, 27-29) (calculation details are provided in section **S5**, SI). In contrast to the quinones, the one electron reduction of DQ^{2+} to the radical $DQ^{\bullet+}$ is not coupled to proton transfer, resulting in $n_{H+}(n_{e-})^{-1} \approx 0$ at pH 7 and 9. Good agreement between experimental and calculated values demonstrates that the bulk electrolysis setup allowed for an accurate quantification of proton and electron transfers.
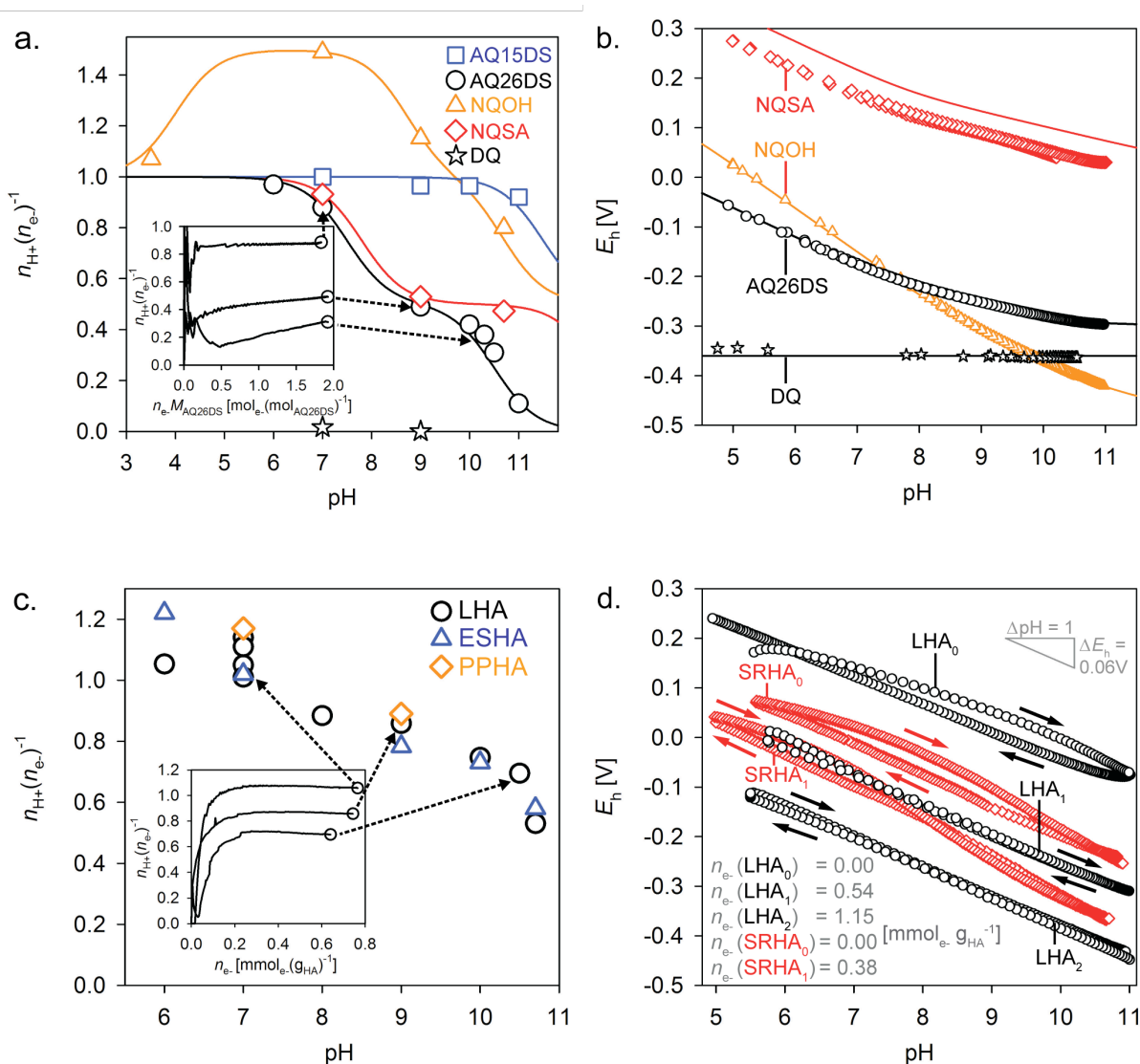
Figure 4. a. Effect of pH on the molar ratio of protons to electrons, $n_{H+}(n_{e-})^{-1}$ transferred to diquat (DQ), and the quinones 9,10-anthraquinone-2,6-disulfonic acid (AQ26DS), 9,10-anthraquinone-1,5-disulfonic acid (AQ15DS), 1,4-naphthoquinone-4-sulfonic acid (NQSA), and 2-hydroxy-1,4-naphthoquinone (NQOH) during acid-titration coupled bulk electrolysis. The solid lines represent the theoretical $n_{H+}(n_{e-})^{-1}$ calculated from published standard reduction potentials, E_h^0, and acidity constants of the quinones/hydroquinones. Calculations were done relative to the unreduced quinone. Inset: Corresponding changes in $n_{H+}(n_{e-})^{-1}$ with n_{e-} during bulk electrolysis of AQ26DS at pH 7, 9, and 10.5, where M_{AQ26DS} is the molar mass of AQ26DS. **b.** Potentiometric E_h-pH titration curves for AQ26DS, NQSA, NQOH, and DQ reduced to 50% of their electron accepting capacities. **c.** Effect of pH on $n_{H+}(n_{e-})^{-1}$ transferred to Leonardite (LHA), Elliott Soil (ESHA), and Pahokee Peat (PPHA) humic acids. Inset: Changes in $n_{H+}(n_{e-})^{-1}$ with n_{e-} for LHA at pH 7, 9, and 10.5. **d.** Potentiometric E_h-pH titration curves for LHA pre-reduced by bulk electrolysis to n_{e-}= 0.00, 0.54, and 1.15

78

$mmol_e$-g_{LHA}^{-1}, and for SRHA at n_{e-}= 0.00, and 0.38 $mmol_e$-$(g_{SRHA})^{-1}$. The arrows indicate the direction of titration.

The reduction of AQ26DS, AQ15DS, and NQSA exhibited $n_{H+}(n_{e-})^{-1} \approx 1$ at pH< pK_{a1} of the corresponding hydroquinone species, consistent with a $2e^-$, $2H^+$ transfer to the quinone to form the hydroquinone. Ratios of $1 \leq n_{H+}(n_{e-})^{-1} \leq$ 1.5 for the reduction of NQOH at circumneutral pH reflected the transfer of up to three protons per two electrons, as the hydroxy substituent is deprotonated in the quinone (acidity constant, $pK_{a, ox}$= 3.94) but protonated in the hydroquinone ($pK_{a,1}$= 8.7) (16). The inset shows the change of $n_{H+}(n_{e-})^{-1}$ during the bulk electrolysis of AQ26DS. At less than 25% reduction (i.e., $n_{e-}*M_{AQ26DS}$ < 0.5 mol_{e-} $(mol_{AQ26DS})^{-1}$), electron transfer to AQ26DS was too fast for automated acid titration, resulting in large variations in $n_{H+}(n_{e-})^{-1}$. At alkaline pH, the gradual increase in $n_{H+}(n_{e-})^{-1}$ at $n_{e-}*M_{AQ26DS}$> 0.5 $mol_{e-}(mol_{AQ26DS})^{-1}$ may have resulted from one electron reductions to form the semiquinone radical anion, consistent with calculations (Figures **S8** and **S9**, SI).

Figure **4b** shows potentiometric E_h-pH titrations of solutions containing model quinones or diquat reduced to 50% of their respective electron accepting capacities. E_h-pH data for AQ26DS at additional extents of reduction are provided in Figure **S10**, SI. The measured E_h-pH dependencies of DQ, AQ26DS, and NQOH were in good agreement with the E_h-pH dependencies calculated from literature E_h^0 and pK_a values (solid lines; Table **S2**, SI) (15, 16, 27-29). The slopes $\Delta E_h(\Delta pH)^{-1}$= -0.09 V for NQOH, -0.06 V for AQ26DS and NQSA, and 0.0 V for DQ at circumneutral pH were consistent with $n_{H+}(n_{e-})^{-1}$= 1.5, 1.0, and 0.0, respectively, measured during bulk electrolysis coupled to automated acid titration. The experimental E_h-pH curve for NQSA was about 0.06 V lower than expected, corresponding to about 90% instead of 50 % reduction. It is conceivable that NQSA became partially reduced during storage in the glovebox prior to electrochemical reduction due to its relatively high standard reduction potential.

Figure **4c** shows the pH dependence of $n_{H+}(n_{e-})^{-1}$ during bulk electrolysis of LHA, PPHA and ESHA. For LHA and ESHA, $n_{H+}(n_{e-})^{-1}$ decreased continuously with increasing pH from between 1.0 and 1.2 at pH $\leq$7 to values smaller than 0.8 at pH >10. The $n_{H+}(n_{e-})^{-1}$ for PPHA, determined at pH 7 and 9, were similar to those of LHA and ESHA at the same pH. The gradual decrease

in $n_{H+}(n_{e-})^{-1}$ with increasing pH implies that the reducible moieties in HA have a wide distribution in pK_a values. Values of $n_{H+}(n_{e-})^{-1}$ larger than unity at pH< 7 are consistent with the presence of hydroxy-substituted quinone moieties in the HA (see NQOH in Figure **4a**). The presence of hydroxy-quinones in LHA, ESHA, and PPHA is reasonable considering their high O/C ratios (0.49, 0.59 and 0.66 mol_O mol_C^{-1}) and high titrated phenolic O contents (1.09, 1.08, and 1.47 mmol(g_{HA})$^{-1}$) (30). Values of $n_{H+}(n_{e-})^{-1}$ smaller than unity at pH> 7 that decreased with increasing pH suggest that a large number of reduced moieties deprotonated at alkaline pH. The transfers of electrons and protons to LHA, ESHA, and PPHA during reduction are expected to result in increasing H^+ buffering capacity of the HA with increasing extent of reduction. A significant increase in phenol-type proton-binding sites at pH> 8 upon HA reduction was previously demonstrated by Maurer et al. (18).

Over the course of the reduction, $n_{H+}(n_{e-})^{-1}$ of all HA initially increased and then leveled off, as shown for LHA reduction at pH 7, 9, and 10.5 in the inset of Figure **4c**. Increasing $n_{H+}(n_{e-})^{-1}$ during the initial stages of the reduction may have resulted from semiquinone radical formation, consistent with theory for quinone reduction (details in Figure **S8** and **S9**, SI) (15, 17) and the finding of a transient increase in the radical content during chemical reduction of a soil fulvic acid, as measured by EPR spectroscopy (11). Yet, other explanations for the gradual increase in $n_{H+}(n_{e-})^{-1}$ during bulk electrolysis are also possible, including a delayed proton uptake caused by slow structural rearrangements of HA (31).

Figure **4d** shows the E_h-pH curves for unreduced and reduced SRHA and LHA at different n_{e-}. Additional data for ESHA and PPHA are provided in Figure **S11**, SI. The E_h-pH titrations for unreduced LHA_0 and $SRHA_0$ were conducted in the absence of mediator due to the lack of suitable compound with sufficiently high E_h^0 at the time of the experiments. The absence of a mediator likely resulted in redox non-equilibria between the Pt electrode and the unreduced HAs during the titrations. Non-equilibria may explain the hysteresis in the titration curves with higher E_h values during base than during acid titrations. The differences in E_h were several tens of millivolts (Table **S3**), which is substantial considering that E_h is logarithmically related to the concentration of the redox-active moieties. Other processes may, however, also

have contributed to hysteresis, including changes in HA aggregation state with pH, previously shown to cause hysteresis in proton binding by HA (31).

HA reduction shifted the E_h-pH curves towards lower potentials (Figure **4d**). LHA_1, LHA_2, and $SRHA_1$ solutions contained small DQ concentrations to facilitate attainment of redox equilibria in E_h-measurements (Figure **S12**). Except for $SRHA_1$, the E_h-pH curves of all HAs, including PPHA and ESHA, exhibited slopes between $\Delta E_h(\Delta pH)^{-1}$= -0.048 V and -0.064 V (Table **S3**, SI) at circumneutral pH, consistent with previously published values of -0.044 V and -0.065V and for two unreduced HA (19, 20). The slopes of the E_h-pH titration curves suggest the uptake of 0.81 to 1.08 moles of H^+ per mole of e- by the four tested HA, in good agreement with $n_{H+}(n_{e-})^{-1} \approx 1$ for LHA, PPHA, and ESHA during bulk electrolysis at circumneutral pH. It is, however, important to note that only those moieties that were reduced during bulk electrolysis contributed to the measured $n_{H+}(n_{e-})^{-1} \approx 1$, whereas all moieties that exchanged current with the Pt redox electrode contributed to the measured E_h. Hence, moieties with high standard reduction potentials (e.g., benzohydroquinones $E_h^0 > 0.2V$) that were already reduced prior to bulk electrolysis of HA may have contributed to measured E_h values but not to $n_{H+}(n_{e-})^{-1}$. The presence of such reduced moieties in untreated HA is supported by their significant electron donating capacities under mildly oxidizing conditions (e.g., (8, 10, 18)). A higher abundance of such moieties in SRHA than LHA may explain the lower potentials measured for $SRHA_0$ compared to LHA_0 (Figure **4d**).

Apparent standard reduction potential distribution of reducible moieties in HA. Figure **5a,b** show the results of a detailed analysis of the effect of HA redox state on E_h for LHA (pH 7 and 9), SRHA, and ESHA (both at pH 7). All E_h measurements were conducted in the presence of small concentrations of DQ and EV to facilitate redox equilibration between the HA and the redox electrode. Attainment of equilibria is supported by the following findings. First, as shown for LHA (Figure **S13a**, SI), the decrease in E_h with increasing n_{e-} was reproducible. Second, potentiometric E_h measurements of ESHA resulted in comparable E_h-n_{e-} dependencies when using Pt, Au, and glassy carbon electrodes (Figure **S13b**, SI). These materials are expected to have different exchange current densities with redox couples in solution and hence would have resulted in different E_h values if equilibrium had not been attained (32-34).

81

Third, the E_h-n_{e-} curve for AQ26DS determined by the same experimental approach was in agreement with the curve calculated from literature E_h^0(pH 7) values (Figure **S14**, SI).

The E_h of all three tested HA decreased with increasing n_{e-} (Figure **5a**) and covered wide E_h ranges > 0.4 V for LHA and ESHA and > 0.2 V for SRHA. The wide E_h ranges indicate wide distributions in the reduction potentials of the reducible moieties. The E_h-n_{e-} curve and the corresponding distribution of $E_{h,i}^{0}*$ for LHA shifted by approximately -0.12 V from pH 7 to pH 9 (Figure **5a**, inset). This shift is consistent with equimolar proton and electron transfers to the reducible moieties in HA, which would result in a shift of -0.059 V at 25°C per pH according to the Nernst equation.
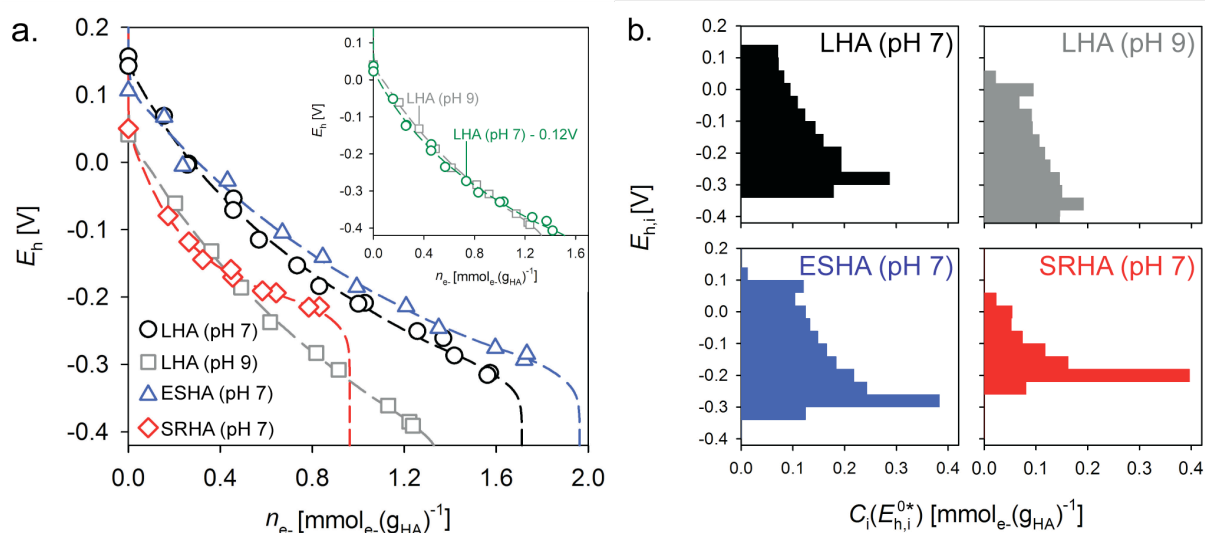
Figure 5 a. Change in the reduction potential E_h of Leonardite humic acid (LHA; pH 7 and 9), Elliot Soil humic acid (ESHA; pH 7), and Suwanee River humic acid (SRHA; pH 7) with increasing moles of electrons, n_{e-}, transferred per mass of HA. The dashed lines represent fits by a model assuming i= 16 discrete types of reducible moieties with apparent standard reduction potentials $E_{h,i}^{0}*$(pH 7) and $E_{h,i}^{0}*$(pH 9) between +0.2 V and -0.4 V. Inset: Overlap in the E_h-n_{e-} data of LHA at pH 9 and at pH 7 following subtraction of ΔE_h= 0.12 V. **b.** Fitted $E_{h,i}^{0}*$(pH) distributions of the reducible moieties in LHA (pH 7 and 9), and in ESHA and SRHA at pH 7, where $C_i(E_{h,i}^{0}*$(pH)) are the molar concentrations of moieties with $E_{h,i}^{0}*$(pH).

The decrease in E_h was steep at low n_{e-} and leveled off at higher n_{e-}, suggesting increasing redox buffering and hence an increase in the abundance of reducible moieties with decreasing E_h. This trend is also reflected in the

$E_{h,i}^{0}$*(pH) distributions of the reducible moieties obtained from fits of equation 1 to the experimental data (Figure **5b**). The two terrestrial HA, LHA and ESHA, showed similar E_h-n_{e^-} dependencies and $E_{h,i}^{0}$*(pH 7) distributions. In comparison, SRHA showed a steeper decrease in E_h at low n_{e^-} and larger redox buffering around E_h= -0.2 V (Figure **5a**), reflected in the overall narrower E_h^{0}*(pH 7) distribution (Figure **5b**). We previously demonstrated strong, positive correlations of HS electron accepting capacities with HS aromaticities and C/H ratios (8), which are higher for LHA and ESHA than for SRHA. The differences in the $E_{h,i}^{0}$*(pH 7) distributions between SRHA and the two terrestrial HA may therefore have resulted from a higher abundance of polycondensated quinone components (e.g., naphtho- and anthraquinones) with lower E_h^{0} in LHA and ESHA than in SRHA.

3.4. Environmental implications

This work has several implications. First, we demonstrated that electron transfer to HA also resulted in proton uptake and that the reduction potential E_h of HA was strongly pH dependent This implies that solution pH has a strong effect on the thermodynamics of electron transfer reactions involving HA. Accurate control and/or monitoring of pH therefore are required when interpreting HA redox dynamics, measured both in laboratory experiments and in the field.

Second, we showed that HA contain reducible moieties that cover a wide range of apparent standard reduction potentials E_h^{0}*. This range covered 0.2 V for SRHA and 0.4 V for LHA and ESHA, at pH 7. This finding suggests that HA contain chemically diverse electron accepting moieties, in line with the previously established chemical complexity and heterogeneity of HA.

Third, we evaluated the distribution in the standard reduction potentials E_h^{0}*(pH) of the reducible moieties in different HA. The distributions allow assessing the thermodynamics of electron transfer to HA under different redox conditions. Figure **6** compares the distribution of E_h^{0}* of the reducible moieties in SRHA and LHA to the reduction potentials of important biogeochemical redox couples and of selected organic and inorganic pollutants, all at pH 7. Electron transfer to HA is expected to occur under both iron and sulfate reducing conditions. A large fraction of the reducible moieties in the studied HA

had higher E_h^0* (pH 7) than the CO_2/CH_4 couple. This finding supports that electron transfer to HA suppresses methanogenesis from peat and bog systems (7). Furthermore reduced HA contain moieties with sufficiently low E_h^0*(pH 7) to reduce iron phases as well as numerous redox-active organic and inorganic pollutants, including nitrobenzene, carbon tetrachloride, and chromium, consistent with experimental observations (6, 10, 36, 37).
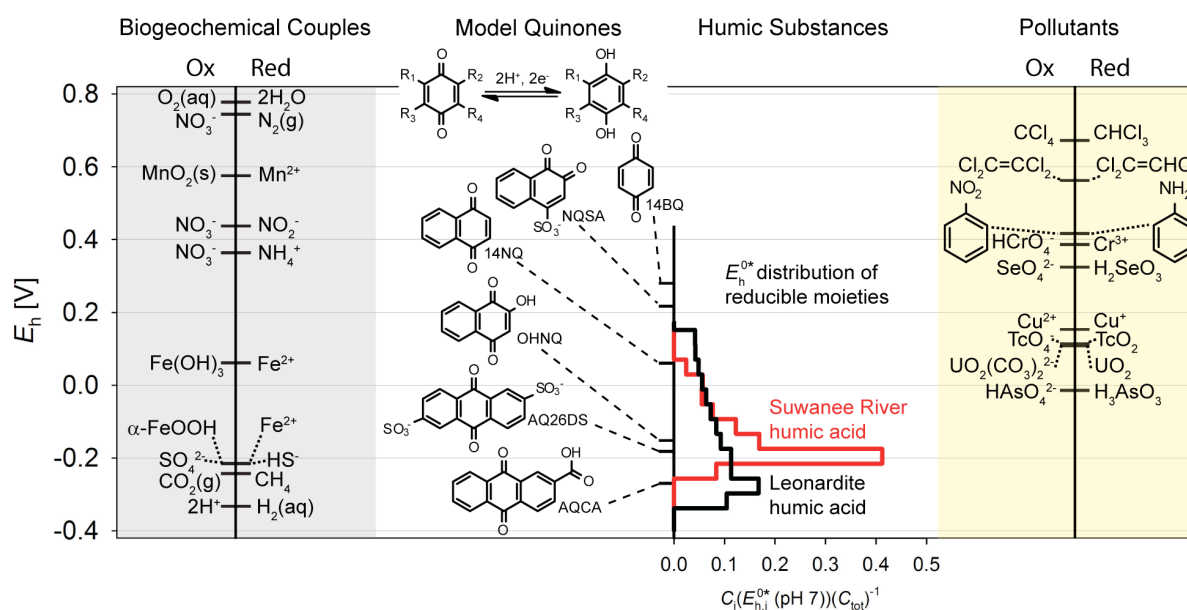
Figure 6. Estimated distributions of apparent standard reduction potentials at pH 7, E_h^0*(pH 7), of reducible moieties in two model humic substances, Leonardite and Suwannee River humic acids, compared to the standard reduction potentials E_h^0(pH 7) of model quinones and the E_h^0(pH 7) of selected biogeochemical and pollutant redox couples (38-42). For redox reactions involving solids, the dissolved species concentrations were set to 10^{-6} M, and the concentration of HCO_3^- to 10^{-3} M. Details on the E_h calculations are provided in Table **S4** in the Supporting Information. The distributions exclude moieties that were already reduced prior to bulk electrolysis.

Fourth, the protonation equilibria of reduced moieties in HA and the range in reduction potentials support quinone components as major electron accepting moieties in HA (Figure **6**). We previously established that terrestrial HS have a larger total number of reducible moieties per unit mass than mixed aquatic-terrestrial and microbial HS (8). The results from this work suggest that the reducible moieties in terrestrial HS cover a wider range in E_h^0 that extend to lower values as compared to the moieties in mixed aquatic-terrestrial HS. HS chemical composition therefore strongly affects not only the total number of

reducible moieties but also their potential distribution. The effects of source material and chemical composition on the pH and E_h characteristics of oxidizable moieties will be addressed in forthcoming work.

Fifth, beyond the direct implications for dissolved HS, this work further advances the use of analytical electrochemistry to characterize the redox properties of organic and mineral environmental phases. These may include particulate organic matter and iron-containing minerals.

3.5. References

1.   Lovley, D. R.; Coates, J. D.; Blunt-Harris, E. L.; Phillips, E. J. P.; Woodward, J. C., Humic substances as electron acceptors for microbial respiration. *Nature* **1996,** *382*, 445-448.

2.   Scott, D. T.; McKnight, D. M.; Blunt-Harris, E. L.; Kolesar, S. E.; Lovley, D. R., Quinone moieties act as electron acceptors in the reduction of humic substances by humics-reducing microorganisms. *Environ. Sci. Technol.* **1998,** *32*, 2984-2989.

3.   Coates, J. D.; Ellis, D. J.; Blunt-Harris, E. L.; Gaw, C. V.; Roden, E. E.; Lovley, D. R., Recovery of humic-reducing bacteria from a diversity of environments. *Appl. Environ. Microbiol.* **1998,** *64*, 1504-1509.

4.   Lovley, D. R.; Fraga, J. L.; Coates, J. D.; Blunt-Harris, E. L., Humics as an electron donor for anaerobic respiration. *Environ Microbiol* **1999,** *1*, 89-98.

5.   Coates, J. D.; Cole, K. A.; Chakraborty, R.; O'Connor, S. M.; Achenbach, L. A., Diversity and ubiquity of bacteria capable of utilizing humic substances as electron donors for anaerobic respiration. *Appl. Environ. Microbiol.* **2002,** *68*, 2445-2452.

6.   Dunnivant, F. M.; Schwarzenbach, R. P.; Macalady, D. L., Reduction of substituted nitrobenzenes in aqueous solutions containing natural organic matter *Environ. Sci. Technol.* **1992,** *26*, 2133-2141.

7.   Heitmann, T.; Goldhammer, T.; Beer, J.; Blodau, C., Electron transfer of dissolved organic matter and its potential significance for anaerobic respiration in a northern bog. *Glob. Change Biol.* **2007,** *13*, 1771-1785.

8.   Aeschbacher, M.; Sander, M.; Schwarzenbach, R. P., Novel electrochemical approach to assess the redox properties of humic substances. *Environ. Sci. Technol.* **2010,** *44*, 87-93.

9.   Ratasuk, N.; Nanny, M. A., Characterization and quantification of reversible redox sites in humic substances. *Environ. Sci. Technol.* **2007,** *41*, 7844-7850.

10.   Bauer, I.; Kappler, A., Rates and extent of reduction of Fe(III) compounds and O_2 by humic substances. *Environ. Sci. Technol.* **2009,** *43*, 4902-4908.

11.   Senesi, N.; Chen, Y.; Schnitzer, M., Role of free radicals in oxidation and reduction of fulvic acid. *Soil. Biol. Biochem.* **1977,** *9*, 397-403.

12.   Nurmi, J. T.; Tratnyek, P. G., Electrochemical properties of natural organic matter (NOM), fractions of NOM, and model biogeochemical electron shuttles. *Environ. Sci. Technol.* **2002,** *36*, 617-624.

13.   Schwarzenbach, R. P.; Stierli, R.; Lanz, K.; Zeyer, J., Quinone and iron porphyrin mediated reduction of nitroaromatic compounds in homogeneous aqueous solution. *Environ. Sci. Technol.* **1990,** *24*, 1566-1574.

14.   Borch, T.; Kretzschmar, R.; Kappler, A.; Van Cappellen, P.; Ginder-Vogel, M.; Voegelin, A.; Campbell, K., Biogeochemical redox processes and their impact on contaminant dynamics. *Environ. Sci. Technol.* **2010,** *44*, 15-23.

15.   Gamage, R.; McQuillan, A. J.; Peake, B. M., Ultraviolet visibile and electron paramagnetic resonance spectroelectrochemical studies of the reduction products of some anthraquinone sulfonates in aqueous solutions *J. Chem. Soc. Faraday. T.* **1991,** *87*, 3653-3660.

16.   Clark, W., *Oxidation-Reduction Potentials of Organic Systems.* Baltimore, 1960.

17.   Laviron, E., Electrochemical reactions with protonations at equilibrium. 8. The 2 e, 2 H+ reaction (9-member square scheme) for a surface or for a heterogeneous reaction in the absence of disproportionation and dimerization reactions. *J. Electroanal. Chem.* **1983,** *146*, 15-36.

18.   Maurer, F.; Christl, I.; Kretzschmar, R., Reduction and reoxidation of humic acid: Influence on spectroscopic properties and proton binding. *Environ. Sci. Technol.* **2010,** *44*, 5787-5792.

19.   Osterberg, R.; Shirshova, L., Oscillating, nonequilibrium redox properties of humic acids. *Geochim. Cosmochim. Acta.* **1997,** *61*, 4599-4604.

20.   Sachs, S.; Bernhard, G., Humic acid model substances with pronounced redox functionality for the study of environmentally relevant interaction processes of metal ions in the presence of humic acid. *Geoderma* **2011,** *162*, 132-140.

21.   Tratnyek, P. G.; Wolfe, N. L., Characterization of the reducing properties of anaerobic sediment slurries using redox indicators. *Environ. Toxicol. Chem.* **1990,** *9*, 289-295.

22. Fultz, M. L.; Durst, R. A., Mediator compounds for the electrochemical study of biological redox systems - a compilation. *Anal. Chim. Acta.* **1982,** *140*, 1-18.

23. Tratnyek, P. G.; Reilkoff, T. E.; Lemon, A. W.; Scherer, M. M.; Balko, B. A.; Feik, L. M.; Henegar, B. D., Visualizing redox chemistry: Probing environmental oxidation–-reduction reactions with indicator dyes. *Chem. Educator* **2001,** *6*, 172-179.

24. Wang, D.; Crowe, W. E.; Strongin, R. M.; Sibrian-Vazquez, M., Exploring the pH dependence of viologen reduction by alpha-carbon radicals derived from Hcy and Cys. *Chemical Communications* **2009**, 1876-1878.

25. Helburn, R. S.; Maccarthy, P., Determination of some redox properties of humic acid by alkaline ferricyanide titration. *Anal. Chim. Acta.* **1994,** *295*, 263-272.

26. Fimmen, R. L.; Cory, R. M.; Chin, Y. P.; Trouts, T. D.; McKnight, D. M., Probing the oxidation-reduction properties of terrestrially and microbially derived dissolved organic matter. *Geochim. Cosmochim. Acta.* **2007,** *71*, 3003-3015.

27. Rosso, K. M.; Smith, D. M. A.; Wang, Z. M.; Ainsworth, C. C.; Fredrickson, J. K., Self-exchange electron transfer kinetics and reduction potentials for anthraquinone disulfonate. *J. Phys. Chem. A.* **2004,** *108*, 3292-3303.

28. Buffle, J.; Martell, A. E., Metal-ion catalyzed oxidation of ortho-dihydroxy aromatic compounds by oxygen .1. Redox and acid-base properties of system 1,2-naphthoquinone-4-sulfonate-1,2-dihydroxynaphthalene-4-sulfonate. *Inorg. Chem.* **1977,** *16*, 2221-2225.

29. Rao, P. S.; Hayon, E., Ionization constants and spectral characteristics of some semiquinone radicals in aqueous solution. *J. Phys. Chem. US.* **1973,** *77*, 2274-2276.

30. Ritchie, J. D.; Perdue, E. M., Proton-binding study of standard and reference fulvic acids, humic acids, and natural organic matter. *Geochim. Cosmochim. Acta.* **2003,** *67*, 85-96.

31. Cooke, J. D.; Hamilton-Taylor, J.; Tipping, E., On the acid-base properties of humic acid in soil. *Environ. Sci. Technol.* **2007,** *41*, 465-470.

32.   Norskov, J. K.; Bligaard, T.; Logadottir, A.; Kitchin, J. R.; Chen, J. G.; Pandelov, S., Trends in the exchange current for hydrogen evolution. *J. Electrochem. Soc.* **2005,** *152*, J23-J26.

33.   Norskov, J. K.; Greeley, J.; Jaramillo, T. F.; Bonde, J.; Chorkendorff, I. B., Computational high-throughput screening of electrocatalytic materials for hydrogen evolution. *Nat. Mater.* **2006,** *5*, 909-913.

34.   Shi, Z.; Nurmi, J. T.; Tratnyek, P. G., Effects of nano zero-valent iron on oxidation-reduction potential. *Environ. Sci. Technol.* **2011**.

35.   Kujawinski, E. B.; Hatcher, P. G.; Freitas, M. A., High-resolution Fourier transform ion cyclotron resonance mass spectrometry of humic and fulvic acids: Improvements and comparisons. *Anal. Chem.* **2002,** *74*, 413-419.

36.   Curtis, G. P.; Reinhard, M., Reductive dehalogenation of hexachloroethane, carbon tetrachloride, and bromoform by anthraquinone disulfonate and humic acid. *Environ. Sci. Technol.* **1994,** *28*, 2393-2401.

37.   Wittbrodt, P. R.; Palmer, C. D., Reduction of Cr(VI) in the presence of excess soil fulvic acid. *Environ. Sci. Technol.* **1995,** *29*, 255-263.

38.   Schwarzenbach, R. P., Gschwend, P.M, Imboden, D. M, *Environmental Organic Chemistry*. 2nd ed.; John Wiley & Sons Hoboken, NJ, 2003.

39.   Haynes, W. M., CRC handbook of chemistry and physics. In 91st ed.; CRC Press: Boca Raton, 1999.

40.   Brooks, S. C.; Fredrickson, J. K.; Carroll, S. L.; Kennedy, D. W.; Zachara, J. M.; Plymale, A. E.; Kelly, S. D.; Kemner, K. M.; Fendorf, S., Inhihition of bacterial U(VI) reduction by calcium. *Environ. Sci. Technol.* **2003,** *37*, 1850-1858.

41.   Islam, F. S.; Gault, A. G.; Boothman, C.; Polya, D. A.; Charnock, J. M.; Chatterjee, D.; Lloyd, J. R., Role of metal-reducing bacteria in arsenic release from Bengal delta sediments. *Nature* **2004,** *430*, 68-71.

42.   Stumm, W.; Morgan, J. J., *Aquatic chemistry: chemical equilibria and rates in natural waters*. 3rd ed.; Wiley: New York, 1996; p xvi, 1022 p.

3.6. Supporting Information Chapter 3

In the manuscript and in the supporting information, electron and proton transfers to humic acids (HA) during electrochemical reduction are given as the number of electrons and protons, n_{e^-} and n_{H^+}, transferred per unit HA mass. The units are $[mmol_{e^-}(g_{HA})^{-1}]$ for n_{e^-} and $[mmol_{H^+}(g_{HA})^{-1}]$ for n_{H^+}. Accordingly, the redox states of HAs are given as n_{e^-} relative to the respective unreduced HAs. All reduction potentials E_h are referenced against the standard hydrogen electrode. Standard potentials are given for T= 25°C and for a partial pressure of the gaseous species of 101.325 kPa (1atm).

Section S1. Quinone redox chemistry

The redox properties of model quinones have been extensively studied in analytical electrochemistry [1]. Quinones exist in three oxidation states, which can interconvert via single electron transfer reactions (Scheme **S1**): the quinone (Q), the semiquinolate anion (Q$^{\bullet-}$), and the quinolate dianion (Q^{2-}). Each of these species can accept one or two protons, depending on the solution pH. The resulting nine-membered square scheme is shown in Scheme **S1** [2, 3].
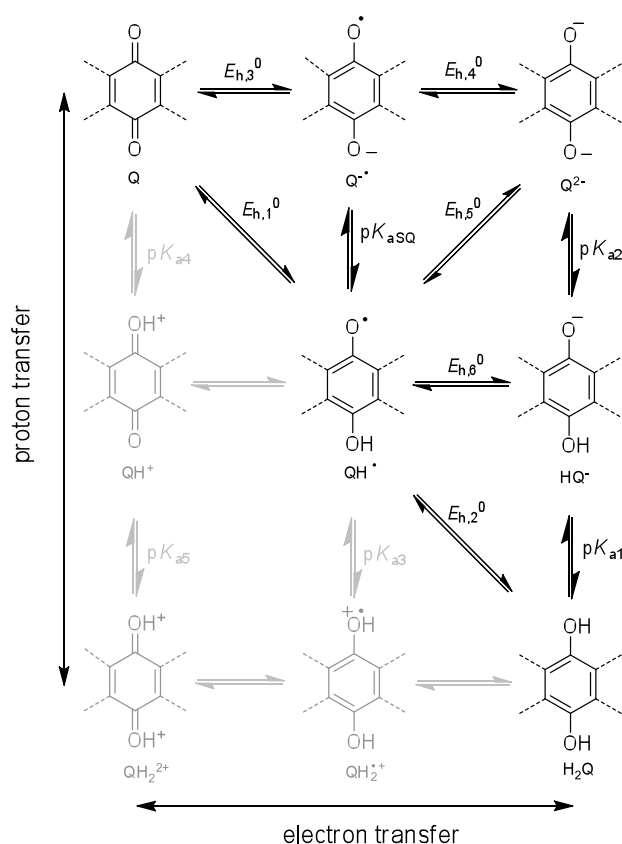
Scheme S1. Nine membered square scheme for the reduction of the quinone (Q) to the quinonolate dianion (Q^{2-}) via the semiquinolate ($Q^{\bullet-}$) (top horizontal line). Also shown are the protonation states in the vertical direction. The pK_a values represent the acid dissociation constants. Prevalent species under environmentally relevant pH conditions are depicted in black. The species depicted in grey are present only in very small concentrations under environmental conditions.

Speciation calculations. The equilibrium speciation of quinones as a function of solution pH and E_h has been treated in detail in [1, 2]. In general, the acidity constants pK_{a3}, pK_{a4}, and pK_{a5} are below the pK_{SQ} of the semiquinolate/semiquinone radical pair ($Q^{\bullet-}/QH^{\bullet}$), which itself is below 6 for most model quinones [2, 4-6]. Therefore, the concentrations of the species QH_2^{2+}, QH^+, $QH_2^{\bullet+}$ (grey structures in Scheme **S1**) are expected to be negligible under environmental pH conditions. These three species are not further considered in the following calculations.

The equations describing the quinone speciation were derived from equations **S1** to **S4**, whereby {activities} were approximated by [concentrations]. In the equations, AH and A$^-$ are the protonated and deprotonated species, respectively; $A_{ox,i}$, $A_{red,j}$ represent the oxidized and the reduced species, respectively; $v_{ox,i}$, $v_{red,j}$ are the stoichiometric coefficients; n is the number of electrons transferred per $\sum_i v_{ox,i} A_{ox,i}$, E_h [V] and E_h^0 [V] are the reduction potential and the standard reduction potential, respectively, and R [J(Kmol)$^{-1}$], T [K], and F [C(mol)$^{-1}$] are the universal gas constant, the absolute temperature, and the Faraday constant, respectively. Equations **S5-S7** represent the proton transfer equilibria and equations **S8-S9** the electron transfer equilibria. The total quinone concentration [Q_{tot}] is kept constant (Equation **S10**).

The proton transfer equilibrium is given as:

$$HA = A^- + H^+ \tag{S1}$$

$$pH = pK_a + Log\frac{\{A^-\}}{\{HA\}} \tag{S2}$$

The electron transfer equilibrium between different species of one redox-active compound is given by the Nernst equation [7]:

$$\sum_i \nu_{ox,i}A_{ox,i} + n_{e^-} = \sum_j \nu_{red,j}A_{red,j} \tag{S3}$$

$$E_h = E_h^0 - \frac{RT}{nF}Ln\frac{\prod_j \{A_{red,j}\}\nu_{red,j}}{\prod_i \{A_{ox,i}\}\nu_{ox,i}} \tag{S4}$$

The equations describing the redox speciation of a given quinone compound are:

$$pH = pK_{a1} + Log\frac{[HQ^-]}{[H_2Q]} \tag{S5}$$

$$pH = pK_{a2} + Log\frac{[Q^{2-}]}{[HQ^-]} \tag{S6}$$

$$pH = pK_{aSQ} + Log\frac{[Q^{\bullet-}]}{[HQ^\bullet]} \tag{S7}$$

$$E_h = E_{h,2}^0 - a\,Log\frac{[HQ^\bullet]}{[Q]10^{-pH}} \qquad \left(a = \frac{Ln(10)\,RT}{F}\right) \tag{S8}$$

$$E_h = E_{h,1}^0 - a \, Log \frac{[H_2Q]}{[HQ^\bullet]10^{-pH}} \qquad (S9)$$

$$[Q]_{tot} = [Q]+[Q^{2-}]+[HQ^-]+[H_2Q]+[HQ^\bullet]+[Q^{\bullet-}] \qquad (S10)$$

The speciation of a given quinone as a function of E_h and pH can be obtained by solving equations **S5-S10**. Using the quinone species, Q, as reference, the ratio of protons to electrons, $n_{H+}(n_{e-})^{-1}$, transferred during the reduction (Eq. **S11**) and the degree of reduction, expressed as conversion factor r (Eq. **S12**), are given as:

$$\frac{n_{H+}}{n_{e-}} = \frac{[HQ^-]+2[H_2Q]+[HQ^\bullet]}{2[Q^{2-}]+2[HQ^-]+2[H_2Q]+[HQ^\bullet]+[Q^{\bullet-}]} \qquad (S11)$$

$$r = \frac{n_{e-}}{2[Q]_{tot}} = \frac{2[Q^{2-}]+2[HQ^-]+2[H_2Q]+[HQ^\bullet]+[Q^{\bullet-}]}{2[Q]+2[Q^{2-}]+2[HQ^-]+2[H_2Q]+[HQ^\bullet]+[Q^{\bullet-}]} \qquad (S12)$$

Section S2. Materials and Methods

Metal content of humic acids

Table S1. Metal contents of the humic acids were quantified by ICP-OES (Varian Vista-MPX).

Humic acid	Nr.	Fe [$\mu mol(g_{HA})^{-1}$]	Cu [$\mu mol(g_{HA})^{-1}$]	Mn [$\mu mol(g_{HA})^{-1}$]
Suwannee River II	2S101H	22.9±0.5	0.46±0.02	<<0.3μM[a]
Elliott Soil	1S102H	19.6±0.3	4.69±0.14	<<0.3μM[a]
Leonardite	1S104H	10.0±0.3	0.11±0.01	<<0.3μM[a]
Pahokee Peat	1R103H	49.6±0.9	0.31±0.02	<<0.3μM[a]

[a]The lowest standard used contained 10 ppm of Mn, which corresponded to ~0.31-0.35 mmol$(g_{HA})^{-1}$ in the 0.5 gL^{-1}LHS solutions. The concentrations of Mn in the 0.5 gL^{-1}HS solutions were much below this concentration and hence not accurately quantifiable.

Mediated electrochemical reduction (MER) was conducted as described in [8]. In brief, the same electrochemical equipment as for bulk reduction of humic acid was used, except for the working electrode, which was replaced by a reticulated vitreous carbon electrode (Bioanalytical Systems Inc., West Lafayette, IN, USA). To quantify the HS redox states, the electrochemical cell was filled with 78 to 80 mL of background electrolyte (0.1 M KCl, 0.1 M phosphate, adjusted to pH 7) and the electrode was equilibrated to the potential E_h= -0.49 V. The electron transfer mediator diquat was then added to the solution by spiking 2 mL of a 5 mM aqueous stock solution into the cell. Upon re-attainment of background currents, the analyte samples (i.e., HAs or model quinones) were spiked to the cell. The resulting current peaks were integrated to obtain the number of transferred electrons. The redox state of each HA sample was calculated as the difference in electron content relative to an untreated (i.e. non pre-reduced or pre-oxidized) standard sample (e.g., samples S_0 in the cyclic voltammetry experiments in the manuscript).

Cyclic voltammetry experiments were conducted in custom-made, small volume cells. The cyclic voltammograms (CVs) were measured using a 3 mm diameter glassy carbon working electrode, a Pt wire counter electrode (Voltalab, Radiometer Analytical SAS, Lyon, France) and an Ag/AgCl reference electrode (Bioanalytical Systems Inc., West Lafayette, IN, USA). All CV measurements were conducted in an anoxic glovebox (O_2 concentration < 0.1 ppm). The CV scans were started at the upper vertex potential. Ten cycles were recorded at scan rates v= 0.1 and 0.075 Vs^{-1}, and five cycles were recorded at scan rates v= 0.5, 0.25 and 0.01 Vs^{-1}. In all cases, the last scan of each run is reported. The glassy carbon electrodes were cleaned in between each series of CV experiments by successive polishing of the electrode surface with 1.0 and 0.05 μm aluminum oxide Micopolish II powder on TexMet 1500 polishing pads (all from Buehler, Lake Bluff, USA). Following the polishing step, the electrodes were thoroughly rinsed with water.

Section S3. Parameterization of the E_h-n_{e^-} curves

A model was developed to describe the dependence of the reduction potential E_h of HA solutions on the number of electrons, n_{e^-}, transferred per unit mass of humic acid during electrochemical reduction. All E_h measurements were conducted in HA solutions containing low concentrations of redox mediators (diquat or ethylviologen, unless stated otherwise).

The model assumes redox equilibria between the electrode, the mediators, and all redox couples in the HA. Under these conditions all redox couples in the HA and the mediator satisfy the Nernst equation (equation **S4**). In the model, the reducible moieties in HA are descretized into i different redox couples. The Nernst equation for the i-th redox couple and for the mediator are given in equations **S13** and **S14**, respectively. In both cases, {activities} were approximated by [concentrations]. $A_{red,i}$ and $A_{ox,i}$ are the oxidized and reduced moieteis of the i-th couple, respectively. med_{red} and med_{ox} refer to the oxidized and reduced redox mediator molecules, respectively. $E_{h,i}^0(pH)$ and $E_{h,med}^0(pH)$ are the standard reduction potentials for the i-th redox couple in HA and the mediator, respectively, adjusted to the given solution pH (i.e., standard conditions except for the pH).

$$E_h = E_{h,i}^0(pH) - aLog\frac{[A_{red,i}]}{[A_{ox,i}]} \qquad \text{where } a = \frac{Ln(10)RT}{F} \qquad (S13)$$

$$E_h = E_{h,med}^0(pH) - aLog\frac{[med_{red}]}{[med_{ox}]} \qquad (S14)$$

This work focuses on the reducible moieties in HA. Note that moieties that were already reduced in the untreated HA are not described by the model (as these moieties did not accept electrons during the electrochemical reduction). Equation **S15** is obtained by expressing [$A_{red,i}$] in equation **S13** by the number of electrons transferred, $n_{e^-,i}$, to the i-th redox couple per unit HA mass and by expressing [$A_{ox,i}$] as the difference in the the total moles of the i-th redox couple per mass of HA, C_i, minus $n_{e^-,i}$. Solving for $n_{e^-,i}$ yields equation **S16**.

$$E_h = E_{h,i}^0(\text{pH}) - a\text{Log}\frac{n_{e-,i}}{C_i - n_{e-,i}} \tag{S15}$$

$$\Rightarrow n_{e-,i} = \frac{10^{\frac{E_{h,i}^0(\text{pH})}{a}} C_i}{10^{\frac{E_h}{a}} + 10^{\frac{E_{h,i}^0(\text{pH})}{a}}} \tag{S16}$$

The analogous equations for the mediator are:

$$E_h = E_{h,med}^0(\text{pH}) - a\text{Log}\frac{n_{e-,med}}{C_{med} - n_{e-,med}} \tag{S17}$$

$$\Rightarrow n_{e-,med} = \frac{10^{\frac{E_{h,med}^0(\text{pH})}{a}} C_{med}}{10^{\frac{E_h}{a}} + 10^{\frac{E_{h,med}^0(\text{pH})}{a}}} \tag{S18}$$

The overall electron balance is given by equation **S19**. Combining it with equations **S16** and **S18** yields equation **S20** that relates the overall number of electrons transferred, n_{e-}, per unit mass of HA to C_i, E_h and $E_{h,i}^0$. The second term on the right side of equation **S20** can be neglected because the mediator concentration was small compared to the total concentration of electron accepting moieties in the HA (i.e. $C_{med} << \sum_i C_i$), resulting in equation **S21**. This equation was used to describe the experimentally measured decrease in E_h with increasing n_{e-}.

$$n_{e-} = \sum_i n_{e-,i} + n_{e-,med} \tag{S19}$$

$$\Rightarrow n_{e-,i} = \sum_i \frac{10^{\frac{E_{h,i}^0(\text{pH})}{a}} C_i}{10^{\frac{E_h}{a}} + 10^{\frac{E_{h,i}^0(\text{pH})}{a}}} + \frac{10^{\frac{E_{h,med}^0(\text{pH})}{a}} C_{med}}{10^{\frac{E_h}{a}} + 10^{\frac{E_{h,med}^0(\text{pH})}{a}}} \tag{S20}$$

$$\text{For } C_{\text{med}} \ll \sum_i C_i \qquad n_{\text{e-},i} = \sum_i \frac{10^{\frac{E^0_{h,i}(pH)}{a}} C_i}{10^{\frac{E_h}{a}} + 10^{\frac{E^0_{h,i}(pH)}{a}}} \qquad (S21)$$

The potential range from E_h= +0.2 V to -0.4 V was divided into i= 16 equally sized potential intervals centered around discrete $E_{h,i}^0$(pH) values. Discretization by a relatively large number of i=16 redox couples with different $E_{h,i}^0$(pH) was required to obtain smooth fits of the experimental E_h-n_{e-} data which covered a wide E_h range. The C_i for each $E_{h,i}^0$(pH) were fitted. The boundary conditions implemented were (i) the total moles of reducible moieties per mass of HA, $C_{\text{tot}} = \sum_{i=1}^{16} C_i$, was set equal to the respective HA electron accepting capacity reported in [8], and (ii) $0 < C_i <$ EAC for all i.

The experimental decrease in E_h with increasing n_{e-} for three tested HAs is shown in Figure **5a** in the manuscript. The data for all HA show continuous decreases in E_h with increasing degrees of reduction. This finding meets with the expectation of continuous distributions in E_h^0(pH) of the reducible moieties in the HAs. Continuous E_h–n_{e-} curves are further supported by (i) the high reproducibility of the E_h-n_{e-} data in duplicate reduction experiments, as shown for LHA at pH 7 in Figure **S13a**, (ii) overlapping E_h-n_{e-} relationships obtained by different redox electrode materials, as shown for EHSA at pH 7 in Figure **S13b**, and (iii) overlap of the E_h-n_{e-} dependency of LHA at pH 9 and of the E_h-n_{e-} dependency at pH 7 after being shifted by –0.12 V (inset in Figure **5a** in the manuscript).

Interpolation of the experimental E_h-n_{e-} data. The E_h-n_{e-} data for Elliot Soil humic acid (pH 7) from Figure **5a** is re-plotted in Figure **S1** (blue triangles) and serves as an example in the following discussion. The slight scatter in the experimental data results in several distinct inflection points (red line in Figure **S1a**) in the fitted E_h-n_{e-} dependence by equation **S21**. These inflection points are particularly evident at low n_{e-} at which the experimental data show more scatter and at which adjacent data points have large differences in E_h. The corresponding distribution of $E_{h,i}^0$(pH7) for ESHA are uneven (Figure **S1b**), contrary to expectation.

This apparent fitting artifact was resolved by interpolation of the experimental E_h-n_{e^-} data prior to fitting of Equation **S21**. A seven parameter (a, b_1, b_2, b_3, t_1, t_2, and t_3) exponential function was used for the interpolation (equation **S22**). Equation **S22** served to convert the experimental E_h-n_{e^-} data into a smooth E_h-n_{e^-} curve.

$$n_{e^-}(E_h) = a + b_1 e^{-t_1 E_h (pH)} + b_2 e^{-t_2 E_h (pH)} + b_3 e^{-t_3 E_h (pH)} \qquad (S22)$$

The resolution of the interpolated data was set to $\Delta E_h = 0.002$ V (black circles in Figure **S1a**). Fits of the interpolated data resulted in an even distribution of $E_{h,i}^0$(pH 7) consistent with expectations (Figure **S1c**). Interpolation did not affect the general trend of an increase in the abundance of reducible moieties with decreasing E_h.
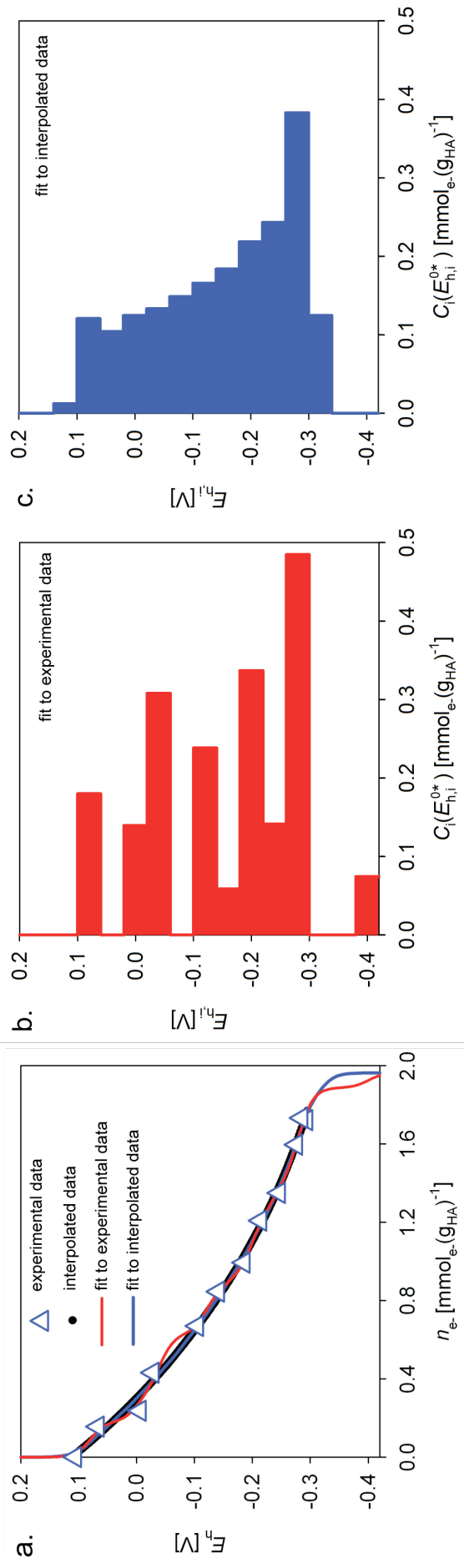
Figure S1. Experimental and fitted reduction potentials, E_h, as a function of the number of electrons n_{e-} transferred per unit mass of Elliott Soil humic acid at pH 7. **a.** The blue triangles represent the experimental data. The black line is composed of values interpolated from the experimental E_h-n_{e-} data as described in the text. The red and blue curves represent the fits of equation **S21** to the measured and interpolated data, respectively. **b,c**. The distributions in the standard reduction potentials $E_{h,i}^0$(pH 7) of the reducible moieties in Elliott Soil HA obtained by fitting equation S21 to the measured experimental (red bars; panel a) and interpolated (blue bars; panel c) data.

Results and Discussion

Section S4. Cyclic voltammetry experiments

Figures **S2** to **S7** show the result of selected cyclic voltammetry experiments, as described in details in the figure legends.
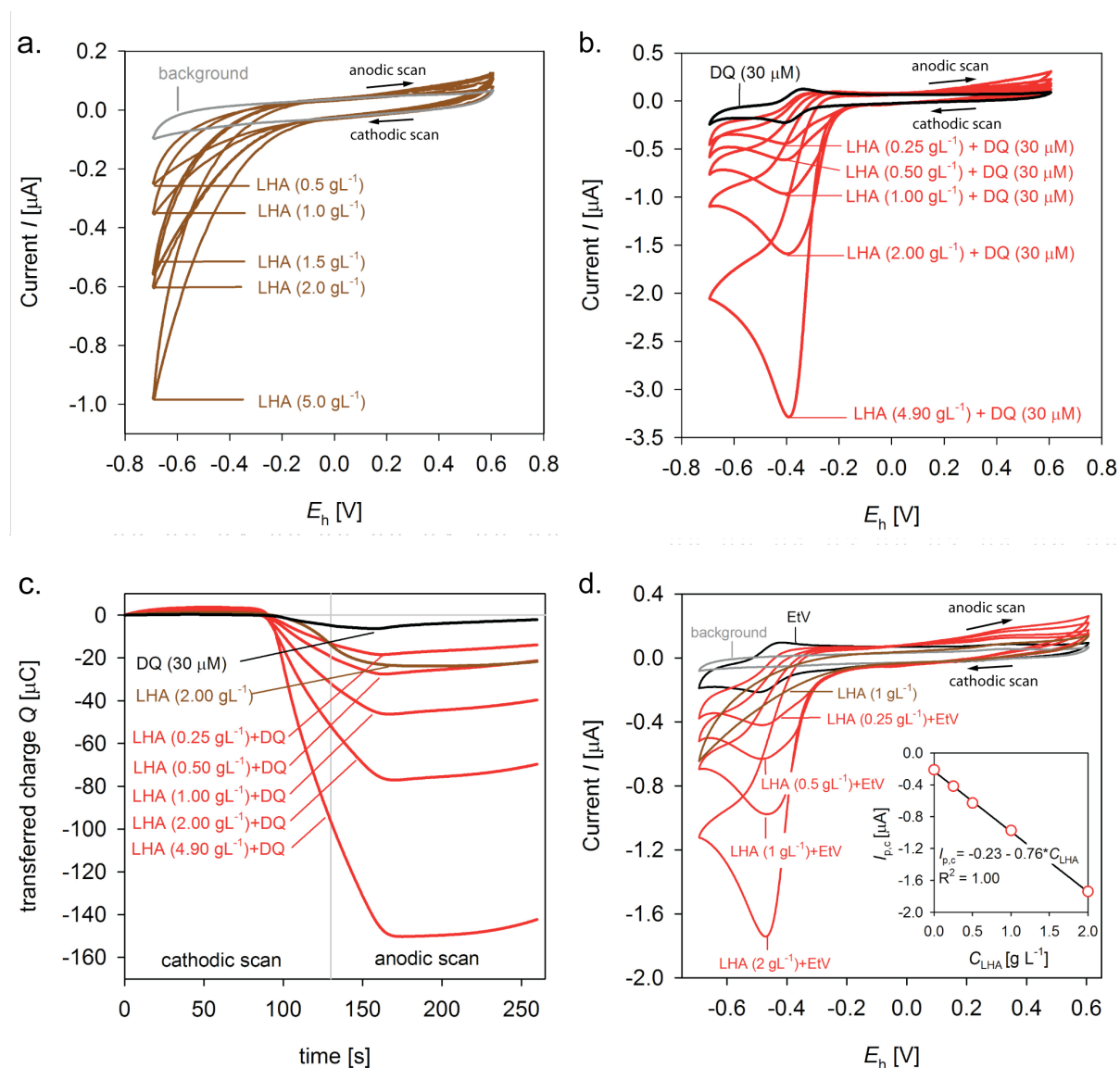
Figure S2. a. Cyclic voltammograms (CVs) of Leonardite Humic acid (LHA) at various concentrations (brown traces) in the absence of electron transfer mediator and of background electrolyte in the absence of LHA (grey trace). **b.** CVs of LHA at various concentrations in the presence of 30 μM of the electron transfer mediator diquat (DQ) (red traces; concentration C_{DQ}= 30 μM), and of DQ at the same concentration in the absence of LHA (black trace). **c.** Results of a chronocoulometric analysis of the CVs of LHA at different

concentrations in the presence of diquat (DQ) (30 µM) (red traces) (panel b), and of non-reduced LHA in the absence of DQ (brown trace), and of only DQ (black trace). The vertical grey line represents the first vertex potential E_h= -0.69 V at which the scanning direction was changed from cathodic to anodic. **d.** CVs of background electrolyte (grey trace), the redox mediator ethylviologen (EtV) (black trace; concentration C_{EtV}= 20 µM), LHA (brown trace; C_{LHA}= 2 g_{LHA} L^{-1}), and for LHA solutions containing small concentrations of EtV (red traces; C_{LHA} from 0.25 to 2 gL^{-1}; C_{EtV}= 20 µM). Inset: Linear increase in the catalytic cathodic peak current, $I_{p,c}$, with increasing C_{LHA} at constant C_{EtV}= 20 µM. All CVs were measured at pH 7 (0.1 M KCl and 0.1 M phosphate buffer) and at scan rates of v= 0.01 V s^{-1}.

Figure **S3** shows that the cathodic and anodic peak currents of the CVs of DQ correlated linearly with the concentration of DQ (panels **a** and **b**). The difference in peak current potentials, $E_{p,a}$-$E_{p,c}$, remained constant at approximately 60-70 mV independent of the scan rate v (panel **c**) and the cathodic peak current scaled linearly with the square root of the scan rate, $v^{0.5}$ (panel **d**). These findings demonstrate fast and fully reversible electron transfer to DQ at the electrode surface.
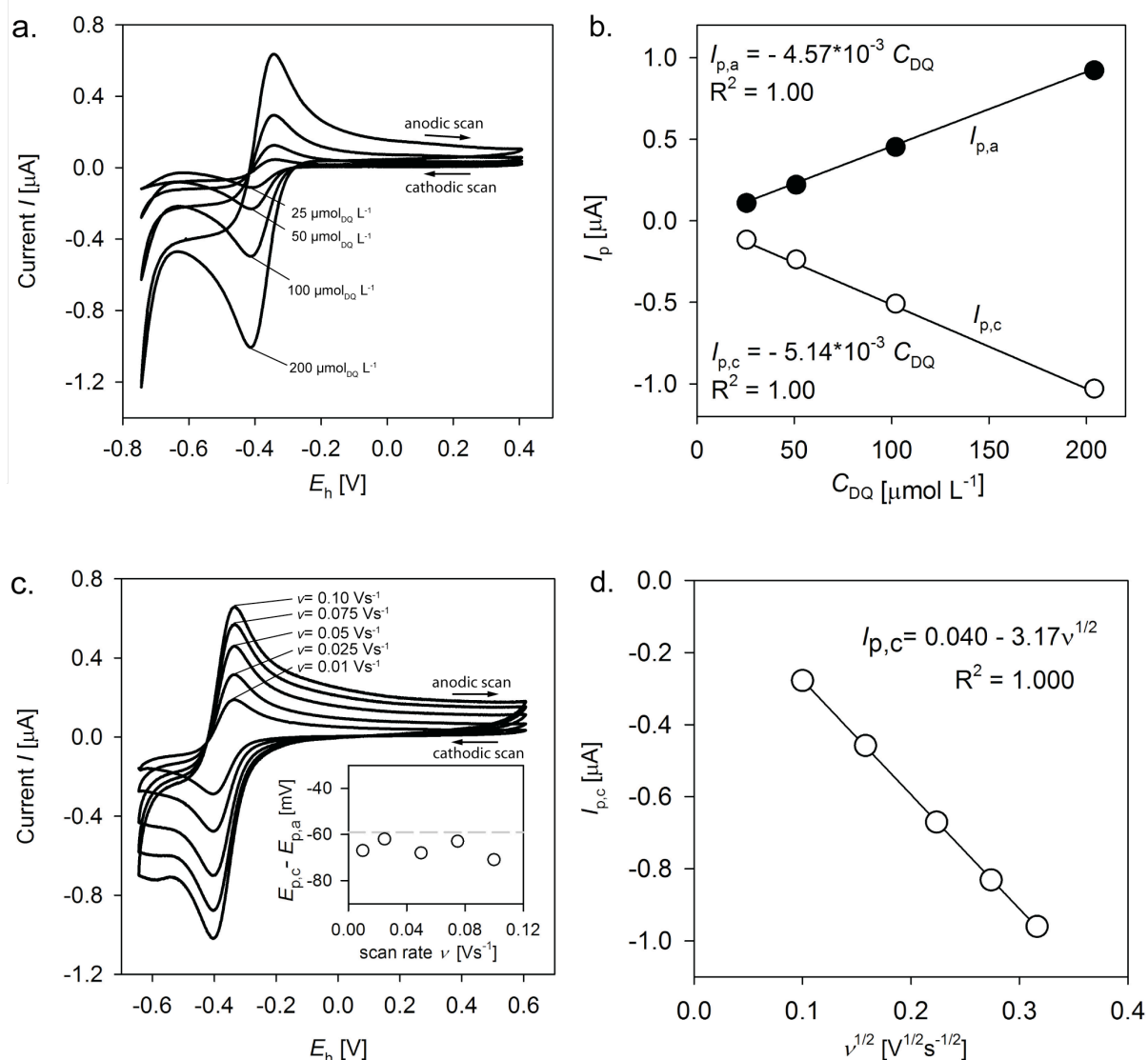
Figure S3. Cyclic voltammograms of the electron transfer mediator diquat (DQ) showing reversible redox behavior at the electrode. **a.** Cyclic voltammograms (CVs) of DQ as a function of DQ concentration, C_{DQ}, at a constant scan rate $v = 0.01$ V s^{-1}. **b.** Linear correlation of the cathodic and anodic peak currents, $I_{p,c}$ and $I_{p,a}$, with C_{DQ}. **c.** CVs of DQ at $C_{DQ} = 30$ μM as a function of the scan rate v. Inset: Differences in the cathodic and anodic peak current potentials, $E_{p,c} - E_{p,a}$, at different scan rates v. **d.** Linear correlation of cathodic peak currents, $I_{p,c}$, with the square root of the scan rate, $v^{0.5}$. All CVs were measured at pH 7 in 0.1 M KCl and 0.1 M phosphate buffer.
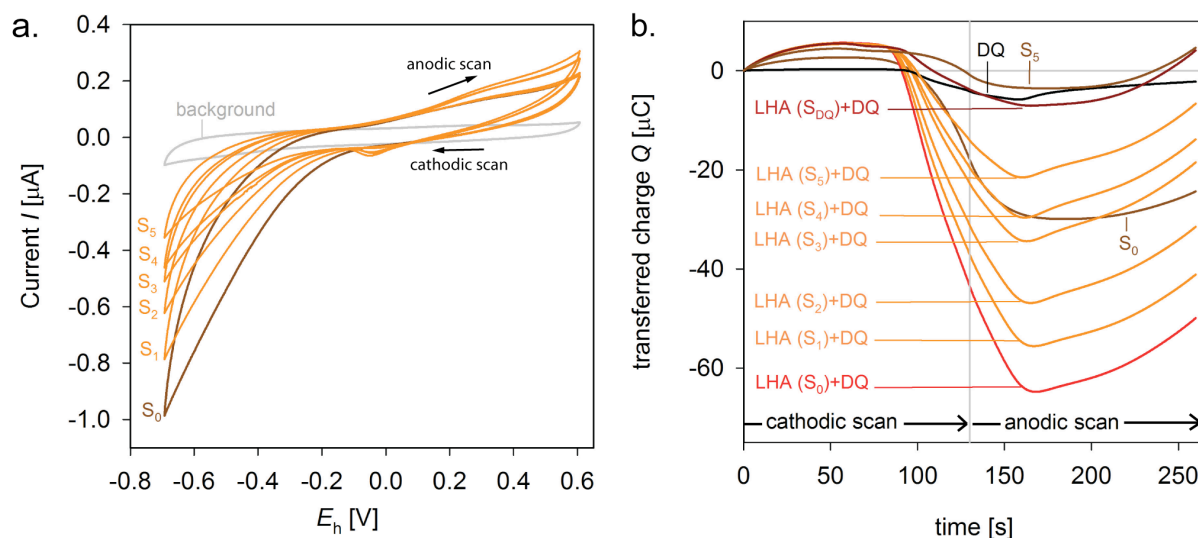
Figure S4. Effect of electrochemical pre-reduction of Leonardite humic acid (LHA) on its cyclic voltammograms (CVs) collected in the absence and in the presence of the electron transfer mediator diquat (DQ). **a.** CVs of LHA pre-reduced to different extents in the absence of DQ. The extent of pre-reduction increased from sample S_0 (unreduced) to S_5, as described in the manuscript. **b.** Results of chronocoulometric analysis of the CVs of (i) samples S_0 to S_5 and of sample S_{DQ} in the presence of small concentrations of DQ (C_{DQ}= 30 µM) (original CV data shown in Figure **1b** in the manuscript), (ii) of unreduced and extensively pre-reduced LHA (sample S_5) in the absence of DQ, and (iii) of only DQ (trace DQ). The vertical grey line represents the first vertex potential of E_h= -0.69 V at which the scanning direction was changed from cathodic to anodic. All CVs were measured at pH 7 in 0.1 M KCl and 0.1 M phosphate buffer and at scan rates of v= 0.01 V s^{-1}.
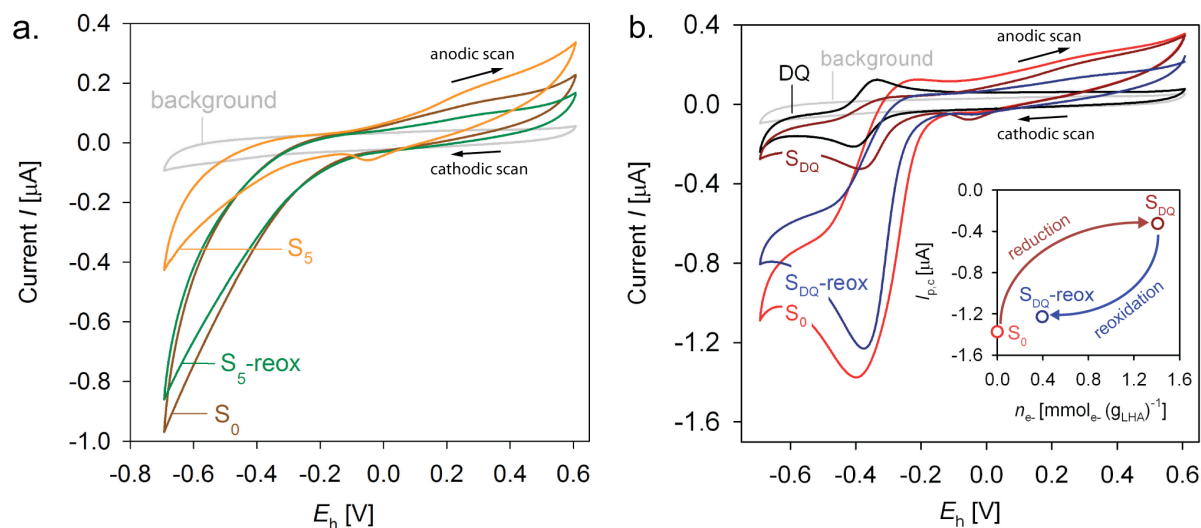
Figure S5. Effect of oxidation of pre-reduced Leonardite humic acid (LHA, C_{LHA}= 2gL^{-1}) with O$_2$ on the cyclic voltammograms (CVs) measured in the absence and presence of the electron transfer mediator diquat (DQ). **a.** CVs of unreduced LHA (sample S$_0$), electrochemically pre-reduced LHA (sample S$_5$), and sample S$_5$ re-oxidized by excess O$_2$ (sample S$_5$-reox) in the absence of mediator DQ. **b.** CV of unreduced LHA (sample S$_0$), electrochemically pre-reduced LHA (sample S$_{DQ}$), and sample S$_{DQ}$ re-oxidized by excess O$_2$ (sample S$_{DQ}$-reox) in the presence of small concentrations of DQ (C_{DQ}= 30 µM). Inset: Cathodic peak currents, $I_{p,c}$, versus the number of electrons n_{e-} transferred per unit mass LHA in samples S$_{DQ}$ and S$_{DQ}$-reox relative to the unreduced LHA in sample S$_0$. All CVs were measured at pH 7 in 0.1 M KCl and 0.1 M phosphate buffer and at scan rates of v= 0.01 V s^{-1}.
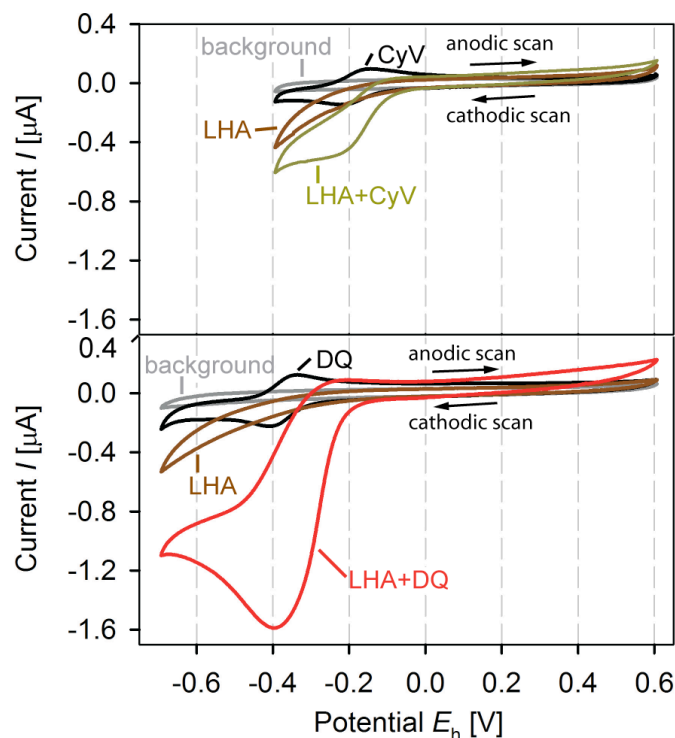
Figure **S6**. Cyclic voltammograms of background buffer (grey trace), of the redox mediators cyanoviologen (CyV; top) and diquat (DQ; bottom) (black traces; concentration $C_{mediator}$= 30 µM), of Leonardite humic acid standard (LHA) (brown trace; C_{LHA}= 2 gL^{-1}), and of LHA in the presence of CyV (yellow trace; top) and DQ (red trace; bottom) (C_{LHA}= 2 gL^{-1}; $C_{mediator}$= 30 µM).
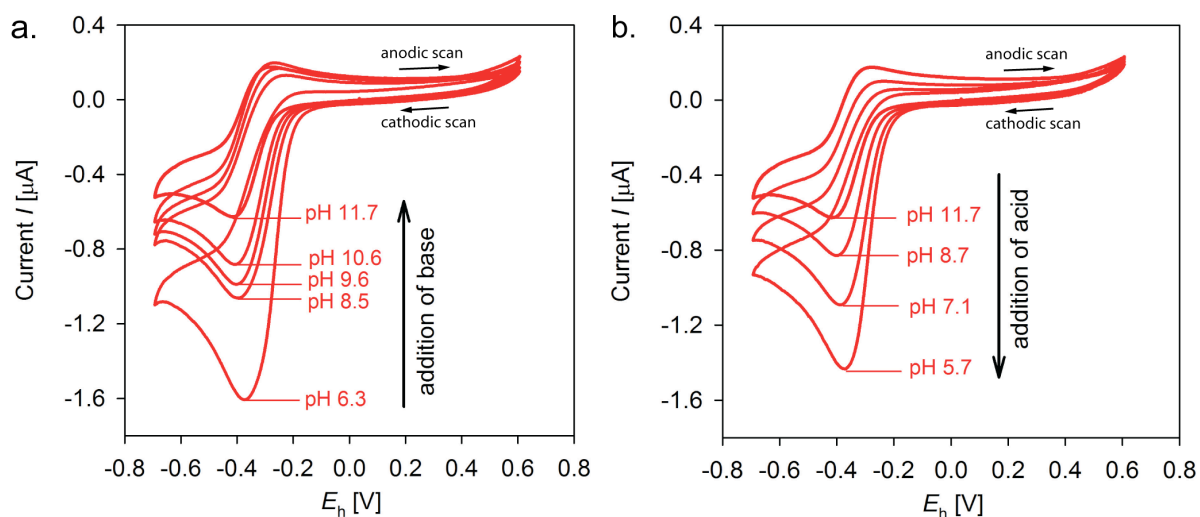
Figure S7. Effect of the solution pH on the cyclic voltammograms of Leonardite humic acid (LHA; 2 gL^{-1}; unreduced) in background electrolyte (0.1 M KCl) in the presence of small concentrations, C_{DQ}= 30 µM, of the electron transfer mediator diquat (DQ). **a.** Decreasing

108

catalytic cathodic currents and increasing shifts in the onsets of the cathodic waves towards lower reduction potentials E_h with increasing pH. **b.** Increasing catalytic cathodic currents and increasing shifts in the onset of the cathodic wave towards higher reduction potentials E_h with decreasing pH. All experiments were carried out at a scan rate $v = 0.01$ V s^{-1}.

Section S5. Model quinones

Table **S2** compiles literature values for the standard reduction potentials E_h^0 and the acidity constants, pK_a, for the tested model quinones.

Table S2. The chemical structures of the tested model quinones and the respective electron and proton transfer equilibria. $E_{h,12}^0$ and $E_{h,12}^0$ (pH 7) correspond to the standard reduction potentials at pH 0 and pH 7, respectively, for the two electron reduction from the quinone to the hydroquinone. The one electron reduction potentials $E_{h,1}^0$ and $E_{h,2}^0$ are given for AQ26DS and are depicted in Scheme **S1**. pK_{a1} and pK_{a2} are the two acidity constants for the hydroquinone, pK_{aSQ} the acidity constant for the semiquinone SQ, and $pK_{a,ox}$ corresponds to the acidity constants for the hydroxy moiety of the unreduced NQOH.

Name	Quinone structure	Semiquinone structure	Hydroquinone structure	$E_{h,12}^0$ [V]	$E_{h,12}^0$ (pH7) [V]	$pK_{a,ox}$	pK_{a1}	pK_{a2}	pK_{aSQ}	Comments
1,2-Naphthoquinone-4-sulfonate (NQSA)	(structure)	(structure)	(structure)	0.628 [a]		-	7.8 [a] 8.14 [d]	12.6 [d]	n.a.	
2-Hydroxy-1,4-naphthoquinone (NQOH)	(structure)	(structure)	(structure)	0.351 [a]	-0.152 [a]	4.0 [a]	8.7 [a]	10.7 [a]	4.7 [c]	
9,10-Anthraquinone-2,6-disulfonate (AQ26DS)	(structure)	(structure)	(structure)	0.229 [a]	-0.182 [a]	-	8.1 [a] 7.5 [b]	10.5 [a]	3.2 [c]	$E_{h,1}^0$ = -0.066 [V] [e] $E_{h,2}^0$ = 0.522 [V] [e]
9,10-Anthraquinone-1,5-disulfonate (AQ15DS)	(structure)	(structure)	(structure)	0.239 [a]	-0.174 [a]	-	11.5 [a]	n.m. [a]	3.9 [b]	

References: [a] [9], [b] [1], [c] [4], [d] [10], [e] [11], n.m.: not measureable, n. a.: not available

Electron and proton transfer equilibria to 9,10-Anthraquinone-2,6-disulfonate (AQ26DS). The electron and proton transfer equilibrium constants in equations **S5** to **S12** have been reported in the literature for the model quinone AQ26DS (see Table **S2**). The compiled values were used to calculate the equilibrium speciation of AQ26DS as a function of solution pH and reduction potential E_h. The results of the calculations are shown in Figure **S8a**. Notably, reduction of AQ26DS (= species Q in scheme **S1**) at pH < pK_{a1} results in the formation of AQDSH$_2$ as predominant species as the standard reduction potential for the first electron transfer from AQDS to AQDSH$^{\bullet}$ is lower than that for the second electron transfer from AQDSH$^{\bullet}$ to AQDSH$_2$. The semiquinone species AQDSH$^{\bullet}$ or AQDS$^{\bullet-}$ become predominant only at high pH and at intermediate extents of reduction (depicted by the orange area in Figure **S8a**).

Figure S**8b** shows a Pourbaix E_h-pH diagram for AQ26DS. This diagram is a projection of the species distribution in Figure **S8a** onto the E_h-pH plane [12]. The predominant species in each stability field are given in bold letters. The lines in the diagram correspond to equal concentrations of the respective oxidized and reduced or protonated and deprotonated species. Solid and dashed lines are for the predominant and minor species, respectively.

The reduction potential E_h for the AQ26DS system was also calculated at different pH values as a function of the degree of reduction, expressed as conversion factor r (Figure **S9a**). At high pH >11, electron transfer to AQ26DS is no longer coupled to proton transfer, resulting in overlapping E_h-r curves at pH 11 and 13. At these pH values, redox buffering occurred over a wider E_h range as compared to lower pH ≤9. The wider buffering range reflects that the semiquinone is formed from the quinone at a higher reduction potential than the potential for the reduction of the semiquinone to the fully deprotonated hydroquinone (diphenolate). Conversely, at lower pH ≤9, the reduction proceeds directly from the quinone to the hydroquinone.

Figure S**9b** shows the ratio of protons and electrons, $n_{H+}(n_{e-})^{-1}$, transferred to AQ26DS as a function of the conversion factor r. At low pH the final $n_{H+}(n_{e-})^{-1}$ is close to unity, reflecting that the transfer of 2e$^-$ to the quinone to form the hydroquinone is coupled to the transfer of 2H$^+$. Increasing the pH results in

111

successive deprotonation of the hydroquinone and therefore in decreasing final $n_{H+}(n_{e-})^{-1}$. The gradual increase in $n_{H+}(n_{e-})^{-1}$ with r, particularly evident at high pH, is due to the formation of the semiquinone which is not coupled to the transfer of protons at pH $>pK_{aSQ} = 3.2$. Subsequent electron transfer to the semiquinone to form the fully reduced hydroquinone species is coupled to the transfer of up to two protons per electron. Figure **S9c** shows the theoretical E_h-pH curves of AQ26DS at different degrees of reduction, expressed by the conversion factor r. For a given pH and r, the slope of the E_h-pH curve corresponds to the $n_{H+}(n_{e-})^{-1}$ multiplied by -0.059 V (for T= 25°C).
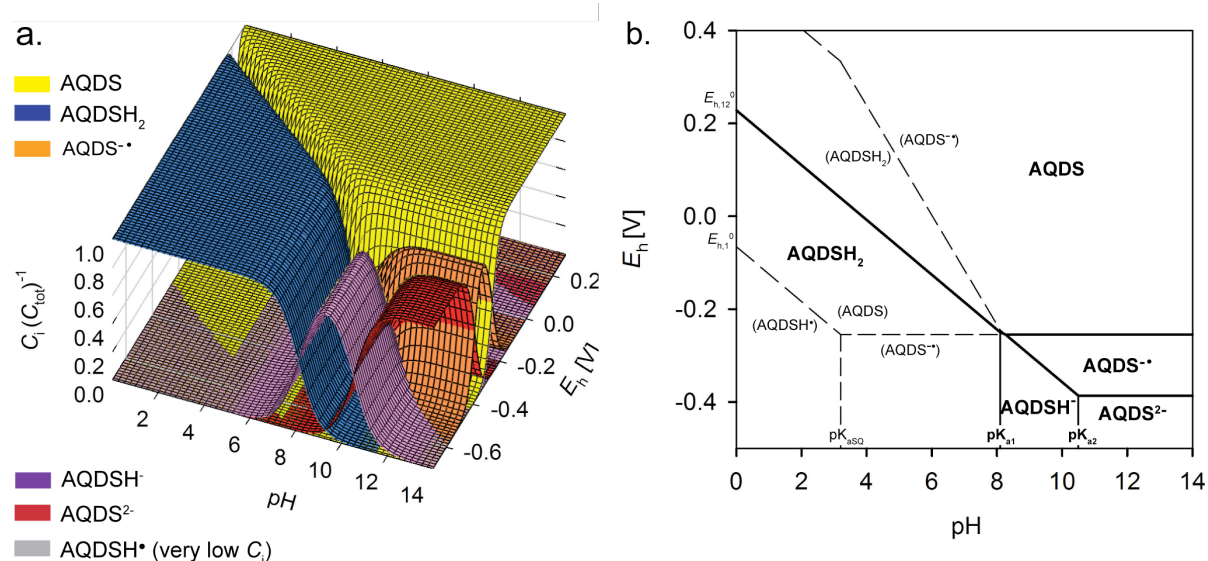
Figure S8. **a.** Distribution of 9,10-Anthraquinone-2,6-disulfonate (AQ26DS) species as a function of pH and reduction potential E_h. The species are the oxidized anthraquinone (AQDS; yellow), the hydroquinone (AH₂QDS; blue), the semiquinone radical (AHQDS$^{\bullet}$; grey, present at only very small concentrations), the semiquinone radical anion (AQDS$^{\bullet-}$; orange), the hydroquinone monophenolate (AHQDS$^-$; purple), and the hydroquinone di-phenolate (AQDS^{2-}; red) **b.** Pourbaix diagram for AQ26DS.
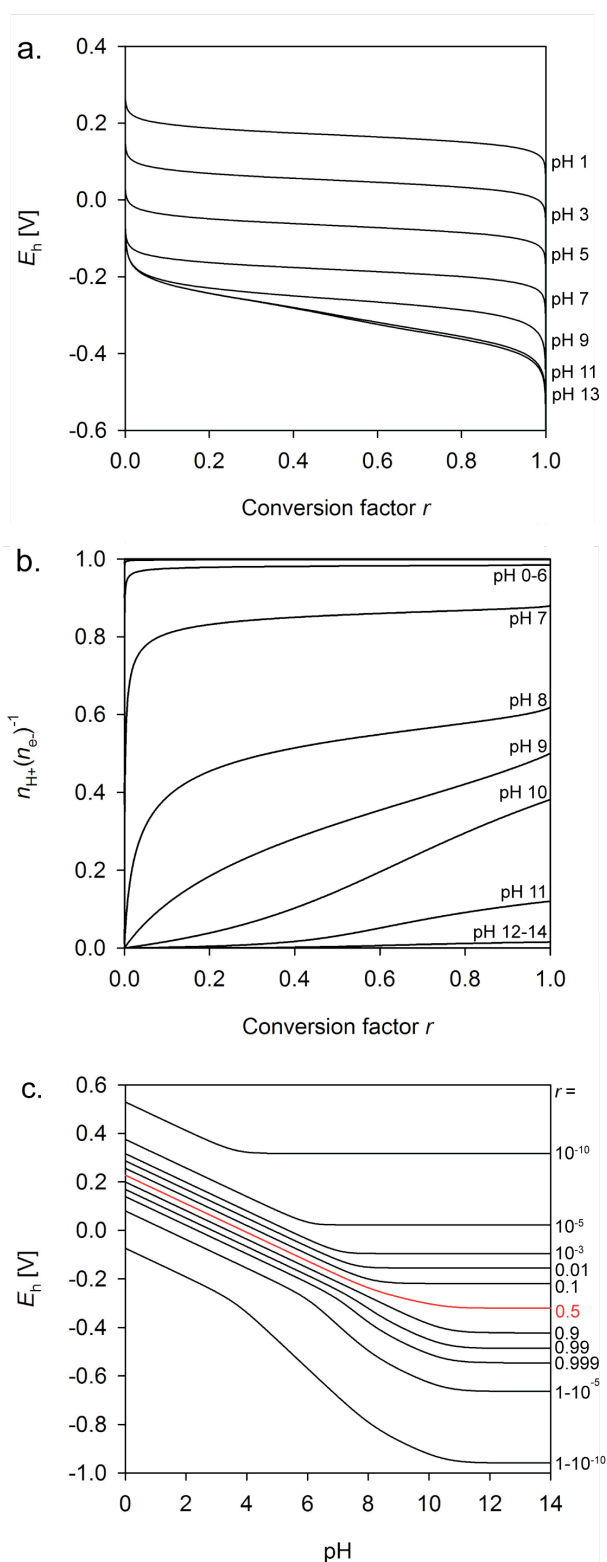
Figure S9. **a.** Change in AQ26DS reduction potential E_h with increasing degree of reduction, expressed as conversion factor r, at different solution pH. **b.** Change in the ratio of protons to electrons, $n_{H+}(n_{e-})^{-1}$, transferred to AQ26DS with increasing r at different pH. **c.** Change in E_h with increasing pH at different r.

Calculation of final $n_{H^+}(n_{e^-})^{-1}$ ratios for the complete reduction of model quinones. The final $n_{H^+}(n_{e^-})^{-1}$ ratios were calculated under the assumption of complete reduction (i.e. *r* close to 1). Under these conditions, the equilibrium concentration of the semiquinone is very small and was neglected in the calculations.

(i) AQ26DS, AQ15DS, NQSA. Equations **S5** and **S6** (Q = AQ26DS, AQ15DS, or NQSA) were combined by mass balancing the predominant quinone species, as described in equation **S23**. Note that the semiquinone concentration could be neglected under the assumption of complete quinone reduction (i.e., *r* approaches 1). The final ratio of protons and electrons, $n_{H^+}(n_{e^-})^{-1}$, transferred to the quinone was calculated as a function of pH using equation **S24**. For *AQ15DS,* formation of the quinolate species Q^{2-} was neglected due to the high $pK_{a2} = 12.6$ (Table **S2**).

$$[Q_{tot}] = [Q^{2-}] + [HQ^-] + [H_2Q] \tag{S23}$$

$$\left(\frac{n_{H^+}}{n_{e^-}}\right)_{final} = \frac{[HQ^-] + 2[H_2Q]}{2[Q_{tot}]} \tag{S24}$$

(ii) NQOH. Calculations on NQOH required accounting for the protonation equilibrium of the hydroxyl substituent on the 1,4-quinone system (Scheme **S2**), given by equation **S25**. The reduced species Q^{3-} was neglected in the calculations (Scheme **S2**) due to the (unknown) high pK_a value for the deprotonation of the third proton of the hydroquinone. The $n_{H^+}(n_{e^-})^{-1}$ ratio as a function of pH was calculated using equation **S26**.

114
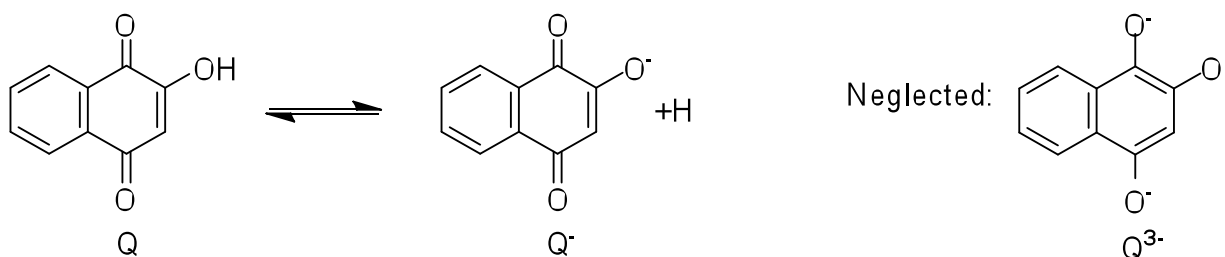
Scheme S2: Protonation equilibrium ($pK_a = 4$) for the hydroxyl substituent in NQOH.

$$pH = pK_{aox} + Log\left(\frac{[Q^-]}{[Q]}\right) \tag{S25}$$

$$\left(\frac{n_{H^+}}{n_{e-}}\right)_{final} = \frac{3[H_2Q] + 2[HQ^-] + [Q^{2-}] - [Q]}{2[Q_{tot}]} \tag{S26}$$

Calculation of E_h-pH dependencies of NQOH and NQSA. The extent of reduction (i.e., the conversion factor r) of the quinone remains constant in E_h-pH titrations in which there is no electron transfer to and from the quinone. Figure **S10** shows the calculated E_h-pH dependencies for AQ26DS at different degrees of reduction, expressed by the conversion factor r (grey dashed lines) The E_h-pH dependencies for NQOH and NQSA were calculated for a conversion factor $r = 0.5$. At this r, the semiquinone radical could be omitted from the calculation because the concentration of the fully oxidized species (i.e., the quinone) equals the total concentration of fully reduced species (i.e., the hydroquinone and its mono- and diphenolate), independent of solution pH. Equations **S8** and **S9** were replaced by equation **S27** and equation **S12** was replaced by equation **S28**. The E_h-pH dependencies for NQSA were calculated by combining equations **S5**, **S6**, **S27**, and **S28**. Calculations for NQOH also accounted for the protonation equilibrium of the hydroxy substituent (equation **S25**).

$$E_h = E^0_{h,12} - \frac{a}{2} Log\left(\frac{[H_2Q]}{[Q](10^{-pH})^2}\right) \tag{S27}$$

$$r = \frac{n_{e-}}{2[Q]_{tot}} = \frac{[Q^{2-}] + [HQ^-] + [H_2Q]}{[Q] + [Q^-] + [Q^{2-}] + [HQ^-] + [H_2Q]} = 0.5 \tag{S28}$$
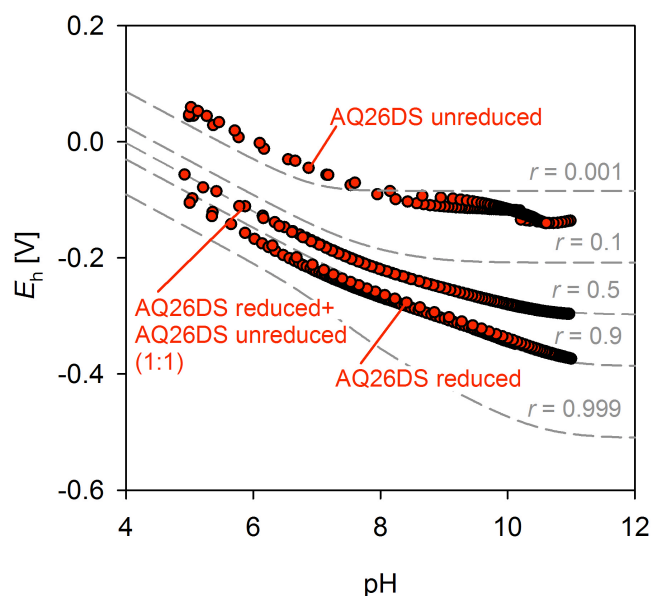
Figure S10. Dependence of the reduction potential E_h of 9,10-Anthraquinone-2,6-disulfonate (AQ26DS) on the solution pH and the extent of AQ26DS reduction. The red circles correspond to experimental data for AQ26DS at different degrees of reduction. The grey dashed lines correspond to the calculated E_h-pH dependencies calculated from literature reduction potentials and pK_a values of the major AQ26DS species, as a function of the conversion factor r. r varies between 0 and 1 for unreduced and fully reduced AQ26DS, respectively. The experimental and calculated dependencies are in good agreement. The higher variations in the experimental data for unreduced AQ26DS likely resulted from the low redox buffering in these systems (very low concentrations of reduced species).

Section S6. Potentiometric E_h-pH titrations of humic acids
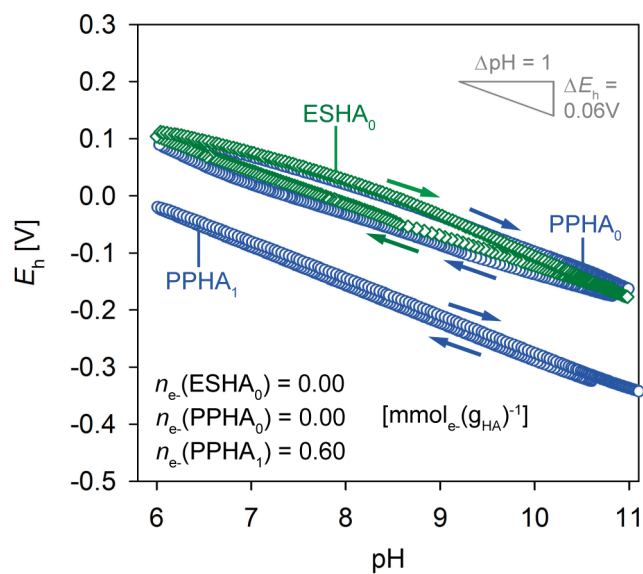
Figure S11. Potentiometric E_h-pH titration curves for unreduced Elliott soil humic acid (ESHA$_0$) and unreduced and reduced Pahokee Peat humic acid (PPHA$_0$ and PPHA$_1$, respectively). The arrows indicate the direction of titration. n_{e^-} corresponds to the number of electrons transferred per unit mass of HA.

Table S3. Slopes of E_h-pH curves obtained from redox titrations of Leonardite humic acid (LHA), Suwanee River humic acid (SRHA), Elliot soil humic acid (ESHA), and Pahokee Peat humic acid (PPHA) at different extents of reduction, expressed as the number of electrons transferred, n_{e-}, per unit mass of HA. $\Delta E_h(\Delta pH)^{-1}$ values correspond to the slopes of the titration curves, Δt specifies the duration of the base and acid titrations between pH 6 and pH 10.5. E_h (pH 7) corresponds to the measured reduction potential at pH 7.

Humic acid	Titration direction	Extent of reduction n_{e-} [mmol$_{e-}$(g$_{HA}$)$^{-1}$]	$\Delta E_h (\Delta pH)^{-1}$ [V] [a] average ± stdev		Δt [h] pH 6-10.5	E_h (pH 7) [V]	E_h (pH 9) [V]
			pH 7-8	pH 6-10.5			
LHA	pH down	0	-0.056±0.004	-0.055±0.007	28	0.123	0.011
	pH up	0	-0.042±0.002	-0.049±0.013	13	0.143	0.054
	pH down	0.54	-0.058±0.003	-0.059±0.005	13	-0.081	-0.196
	pH up	0.54	-0.066±0.005	-0.060±0.013	43	-0.077	-0.200
	pH down	1.15	-0.060±0.002	-0.060±0.005	14	-0.201	-0.328
	pH up	1.15	-0.062±0.002	-0.060±0.007	22	-0.198	-0.320
SRHA	pH down	0	-0.063±0.016	-0.062±0.016	23	-0.011	-0.145
	pH up	0	-0.054±0.013	-0.064±0.021	27	0.022	-0.104
	pH down	0.38	-0.063±0.013	-0.072±0.016	22	-0.099	-0.236
	pH up	0.38	-0.091±0.017	-0.077±0.023	27	-0.067	-0.249
ESHA	pH down	0	-0.058±0.010	-0.058±0.018	23	0.043	-0.069
	pH up	0	-0.048±0.009	-0.059±0.019	28	0.076	-0.033
PPHA	pH down	0	-0.053±0.009	-0.057±0.013	26	0.02	-0.087
	pH up	0	-0.050±0.008	-0.054±0.018	28	0.068	-0.035
	pH down	0.6	-0.069±0.013	-0.068±0.012	26	-0.089	-0.224
	pH up	0.6	-0.065±0.007	-0.065±0.009	27	-0.081	-0.210

[a] Calculated as $\frac{1}{n}\sum_{i=1}^{n}\frac{E_h(pH_{i+1}) - E_h(pH_i)}{pH_{i+1} - pH_i}$, where i and $i+1$ are two consecutive data points on the E_h-pH titration curve.
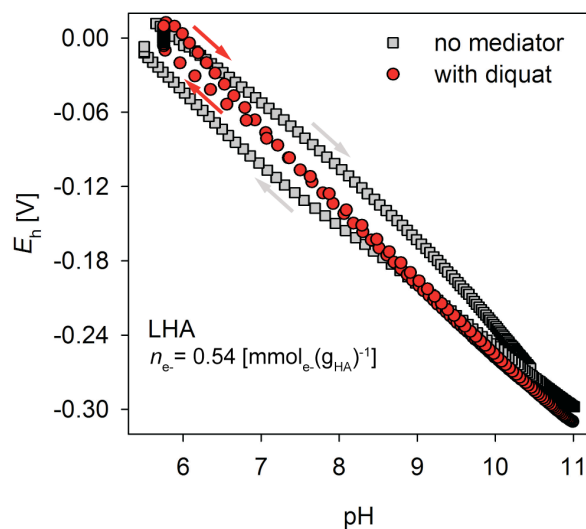
Figure S12. Potentiometric E_h-pH curves of reduced Leonardite humic acid (2 gL^{-1}; pH 7, n_{e-} = 0.54 mmol$_{e-}$(g$_{LHA}$)$^{-1}$) in the absence and in the presence of small concentrations of the redox mediator diquat (C_{DQ}= 28 µM). The arrows indicate the titration direction. The E_h-pH data in the presence of DQ is reproduced from Figure **4d** in the manuscript. The figure shows that DQ facilitates attainment of redox equilibria, and thereby eliminates hysteresis in the E_h-pH titration data.

Section S7. Change in the reduction potential E_h with increasing extent of HA reduction

Figure **S13** shows the dependencies of the reduction potentials E_h on the number of transferred electrons, n_{e-}, per unit masses of Leonardite humic acid (LHA) (panel a) and of Elliot Soil humic acid (ESHA) (panel b), both at pH 7.

119
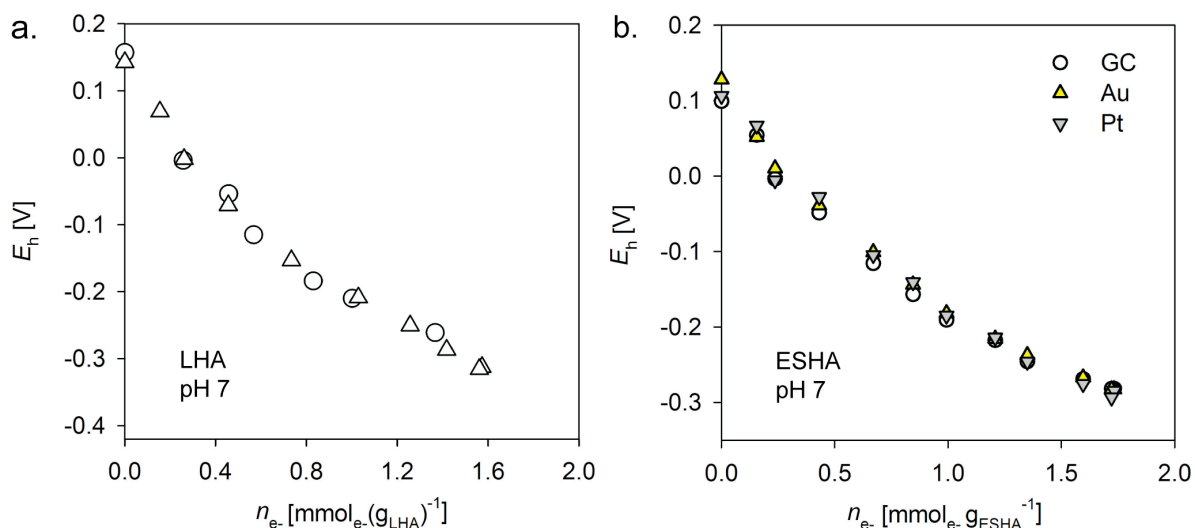
Figure S13. a. Reproducibility of the decrease in the reduction potential E_h with increasing number of electrons, n_{e-}, transferred per unit mass of Leonardite humic acid standard (LHA). The circles and triangles represent measurements from two independent reduction experiments. **b.** Decrease in E_h of Elliott Soil humic acid Standard (ESHA) samples (1 gL^{-1}; pH 7) with increasing n_{e-}, as measured by a Pt ring redox electrode, a gold ring redox electrode, and a glassy carbon (GC) electrode.
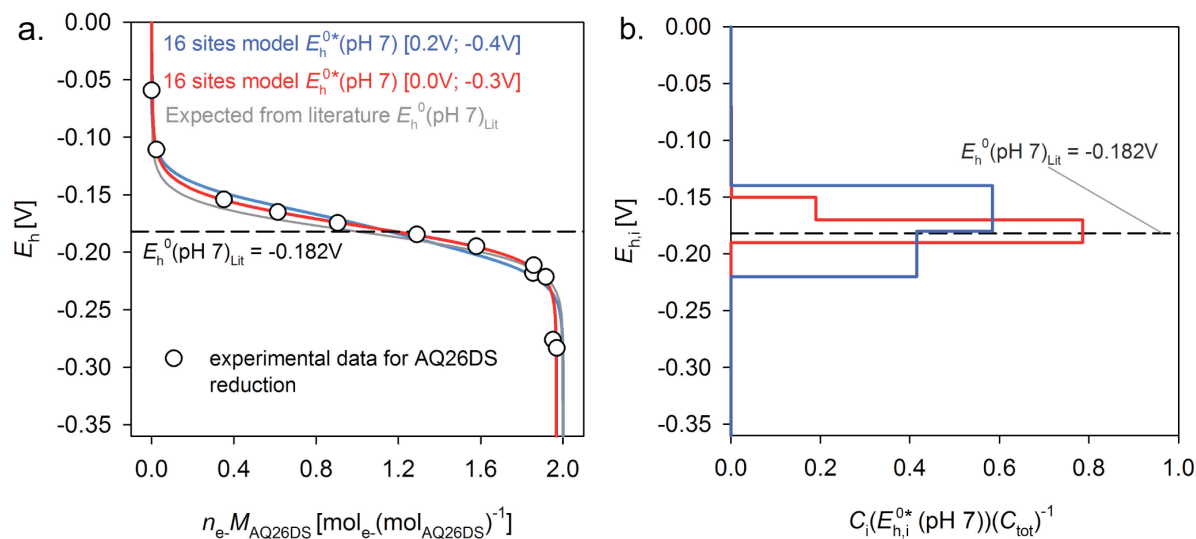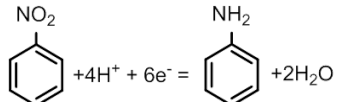
Figure S14. a. Decrease in the reduction potential, E_h, of 9,10-Anthraquinone-2,6-disulfonate (AQ26DS) with increasing extent of reduction as expressed by the number of electrons, n_{e-}, transferred per unit number of quinone. The circles correspond to experimental data. The blue and red curves correspond to the fits of equation S21 to the experimental data with different widths of the fitted potential range. The quality of the fit improved when the potential window was narrowed from $0.2 > E_h > -0.4$ V (blue curve) to $0 > E_h^0 > -0.3$ V (red curve). The

measured data and the model fits agree well with the E_h-n_{e^-} curve calculated from the literature value, E_h^0(pH 7)$_{Lit}$= -0.182 V (grey line) (Table **S2**). **b**. Fitted "distributions" of standard reduction potentials of AQ26DS. The fits in panel a resulted in averaged E_h^0(pH 7) values of -0.173 V and -0.177 V, which corresponded well the to published value of E_h^0(pH 7)$_{Lit}$= -0.182 V (see Table **S2**).

Section S8. Reduction potentials of biogeochemical and pollutant redox couples

Table S4. Reaction equations and corresponding reduction potentials for the biogeochemical and pollutant redox couples shown in Figure **6** in the manuscript.

Ox + m H$^+$ + n e$^-$ = Red	E_h^0 [V]	E_h^0(pH 7)[a] [V]	E_h(pH 7)[b] [V]	Reference
Biogeochemical redox couples				
$O_2(aq) + 4H^+ + 4e^- = 2H_2O$	1.190	0.777	0.777	[13]
$2NO_3^- + 12H^+ + 10e^- = N_2(g) + 6H_2O$	1.240	0.744	0.744	[13]
$NO_3^- + 2H^+ + 8e^- = NO_2^- + H_2O$	0.850	0.437	0.437	[13]
$MnO_2 + 4H^+ + 2e^- = Mn_2^+(10^{-6}\,M) + 2H_2O$	1.224	0.398	0.575	[14]
$NO_3^- + 10H^+ + 8e^- = NH_4^+ + 3H_2O$	0.880	0.364	0.364	[13]
$Fe(OH)_3$ (amorph) $+ e^- + 3H^+ = Fe^{2+}$ (10^{-6} M) + $3H_2O$	0.948	-0.291	0.062	calc[c]
α-FeOOH $+ 3H^+ + e^- = Fe^{2+}$ (10^{-6} M) $+ 2H_2O$	0.670	-0.569	-0.216	calc [c]
$SO_4^{2-} + 9H^+ + 8e^- = HS^- + 4H_2O$	0.250	-0.215	-0.215	[13]
$CO_2(g) + 8H^+ + 8e^- = CH_4(g) + 2H_2O$	0.170	-0.243	-0.243	[13]
$2H^+ + 2e- = H_2(aq)$	0.080	-0.333	-0.333	[13]
Inorganic pollutants				
$HCrO_4^- + 7H^+ + 3e^- = Cr^{3+} + 4H_2O$	1.350	0.386	0.386	[14]
$SeO_4^{2-} + 4H^+ + 2e^- = H_2SeO_3 + H_2O$	1.150	0.324	0.324	calc [c]
TcO_4^- (10^{-6} M) $+ 4H^+ + 3e^- = TcO_2 + 2H_2O$	0.782	0.231	0.113	[14]
$Cu^{2+} + e^- = Cu^+$	0.153	0.153	0.153	[14]
$UO_2(CO_3)_2^{2-}$ (10^{-6} M) $+ 2H^+ + 2e^- = UO_2 + 2HCO_3^-$ (10^{-3} M)	0.521	0.108	0.108	[15]
$HAsO_4^{2-} + 4H^+ + 2e^- = H_3AsO_3 + H_2O$		-0.014	-0.014	[16]
Organic pollutants				
$CCl_4 + H^+ + 2e^- = CHCl_3 + Cl^-$ (10^{-3} M)	0.790	0.584	0.672	[13]
$CHCl_3 + H^+ + 2e^- = CH_2Cl_2 + Cl^-$ (10^{-3} M)	0.680	0.474	0.562	[13]
	0.830	0.417	0.417	[13]

[a] Standard reduction potential at pH 7 E_h^0(pH 7) (i.e. standard conditions except for the pH) calculated from E_h^0 using equation S4. [b] Reduction potentials at pH 7, E_h(pH 7), shown in Figure **6** in the manuscript. E_h(pH 7)

values were calculated from E_h^0 values using equation S4. For reactions involving solid phases, the activities of the dissolved species were set to 10^{-6} M and the activity of HCO_3^- was set to 10^{-3} M. In all other cases the same activities were assumed for the reduced and oxidized species. [3] Calculated from standard Gibbs energies of formation (Table **S5**). All calculations assumed T= 25°C.

Table S5. Standard Gibbs energies of formation, ΔG_f^0, used for the calculation of reduction potentials in Table **S4**.

Species	ΔG_f^0 [J mol^{-1}]	Reference
SeO_4^{2-} (aq)	-441.40	[17]
H_2SeO_3 (aq)	-426.20	[17]
α-FeOOH (Goethite)	-488.60	[17]
$Fe(OH)_3$ (amorphous)	-699.00	[17]
Fe^{2+}(aq)	-78.87	[17]
H_2O (l)	-237.18	[17]

References Supporting Information Chapter 3

1.   Gamage, R.; McQuillan, A. J.; Peake, B. M., Ultraviolet visibile and electron paramagnetic resonance spectroelectrochemical studies of the reduction products of some anthraquinone sulfonates in aqueous solutions *J. Chem. Soc. Faraday. T.* **1991,** *87,* (22), 3653-3660.

2.   Laviron, E., Electrochemical reactions with protonations at equilibrium. 8. The 2 e-, 2 H+ reaction (9-member square scheme) for a surface or for a heterogeneous reaction in the absence of disproportionation and dimerization reactions. *J. Electroanal. Chem.* **1983,** *146,* (1), 15-36.

3.   Rich, P. R.; Bendall, D. S., Mechanism for the reduction of cytochromes by quinols in solution and its relevance to biological electron-transfer reactions. *Febs Letters* **1979,** *105,* (2), 189-194.

4.   Rao, P. S.; Hayon, E., Ionization-Constants and Spectral Characteristics of Some Semiquinone Radicals in Aqueous-Solution. *J Phys Chem-Us* **1973,** *77,* (19), 2274-2276.

5.   Wilson, R. L., Semiquinone Free Radicals - Determination of Acid Dissociation Consttants by Pulse Radiolysis. *J Chem Soc Chem Comm* **1971**, (20), 1249-&.

6.   Pal, H.; Palit, D. K.; Mukherjee, T.; Mittal, J. P., One-Electron Reduction of Anthraquinone Sulfonates - a Pulse-Radiolysis Study. *Radiat Phys Chem* **1991,** *37,* (2), 227-235.

7.   Hamann, C. H.; Hamnett, A.; Vielstich, W., *Electrochemistry.* 2nd ed.; Wiley-VCH Verlag: Weinheim, 2007.

8.   Aeschbacher, M.; Sander, M.; Schwarzenbach, R. P., Novel electrochemical approach to assess the redox properties of humic substances. *Environ. Sci. Technol.* **2010,** *44,* (1), 87-93.

9.   Clark, W., *Oxidation-Reduction Potentials of Organic Systems.* Baltimore, 1960.

10.   Buffle, J.; Martell, A. E., Metal-Ion Catalyzed Oxidation of Ortho-Dihydroxy Aromatic-Compounds by Oxygen .1. Redox and Acid-Base Properties of System 1,2-Naphthoquinone-4-Sulfonate-1,2-Dihydroxynaphthalene-4-Sulfonate. *Inorg Chem* **1977,** *16,* (9), 2221-2225.

11. Rosso, K. M.; Smith, D. M. A.; Wang, Z. M.; Ainsworth, C. C.; Fredrickson, J. K., Self-exchange electron transfer kinetics and reduction potentials for anthraquinone disulfonate. *J Phys Chem A* **2004,** *108*, (16), 3292-3303.

12. Bailey, S. I.; Ritchie, I. M.; Hewgill, F. R., The Construction and Use of Potential-Ph Diagrams in Organic Oxidation-Reduction Reactions. *J Chem Soc Perk T 2* **1983**, (5), 645-652.

13. Schwarzenbach, R. P.; Gschwend, P. M.; Imboden, D. M., *Environmental organic chemistry*. 2nd ed.; Wiley: Hoboken, N.J., 2003; p xiii, 1313 p.

14. Haynes, W. M. e., CRC handbook of chemistry and physics. In 91st ed. ed.; CRC Press: Boca Raton, 1999.

15. Brooks, S. C.; Fredrickson, J. K.; Carroll, S. L.; Kennedy, D. W.; Zachara, J. M.; Plymale, A. E.; Kelly, S. D.; Kemner, K. M.; Fendorf, S., Inhihition of bacterial U(VI) reduction by calcium. *Environmental Science & Technology* **2003,** *37*, (9), 1850-1858.

16. Islam, F. S.; Gault, A. G.; Boothman, C.; Polya, D. A.; Charnock, J. M.; Chatterjee, D.; Lloyd, J. R., Role of metal-reducing bacteria in arsenic release from Bengal delta sediments. *Nature* **2004,** *430*, (6995), 68-71.

17. Stumm, W.; Morgan, J. J., *Aquatic chemistry: chemical equilibria and rates in natural waters*. 3rd ed.; Wiley: New York, 1996; p xvi, 1022 p.

Chapter 4

Antioxidant properties of humic substances

This Chapter is in review for publication in *Environmental Science and Technology*:

Michael Aeschbacher, Cornelia Graf, René P. Schwarzenbach, Michael Sander; Antioxidant properties of humic substances

Abstract

Humic substances (HS) are heterogeneous, redox-active organic macromolecules. While electron transfer to and from HS under reducing conditions is well investigated, comparatively little is known on the electron donating properties of HS under oxic conditions. In this work the electron donating capacities (EDCs) of HS were determined as a function of the redox potential E_h and the pH using electrochemical oxidation with 2,2'-azino-bis(3-ethylbenzthiazoline-6-sulfonic acid) as electron transfer mediator. Electrochemical oxidation of three model HAs was largely irreversible and their EDCs continuously increased with increasing E_h and pH. The results suggest that HS contain moieties that donate electrons over a wide potential range and that oxidation of these moieties is coupled to the release of protons. At a given pH and E_h, the EDCs of HS correlated well with their titrated phenol contents, consistent with phenolic moieties as major electron donating groups in HS. Comparing the EDCs of 15 HS with their electron accepting capacities (EACs) determined in earlier work, aquatic HS had higher EDCs but lower EACs than terrestrial HS of comparable aromaticities. The results indicate that oxidative transformation of HS in the environment result in a depletion of electron donating phenolic moieties relative to the electron accepting quinone moieties.

4.1. Introduction

Humic substances (HS) are mixtures of complex organic macromolecules that play important roles in biogeochemical and in pollutant redox reactions. For these reasons, HS redox properties have received considerable interest. Previous studies focused primarily on assessing HS electron accepting and donating properties under reducing conditions.[1-9] Several studies reported largely reversible electron transfer to the reducible moieties in HS,[1, 5, 7] and strong correlations of HS electron accepting capacity (EAC) (i.e., the moles of electrons transferred to a given HS mass at a given pH and reduction potential E_h) with HS aromaticity.[2, 4, 7] Furthermore, reduction of HS was found to occur over wide potential ranges and to be coupled to pH-dependent proton uptake.[8] These findings suggested quinones as major reducible moieties in HS. [2, 4-6]

Comparatively little is known about the electron donating properties of HS under oxic conditions. In previous studies, HS electron donating capacities (EDCs) (i.e., the moles of electrons donated by a given HS mass at a given pH and applied potential E_h) were quantified indirectly by measuring the reduction of added chemical oxidants (e.g., ferricyanide, Fe^{3+} citrate, and iodine) in batch equilibration experiments or by potentiometric redox titrations.[6, 10-16] Polyphenolic moieties from higher plant precursors, including lignin and tannins, were suggested as major electron donating moieties, based on the findings of increasing EDCs with increasing solution pH,[11-16] the release of protons upon oxidation of a humic acid (HA),[11] and comparable pH dependencies of the redox titration curves of a HA and of phenol and hydroquinone mixtures.[11]

Polyphenols have antioxidant properties.[17, 18] Phenolic moieties in HS are therefore expected to affect the concentration and lifetimes of reactive oxidants in soils and aquatic systems and thereby affect a number of important processes. Phenolic moieties in HS may protect other functional groups from oxidative breakdown and therefore play an important role in the environmental recalcitrance of HS.[19-21] Furthermore, recent evidence suggests beneficial effects of the antioxidant properties of HS on the activity of soil-dwelling organisms: exposure of the nematode *Caenorhabditis elegans* to HS enriched with electron donating moieties increased its tolerance to thermal stress and extended its

lifespan.[22] The antioxidant properties of HS likely also affect the redox dynamics of other chemical species in natural and engineered systems. For instance, dissolved HS may decrease indirect photolysis of organic pollutants in surface waters both by quenching reactive oxygen species and by donating electrons to radical pollutant intermediates, thereby reducing them back to parent pollutant molecules.[23, 24] Similar inhibitory effects of HS are conceivable for oxidative pollutant transformations in other systems, for instance on manganese dioxide surfaces in soils.[25, 26] In water treatment facilities, electron donation by HS increases the amount of chemical oxidants that is required to disinfect and remove pollutants from the water.[27-29] Despite the importance of HS antioxidant properties, they have been so far only poorly characterized.

The main objective of this work was to characterize HS antioxidant properties as a function of E_h, pH, and HS source material to obtain insight into the reactivity and the chemical nature of the oxidizable moieties in HS. To this end, we quantified the EDCs of a representative number of terrestrial and aquatic HS and NOM samples over wide E_h and pH ranges. We used mediated electrochemical oxidation (MEO), a novel approach that relies on the use of 2,2'-azino-bis(3-ethylbenzothiazoline-sulfonic acid) to mediate electron transfer from the oxidizable moieties in HS to the working electrodes. Finally the EDC values of the studied HS were compared to their respective EAC values[7] to assess the effects of HS origin and transformation history on HS redox properties.

4.2. Materials and Methods

Chemicals. Diquat dibromide monohydrate (DQ, 99.5%) was from Supelco. Sodium hydroxide, hydrochloric acid, acetic acid, potassium chloride, boric acid, sodium bicarbonate, citric acid monohydrate (all puriss. p.a.), and 2,2'-azino-bis(3-ethylbenzthiazoline-6-sulfonic acid) diammonium salt (> 99%) (ABTS) were from Fluka. Sodium phosphate dibasic dihydrate (puriss. p.a.) was from Sigma.

Humic substances, natural organic matter samples, and model antioxidants. Aldrich humic acid (AHA) was from Sigma-Aldrich. All other humic and fulvic acids (HA and FA) and the NOM samples were from the International Humic Substances Society (St. Paul, MN, USA) and included

Suwannee River HA Standard II (SRHA), Elliott Soil HA Standard (ESHA) and FA Standard III (ESFA), Leonardite HA Standard (LHA), Pahokee Peat HA Standard II (PPHAS), HA Reference (PPHAR), and FA Standard II (PPFA), Washkish Peat HA Reference (WPHA), Nordic Aquatic HA (NAHA) and FA (NAFA) References, Pony Lake FA Reference (PLFA), and Suwannee River and Nordic Reservoir NOM (SRNOM and NRNOM). Lignin (alkali; average molecular weight ~10,000 Da), L-ascorbic acid ($\geq$ 99.0%) were from Fluka, and ($\pm$)-6-Hydroxy-2,5,7,8-tetramethylchromane-2-carboxylic acid (Trolox®; 97%) was from Aldrich.

Solutions. All solutions were prepared with nanopure water (resistivity> 18 MΩcm; Barnstead NANOpure System). Solutions for electrochemical experiments contained 0.1M KCl as electrolyte and 0.1 M of pH buffers (acetate at pH 5; citrate at pH 6; phosphate at pH 7, 8, and 12, borate at pH 9 and 10, and carbonate at pH 10 and 11).

Electrochemical experiments. All experiments were controlled with CHInstruments 630C or 630D electrochemical analyzers (Austin, TX) or an Autolab PG302 (EcoChemie B.V., Netherlands). Potentials were measured vs. Ag/AgCl but are reported vs. the standard hydrogen electrode (SHE).

Cyclic voltammetry experiments were conducted inside the glovebox (N_2 atmosphere, O_2 < 0.1 ppm; 25$\pm$1 °C) in 4-5 mL solutions with a 3 mm diameter glassy carbon disk working electrode, a platinum wire counter electrode (both Radiometer Analytical), and an Ag/AgCl reference electrode (Bioanalytical Systems Inc.). The WE was polished and cleaned before each series of scans.[8] Cyclic voltammograms (CVs) were collected in pH-buffered solutions in the absence of ABTS and SRHA, in the presence of either ABTS (concentration C_{ABTS}= 30 µM) or SRHA (C_{SRHA}= 0.1 to 2 gL^{-1}), and in the presence of ABTS (C_{ABTS}= 30 µM) and SRHA (various C_{SRHA}). The cathodic and anodic vertex potentials were at E_h= -0.1 V and + 0.9 V, respectively, and the scan rate was v= 0.01 Vs^{-1} unless stated differently.

HA bulk oxidation experiments to assess the reversibility of HA oxidation were conducted in an anoxic glovebox. Water, buffer solutions, and diluted acids and bases were made anoxic by purging with argon for two hours at 150°C and for one hour at room temperature prior to transfer to the glovebox. All other solutions were prepared inside the glovebox by dissolving the

chemicals in anoxic water or buffer. SRHA, LHA, and ESHA were dissolved in pH 7 solutions (0.1 M KCl, 0.1 M phosphate) at concentrations of 2 gL^{-1}. After dilution to 0.4 gL^{-1}, 121 mL of the solutions were transferred into electrochemical cells containing a reticulated vitreous carbon WE polarized to E_h= 0.725 V, an Ag/AgCl reference electrode, and a coiled platinum wire auxiliary electrode (all from Bioanalytical Systems). Over the course of the oxidation, small amounts of ABTS were repeatedly spiked to the cell to sustain electron transfer mediation. Decreasing mediation likely resulted from slow loss of ABTS$^{\bullet+}$ by reaction with oxidized HS components. The total moles of ABTS spiked were, however, small compared to the moles of electrons, $n_{e^-}^{bulk\ oxidation}$ [mmol$_{e^-}$ (g$_{HA}$)$^{-1}$], transferred from the HAs to the WE during bulk oxidation (i.e., 1.6% for ESHA and LHA and 2.4% for SRHA). $n_{e^-}^{bulk\ oxidation}$ were determined by direct integration of the oxidative currents. No background current correction was required because oxidative currents in solutions without HA were negligibly small. Over the course of the oxidation, aliquots were withdrawn from the cell and analyzed for changes in HS UV-visible light absorption (Varian Cary 100 Spectrophotometer; 1 cm Quartz Helma Suprasil® cells), in the EDCs of the HS by MEO (see below) at E_h= 0.725 V and pH 7 (i.e., the same E_h as used during bulk oxidation), and in the EACs of the HS by mediated electrochemical reduction (MER) at E_h= -0.49 V and pH 7, as described earlier.[7]

Mediated electrochemical oxidation (MEO) according to Aeschbacher et al.[7] was used to quantify the EDCs of HS, NOM, and model antioxidants Trolox® and ascorbic acid (chemical structures in Figure **S1**). MEO was carried out in electrochemical cells containing pH buffered solutions with the same electrodes as used for HA bulk oxidation. ABTS was spiked into the cell to a total concentration of C_{ABTS}^{total}= 0.13 mM, which was the lowest concentration at which EDCs were independent of C_{ABTS} (Figure **S2**). At this concentration ABTS was oxidized at the WE, resulting in oxidative current peaks. Baseline currents were re-attained upon attainment of redox equilibrium between the ABTS$^{\bullet+}$/ABTS couple and the WE. Small volumes of HS/NOM/antioxidant solutions were subsequently spiked into the electrochemical cell. Electron donation by the HS/NOM/antioxidant to ABTS$^{\bullet+}$ formed ABTS, which was rapidly re-oxidized at the WE, resulting in oxidative current peaks. Peak integration yielded the EDC. Trolox® and ascorbic acid served to validate the experimental setup. The EDCs of SRHA, ESHA, and LHA were determined

over a wide E_h and pH range (i.e., 0.548V to 0.725V and pH 5 to 12). The EDCs of all 15 HS and NOM samples were determined at E_h= 0.607V and 0.725V for pH 7 and at E_h= 0.607V for pH 9. The upper potential limit of E_h= 0.725V was chosen because higher applied E_h resulted in large background currents (> 100μA), likely due to ABTS-mediated oxidation of water and/or the WE material.

4.3. Results and Discussion

Validation of mediated electrochemical oxidation. Cyclic voltammetry was used to demonstrate that ABTS mediates electron transfer from SRHA, which was used as model HS, to the WE. The cyclic voltammograms (CVs) collected in solutions containing only ABTS showed fast and fully reversible one electron oxidation of ABTS to ABTS$^{\bullet+}$ with anodic and cathodic waves centered at E_h= 0.69V (Figures **1a** and **S3**), in good agreement with the reported standard reduction potential of E_h^0(ABTS$^{\bullet+}$/ABTS)= 0.68V.[30] The CVs collected in SRHA-containing solutions showed higher oxidative currents during anodic scanning at E_h> 0.6 than the CVs collected in background electrolyte solution (Figure **1a**), demonstrating that SRHA was directly oxidized at the WE. However, the CVs were featureless, suggesting sluggish electron transfer from the oxidizable moieties in SRHA to the WE. Conversely, the CVs collected in SRHA-solutions in the presence of low ABTS concentrations showed much higher oxidative currents during anodic scanning than the CVs in solutions containing either only ABTS or only SRHA. The anodic peak currents, $I_{p,a}$, in the SRHA-ABTS systems increased linearly with SRHA concentration, C_{SRHA}, up to about 0.5 g$_{SRHA}$ L^{-1} (inset Figure 1a; Figure **S4a** for all CVs). At higher C_{SRHA}, $I_{p,a}$ was no longer proportional to C_{SRHA} (data not shown), possibly due to passivation of the WE by adsorption of SRHA oxidation products. The finding of catalytic current peaks in the SRHA-ABTS systems and of linearity between $I_{p,a}$ and C_{SRHA} over a wide C_{SRHA} range demonstrate that ABTS effectively mediated the electron transfer from SRHA to the WE. Mediated oxidation is also evident from chronocoulometric analysis of the CVs: for instance, at C_{SRHA}= 0.5 gL^{-1}, each mole of ABTS mediated the transfer of up to 7.5 moles of electrons from SRHA to the WE (Figure **S4**).

We validated the MEO setup used to quantify EDC values by analyzing Trolox® and ascorbic acid (Vitamin C), two commonly used model antioxidants. In MEO, small volumes containing the analyte are spiked to pH-buffered solution containing ABTS in bulk electrolysis cells, followed by integration of the resulting oxidative current peaks. Figure **S5** shows that the MEO of Trolox® and Vitamin C at E_h= 0.607V and pH 7 resulted in sharp and baseline-separated oxidative current responses. Integration of these peaks yielded the numbers of electrons transferred, n_{e-}, which were linearly proportional to the moles of spiked antioxidant (insets in Figure **S5**). The slopes of the regression lines for Trolox® and Vitamin C were 1.95±0.01 and 1.88±0.02 $\text{mmol}_{e-}(\text{mmol}_{antioxidant})^{-1}$ (± half of the 95% confidence interval), respectively, in good agreement with the expected EDCs of 2 mmol_{e-} $(\text{mmol}_{antioxidant})^{-1}$ for both antioxidants at this E_h.[31] Thus the recovery by MEO was 98±1 % and 94±1 % of the EDC of spiked Trolox ® and Vitamin C, respectively.
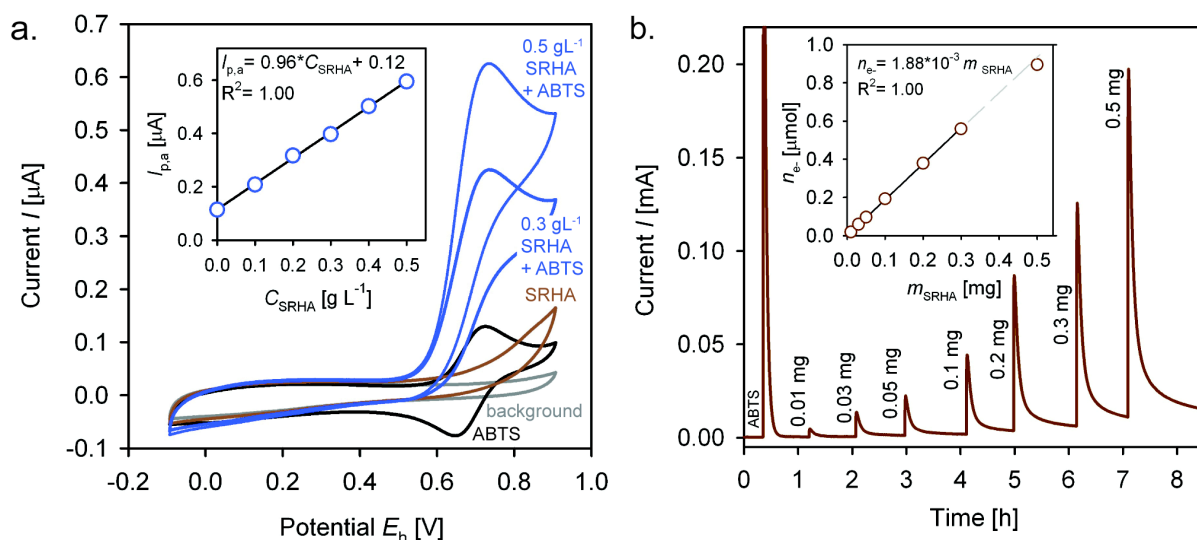
Figure 1a. Cyclic voltammograms (CVs) collected in solutions containing only background electrolyte (grey trace), only 2,2'-azino-bis(3-ethylbenzthiazoline-6-sulfonic acid) (ABTS; black trace), only Suwanee River Humic Acid (SRHA; brown trace), and both SRHA and ABTS (blue trace at different concentrations of SRHA, C_{SRHA}). Inset: Linear dependency of the oxidative peak current, $I_{p,a}$, on C_{SRHA}. **b.** Oxidative current responses to spikes of ABTS and to spikes of increasing SRHA masses, m_{SRHA}, (E_h= 0.607 V and pH 7). Inset: Plot of moles of electrons, n_{e-}, transferred from SRHA to the working electrode versus m_{SRHA}. The highest spiked SRHA mass of 500 µg was not included in the regression analysis as it

resulted in oxidative currents slightly smaller than expected based on the linear response to spikes of lower m_{SRHA}.

Figures **1b** and **S6** show the oxidative current responses to spikes of increasing amounts of SRHA and LHA, respectively (E_h= 0.607 V, pH 7). Compared to the model antioxidants, the current peaks of HA were broader, indicating slower ABTS-mediated electron transfer from the HA than from the model antioxidants to the WE. Yet, at spiked HA masses $m_{HA}\leq$ 0.3 mg, background currents were re-attained within 50 min of spiking. Integration of the baseline-separated peaks showed that n_{e^-} were directly proportional to m_{HA} for both SRHA and LHA (insets in Figures **1b** and **S6**). The slopes of the regression lines of 1.88±0.04 and 1.33±0.02 mmol$_{e^-}$(g$_{HA}$)$^{-1}$ (± half of the 95% confidence interval) corresponded to the EDCs of SRHA and LHA, respectively, under the given E_h and pH conditions. Spikes with $m_{HA}>$ 0.3 mg resulted in n_{e^-} values that were smaller than expected based on the linear n_{e^-}-m_{HA} dependencies determined at lower m_{HA}, likely due to incomplete oxidation of larger HA amounts over 50 min.

MEO has two major advantages over previously employed methods to quantify EDCs, including assays that rely on the reductive decolorization of ABTS$^{\bullet+}$ to ABTS, [19, 21, 32, 33] and potentiometric redox titrations with chemical oxidants.[10-16] First, the EDCs are directly quantified in MEO by chronocoulometric analysis of oxidative current peaks and not indirectly via changes in the absorbance of added oxidants or the solution E_h. Second, the E_h in MEO is accurately controlled by a potentiostat, is independent of solution pH, and remains constant during HS oxidation, as ABTS$^{\bullet+}$ reduced to ABTS is constantly regenerated by oxidation at the WE. These advantages in combination with the quantitative and reproducible detection of model antioxidants, and the linear response of n_{e^-} to m_{HA} up to $m_{HA}\leq$ 0.25 mg$_{HA}$ demonstrated the suitability of MEO for a systematic assessment of the E_h- and pH-dependencies of the EDCs of HS.

Reversibility of HS oxidation. The reversibility of HS oxidation provides information on the chemical nature of the electron donating moieties in HS. Furthermore, the reversibility data allows assessing whether the pool of these moieties, and hence the antioxidant capacity, is depleted during oxidation. HS

oxidation reversibility was determined for SRHA, ESHA, and LHA, which were selected to represent aquatic, terrestrial, and lignite-derived HAs, respectively.

Figures **2a,b** show the changes in EDC and EAC, ΔEDC and ΔEAC, with increasing moles of electrons, $n_{e\text{-}}^{\text{bulk oxidation}}$, transferred from SRHA, ESHA, and LHA during their bulk oxidation. In the initial stages of the bulk oxidation ($n_{e\text{-}}^{\text{bulk oxidation}} \leq 1 \text{ mmol}_{e\text{-}} (g_{HA})^{-1}$), ΔEDC decreased to the same extent as $n_{e\text{-}}^{\text{bulk oxidation}}$ increased (Figure **2a**; data on the 1:1 line), demonstrating that MEO quantitatively detected the depletion of oxidizable moieties in the HA during bulk oxidation. Conversely, at $n_{e\text{-}}^{\text{bulk oxidation}} > 0.8\text{-}1 \text{ mmol}_{e\text{-}} (g_{HA})^{-1}$, the decrease in EDC was smaller than expected based on the increase in $n_{e\text{-}}^{\text{bulk oxidation}}$. Most likely, this finding reflected a slight overestimation of $n_{e\text{-}}^{\text{bulk oxidation}}$ due to the repeated electrochemical oxidation of some redox-active HA moieties that were unstable in the oxidized form under reducing conditions inside the glovebox (e.g., quinones with high standard reduction potential). However, more important for the assessment of reversibility, ΔEDC values of the HAs increased only slightly compared to $n_{e\text{-}}^{\text{bulk oxidation}}$ (Figure **2b**). For the last samples withdrawn during bulk oxidation, ΔEAC were merely 14%, 22%, and 17% of the $n_{e\text{-}}^{\text{bulk oxidation}}$ values of SRHA, ESHA, and LHA, respectively, demonstrating that the oxidation of all three HAs was largely irreversible. Hydroquinone moieties, which are reversibly oxidized to quinones, therefore contributed little to $n_{e\text{-}}^{\text{bulk oxidation}}$. Irreversible HA oxidation is consistent with the oxidation of phenolic moieties to phenolate radicals which are known to rapidly undergo irreversible coupling reactions.[31] The finding of irreversible oxidation strongly suggests that HS oxidations in the environment result in an irreversible depletion of their electron donating moieties.

ABTS-mediated bulk oxidation of the three HAs did not alter their UV-visible absorbance spectra (Figure **S7**). Combined with the slight increase in EAC during bulk oxidation, this finding suggests that ABTS$^{\bullet+}$ did not destroy aromatic and quinone moieties in the HAs. This is supported by previous work, which showed that ABTS$^{\bullet+}$ oxidizes aromatic Ar–OH and Ar–NH$_2$ moieties but leaves aromatic rings intact.[26, 34] ABTS$^{\bullet+}$ therefore is a more selective oxidant than ozone and chlorine, which decrease the UV absorbance of HAs and hence their aromaticity.[35-39] Note that HS reduction, in contrast to the oxidation shown here, resulted in pronounced changes in the HS UV-visible absorbance spectra.[1,

[40, 41] These changes were hypothesized to result from the reduction of quinones and aromatic ketones that act as acceptors in charge transfer complexes in HS that give rise to the long-wavelength absorbance.[40, 42] The finding in this work of unaltered optical properties of the tested HA upon their electrochemical oxidation therefore suggests that the moieties that were oxidized by this method are not part of tentative charge-transfer complexes.
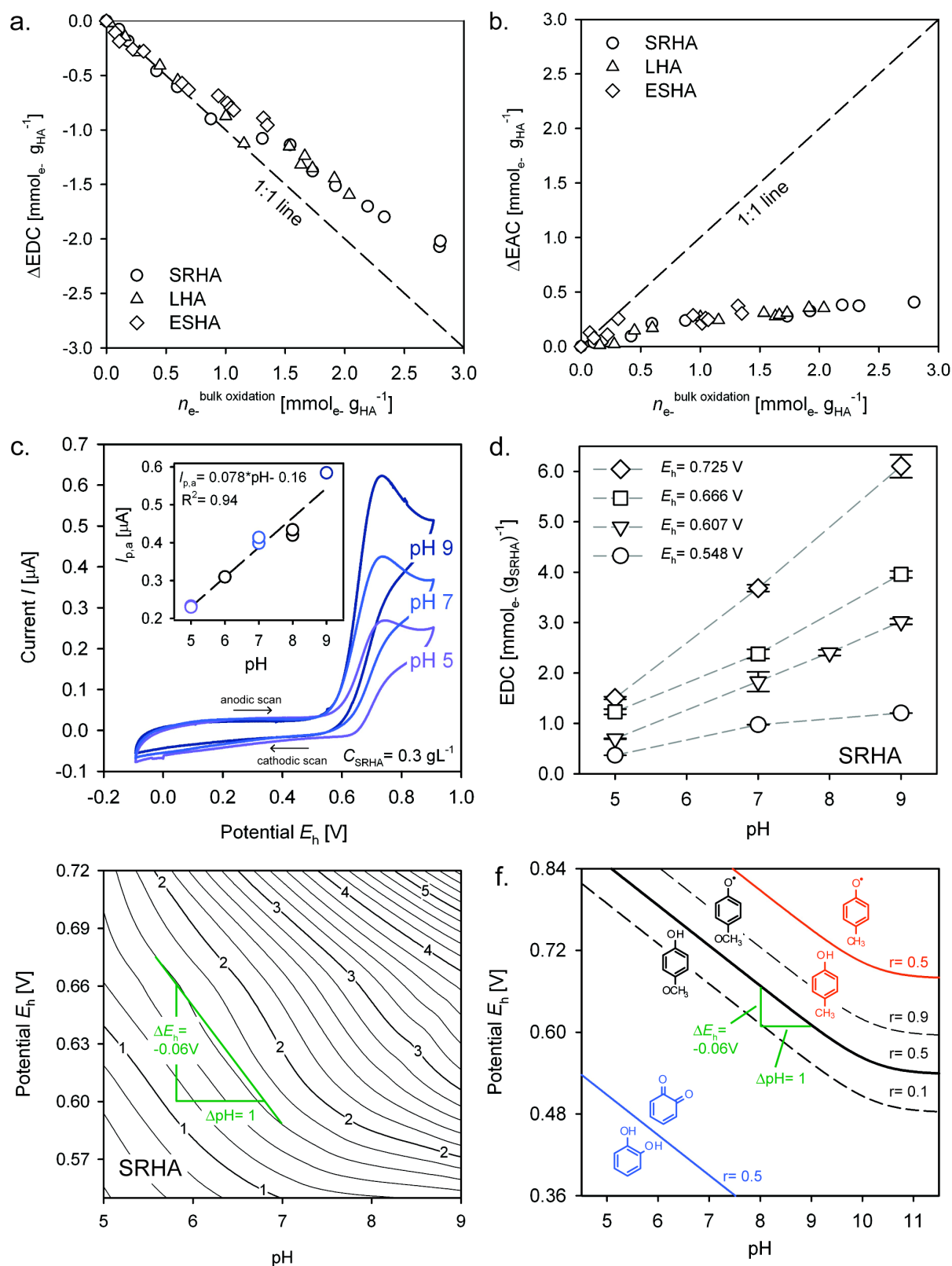
Figure 2. a,b. Decrease in the electron donating capacity (ΔEDC) and increase in the electron accepting capacity (ΔEAC) of SRHA, Leonardite Humic Acid (LHA), and Elliot Soil Humic Acid (ESHA) as a function of the moles of electrons, $n_{e^-}^{bulk\ oxidation}$, transferred from the HAs

during their bulk oxidation. **c.** Cyclic voltammograms (CVs) of Suwanee River Humic Acid (SRHA; concentration C_{SRHA}= 0.3 gL^{-1}) and 2,2'-azino-bis(3-ethylbenzthiazoline-6-sulfonic acid) (ABTS) collected in solutions at pH 5, 7, and 9. Inset: Dependence of the catalytic peak current, $I_{p,a}$, on solution pH. All CVs were collected at scan rates of v= 0.01 V s^{-1} and the concentration of ABTS, if present, was C_{ABTS}= 30 μM. **d.** Electron donating capacities of SRHA as a function of solution pH and applied redox potential E_h. **e.** Iso-EDC contour plots of SRHA in units of mmol$_{e-}$ (g$_{SRHA}$)$^{-1}$ as a function of E_h and pH. The green reference line has a slope of ΔE_h= -0.060 V per pH. **f.** E_h-pH dependencies of the oxidation of 4-methoxyphenol, 4-methylphenol, and 1,2-dihydroxy-benzene. The solid lines corresponds to the standard reduction potentials, E_h^0, at which a fraction of r= 0.5 of the compound is in its oxidized form. The dashed lines correspond to r= 0.1 and r= 0.9 for 4-methoxyphenol.

pH- and E_h-dependencies of HS oxidation. CVs collected in SRHA solutions containing ABTS showed increasing oxidative currents with increasing solution pH (Figure **2c**). This increase must have resulted from more favorable electron donation by oxidizable moieties in SRHA, as solution pH did not affect the CVs of only ABTS (Figure **S3**) and the EDCs of the model antioxidant Trolox® (Figure **S8**). Based on the pH-independent speciation and E_h^0= 0.68V of the ABTS$^{•+}$/ABTS couple at pH> 2.1[30] (Figure **S9**), ABTS as a mediator could be used to systematically investigate the effects of E_h and pH on oxidation. We quantified the EDCs of SRHA, ESHA, and LHA over wide pH and E_h ranges. The results for SRHA are discussed in detail in the following. Similar results were obtained for ESHA and LHA (Figures **S10** and **S11**) and referred to only if they significantly differ from the SRHA results.

At E_h= 0.55 V and pH 7, the EDCs of the three tested HAs ranged from 0.3 to 1.0 mmol$_{e-}$(g$_{HA}$)$^{-1}$. As expected, these values were larger than the reported EDCs of 0.13 and 0.07 mmol$_{e-}$(g$_{HA}$)$^{-1}$ for LHA and ESHA, respectively, determined by redox titrations with the milder oxidant Fe^{3+}-citrate (E_h^0= 0.37 V).[16] The EDCs of SRHA, ESHA, and LHA steadily increased with increasing E_h and pH to values > 5 mmol$_{e-}$ g$_{HA}^{-1}$ at E_h= 0.73 V and pH≥ 8 (Figures **2d, S10**, and **S11** for SRHA, ESHA, and LHA, respectively). The increase in EDCs with pH and E_h demonstrates that electron donation from moieties in the HAs became more feasible with increasing E_h and pH, consistent with the results from the CV experiments (Figure **2c**) and from previous studies.[11-16] The strong pH dependence of the EDCs suggests that electron donation from oxidizable moieties in HS is coupled to proton release.

The E_h- and pH dependencies of EDCs are re-plotted as iso-EDC contour plots in Figures **2e**, **S10**, and **S11** for SRHA, ESHA and LHA, respectively. The iso-EDC contour lines had slopes of approximately -0.06 V per pH (i.e., green lines in the Figures) at pH< 8. At higher pH, the slopes for SRHA and LHA tended to become less negative with increasing pH. Phenols have very similar E_h-pH dependencies, as shown in Figure **2f** for the one electron oxidation of 4-methoxyphenol and 4-methylphenol to the respective phenol radicals. At pH below the acidity constant, p$K_{a\ phenol}$, of the phenol, the one electron oxidation is coupled to the release of one proton, resulting in a slope of –0.059V per pH (T= 25°C). The phenol radicals are not protonated at environmentally relevant pH (pK_a< 0[43]). At pH> p$K_{a\ phenol}$, the one electron oxidation of the phenolate species is not coupled to proton release, such that E_h is pH independent. Similar pH dependencies of the E_h of phenols and the iso-EDC contour lines of the HAs and support phenolic moieties as major electron donating moieties in the HAs.

The EDCs of the HAs steadily increased from E_h= 0.55V to 0.73V, whereas model phenols are oxidized over a relatively narrow E_h range (i.e., from 10% oxidized at E_h^0 – 0.059V to 90% at E_h^0 + 0.059V, as shown for 4-methoxyphenol in Figure **2d**). Figure **2d** also shows the pH dependence of E_h^0 for the two-electron redox couple 1,2-benzoquinone/1,2-dihydroxybenzene. The E_h^0 of this couple lies at the higher end of the potential range of quinones, since the E_h^0 decrease from 1,2- to 1,4-substituted quinones and with increasing ring condensation from benzo-, to naphtha-, to anthraquinones.[8, 44] The majority of the electron donating moieties in the HAs were, however, oxidized at E_h much higher than the E_h^0 for the oxidation of 1,2-benzohydroquinone. These findings suggest that the HA contained phenolic moieties with a wide distribution of E_h^0 and that hydroquinones contributed little to the EDCs of the HAs, consistent with the irreversibility of HA oxidation.

The increase in the EDCs of the HAs with E_h and pH likely reflected an increase in the thermodynamic feasibility of one-electron oxidation of phenolic moieties.[45-47] Increasing EDC with increasing pH may also have resulted from faster oxidation kinetics of phenolate than phenolic moieties.[47] Studies with low molecular weight phenols showed that faster phenolate oxidation results in strong linear correlations of the total oxidation rate of phenols with the phenolate concentration.[45, 46] Consistently, the EDCs of SRHA, LHA, and

ESHA at pH> 7 increased with their corresponding titrated charges q_{TOT}[48] (Figure **S12**) and hence their phenolate concentrations.

Dependence of the EDCs of HS and NOM on their source material. Figure **3a** shows the EDCs of eight humic acids (HA), five fulvic acids (FA), and two NOM samples of terrestrial, aquatic, and industrial origin, quantified at three selected E_h-pH combinations. All EDC values are provided in Table **S1**. At E_h= 0.61V and pH 7, the EDCs ranged from 0.47±0.01 $mmol_{e^-}(g_{PLFA})^{-1}$ for Pony Lake FA (PLFA) to 2.65±0.05 $mmol_{e^-}(g_{WPHA})^{-1}$ for Washkish Peat HA (WPHA). The data shows that, with the exception of PLFA, the aquatic HS had higher EDC values than the terrestrial HS. The EDCs of all HS increased by a factor of two or more when increasing the applied potential by ΔE_h= 0.12V from 0.61 V to 0.73V while maintaining pH 7. A slightly smaller increase in the EDCs of all HS resulted when the pH was increased from pH 7 to 9 while maintaining E_h= 0.61V. All HSs therefore contained oxidizable moieties with comparable E_h- and pH dependencies.

The EDC values (E_h= 0.61V; pH 7) of ten of the 12 tested natural HS showed a strong linear correlation to their titrated phenol contents Ar-OH (Figure **3b**; Table **S2**), strongly supporting phenolic moieties as major contributors to the EDCs. PLFA and WPHA were omitted from the correlation analysis as no titration data was available for these HS. Note that the titrated phenol contents were operationally defined as twice the titrated charge density between pH 8 and 10. It is conceivable that the tested HS contain phenolic moieties that deprotonate at much lower pH, including hydroxy-substituted quinones with acidity constants of pK_a<< 8.[44] Furthermore, at high titration rates, acid-base non-equilibria may largely affect the titrated phenol contents.[48, 49] The resulting uncertainties in the phenol contents may explain why some of the EDCs measured at the higher potential E_h= 0.73V were larger than the estimated phenol contents (see Table **S1**). It is also possible that, in addition to phenols, nitrogen containing functional groups, such as aromatic amines contributed to the EDCs at higher E_h. Conversely, the Fe, Cu and Mn contents in all HS, except Aldrich HA, were too small to have significantly contributed to the measured EDCs (Table **S2**).
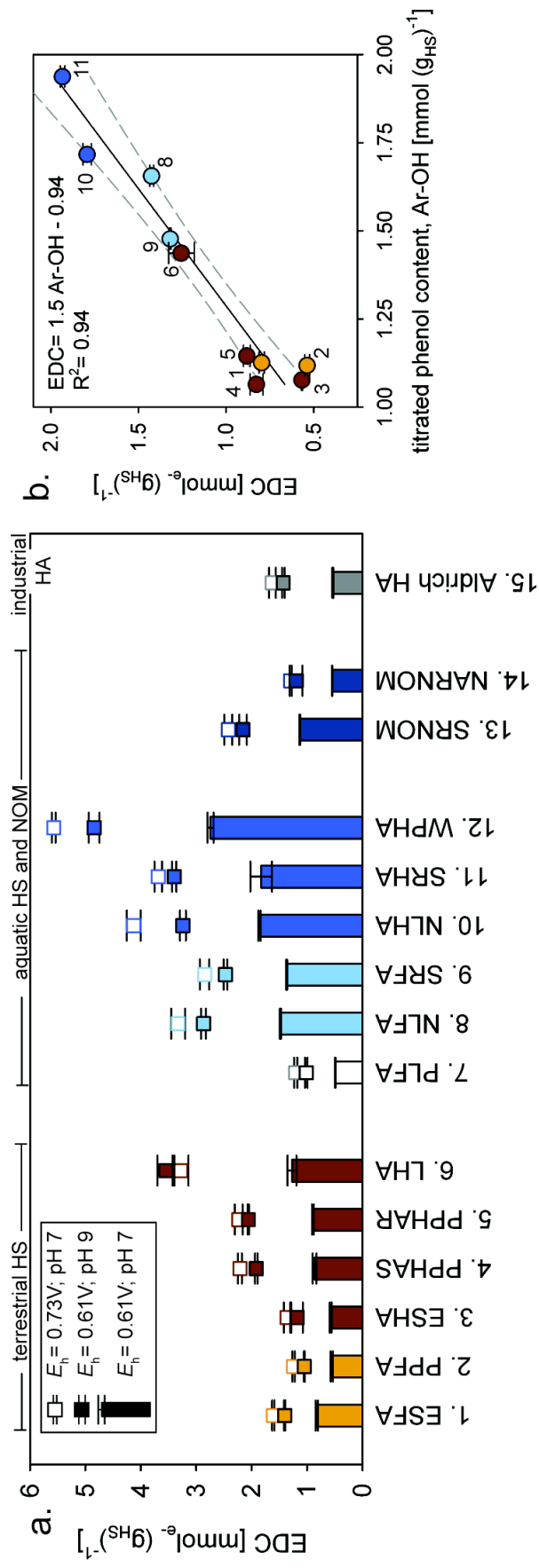
Figure 3. a. Electron donating capacities (EDCs) of 15 humic substances (HS) and natural organic matter (NOM) samples at an applied potential of $E_h = 0.61$ V at pH 7 and 9 and at $E_h = 0.73$ V at pH 7. The brown and blue bars represent HS and NOM of terrestrial and aquatic origins, respectively. Aldrich humic acid (AHA; grey bar) is an industrially extracted HA. **b.** Plot of the EDCs ($E_h = 0.61$V, pH 7) of ten HS versus their titrated phenol contents, Ar-OH.[48]

Abundances of electron donating and accepting moieties as a function of HS origin. Figure **4a** and Table **S1** give an overview of the EDC and EAC values of all tested HS and NOM quantified at pH 7 and E_h= 0.61 V and E_h= -0.49, respectively. The data show that terrestrial HS tend to have smaller EDCs but larger EACs than the aquatic HS and NOM samples. This is evident also from Figure **4b,** in which the EDCs are plotted versus the EACs. While the absolute EDC and EAC values and therefore the positions of the tested HS and NOMs relative to the 1:1 line depend on pH and E_h, these two variables do not affect the relative differences in the EDC to EAC ratios between the terrestrial and the aquatic HS and NOMs (Table **S1**). In Figure **4c** the EDC and EAC values of 13 of the 15 tested samples are compared based on their aromaticities estimated from ^{13}C-NMR spectra[50] (Table **S2**). PPHAR and AHA were not included in the analysis, because their ^{13}C-NMR spectra have not been reported. Plots of the EDCs of all 13 HS and NOM samples versus their aromaticities reveal that aquatic HS and NOM have higher EDCs than terrestrial HS of comparable aromaticity. A strong correlation (R^2= 0.88) was, found for the aquatic HS and NOMs and a weaker correlation (R^2= 0.32) for the terrestrial HS. At the same time, the EACs of all 13 HS and the two NOM samples strongly correlate with aromaticity (R^2= 0.85), consistent with quinones as major reducible moieties. The data in Figure **4c** suggest that aquatic HS and NOM samples have higher phenol to quinone ratios than terrestrial HS.
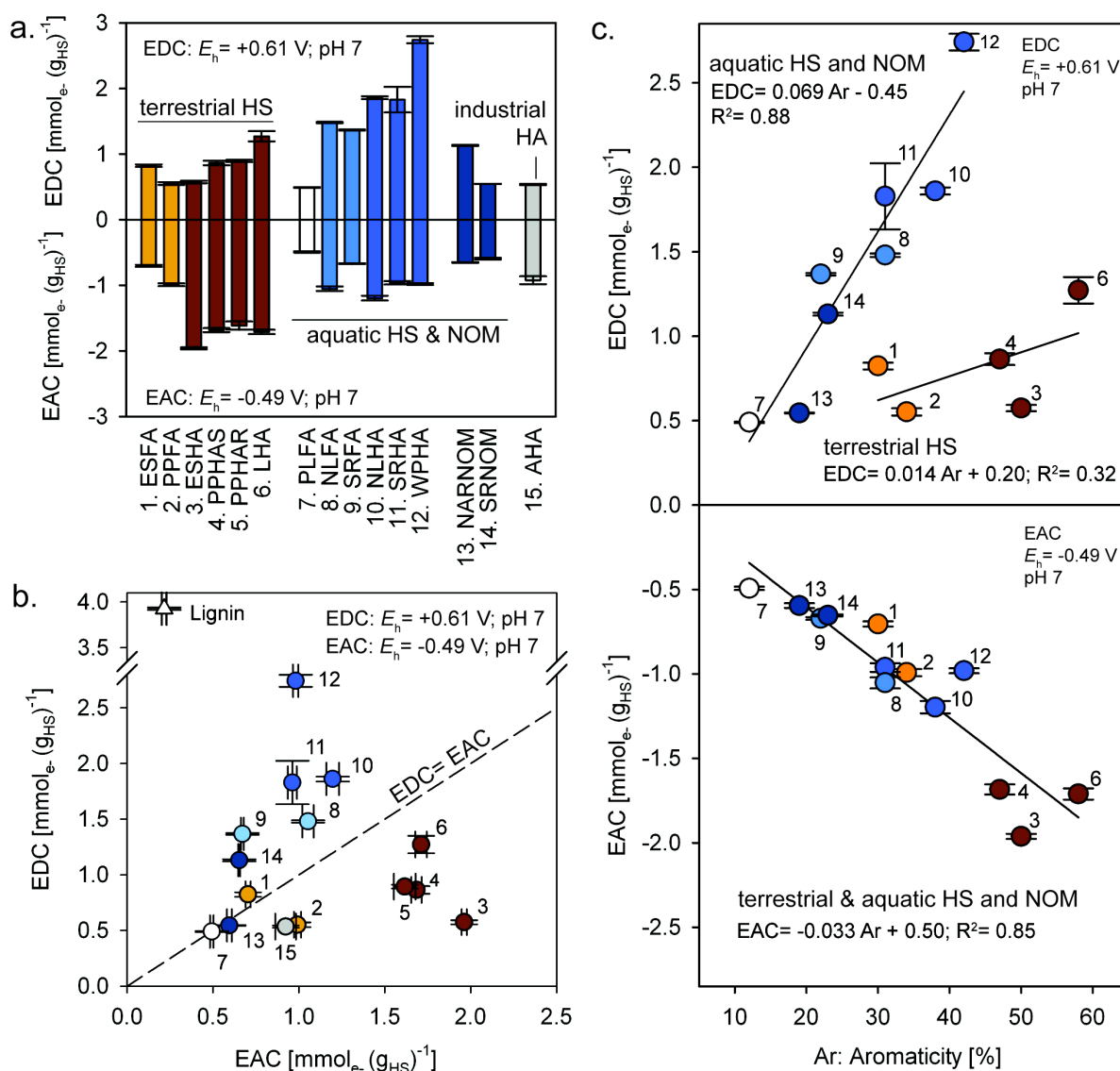
Figure 4. a. Electron donating capacities (EDCs; E_h= 0.61V, pH 7) and electron accepting capacities (EACs; E_h= -0.49 V, pH 7; data for HS from Aeschbacher et al.[7]) of terrestrial HS (brown bars), aquatic HS and NOM (blue bars), and of industrial Aldrich humic acid (grey bar). **b.** Data from panel a re-plotted as EDCs versus EACs. **c.** EDCs and EACs of 13 HS and NOM samples of terrestrial and aquatic origin versus their ^{13}C-NMR estimated aromaticities (from http://www.ihss.gatech.edu/).

Aquatic HS isolated from rivers, streams, and lakes are commonly much younger than terrestrial HS isolated from soils (i.e., several hundred to several thousand years of age), as inferred from ^{14}C dating.[51] The higher phenolic contents and, hence, EDCs in aquatic than terrestrial HS and NOMs of comparable aromaticity therefore likely reflect lower extents of oxidative transformations of polyphenolic precursor materials from higher plants in

aquatic than in terrestrial HS and NOMs. Note that lignin, a major constituent of higher plant cell walls, which is considered an important precursor for aquatic and terrestrial HS, showed very high EDC but low EAC values (Figure **4b**; Table **S1**), reflecting the high phenol and low quinone contents of lignin.[52] Washkish Peat HA, which showed the highest EDC values among the tested HS and NOMs, was isolated from a sphagnum bog peat containing poorly degraded, polyphenolic plant materials, including lignin and tannins.[53] The slow degradation of polyphenolic plant precursors in water saturated bogs and peats has been linked to low activities of phenol oxidases in such systems.[54] Suwannee River and Nordic Lake HS and NOM were isolated from inland water systems. HS from such systems typically show higher phenolic content than terrestrial HS, based on ^{13}C-NMR.[51] Ultrahigh resolution mass spectrometry and NMR provided evidence for lignin-derived structures in SRHA.[55-57] Pony Lake fulvic acid (PLFA) showed the lowest EDC and EAC values. PLFA represents an aquatic end member among the aquatic HS as it originates from a costal pond in Antarctica with organic matter input only from lower plants, lichen, and microorganisms.[58] Based on the relatively high N and S contents in PLFA,[59] moieties containing these heteroatoms may also have contributed to its redox capacity. Elliott Soil and Pahokee Peat HS originate from agricultural soils and, in contrast to aquatic HS, are expected to be composed of highly degraded precursor materials. Extensive degradation of plant-derived precursors in such systems is supported by recent findings that lignin does not accumulate in the refractory C pool of arable and grassland soils.[60, 61] Leonardite HA is extracted from a lignite coal and is composed of highly processed and diagenetically altered organic molecules with high aromaticity that give rise to a high EAC and relatively low EDC values.

The lower EAC values in aquatic than terrestrial HS and NOMs at comparable aromaticities may have resulted from a relative enrichment of electron accepting quinone moieties that were present already in the source material[52] and/or from the neo-formation of quinone moieties during the oxidative transformation of HS precursors and HS. Quinone formation was demonstrated during the enzymatic oxidation of lignin model compounds by laccases and manganese peroxidases isolated from white rot fungi.[62, 63] Furthermore, quinones may form upon reaction of hydroxyl radicals ($\bullet$OH) with aromatic and phenolic structures.[64] It has been hypothesized that the degradation

of lignin and HS by white rot fungi involves •OH formed via Fenton chemistry.[65-68] Furthermore, •OH may be formed during HS photolysis,[69] and HS redox cycling in the dark.[70]

The results of this work suggest that abiotic and biotic oxidation reactions of HS and NOM in the environment result in the preferential loss of electron-donating phenolic moieties over electron-accepting quinone moieties. This work supports the hypothesis that the presence of phenolic moieties with antioxidant properties in HS and NOM slows down the oxidative transformation of other moieties in HS and NOM and hence increases their recalcitrance in oxidative environments.[19-21]

4.4. Applications

The novel mediated electrochemical oxidation (MEO) method presented in this paper allows for accurate and direct quantification of the electron donating capacities of HS as a function of redox potential E_h and pH. MEO is highly sensitive with detection limits of a few μg of HS.

This work demonstrates that HS and NOM contain phenolic electron-donating moieties that cover a wide range of one-electron oxidation potentials. These moieties may act as antioxidants and thereby affect biogeochemical and pollutant redox reactions in both natural and engineered systems. For instance, this work supports the hypothesis that the inhibitory effect of HS on indirect phototransformation rates of organic pollutants results from electron donation from phenolic moieties in the HS to pollutant oxidation intermediates.[23, 24] Future studies would benefit from a combined photochemical and electrochemical approach that can relate differences in the inhibitory effects among HS to the differences in their EDCs.

MEO may be used in drinking water facilities to determine the dose of oxidants, such as ozone or chlorine that need to be added to the water for disinfection, pollutant degradation, decolorization, and odor control. At present, drinking water treatment facilities lack suitable approaches to monitor the changes in the EDCs and hence chemical oxidant demand of the incoming water in real time. Measurements of the EDCs of NOM-containing waters may also help to assess their potential for disinfection byproduct formation, as electron-donating moieties in NOM play a role in this process.[27-29]

This work provides evidence for pronounced and systematic effects of HS source material and age on the relative abundances of electron accepting and donating moieties in HS and NOM. The hypothesis that (poly)phenolic moieties originating from higher plants are preferentially oxidized in HS may be tested by quantifying the EDCs of HS sampled along natural gradients of organic matter decomposition, such soil profiles or an estuary. The depletion of electron donating moieties during oxidative transformation of HS can be further investigated in the laboratory by quantifying the changes in the EDCs of plant-derived polyphenols, HS, and NOM over the course of abiotic and enzymatic oxidations.

4.5. References

1. Maurer, F.; Christl, I.; Kretzschmar, R., Reduction and reoxidation of humic acid: Influence on spectroscopic properties and proton binding. *Environ Sci Technol* **2010,** *44*, 5787-5792.

2. Nanny, M. A.; Ratasuk, N., Characterization and quantification of reversible redox sites in humic substances. *Environmental Science & Technology* **2007,** *41*, 7844-7850.

3. Lovley, D. R.; Coates, J. D.; Blunt-Harris, E. L.; Phillips, E. J. P.; Woodward, J. C., Humic substances as electron acceptors for microbial respiration. *Nature* **1996,** *382*, 445-448.

4. Scott, D. T.; McKnight, D. M.; Blunt-Harris, E. L.; Kolesar, S. E.; Lovley, D. R., Quinone moieties act as electron acceptors in the reduction of humic substances by humics-reducing microorganisms. *Environ Sci Technol* **1998,** *32*, 2984-2989.

5. Bauer, I.; Kappler, A., Rates and extent of reduction of Fe(III) compounds and O_2 by humic substances. *Environ Sci Technol* **2009,** *43*, 4902-4908.

6. Bauer, M.; Heitmann, T.; Macalady, D. L.; Blodau, C., Electron transfer capacities and reaction kinetics of peat dissolved organic matter. *Environ Sci Technol* **2007,** *41*, 139-145.

7. Aeschbacher, M.; Sander, M.; Schwarzenbach, R. P., Novel electrochemical approach to assess the redox properties of humic substances. *Environ Sci Technol* **2010,** *44*, 87-93.

8. Aeschbacher, M.; Vergari, D.; Schwarzenbach, R. P.; Sander, M., Electrochemical analysis of proton and electron transfer equilibria of the reducible moieties in humic acids. *Environmental Science & Technology* **2011,** *45*, 8385-8394.

9. Nurmi, J. T.; Tratnyek, P. G., Electrochemical properties of natural organic matter (NOM), fractions of NOM, and model biogeochemical electron shuttles. *Environmental Science & Technology* **2002,** *36*, 617-624.

10. Visser, S. A., Oxidation-Reduction Potentials + Capillary Activities of Humic Acids. *Nature* **1964,** *204*, 581-&.

11. Helburn, R. S.; Maccarthy, P., Determination of some redox properties of humic acid by alkaline ferricyanide titration. *Analytica Chimica Acta* **1994,** *295*, 263-272.

12. Matthiessen, A., Determining the redox capacity of humic substances as a function of pH. *Vom Wasser* **1995,** *84*, 229-235.

13. Matthiessen, A., *Evaluating the redox capacity and the redox potential of humci acids by redox titrations.* 1994; p 187-192.

14. Skogerboe, R. K.; Wilson, S. A., Reduction of ionic species by fulvic acid. *Analytical Chemistry* **1981,** *53*, 228-232.

15. Struyk, Z.; Sposito, G., Redox properties of standard humic acids. *Geoderma* **2001,** *102*, 329-346.

16. Peretyazhko, T.; Sposito, G., Reducing capacity of terrestrial humic acids. *Geoderma* **2006,** *137*, 140-146.

17. RiceEvans, C. A.; Miller, N. J.; Paganga, G., Structure-antioxidant activity relationships of flavonoids and phenolic acids. *Free Radical Biology and Medicine* **1996,** *20*, 933-956.

18. Bravo, L., Polyphenols: Chemistry, dietary sources, metabolism, and nutritional significance. *Nutrition Reviews* **1998,** *56*, 317-333.

19. Rimmer, D. L.; Smith, A. M., Antioxidants in soil organic matter and in associated plant materials. *European Journal of Soil Science* **2009,** *60*, 170-175.

20. Rimmer, D. L., Free radicals, antioxidants, and soil organic matter recalcitrance. *European Journal of Soil Science* **2006,** *57*, 91-94.

21. Rimmer, D. L.; Abbott, G. D., Phenolic compounds in NaOH extracts of UK soils and their contribution to antioxidant capacity. *European Journal of Soil Science* **2011,** *62*, 285-294.

22. Menzel, R.; Menzel, S.; Tiedt, S.; Kubsch, G.; Stoesser, R.; Baehrs, H.; Putschew, A.; Saul, N.; Steinberg, C. E. W., Enrichment of Humic Material with Hydroxybenzene Moieties Intensifies Its Physiological Effects on the Nematode Caenorhabditis elegans. *Environmental Science & Technology* **2011,** *45*, 8707-8715.

23. Wenk, J.; von Gunten, U.; Canonica, S., Effect of Dissolved Organic Matter on the Transformation of Contaminants Induced by Excited Triplet States and the Hydroxyl Radical. *Environmental Science & Technology* **2011,** *45*, 1334-1340.

24. Canonica, S.; Laubscher, H. U., Inhibitory effect of dissolved organic matter on triplet-induced oxidation of aquatic contaminants. *Photochemical & Photobiological Sciences* **2008,** *7*, 547-551.

25. Laha, S.; Luthy, R. G., Oxidation of Aniline and Other Primary Aromatic-Amines by Manganese-Dioxide. *Environmental Science & Technology* **1990,** *24*, 363-373.

26. Skarpeli-Liati, M.; Jiskra, M.; Turgeon, A.; Garr, A. N.; Arnold, W. A.; Cramer, C. J.; Schwarzenbach, R. P.; Hofstetter, T. B., Using Nitrogen Isotope Fractionation to Assess the Oxidation of Substituted Anilines by Manganese Oxide. *Environmental Science & Technology* **2011,** *45*, 5596-5604.

27. Norwood, D. L.; Christman, R. F.; Hatcher, P. G., Structural characterization of aquatic humic material. 2. Phenolic content and its relationship to chlorination mechanism in an isolated aquatic fulvic acid *Environmental Science & Technology* **1987,** *21*, 791-798.

28. von Gunten, U., Ozonation of drinking water: Part I. Oxidation kinetics and product formation. *Water Research* **2003,** *37*, 1443-1467.

29. von Gunten, U., Ozonation of drinking water: Part II. Disinfection and by-product formation in presence of bromide, iodide or chlorine. *Water Research* **2003,** *37*, 1469-1487.

30. Scott, S. L.; Chen, W. J.; Bakac, A.; Espenson, J. H., Spectroscopic Parameters, Electrode-Potentials, Acid Ionization-Constants, and Electron-Exchange Rates of the 2,2'-Azinobis(3-Ethylbenzothiazoline-6-Sulfonate) Radicals and Ions. *Journal of Physical Chemistry* **1993,** *97*, 6710-6714.

31. Steenken, S.; Neta, P., One-Electron Redox Potentials of Phenols - Hydroxyphenols and Aminophenols and Related-Compounds of Biological Interest. *Journal of Physical Chemistry* **1982,** *86*, 3661-3667.

32. Huang, D. J.; Ou, B. X.; Prior, R. L., The chemistry behind antioxidant capacity assays. *Journal of Agricultural and Food Chemistry* **2005,** *53*, 1841-1856.

33. Re, R.; Pellegrini, N.; Proteggente, A.; Pannala, A.; Yang, M.; Rice-Evans, C., Antioxidant activity applying an improved ABTS radical cation decolorization assay. *Free Radical Biology and Medicine* **1999,** *26*, 1231-1237.

34. Bourbonnais, R.; Leech, D.; Paice, M. G., Electrochemical analysis of the interactions of laccase mediators with lignin model compounds. *Biochimica Et Biophysica Acta-General Subjects* **1998,** *1379*, 381-390.

35. Volk, C.; Roche, P.; Joret, J. C.; Paillard, H., Comparison of the effect of ozone, ozone-hydrogen peroxide system and catalytic ozone on the biodegradable organic matter of a fulvic acid solution. *Water Research* **1997,** *31*, 650-656.

36. Li, C. W.; Benjamin, M. M.; Korshin, G. V., Use of UV spectroscopy to characterize the reaction between NOM and free chlorine. *Environmental Science & Technology* **2000,** *34*, 2570-2575.

37. Korshin, G. V.; Li, C. W.; Benjamin, M. M., Monitoring the properties of natural organic matter through UV spectroscopy: A consistent theory. *Water Research* **1997,** *31*, 1787-1795.

38. Chin, Y. P.; Aiken, G.; Oloughlin, E., Molecular-Weight, Polydispersity, and Spectroscopic Properties of Aquatic Humic Substances. *Environmental Science & Technology* **1994,** *28*, 1853-1858.

39. Weishaar, J. L.; Aiken, G. R.; Bergamaschi, B. A.; Fram, M. S.; Fujii, R.; Mopper, K., Evaluation of specific ultraviolet absorbance as an indicator of the chemical composition and reactivity of dissolved organic carbon. *Environmental Science & Technology* **2003,** *37*, 4702-4708.

40. Boyle, E. S.; Guerriero, N.; Thiallet, A.; Del Vecchio, R.; Blough, N. V., Optical Properties of Humic Substances and CDOM: Relation to Structure. *Environmental Science & Technology* **2009,** *43*, 2262-2268.

41. Ma, J. H.; Del Vecchio, R.; Golanoski, K. S.; Boyle, E. S.; Blough, N. V., Optical properties of humic substances and CDOM: Effects of borohydride reduction. *Environmental Science & Technology* **2010,** *44*, 5395-5402.

42. Del Vecchio, R.; Blough, N. V., On the origin of the optical properties of humic substances. *Environmental Science & Technology* **2004,** *38*, 3885-3891.

43. Jovanovic, S. V.; Tosic, M.; Simic, M. G., Use of the Hammett Correlation and Sigma+ for Calculation of One-Electron Redox Potentials of Antioxidants. *Journal of Physical Chemistry* **1991,** *95*, 10824-10827.

44. Clark, W., *Oxidation-Reduction Potentials of Organic Systems.* Baltimore, 1960.

45. Canonica, S.; Tratnyek, P. G., Quantitative structure-activity relationships for oxidation reactions of organic chemicals in water. *Environmental Toxicology and Chemistry* **2003,** *22*, 1743-1754.

46. Tratnyek, P. G.; Hoigne, J., Kinetics of Reactions of Chlorine Dioxide (Oclo) in Water .2. Quantitative Structure-Activity-Relationships for Phenolic-Compounds. *Water Research* **1994,** *28*, 57-66.

47. Alfassi, Z. B.; Huie, R. E.; Neta, P., Substituent Effects on Rates of One-Electron Oxidation of Phenols by the Radicals ClO2, NO2, and SO3-. *Journal of Physical Chemistry* **1986,** *90*, 4156-4158.

48. Perdue, E. M.; Ritchie, J. D., Proton-binding study of standard and reference fulvic acids, humic acids, and natural organic matter. *Geochimica Et Cosmochimica Acta* **2003,** *67*, 85-96.

49. Cooke, J. D.; Hamilton-Taylor, J.; Tipping, E., On the acid-base properties of humic acid in soil. *Environ Sci Technol* **2007,** *41*, 465-470.

50. Thorn, K. A.; Folan, D. W.; MacCarthy, P. *Characterization of the International Humic Substances Society Standard and Reference Fulvic and Humic Acids by Solution State Carbon-13 (13C) and Hydrogen-1 (1H) Nuclear Magnetic Resonance Spectrometry*; U.S. Geological Survey: Denver, CO, 1989; p 93 pp.

51. Malcolm, R. L., The uniqueness of humic substances in each of soil, stream and marine environments. *Analytica Chimica Acta* **1990,** *232*, 19-30.

52. Argyropoulos, D. S.; Zhang, L. M., Semiquantitative determination of quinonoid structures in isolated lignins by P-31 nuclear magnetic resonance. *Journal of Agricultural and Food Chemistry* **1998,** *46*, 4628-4634.

53. Lewis, R. L. *Soil survey of Carlton County, Minnesota*; United States Department of Agriculture - Soil Conservation Service; Minnesota Agricultural Experiment Station: Minessota, 1978.

54. Freeman, C.; Ostle, N.; Kang, H., An enzymic 'latch' on a global carbon store - A shortage of oxygen locks up carbon in peatlands by restraining a single enzyme. *Nature* **2001,** *409*, 149-149.

55. Cooper, W. T.; Stenson, A. C.; Marshall, A. G., Exact masses and chemical formulas of individual Suwannee River fulvic acids from ultrahigh resolution electrospray ionization Fourier transform ion

cyclotron resonance mass spectra. *Analytical Chemistry* **2003,** *75*, 1275-1284.

56. Lambert, J.; Haiber, S.; Herzog, H.; Burba, P.; Gosciniak, B., Two-dimensional NMR studies of size fractionated Suwannee River Fulvic and Humic Acid Reference. *Environmental Science & Technology* **2001,** *35*, 4289-4294.

57. Freitas, M. A.; Kujawinski, E. B.; Hatcher, P. G., High-resolution Fourier transform ion cyclotron resonance mass spectrometry of humic and fulvic acids: Improvements and comparisons. *Analytical Chemistry* **2002,** *74*, 413-419.

58. McKnight, D. M.; Brown, A.; Chin, Y. P.; Roberts, E. C.; Uhle, M., Chemical characterization of dissolved organic material in Pony Lake, a saline coastal pond in Antarctica. *Marine Chemistry* **2004,** *89*, 327-337.

59. Source Materials for IHSS Samples (http://www.humicsubstances.org/sources.html). (accessed 5th January, 2012)

60. Kiem, R.; Kogel-Knabner, I., Contribution of lignin and polysaccharides to the refractory carbon pool in C-depleted arable soils. *Soil Biology & Biochemistry* **2003,** *35*, 101-118.

61. Heim, A.; Schmidt, M. W. I., Lignin turnover in arable soil and grassland analysed with two different labelling approaches. *European Journal of Soil Science* **2007,** *58*, 599-608.

62. Kawai, S.; Umezawa, T.; Higuchi, T., Degradation mechanisms of phenolic beta-1 lignin substructure model compounds by laccase of coriolus versicolor. *Archives of Biochemistry and Biophysics* **1988,** *262*, 99-110.

63. Tuor, U.; Wariishi, H.; Schoemaker, H. E.; Gold, M. H., Oxidation of phenolic arylglycerol beta-aryl ether lignin model compounds by manganese peroxidase from Phenerochaete chrysosporium: Oxidative cleavage of an alpha-carbonyl model compound. *Biochemistry* **1992,** *31*, 4986-4995.

64. Raghavan, N. V.; Steenken, S., Electrophilic reaction of the OH radical with phenol - Determination of the distribution of isomeric dihydroxycyclohexadienyl radicals. *Journal of the American Chemical Society* **1980,** *102*, 3495-3499.

65. Barr, D. P.; Shah, M. M.; Grover, T. A.; Aust, S. D., Production of hydroxyl radical by lignin peroxidase from Phanerochaete chrysosporium. *Archives of Biochemistry and Biophysics* **1992,** *298*, 480-485.

66. Forney, L. J.; Reddy, C. A.; Tien, M.; Aust, S. D., The involvement of hydroxyl radical derived from hydrogen peroxide in lignin degradation by the white rot fungus Phanerochaete chrysosporium. *Journal of Biological Chemistry* **1982,** *257*, 1455-1462.

67. Gomez-Toribio, V.; Garcia-Martin, A. B.; Martinez, M. J.; Martinez, A. T.; Guillen, F., Induction of extracellular hydroxyl radical production by white-rot fungi through quinone redox cycling. *Applied and Environmental Microbiology* **2009,** *75*, 3944-3953.

68. Grinhut, T.; Salame, T. M.; Chen, Y. N.; Hadar, Y., Involvement of ligninolytic enzymes and Fenton-like reaction in humic acid degradation by Trametes sp. *Applied Microbiology and Biotechnology* **2011,** *91*, 1131-1140.

69. Page, S. E.; Arnold, W. A.; McNeill, K., Assessing the contribution of free hydroxyl radical in organic matter-sensitized photohydroxylation reactions. *Environmental Science & Technology* **2011,** *45*, 2818-2825.

70. Page, S. E.; Sander, M.; Arnold, W. A.; McNeill, K., Hydroxyl radical formation upon oxidation of reduced humic acids by oxygen in the dark. *Environmental Science & Technology* **2012,** *asap*.

4.6. Supporting Information Chapter 4

Chemical structures of the model antioxidants Trolox® and Vitamin C

a.

b.
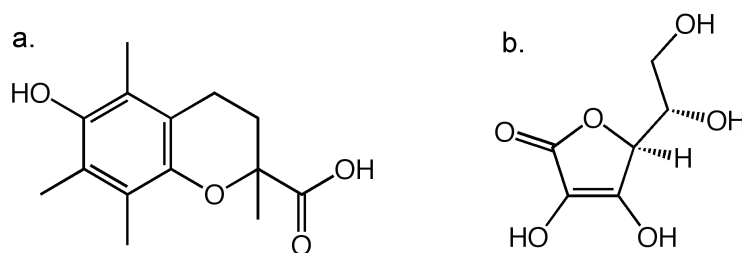
Figure **S1**. Chemical structures of the model antioxidants **a.** 6-hydroxy-2,5,7,8-tetra-methylchroman-2-carboxylic acid (Trolox®), and **b.** 2-Oxo-L-threo-hexono-1,4-lactone-2,3-enediol (*L*-ascorbic acid; Vitamin C).
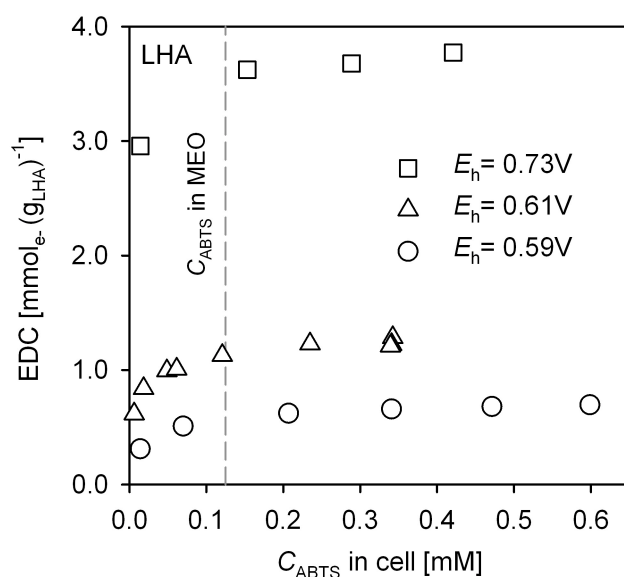
Figure **S2**. Dependence of the electron donating capacity (EDC) of Leonardite Humic Acid (LHA) on the concentration of the mediator 2,2'-azino-bis(3-ethylbenzothiazoline-sulfonic acid) (ABTS) and the applied potential E_h. All measurements were conducted at pH 7.

Cyclic voltammograms of ABTS
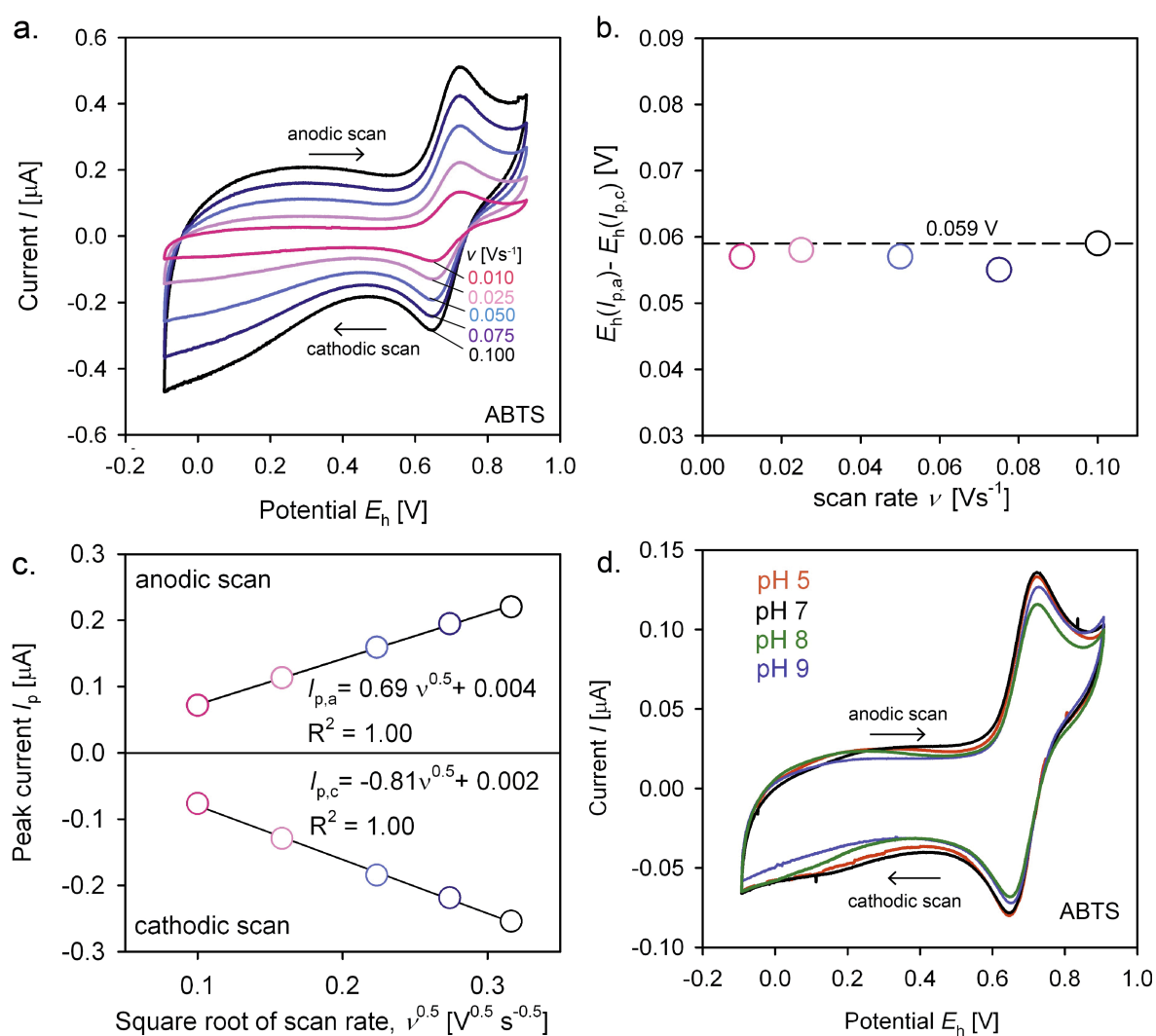
Figure **S3. a.** Cyclic voltammograms of 2,2'-azino-bis(3-ethylbenzothiazoline-sulfonic acid) (ABTS) at different scan rates v from 0.01 to 0.1 V s^{-1} (C_{ABTS}= 30 µM; pH 7). **b.** Difference in the reduction potentials E_h of anodic and cathodic peak currents, $I_{p,a}$ and $I_{p,c}$, versus the scan rate v. **c.** Linear relationship between $I_{p,a}$ and $I_{p,c}$ and the square root of the scan rate, $v^{0.5}$ (C_{ABTS}= 30 µM; pH 7). **d.** CVs of ABTS (C_{ABTS}= 30; v= 0.01 V s^{-1}) at pH 5 to 9.

Chronocoulometric analysis of electron transfer mediation by ABTS
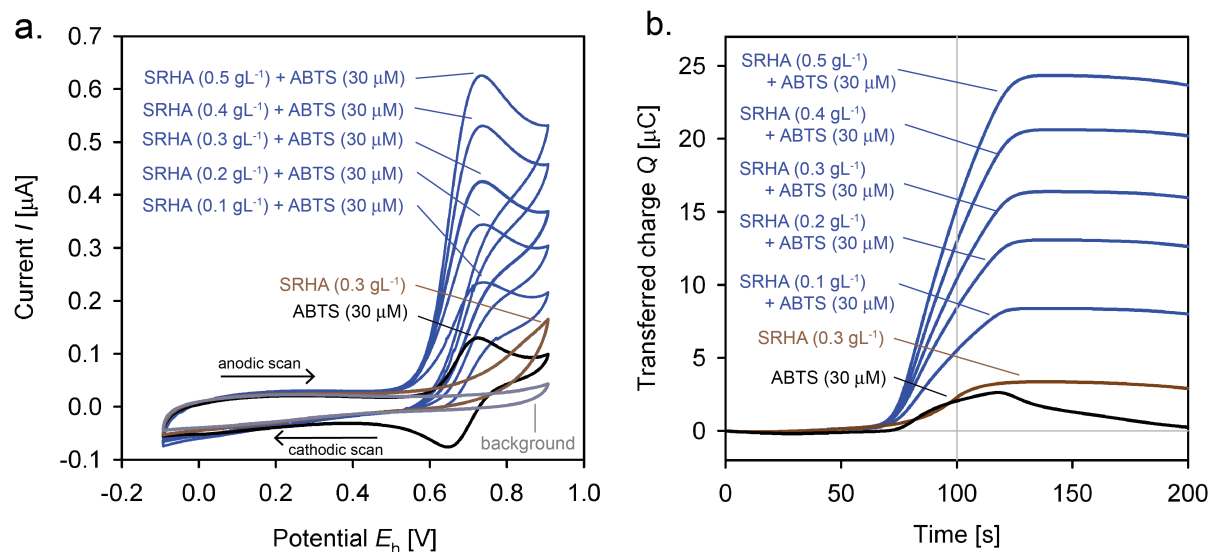
Figure S4. **a.** Cyclic voltammograms (CVs) of solutions containing various concentrations of Suwanee River Humic Acid (SRHA), C_{SRHA}, in the presence of the electron transfer mediator 2,2'-azino-bis(3-ethylbenzothiazoline-sulfonic acid) (ABTS) (blue traces; C_{ABTS}= 30 µM), containing only SRHA (brown trace; C_{SRHA}= 0.3 g L^{-1}) and only ABTS (black trace; C_{ABTS}= 30 µM), and containing no redox-active species (background, grey trace). All CVs were measured at pH 7 (0.1 M KCl and 0.1 M phosphate buffer) and at scan rates of v= 0.01 V s^{-1}. **b.** Results of a chronocoulometric analysis of the CVs of SRHA at different C_{SRHA} in the presence of ABTS (C_{ABTS}= 30 µM; blue traces), and of SRHA in the absence of ABTS (C_{SRHA}= 0.3 g L^{-1}; brown trace), and of only ABTS (C_{ABTS}= 30 µM; black trace). The vertical grey line represents the first vertex potential E_h= 0.9 V at which the scanning direction was changed from anodic to cathodic.

Mediated electrochemical oxidation of the model antioxidants Trolox® and Vitamin C

Figures **S5a,b** show the oxidative current responses to spikes of ABTS (first current peak) and to spikes of increasing moles of Trolox® (peaks 2-7; panel a) and of Vitamin C (peaks 2-7; panel b) measured at E_h= 0.61V and pH 7. The applied potential was about 0.08 V below E_h^0(ABTS$^{•+}$/ABTS), resulting in the oxidation of about 6% of the spiked ABTS to ABTS$^{•+}$. All Trolox® and Vitamin C peaks were sharp and baseline-separated and the corresponding n_{e-} were linearly proportional to the moles of spiked Tolox®, n_{Trolox} (inset panel a) and Vitamin C, $n_{Vitamin C}$ (inset panel b). The slopes of the regression lines were 1.96±0.01 (± half of the 95% confidence interval) mmol$_{e-}$ (mmol$_{Trolox®}$)$^{-1}$ for

Trolox® and 1.88 ± 0.02 mmol$_{e-}$ (mmol$_{\text{Vitamin C}}$)$^{-1}$ for Vitamin C, in good agreement with the expected EDC of 2 mmol$_{e-}$ (mmol$_{\text{antioxidant}}$)$^{-1}$ for both Trolox® and Vitamin C at this E_h.[1] MEO therefore 'recovered' 98 % and 94 % of the EDCs of spiked Trolox ® and Vitamin C, respectively.
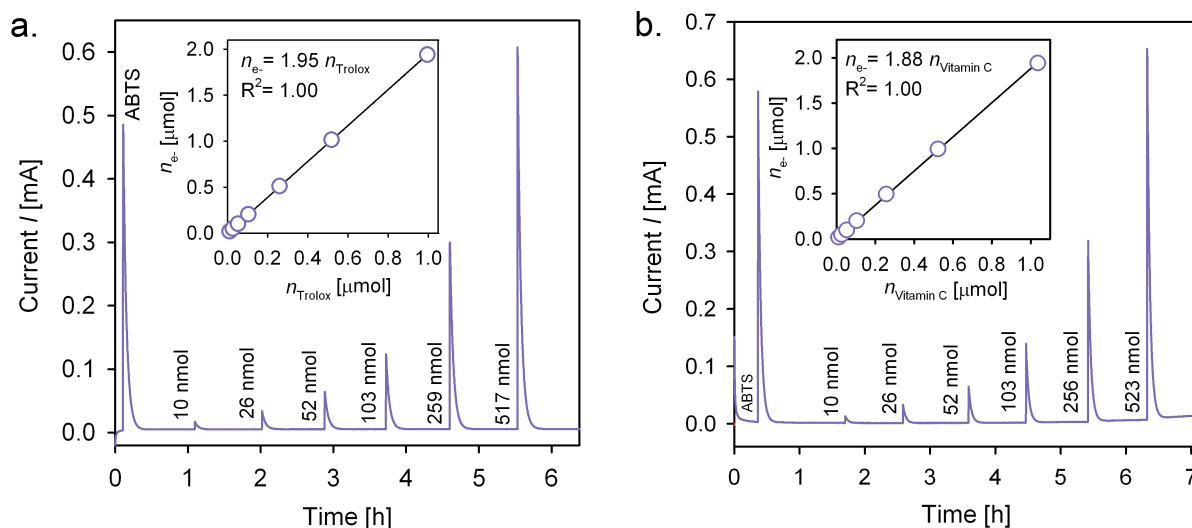
Figure S5. Oxidative current responses to spikes of ABTS and to subsequent spikes of increasing moles, $n_{\text{antioxidant}}$, of the model antioxidants Trolox® (panel a; $n_{\text{Trolox®}} = 10$ nmol to 517 nmol) and Vitamin C (panel b; $n_{\text{Viatmin C}} = 10$ nmol to 523 nmol) ($E_h = 0.61$ V and pH 7). Insets: Linear responses in the moles of electrons, n_{e-}, transferred from the model antioxidants to the working electrode versus $n_{\text{antioxidant}}$.
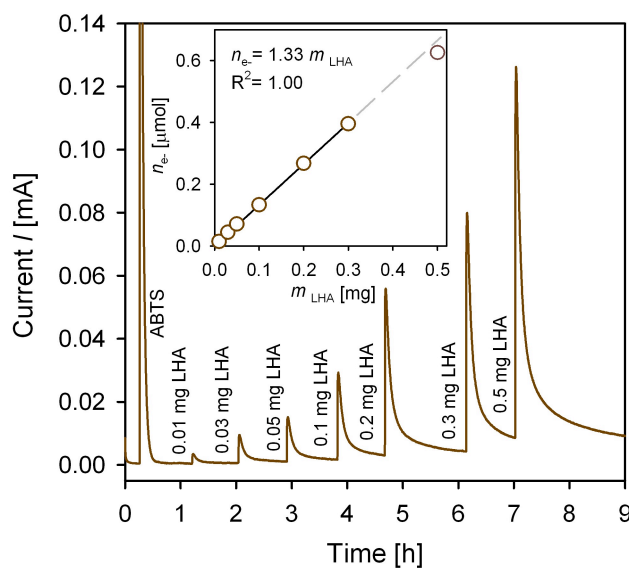
Figure S6. Oxidative current responses to spikes of ABTS and to spikes of increasing masses, m_{HA}, of Leonardite humic acid (LHA; m_{LHA} from 0.01 to 0.50 mg) ($E_h = 0.61$ V and pH 7).

162

Insets: Plots of the moles of electrons, n_{e^-}, transferred from LHA to the working electrode versus m_{LHA}. The highest spiked mass of $m_{LHA}= 0.50$ mg was outside the linear response ranges of the detection method and therefore was not included in the regression analysis.
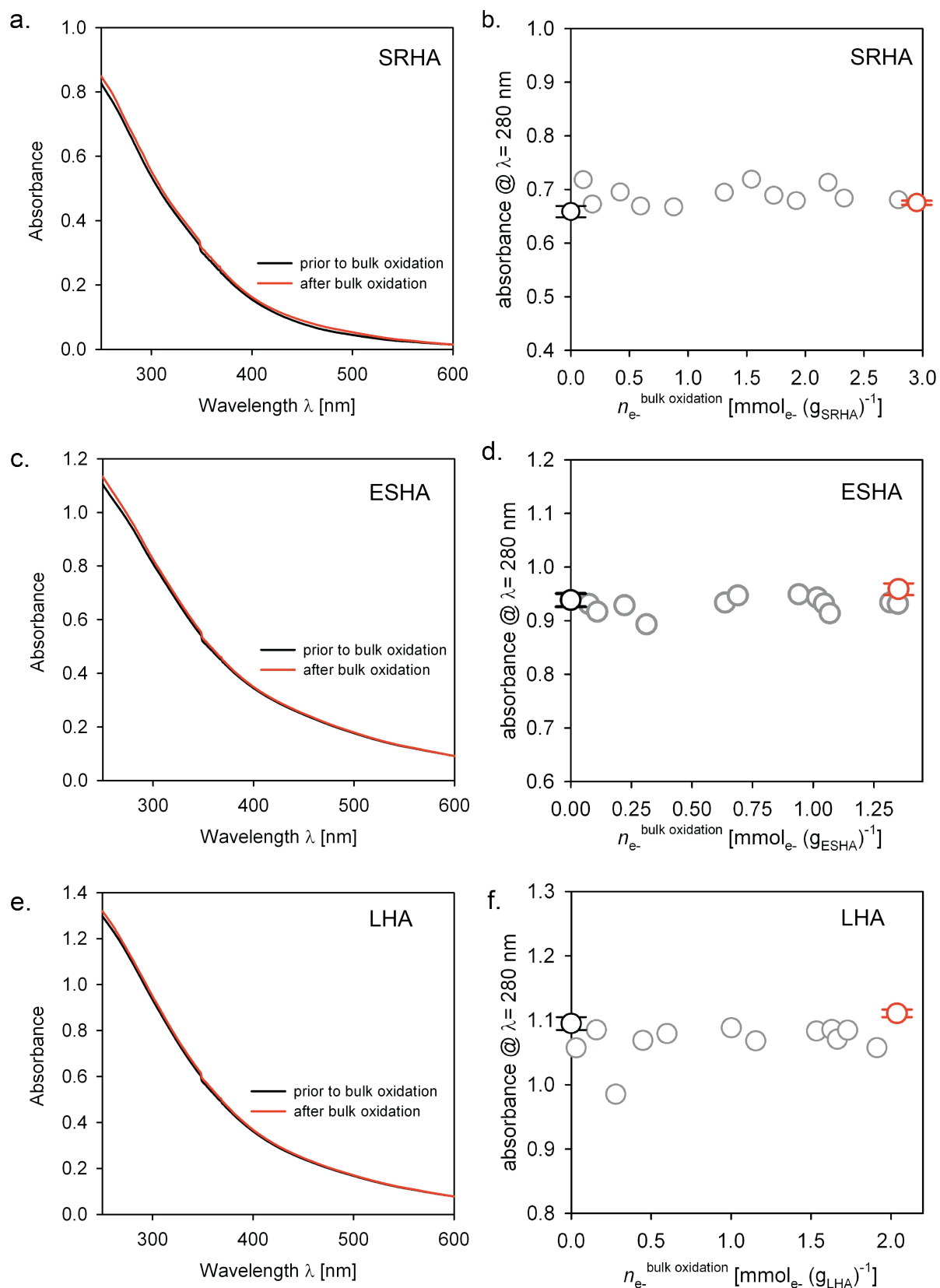
Figure **S7**. UV-visible absorbance spectra of Suwanee River Humic Acid (SRHA; panel a), Elliot Soil humic acid (panel c), and Leonardite Humic Acid (LHA, panel e) prior to (black)

and after (red) electrochemical bulk oxidation. Absorbance of SRHA (panel b), ESHA (panel d), and LHA (panel f) at $\lambda = 280$ nm as a function of the moles of electrons, $n_{e\text{-}}^{\text{bulk oxidation}}$, removed from the three HAs during their mediated electrochemical bulk oxidation.

Effect of pH and E_h on the electron donating capacities of the model antioxidant Trolox®
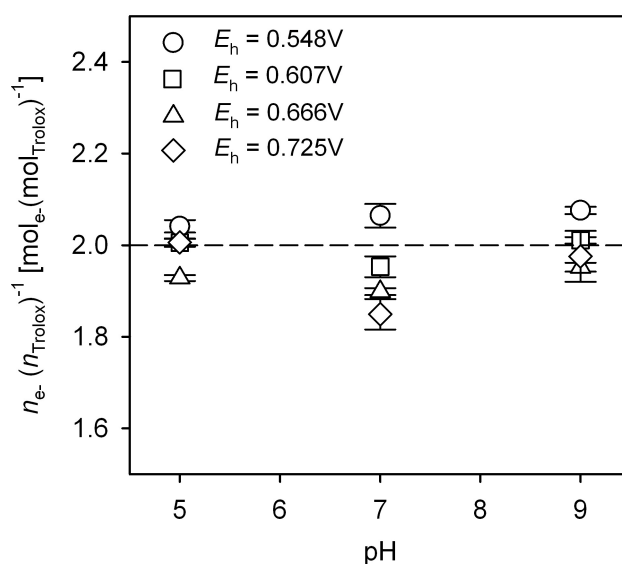
Figure **S8**. Moles of electrons, $n_{e\text{-}}$, transferred to the working electrode per mole of spiked Trolox®, $n_{\text{Trolox®}}$, as a function of applied redox potential E_h and of solution pH. The dashed line at $n_{e\text{-}} (n_{\text{Trolox®}})^{-1} = 2$ corresponds to the expected electron donating capacity of Trolox®.

E_h-pH speciation diagram of 2,2'-azino-bis(3-ethylbenzothiazoline-sulfonic acid)
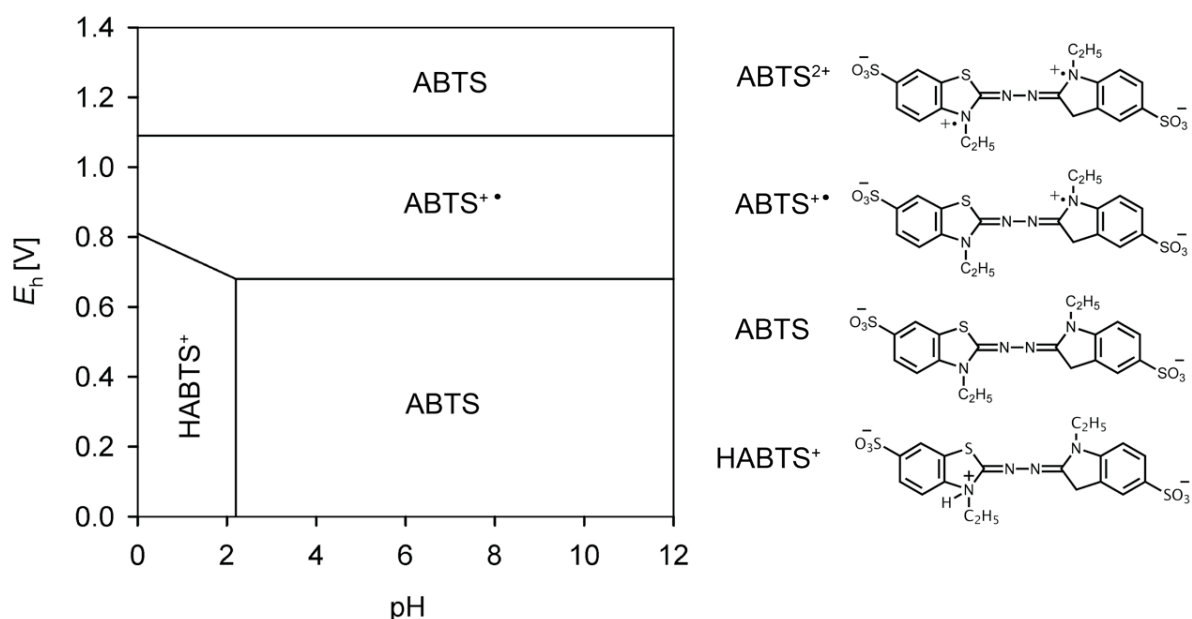
Figure S9. E_h-pH speciation diagram of 2,2'-azino-bis(3-ethylbenzothiazoline-sulfonic acid) (ABTS), calculated using standard reduction potentials and acidity constants from ref[2]. The lines in the diagram correspond to equal concentrations of the respective oxidized and reduced or protonated and deprotonated species.
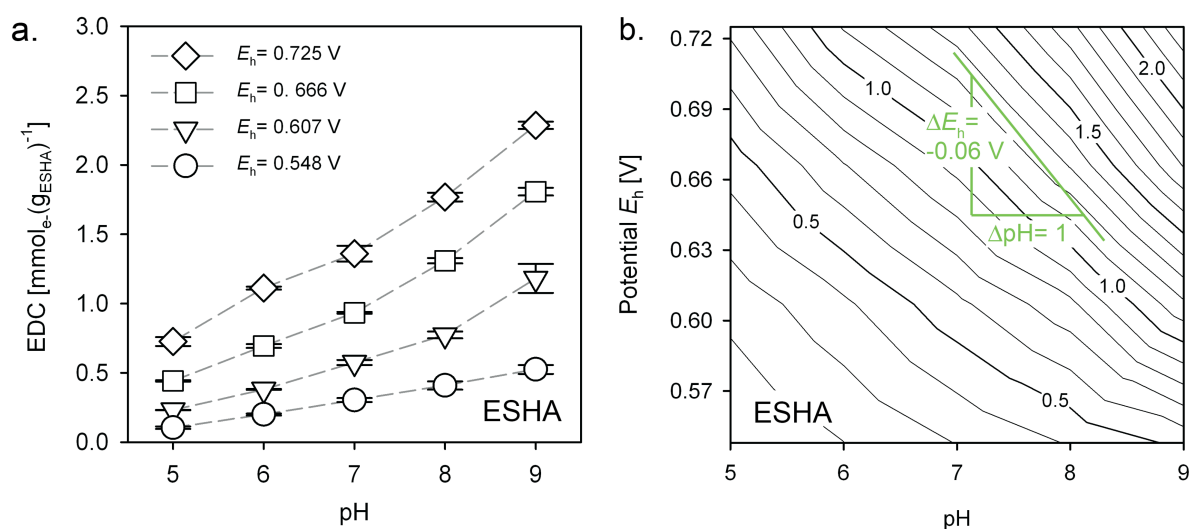
Figure S10. a. Electron donating capacities (EDCs) of Elliot Soil Humic Acid (ESHA) as a function of solution pH and applied potential E_h. **b.** Iso-EDC contour plots in units of mmol$_{e-}$

$(g_{ESHA})^{-1}$ as a function of E_h and pH for ESHA. The reference line has a slope of ΔE_h= -0.060 V per pH.
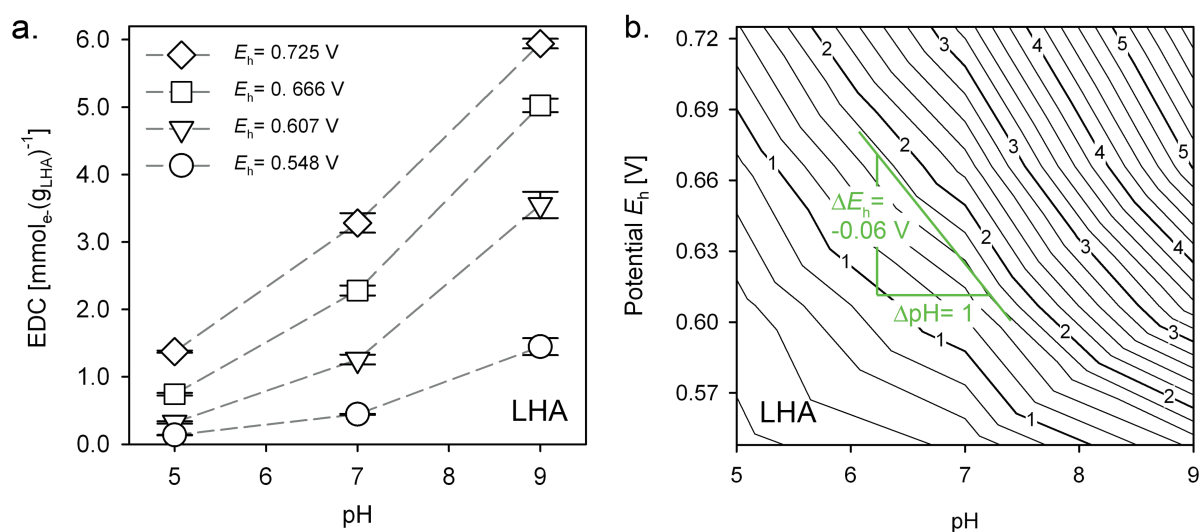
Figure S11. a. Electron donating capacities (EDCs) of Leonardite Humic Acid (LHA) as a function of solution pH and applied potential E_h. **b.** Iso-EDC contour plots in units of mmol$_{e-}$ $(g_{LHA})^{-1}$ as a function of E_h and pH for LHA. The reference line has a slope of ΔE_h= -0.060 V per pH.
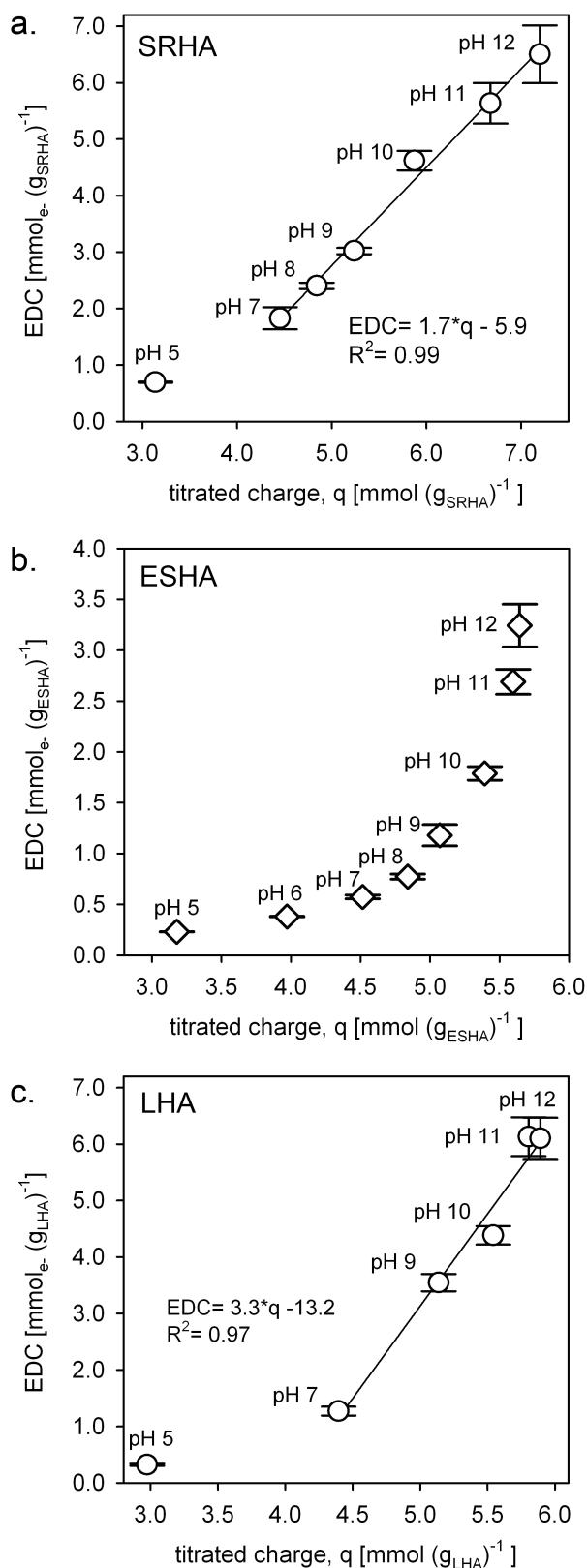
Figure S12. Changes in the electron donating capacities (EDCs) at E_h= 0.61 V of Suwannee River Humic Acid (SRHA; panel a), Elliot Soil Humic Acid (ESHA; panel b), and Leonardite

Humic Acid (LHA, panel c) with the total titrated charges of SRHA, ESHA, and LHA, respectively, as calculated from ref [3]. The pH values at which the EDCs were measured are shown next to the data symbols.

Table S1. Electron donating capacities (EDCs), electron accepting capacities (EAC), and elemental compositions of analyzed humic substances and natural organic matter (NOM) samples. The EDC and EAC values are averages ± standard deviations of at least triplicate measurements.

Humic substance	Number & abbreviation	Cat. Nr.	EDC E_h= 0.61 V pH 7	EDC E_h= 0.73V pH 7	EDC E_h= 0.61V pH 9	EAC[a] E_h= -0.49V pH 7	Elemental composition[b] C	H	O	N	S	C/H
			------- mmol$_{e-}$ (g$_{HS}$)$^{-1}$ -------			mmol$_{e-}$ (g$_{HS}$)$^{-1}$	------- mmol$_{e}$ (g$_{HS}$)$^{-1}$ -------					
Terrestrial Fulvic Acids												
Elliott Soil Fulvic Acid Standard III	1. ESFA	3S102F	704±15	824±20	1607±22	1403±11	40.39	41.28	27.00	2.26	0.37	0.98
Pahokee Peat Fulvic Acid Standard II	2. PPFA	2S103F	992±21	551±22	1242±22	1048±10	42.34	34.71	26.83	1.66	0.23	1.22
Terrestrial Humic Acids												
Elliott Soil Humic Acid Standard	3. ESHA	1S102H	1962±15	574±18	1360±57	1180±105	47.98	36.19	21.11	2.93	0.14	1.33
Pahokee Peat Humic Acid Standard	4. PPHAS	1S103H	1684±30	864±35	2211±34	1916±23	46.41	37.48	23.08	2.61	0.22	1.24
Pahokee Peat Humic Acid Reference	5. PPHAR	1R103H	1616±63	894±17	2233±70	2061±15	46.52	35.11	22.50	2.63	0.21	1.32
Leonardite Humic Acid Standard	6. LHA	1S104H	1711±33	1272±78	3282±145	3546±153	51.79	35.79	19.05	0.86	0.23	1.45
Aquatic Fulvic Acids												
Pony Lake FAR	7. PLFA	1R109F	493±10	490±4	1203±29	1014±22	43.15	52.82	19.37	4.59	0.93	0.82
Nordic Lake Fulvic Acid Reference	8. NLFA	1R105F	1053±33	1480±10	3326±125	2868±44	43.36	39.31	28.07	0.48	0.14	1.10
Suwannee River Fulvic Acid Standard II	9. SRFA	2S101F	671±8	1367±8	2848±85	2473±32	43.33	43.01	26.71	0.48	0.14	1.01
Aquatic Humic Acids												
Nordic Lake Humic Acid Reference	10. NLHA	1R105H	1197±37	1860±21	4128±125	3241±52	44.26	39.27	26.85	0.83	0.18	1.13
Suwannee River Humic Acid Standard II	11. SRHA	2S101H	962±26	1828±196	3684±66	3397±38	43.37	42.03	26.01	0.83	0.17	1.03
Waskish Peat Humic Acid Reference	12. WPHA	1R107H	981±15	2742±54	5573±34	4843±98	44.84	39.45	23.71	1.03	0.11	1.14
Aquatic Natural Organic Matter												
Suwannee River Natural Organic Matter	13. SRNOM	1R101N	653±6	1131±8	2421±72	2155±69	40.83	38.85	24.94	0.73	0.19	1.05
Nordic Lake Natural Organic Matter	14. NLNOM	1R108N	595±14	545±2	1295±18	1195±113	31.31	39.78	n.d.	0.56	n.d.	0.79
Synthetic humic acid												
Aldrich Humic Acid	15. AHA	H16752	923±60	535±10	1625±60	1428±23	46.0	44.4	23.5	0.228	0.727	1.04

[a] data from ref [4], [b] elemental composition corrected for ash content of HA; data from http://www.ihss.gatech.edu/ (accessed 1st January, 2012).

Table S2. Acidic functional group contents, carbon distributions, and metal concentrations of tested humic substances (HS) and natural organic matter (NOM) samples.

Humic substance	Number & abbreviation	Cat. Nr.	Acidic functional groups — Carboxylic mmol (g$_{HS}$)$^{-1}$	Phenolic mmol (g$_{HS}$)$^{-1}$	Aromatic C[a] %	Aliphatic C[b] %	Metal concentrations — Iron μmol g$_{HS}$$^{-1}$	Cu μmol g$_{HS}$$^{-1}$	Mn μmol g$_{HS}$$^{-1}$
Terrestrial Fulvic Acids									
Elliott Soil Fulvic Acid Standard III	1. ESFA	3S102F	6.57	1.13	30	22	3.27±0.03	0.46±0.01	<<0.3[c]
Pahokee Peat Fulvic Acid Standard II	2. PPFA	2S103F	6.43	1.12	34	20	14.72±0.18	0.41±0.03	<<0.3[c]
Terrestrial Humic Acids									
Elliott Soil Humic Acid Standard	3. ESHA	1S102H	4.77	1.08	50	16	19.55±0.27	4.69±0.14	<<0.3[c]
Pahokee Peat Humic Acid Standard	4. PPHAS	1S103H	5.02	1.06	47	19	37.80±1.17	0.28±0.02	<<0.3
Pahokee Peat Humic Acid Reference	5. PPHAR	1R103H	4.96	1.15			49.56±0.87	0.31±0.02	<<0.3
Leonardite humic Acid Standard	6. LHA	1S104H	4.64	1.44	58	14	9.97±0.32	0.11±0.01	<<0.3
Aquatic Fulvic Acids									
Pony Lake FAR	7. PLFA	1R109F			12	61	1.59±0.07	1.28±0.03	<<0.3
Nordic Lake Fulvic Acid Reference	8. NLFA	1R105F	5.81	1.66	31	18	4.89±0.02	0.06±0.02	<<0.3
Suwannee River Fulvic Acid Standard II	9. SRFA	2S101F	5.81	1.48	22	35	6.81±0.11	0.33±0.01	<<0.3
Aquatic Humic Acids									
Nordic Lake Humic Acid Reference	10. NLHA	1R105H	4.82	1.72	38	15	18.15±0.49	0.2±0.02	<<0.3
Suwannee River Humic Acid Standard II	11. SRHA	2S101H	4.76	1.94	31	29	22.91±0.53	0.46±0.02	<<0.3
Waskish Peat Humic Acid Reference	12. WPHA	1R107H			42	18	9.46±0.04	0.73±0.03	<<0.3
Aquatic Natural Organic Matter									
Suwannee River Natural Organic Matter	13. SRNOM	1R101N	4.83	1.93	23	27	n.q	n.q	n.q
Nordic Lake Natural Organic Matter	14. NLNOM	1R108N			19	31	n.q	n.q	n.q
Synthetic humic acid									
Aldrich Humic Acid	15. AHA	H16752					300.73±3.57	0.12±0.02	<<1

[a] obtained from integration of ^{13}C NMR spectra over the chemical shift range of 165-110 ppm; data from http://www.ihss.gatech.edu/ (accessed 1st January, 2012).
[b] obtained from integration of ^{13}C NMR spectra over the chemical shift range of 60-0 ppm; data from http://www.ihss.gatech.edu/ (accessed 1st January, 2012).
[c] filtered with 0.2 μm syringe filters prior to analysis.

References

1.   Steenken, S.; Neta, P., One-Electron Redox Potentials of Phenols - Hydroxyphenols and Aminophenols and Related-Compounds of Biological Interest. *Journal of Physical Chemistry* **1982,** *86*, 3661-3667.

2.   Scott, S. L.; Chen, W. J.; Bakac, A.; Espenson, J. H., Spectroscopic Parameters, Electrode-Potentials, Acid Ionization-Constants, and Electron-Exchange Rates of the 2,2'-Azinobis(3-Ethylbenzothiazoline-6-Sulfonate) Radicals and Ions. *Journal of Physical Chemistry* **1993,** *97,* 6710-6714.

3.   Perdue, E. M.; Ritchie, J. D., Proton-binding study of standard and reference fulvic acids, humic acids, and natural organic matter. *Geochimica Et Cosmochimica Acta* **2003,** *67*, 85-96.

4.   Aeschbacher, M.; Sander, M.; Schwarzenbach, R. P., Novel electrochemical approach to assess the redox properties of humic substances. *Environ Sci Technol* **2010,** *44*, 87-93.

Chapter 5

Assessing the effect of humic acid redox state on organic pollutant sorption by combined electrochemical reduction and sorption experiments

Abstract

Natural organic matter (NOM) is a major sorbent for organic pollutants in soils and sediments. While sorption under oxic conditions has been well investigated, possible changes in the sorption capacity of a given NOM induced by reduction have not yet been studied. Reduction of quinones to hydroquinones, the major redox active moieties in NOM, increases the number of H-bond donating moieties and thus may affect sorption. This work compares the sorption of four non-ionic organic pollutants of different polarities (naphthalene, acetophenone, quinoline, and 2-naphthol), and of the organocation paraquat to unreduced and electrochemically reduced Leonardite Humic Acid (LHA). The redox states of reduced and unreduced LHA in all sorption experiments were stable, as demonstrated by a spectrophotometric 2,6-dichlorophenol indophenol reduction assay. The sorption isotherms of the non-ionic pollutants were highly linear, while paraquat sorption was strongly concentration-dependent. LHA reduction did not result in significant changes in the sorption of all tested compounds, even of the cationic paraquat at pH 7, 9, and 11. This work provides first evidence that changes in NOM redox state do not largely affect organic pollutant sorption, suggesting that current sorption models are applicable both to unreduced and reduced soil and sediment NOM.

5.1. Introduction

Natural organic matter (NOM) is a major environmental sorbent for organic pollutants. The sorption of organic pollutants to NOM is well investigated and understood at the molecular level.[1-11] While all organic pollutants interact with NOM by non-specific van der Waals (vdW) interactions, monopolar (i.e., either H-bond donating or accepting) and bipolar (i.e., H-bond donating and accepting) compounds additionally undergo specific H-bond donor-acceptor (HDA) interactions with polar functional moieties in NOM. Furthermore, organocations may exhibit high affinities to NOM due to strong electrostatic attraction to carboxylate and phenolate moieties.[12] The sorption of polar and cationic organic pollutants therefore depends on the numbers of H-bond donating and H-bond accepting moieties, and of anionic sites in NOM, respectively.[13] In addition, sorption of any organic pollutant depends on NOM cohesive energy, which itself is expected to increase with increasing HDA interactions between polar moieties within the NOM.

The abundance of polar and anionic moieties varies between different types of NOM.[14, 15] The abundance of such moieties may, however, also change for a given NOM when it undergoes chemical reactions. Reduction and oxidation reactions involving NOM are of particular interest, since many contaminated soils, sediments, and aquifers may undergo spatial and temporal changes in redox conditions. For humic acids (HA) and fulvic acids, two major components of NOM, electron accepting capacities of up to two millimoles of electrons per gram have been reported. [16-18] It has been shown that quinone/hydroquinone pairs are major redox-active moieties in NOM that may reversibly undergo reduction and oxidation.[19-21] Reduction of quinones to hydroquinones increases the number of H-bond donating moieties and the deprotonation of the hydroquinones at high pH results in the formation of mono-and diphenolate anions[22, 23] (Table **1**; upper part). The increase in H-bond donating moieties upon reduction may, on the one hand, enhance the sorption of monopolar H-bond accepting and of bipolar organic pollutants. On the other hand, it may render sorption of all organic pollutants energetically less favorable if it increases intra-NOM HDA interactions and hence the cohesive energy of the NOM. Increases in the number of anionic sites upon reduction at

high pH may lead to increased organocation sorption. Finally, reduction may also affect sorption if it alters the conformational structure of NOM aggregates.[24-26]

Only few studies have addressed possible effects of NOM reduction state on the sorption of exclusively apolar organic pollutants. The majority of these studies reported altered organic pollutant sorption upon changes in the redox states of contaminated soils and sediments (e.g., re-aeration of reduced samples).[26-31] The complexity of the investigated systems, however, impaired assessing whether changes in NOM redox state contributed to altered sorption. Coates et al. reported decreased naphthalene sorption to microbially reduced Aldrich HA compared to the unreduced HA.[26] This finding may have reflected an increase in the cohesive energy of the HA upon reduction. None of the previous studies, however, included polar and cationic organic compounds to more selectively probe for changes in the H-donor and acceptor properties and the number of anionic moieties in NOM upon its reduction.

The goal of this work was to assess whether NOM reduction affects its properties as sorbent for organic pollutants. To this end, sorption of five model organic pollutants (Table **1**, lower part) was studied to both unreduced and electrochemically reduced Leonardite humic acid (LHA). The pollutants included the weak H-bond accepting naphthalene (referred to as "apolar" in the following), the monopolar, H-bond accepting acetophenone and quinoline, the bipolar H-bond donating and accepting 2-naphthol, and the organocation paraquat (Table **1**). LHA, a kerogen-derived HA, was chosen because it has been used in previous sorption studies[1, 2, 12] and is well-characterized[14-16] (Table **1**). Furthermore, due to its high aromaticity and C/O ratio, LHA represents a humin-like end-member among the HAs and hence is considered as a model for both HA and humin. Finally, the EAC of LHA is about 1.7 $mmol_{e-}(g_{LHA})^{-1}$, which is among the highest reported values for HA.[16] With quinones as the major reducible moieties in LHA,[16, 22] even partial reduction of LHA results in a significant increase in the number of phenolic H-bond donating sites (see below). LHA was reduced by direct electrochemical reduction.[16] In contrast to previous methods that relied on the use of chemical reductants, the electrochemical reduction allows for a selective electron transfer to reducible moieties to yield reduced HA with well-defined reduction states and devoid of

chemical reductants that can be directly used in subsequent experiments. Both before and after the sorption experiments the redox states of unreduced and reduced LHA were quantified by their reductive decolorization of added 2,6-dichlorophenol indophenol.[16]

Table 1. Upper part: Some important chemical characteristics of unreduced and partially reduced LHA. Lower part: Chemical structures of the probe compounds and their respective interactions with quinone and hydroquinone moieties. vdW: van der Waals interactions, HDA: H-bond donor-acceptor interactions; ES: electrostatic interactions.

Leonardite Humic Acid	Unreduced	Reduced
Structural properties:		

Element	C	H	O	N
mmol $(g_{LHA})^{-1}$	53.1	36.6	19.5	0.9

	Aromatic	Aliphatic
[%]	58	14

$$1 \; mmol_{e-} \, (g_{LHA})^{-1} \longrightarrow$$

	quinones monopolar	hydroquinones bipolar anion at high pH
Phenolic moieties [mmol $(g_{LHA})^{-1}$]:	~1.4	~2.4 (+ 71%)
Carboxylic moieties [mmol $(g_{LHA})^{-1}$]:	~4.6	~4.6

Probe compounds		Interactions with quinones	Interactions with hydroquinones
naphthalene 'apolar'		vdW	vdW (+ HDA) (weak H-bond acceptor)
quinoline monopolar (& ionic)		vdW	vdW + HDA (+ ES, $pK_{a,quin}$= 4.9)
acetophenone monopolar		vdW	vdW + HDA
2-naphthol bipolar		vdW + HDA	vdW + HDA
paraquat monopolar & ionic		vdW (+ ES*)	vdW + HDA + ES

* quinines substituted with acidic functional groups (e.g. carboxyl- and hydroxyl groups)

179

5.2. Materials and Methods

Chemicals. All chemicals were of analytical grade and were used as received. 2,6-dichlorophenol indophenol sodium salt hydrate (DCPIP), 2-naphthol, acetophenone, hydrochloric acid (32%), and sodium hydroxide solutions (32%) were from Fluka, quinoline, naphthalene, and methylviologen dichloride monohydrate (paraquat) were from Sigma Aldrich, sodium dihydrogen phosphate monohydrate, potassium dihydrogen phosphate, sodium hydrogen carbonate, boric acid, and potassium chloride were from Merck AG, and methanol was from Scharlau. All aqueous solutions were prepared with NanoPure water.

Anoxic experiments. Electrochemical reductions and all sorption experiments were conducted in an anoxic glovebox (N_2 atmosphere at 25±1°C, O_2< 0.1ppm; M. Braun Ltd., Germany). Aqueous solutions were made anoxic by purging with argon for 2 hours at 150°C and for 1 hour at room temperature. Methanol was made anoxic by purging with argon for 1 hour.

Sorbent. Leonardite humic acid (LHA) standard was purchased from the International Humic Substances Society (St. Paul, MN, USA) and was used as received. LHA solutions (125mL, $2g_{LHA}L^{-1}$) were prepared in the glovebox by dissolving LHA in aqueous solutions containing 0.1M phosphate (pH 7), borate (pH 9), or carbonate (pH 11) as pH buffers and 0.1M KCl as electrolyte for accurate potential control during electrochemical reduction. The pH was adjusted to ±0.02 pH units by addition of anoxic NaOH (32%). A total of eight batches (I-VIII) of LHA solutions were prepared and stored in light-protected flasks. An aliquot of each batch was withdrawn and used as *unreduced* LHA in the sorption experiments. Another aliquot was reduced electrochemically and then used as *reduced* LHA in the sorption experiments.

Direct electrochemical reduction. LHA was reduced in a bulk electrolysis cell according to Aeschbacher et al.[16] Briefly, 65mL of the LHA solution from each batch were transferred into an electrochemical cell containing a glassy carbon working electrode (Sigradur G®, HTW, Germany), an Ag/AgCl reference electrode, and a coiled platinum wire auxiliary electrode (both from Bioanalytical Systems Inc., West Lafayette, IN, USA). To minimize

re-oxidation of reduced LHA at the auxiliary electrode, the anodic compartment was separated from the cathodic compartment by a porous glass frit. A model 630C potentiostat (CHInstruments, USA) was used to measure the current, I, and to control the potential, E_h, at the working electrode. LHA solutions were reduced under stirring for 60 hours at an E_h= -0.59V (vs. standard hydrogen electrode), the number of electrons, n_{e^-}, transferred per mass of LHA was obtained by integration of reductive currents over time.

Sorption experiments. Sorption experiments were carried out in custom-made dialysis cells.[12] Each cell consisted of two approximately 4mL compartments separated by a dialysis membrane that was impermeable to LHA but permeable to the organic pollutants. Prior to use, the dialysis membranes were immersed in water, and made anoxic by purging with argon for two hours. A 500Da molecular weight cutoff (MWCO) Spectra/Por® cellulose ester membrane (Spectrum Laboratories, USA) was used for all sorption experiments with non-ionic pollutants. Control experiments showed that paraquat diffused very slowly across the 500Da MWCO membrane. To facilitate attainment of diffusive equilibrium, a 2000Da MWCO cellulose membrane (Roth, Germany) was employed for the paraquat experiments instead. Prior to the paraquat sorption experiments, the LHA-solutions were pre-dialyzed against pH-buffered solutions to remove low molecular weight LHA constituents that passed through the 2000Da MWCO membrane. Pre-dialysis was carried out for 7 days in the same dialysis cells subsequently used for sorption. The dialysate was replaced after 2, 4, and 7 days.

All sorption experiments were carried out in triplicates. Sorption experiments with the non-ionic pollutants were run at pH 7 and for quinoline also at pH 9. For each pollutant and at each pH, the sorption experiments were conducted at four different initial pollutant concentrations $C_{i,aq}^0$ in the LHA free dialysis cell (see Supporting Information). Sorption of paraquat was studied at two C_{aq}^0 at pH 7, 9, and 11. Sorption was initiated by filling one of the two compartments of each dialysis cell with 4mL solutions containing reduced or unreduced LHA (2gL^{-1} for the non-ionic pollutants and 0.2gL^{-1} for paraquat) and by filling the second compartment of each cell with solutions containing the organic pollutant. Cells were shaken horizontally for 7 and 8 days in the dark to attain sorption equilibrium of the non-ionic pollutants and paraquat, respectively

181

(see Supporting Information). Three 1 mL aliquots were withdrawn from the LHA-free half-cells and analyzed to determine the aqueous pollutant concentration. For the non-ionic pollutants, 3mL aliquots were withdrawn from the LHA-containing solutions, extracted with 3mL of ethyl acetate, and the pollutant concentration was quantified in the extract. Control experiments demonstrated quantitative extraction by ethyl acetate (see Supporting Information). Concentrations of the non-ionic organic pollutants were quantified by HPLC-UV (Dionex PDA-100, *USA*). The cationic paraquat could not be extracted from LHA-containing half-cells with organic solvents. Paraquat was therefore only quantified in the LHA-free half-cells by derivative spectrophotometry at $\lambda = 241 \text{nm}$[32] to eliminate artifacts resulting from weak UV absorbance of small amounts of LHA that had diffused across the membrane during the sorption experiment. Further details on the quantification of the organic pollutants are provided in the Supporting Information.

The sorbed concentrations of the non-ionic pollutants and of paraquat, $C_{i,LHA}$ [mol $(g_{LHA})^{-1}$)], were calculated according to Equations **1** and **2,** respectively.

$$C_{i,LHA} = \frac{C_{i,LHA\ cell} \cdot V_{LHA\ cell} - C_{i,aq} \cdot V_{buffer\ cell}}{m_{LHA}} \qquad (1)$$

$$C_{i,LHA} = \frac{(C_{i,aq}^{0} - 2 \cdot C_{i,aq}) \cdot V_{buffer\ cell}}{m_{LHA}} \qquad (2)$$

where $C_{i,aq}$ [mol L^{-1}] is the aqueous pollutant concentration, $C_{i,aq}^{0}$ [mol L^{-1}] is the initial aqueous pollutant concentration in the LHA-free solution, $V_{LHA\ cell}$ and $V_{buffer\ cell}$ [L] are the volumes of the LHA-containing and LHA-free solutions, respectively, and m_{LHA} [g] is the mass of LHA in each dialysis cell.

After sorption, the membranes from each dialysis cell were extracted. While only small fractions of quinoline, acetophenone, and paraquat sorbed to the membrane, approximately 30% of the total mass of naphthalene and 2-naphthol sorbed to the membranes. When accounting for these losses, overall high recoveries were found for all compounds (see Supporting Information).

182

The sorption isotherms for the non-ionic pollutants were plotted as $\text{Log}_{10}(C_{i,LHA})$ versus $\text{Log}_{10}(C_{i,aq})$ and fitted by the logarithmized Freundlich equation (Equation **3**) to determine Freundlich affinity coefficients, $K_{i,F}$ [mol^{1-N} L^{N} $(\text{g}_{LHA})^{-1}$], and the Freundlich exponents, N_i:

$$\text{Log}_{10}(C_{i,LHA}) = \text{Log}_{10}(K_{i,F}) + N_i \cdot \text{Log}_{10}(C_{i,aq}) \tag{3}$$

The apparent organic carbon normalized distribution coefficient, $K_{i,OC}$ [L $(\text{kg}_C)^{-1}$], was calculated according to Equation 4. For the non-ionic compounds $K_{i,OC}$ was calculated at $C_{i,aq} = 50$ and $100\mu M$, and $C_{i,LHA}$ was extrapolated from Equation 3. For paraquat, K_{OC} was calculated for the experimental concentrations.

$$K_{i,OC} = \frac{C_{i,LHA}}{f_{OC} \cdot C_{i,aq}} \tag{4}$$

where $f_{oc} = 6.22 \cdot 10^{-4}$ [kg_C $(\text{g}_{HA})^{-1}$] is the ash-corrected organic carbon content of LHA.[15]

Sorption of the non-ionic compounds to unreduced and reduced LHA were compared based on the 95% confidence intervals of the fitted isotherm parameters, $\text{Log}_{10}(K_{i,F})$ and N_i, and based on the prediction intervals for $K_{i,OC}$ obtained at given $C_{i,aq}$ from the fitted isotherm parameters. Paraquat sorption to unreduced and reduced LHA was compared based on the 95% confidence intervals of the concentration-dependent K_{OC} values.

Spectrophotometric redox assay. The redox states of unreduced and reduced LHA were analyzed before and after the sorption experiments by a spectrophotometric assay based on the reductive decolorization of the blue redox dye DCPIP ($\varepsilon = 20.6$ mM^{-1} cm^{-1} at $\lambda = 603$ nm).[16, 33] Aliquots of unreduced and reduced LHA solutions were withdrawn from the respective LHA solutions prior to filling of the dialysis cells and from all half-cells containing LHA solutions after termination of the sorption experiment. Three different volumes of the LHA aliquots were transferred to plastic cuvettes (Brand GMBH, Germany) with solutions containing DCPIP in excess amounts relative to n_{e^-}. A fourth cuvette containing DCPIP was not amended with LHA solutions. The cuvettes were sealed, mixed, and transferred out of the glovebox. The

absorbance spectra of DCPIP were measured (400-800 nm) after a reaction time of approximately 10 min on a Cary100 spectrophotometer (Varian Instruments, USA). The number of electrons transferred from LHA to DCPIP, $n_{e\text{-,DCPIP}}$, was calculated from the decrease in DCPIP absorbance at $\lambda = 603$ nm with increasing LHA concentration and served to quantify the redox state of the LHA samples. Further details are provided in the Supporting Information and in Aeschbacher et al.[16] The kinetics of electron transfer from reduced LHA to DCPIP and the dependence of the detected $n_{e\text{-,DCPIP}}$ on the electrochemically transferred $n_{e\text{-}}$ were analyzed separately.

5.3. Results and Discussion

Electrochemical LHA reduction. The data in Figure **1a** shows the number of electrons, $n_{e\text{-}}$, transferred per mass of LHA during bulk electrolysis of the eight batches of LHA with batches I-VI at pH 7, batch VII at pH 9, and batch VIII at pH 11. As shown previously,[16] LHA-containing solutions showed much higher reductive currents and therefore higher $n_{e\text{-}}$ than LHA-free solutions (data not shown), demonstrating negligible reduction of H^+ to H_2 at the glassy carbon working electrode at the given pH and applied potentials. The rate of electron transfer from the working electrode to LHA gradually decreased over the 60 hours reduction periods. The number of electrons transferred in 60 hours decreased with increasing pH from 1.05 ± 0.08 mmol$_{e\text{-}}$ g$_{LHA}^{-1}$ at pH 7 (average $\pm$ standard deviation of batches I-IV), to 0.76 mmol$_{e\text{-}}$ g$_{LHA}^{-1}$ at pH 9 and pH 11. The $n_{e\text{-}}$ at pH 7 agreed well with a previously published value obtained under the same reduction conditions,[16] demonstrating the high reproducibility of direct electrochemical reduction. The slight variations in $n_{e\text{-}}$ between the different batches at pH 7 likely resulted from small differences in the cell geometries and the kinetics of electron transfer from the electrode to LHA. Slower reductions and lower final $n_{e\text{-}}$ at pH 9 and pH 11 as compared to pH 7 are consistent with the decrease in the reduction potentials of the quinone moieties in LHA with increasing pH.[22]

Direct electrochemical reduction provided reduced LHA samples with known redox states. In contrast to previous reduction methods that rely on the

use of chemical reductants (e.g., [17, 34, 35]), the electrochemical reduction selectively alters the redox state of LHA, which can be used without purification in follow up experiments. Given that electrons are primarily transferred to quinones in LHA,[16, 22] the electrochemical reduction resulted in the formation of approximately 0.5 mmol hydroquinones per gram LHA at pH 7. The reduction therefore significantly altered the chemical structure of LHA as it affected more than 5% of all oxygen atoms and more than 10% of all non-carboxylic oxygen atoms in LHA, and it resulted in a 71% increase in the concentration of phenol moieties (see Table **1**).[14, 15]
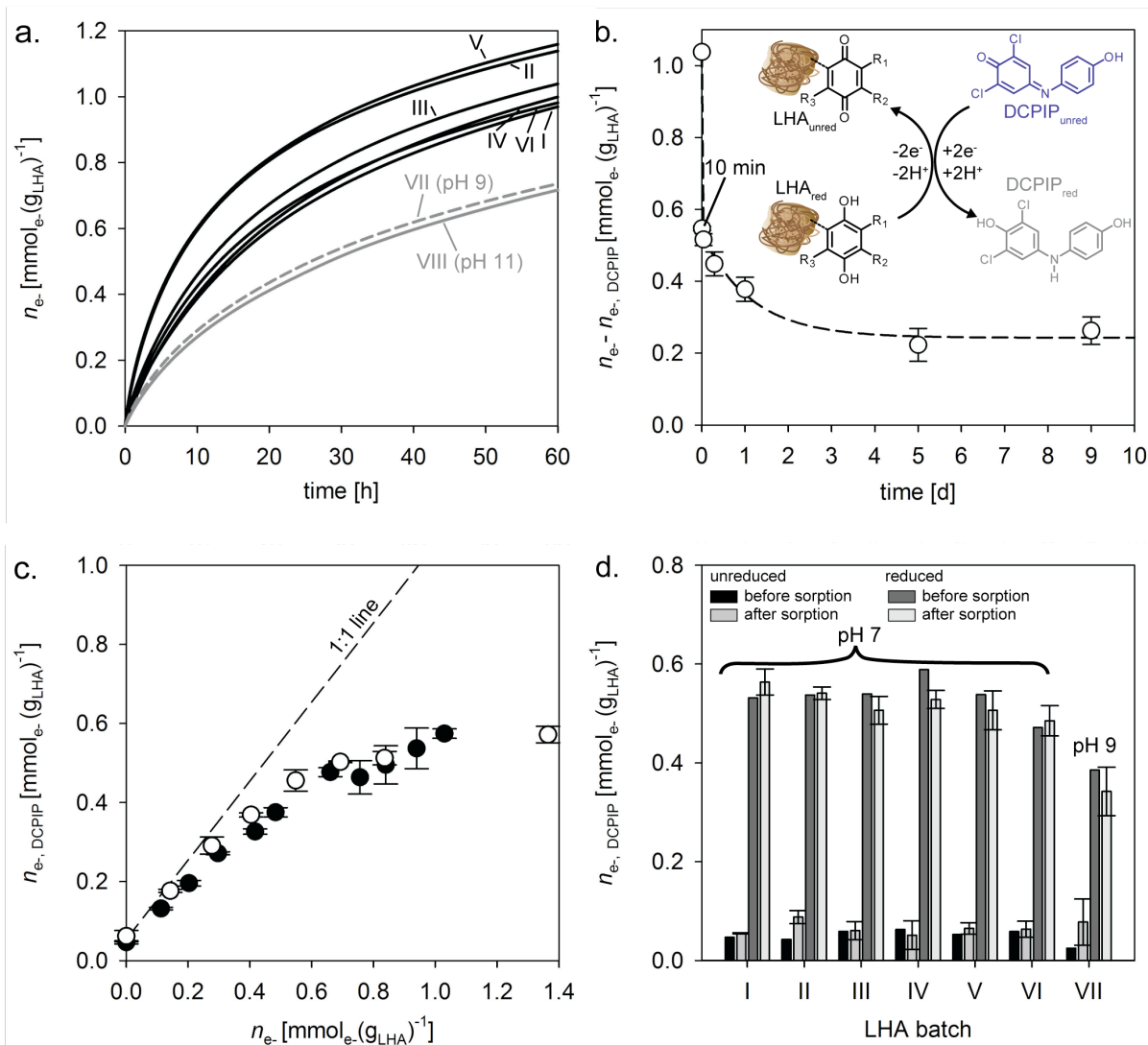
Figure 1. a. The number of electrons, n_{e-}, transferred per mass of Leonardite Humic Acid (LHA) during electrochemical bulk reduction of batches I-VI (pH 7), batch VII (pH 9), and batch VIII (pH 11). **b.** Re-oxidation kinetics of reduced LHA by 2,6-dichlorophenol indophenol (DCPIP) at pH 7. The initial value of $n_{e-}= 1.04$ mmol$_{e-}$ g$_{LHA}^{-1}$ corresponds to the number of electrons transferred to LHA during the direct electrochemical reduction. The other values were calculated by subtracting the number of electrons transferred to DCPIP, $n_{e-,DCPIP}$, from the initial n_{e-} value. **c.** Number of electrons recovered from reduced LHA by DCPIP, $n_{e-,DCPIP}$, versus the moles of electrons transferred to LHA withdrawn from the electrochemical cell in aliquots at different times during direct electrochemical reduction, n_{e-} (duplicate experiments; the error bars represent standard errors). **d.** Number of electrons transferred to DCPIP, $n_{e-,DCPIP}$, from unreduced and reduced LHA for all batches. $n_{e-,DCPIP}$ were quantified prior to and after each sorption experiment. The bars represent averages and the error bars represent standard deviations of $n_{e-,DCPIP}$ for LHA solutions of the respective batch taken from dialysis cells after termination of the sorption experiment.

Stability of the LHA reduction state. All sorption experiments were conducted in an anoxic glovebox because oxygen rapidly and extensively re-oxidizes reduced HA.[16, 36] In order to confirm that reduced LHA solutions were not re-oxidized over the course of the sorption experiments, the redox states of reduced and unreduced LHA were re-analyzed prior to and after the sorption experiments using the recently developed spectrophotometric DCPIP assay.[16] This assay allows for a high sample throughput and thus allowed analyzing LHA samples from all (>100) dialysis cells.

The re-oxidation of electrochemically reduced LHA over time after addition of DCPIP is shown in Figure **1b**. The LHA re-oxidation kinetics were clearly biphasic: about 55% of the electrons transferred to LHA during electrochemical reduction were rapidly transferred to DCPIP within 10 min, while the transfer of the remaining electrons occurred at a much slower rate. After 9 days, DCPIP recovered close to 80% of the electrons transferred to LHA during reduction. The re-oxidation data demonstrates that the reduced moieties in LHA exhibited different electron transfer rates to DCPIP and that about 20% of the reduced moieties were not readily re-oxidized by DCPIP over 9 days. Similar biphasic kinetics and incomplete oxidation were reported for reduced LHA by O_2 [16] and of reduced Pahokee Peat HA by Fe^{3+} complexes.[37] It is reasonable to assume that those moieties in LHA that rapidly transfer electrons to DCPIP also rapidly transfer electrons to O_2.

The number of electrons transferred from reduced LHA to DCPIP, $n_{e-,DCPIP}$, within 10 min of reaction increased with the moles of electrons transferred to LHA during electrochemical reduction, n_{e-} (Figure **1c**), demonstrating that the DCPIP assay was highly sensitive to changes in the LHA redox state. Furthermore, the assay yielded reproducible results, as shown by the good agreement between the duplicate experiments. Consequently, the assay was used to assess whether changes occurred in the redox state of LHA (i.e., re-oxidation of reduced LHA by O_2) during the sorption experiments.

The data in Figure **1d** shows the number of electrons transferred from unreduced and reduced LHA to DCPIP, $n_{e-,DCPIP}$, quantified both prior to and after the sorption experiments. As expected, $n_{e-,DCPIP}$, was much larger for the reduced than for the unreduced LHA samples. Comparable $n_{e-,DCPIP}$ values obtained for reduced LHA at pH 7 (batches I to VI) were consistent with the comparable n_{e-} transferred to these samples during electrochemical reduction (Figure **1a**). The lower $n_{e-,DCPIP}$ values of reduced LHA at pH 9 (batch VII) reflected the lower n_{e-} transferred to the LHA at this pH (Figure **1a**). More importantly, there were no significant differences in the $n_{e-,DCPIP}$ of samples collected from a given batch prior to and after the sorption experiments (Figure **1d**). This finding implies that there were no detectable changes in the reduction states of both the unreduced and reduced LHA during the sorption experiments, which excludes re-oxidation of reduced LHA, for instance by traces of O_2 in the glovebox.

Sorption isotherms. The data in Figure **2a** shows the sorption isotherms of naphthalene, acetophenone, and 2-naphthol at pH 7 and of quinoline at pH 7 and pH 9 to unreduced LHA and the Freundlich isotherm fits to the sorption data. The corresponding Freundlich affinity coefficients, $K_{i,F}$, and the Freundlich exponents, N_i, are provided in Table **2**. Sorption of apolar naphthalene, and the H-bond accepting acetophenone and quinoline at pH 7 were concentration independent, as evident from linear sorption isotherms (i.e., $N_i \approx 1$). Conversely, the sorption of bipolar 2-naphthol was slightly concentration dependent ($N_i \approx 0.80$). These observations suggest that the interaction energies between 2-naphthol molecules and sorption sites in LHA decreased with increasing sorbed concentrations, C_{LHA}. The high affinity sorption sites that were preferentially occupied at low C_{LHA} may have involved

H-bond accepting moieties, given that non-linearity was observed only for bipolar 2-naphthol but not for the apolar and monopolar, H-bond accepting model compounds. Based on the Freundlich model parameters, the organic carbon normalized partition coefficients, $K_{i,OC}$, of the non-ionic pollutants were calculated for solution concentrations of $C_{i,aq}$ equal to 50 and 100 µM (Table **2**). The $K_{i,OC}$ values compare well with literature values (Table **2**).

At pH 7, about 1% of the quinoline in solution was cationic ($pK_{a,quinoline}$= 4.9[38]). Electrostatic attraction of organocations to anionic sites in HA may result in high affinity sorption.[39] For example, sorption of the sulfonamide antibiotic sulfathiazole to LHA is dominated by the cationic species up to 3 pH units above the pK_a value of the aniline moiety in sulfathiazole.[12] To assess the contribution of the quinoline cation to quinoline sorption at pH 7, sorption experiments were also carried out at pH 9 at which less than 0.01% of the quinoline was cationic. Comparable sorption at pH 7 and pH 9 (Figure **2a**, Table **2**), demonstrates that the neutral quinoline dominated sorption at pH 7. These findings are in agreement with previous work by Nielsen and coworkers[40] who reported constant K_{OC} values for quinoline to Aldrich humic acid between pH 7 and pH 12.
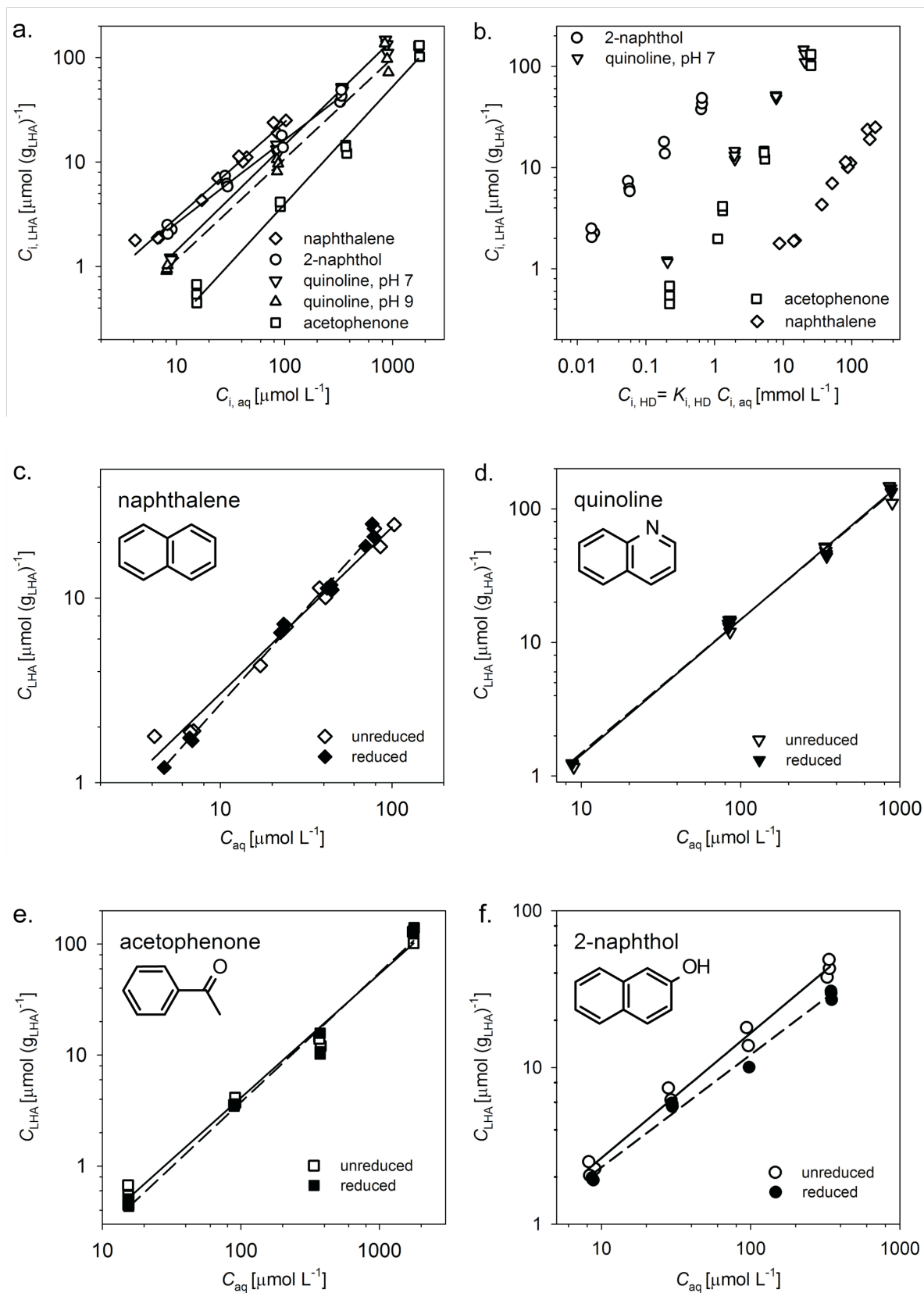
Figure **2**. **a.** Sorption isotherms of naphthalene, acetophenone, and 2-naphthol at pH 7 and of quinoline at pH 7 and 9, to unreduced Leonardite humic acid (LHA). $C_{i,aq}$ and $C_{i,LHA}$ are the equilibrium molar aqueous and sorbed concentrations, respectively. The lines represent fits of the Freundlich model. **b**. Sorption isotherms of naphthalene, acetophenone, quinoline, and 2-naphthol to unreduced LHA at pH 7 re-plotted from panel (a) as $C_{i,LHA}$ versus the calculated dissolved concentrations of the tested compounds in n-hexadecane, $C_{i,HD}$, in equilibrium with $C_{i,aq}$. **c-f.** Sorption isotherms of naphthalene (panel **c**), quinoline (panel **d**), acetophenone (panel **e**), and 2-naphthol (panel **f**) to unreduced LHA (open symbols) and reduced LHA (closed symbols). The solid and dashed lines represent the respective Freundlich model fits.

The contributions of HDA interactions of the compounds with polar moieties in LHA to overall sorption cannot be directly assessed by comparing the isotherms of $C_{i,LHA}$ versus $C_{i,aq}$ (Figure **2a**). Water, and hence $C_{i,aq}$, is not a suitable reference phase for such a comparison as the tested compounds experience large differences in HDA interactions with water molecules. To assess the contribution of HDA interactions of the compounds with polar LHA moieties to total sorption, $C_{i,LHA}$ instead need to be compared on the basis of dissolved concentrations in an apolar phase, in which only vdW interactions occur. n-hexadecane (HD) has previously been used as such a reference phase.[6,41] Partition coefficients between HD and water, $K_{i,HD\text{-}water}$, are reported for numerous organic pollutants.[42]

In Figure **2b**, $C_{i,LHA}$ values from panel a are re-plotted versus the pollutant concentration in n-hexadecane, $C_{i,HD}$, in equilibrium with $C_{i,aq}$. The $C_{i,HD}$ values were calculated by multiplying the experimental $C_{i,aq}$ of each compound, i, with the respective $K_{i,HD\text{-}water}$ value.[42] At the same $C_{i,HD}$, $C_{i,LHA}$ values of the bipolar 2-naphthol were about one order of magnitude larger than those of the monopolar compounds, which again were about an order of magnitude larger than the C_{LHA} of naphthalene. Specific HDA interactions with polar moieties in LHA therefore decreased from naphthol, to acetophenone and quinoline, to naphthalene. The same trend was evident when plotting $K_{i,OC}$ versus $K_{i,HD\text{-}water}$ of the tested compounds (Figure **S1**, Supporting Information). The findings of pronounced HDA interactions between polar moieties in LHA and the polar compounds demonstrate that these compounds were suitable probes to assess whether LHA reduction altered the sorption of polar compounds by increasing the number of H-bond donating moieties. Naphthalene, which may only form relatively weak

HDA interactions with LHA, may selectively probe for changes in the cohesive energy of LHA upon its reduction.

The results of paraquat sorption to LHA at two different concentrations and at pH 7, 9, and 11 are shown in Table **2**. The K_{OC} values of paraquat were highly concentration dependent, and increased from pH 7 to pH 9 and 11. The concentration and pH-dependencies support electrostatic attraction between cationic paraquat and anionic sites in LHA as dominant sorption mechanism. Sorption increased with increasing pH due to an increase in the number of anionic sites that resulted from deprotonation of phenolic moieties (Table **S1**, Supporting Information).

Table 2. Freundlich affinity coefficients, $Log_{10}(K_{i,F})$ [$Log_{10}(mol^{1-N} L^N (g_{LHA})^{-1})$] and the Freundlich exponent N_i (each with ±½ of the 95 % confidence intervals) and the organic carbon normalized distribution coefficients, $Log_{10}(K_{i,OC})$, for the sorption of naphthalene, 2-naphthol, acetophenone, and quinoline to unreduced and reduced Leonardite humic acids (LHA). $Log_{10}(K_{i,OC})$ values were evaluated at aqueous concentrations of $C_{i,aq}=50$ and 100 μmol L^{-1} for the apolar and polar compounds (each with ±½ of the 95 % prediction interval) and of $C_{aq}\approx 25$, 50, and 600 μmol L^{-1} for paraquat. The experimental $Log_{10}(K_{i,OC})$ values are compared to literature values.

Compound	redox state	pH	$Log_{10}(K_{i,F})$	N_i	R^2	n	$Log_{10}(K_{i,OC})$ $C_{i,aq}=50$ μM	$Log_{10}(K_{i,OC})$ $C_{i,aq}=100$ μM	$Log_{10}(K_{i,OC})$ literature
Naphthalene	Unreduced	7	-0.42 ± 0.14	0.90 ± 0.10	0.98	11	2.62 ± 0.15	2.59 ± 0.16	2.87 ± 0.15[a], 2.71[c], 2.53[d]
	Reduced	7	-0.61 ± 0.08	1.04 ± 0.06	0.99	12	2.66 ± 0.08	2.67 ± 0.09	
2-Naphtol	Unreduced	7	-0.37 ± 0.11	0.80 ± 0.06	0.99	11	2.49 ± 0.13	2.43 ± 0.13	2.04[c], 2.09[d]
	Reduced	7	-0.35 ± 0.11	0.72 ± 0.06	0.99	10	2.37 ± 0.12	2.29 ± 0.13	
Acetophenone	Unreduced	7	-1.61 ± 0.21	1.12 ± 0.09	0.99	11	1.79 ± 0.25	1.82 ± 0.24	1.55 ± 0.13[a], 1.44[c], 1.07[d]
	Reduced	7	-1.76 ± 0.21	1.17 ± 0.10	0.99	12	1.73 ± 0.28	1.78 ± 0.28	
Quinoline 7	Unreduced	7	-0.86 ± 0.11	1.01 ± 0.05	1.00	12	2.37 ± 0.11	2.38 ± 0.11	3.05[b], 1.59[c], 1.47[d]
	Reduced	7	-0.83 ± 0.08	1.00 ± 0.04	1.00	13	2.38 ± 0.10	2.38 ± 0.10	
Quinoline 9	Unreduced	9	-0.93 ± 0.18	0.99 ± 0.09	0.99	9	2.26 ± 0.22	2.26 ± 0.22	
	Reduced	9	-0.86 ± 0.14	0.94 ± 0.07	0.99	9	2.23 ± 0.18	2.22 ± 0.18	

Table **2**. Continued

Compound	redox state	pH	C_{aq}	$Log_{10}(K_{OC})$	n	C_{aq}	$Log_{10}(K_{OC})$	n
Paraquat	unred	7	56 ± 2	4.12 ± 0.03	3	673 ± 3	3.27 ± 0.02	2
	Red	7	51 ± 3	4.21 ± 0.05	3	676 ± 18	3.24 ± 0.14	3
	unred	9	29 ± 3	4.62 ± 0.06	3	656 ± 3	3.37 ± 0.02	2
	Red	9	27 ± 4	4.66 ± 0.10	3	640 ± 6	3.44 ± 0.03	3
	unred	11	27 ± 1	4.65 ± 0.03	3	628 ± 22	3.49 ± 0.10	3
	Red	11	27 ± 1	4.65 ± 0.03	3	617 ± 24	3.54 ± 0.11	3

[a]average $K_{i,OC}$ values for different soils and sediments, compiled in ref. [11]. [b]for Aldrich HA from ref. [40], [c]extrapolated from polyparameter linear free energy relationships (ppLFERs) with LHA descriptors from ref. [2] and compound descriptors from refs [42, 43]. [d]extrapolated from ppLFER for Pahokee Peat[4].

Effect of LHA reduction on sorption. The sorption isotherms of naphthalene, 2-naphthol, aceptophenone, and quinoline to unreduced LHA (open symbols) and reduced LHA (closed symbols) are compared in Figures **2c** to **2f**, respectively. The isotherms show that LHA reduction had little, if any, effect on the sorption of the four non-ionic pollutants. The same conclusion can be drawn based on the overlapping confidence intervals of the fitted $K_{i,F}$ and N_i values for sorption to unreduced and reduced LHA (Table **2**).

In Figure **3**, the $Log_{10}(K_{i,OC})$ values for the sorption of all compounds to reduced LHA are plotted versus the corresponding $K_{i,OC}$ values for the sorption to unreduced LHA. For the non-ionic compounds, $K_{i,OC}$ values were calculated at $C_{i,aq}$ equal to 50 and 100 µM from the fitted Freundlich parameters (Table **2**). The apparent K_{OC} values for paraquat were calculated directly from the experimentally determined C_{aq} and C_{LHA} according to equation 4. As for the non-ionic pollutants, sorption of paraquat was not significantly affected by LHA reduction: the confidence intervals of the K_{OC} values for sorption to the oxidized and reduced LHA overlapped, except for sorption of paraquat at the lowest tested concentration at pH 7 (Table **2**).
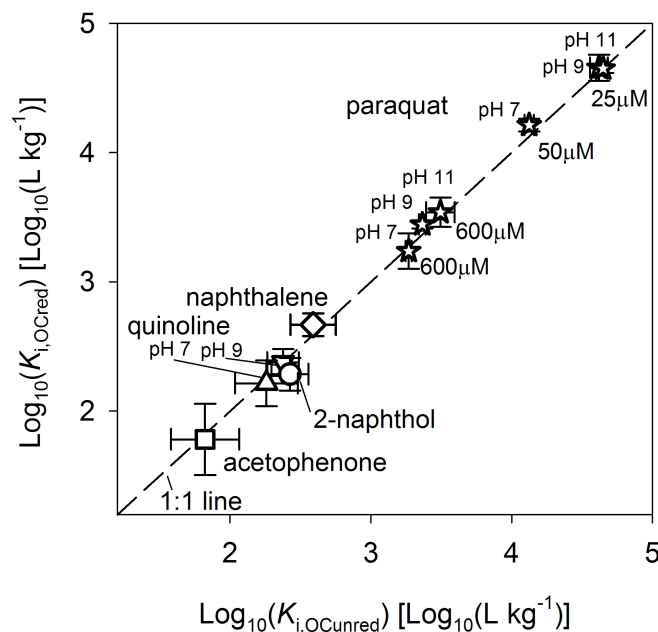
Figure **3**. Logarithms of the organic-carbon normalized distribution coefficients of naphthalene, acetophenone, 2-naphthol, quinoline, and paraquat to reduced Leonardite humic acid (LHA), $Log_{10}(K_{i,OCred})$, versus the corresponding values to unreduced LHA, $Log_{10}(K_{i,OCunred})$. The $K_{i,OC}$ values were calculated for an aqueous concentration of $C_{i,aq} = 100\mu M$ for the apolar and polar compounds and at the specified C_{aq} for paraquat.

The experimental results show that extensive reduction of LHA did not significantly affect the sorption coefficients of the apolar, monopolar, and cationic probe compounds. Several possible explanations for the absence of an observable effect of the LHA redox state on organic pollutant sorption are possible. First, it is possible that the redox active moieties in the HS are situated in microenvironments that were not readily accessible by the organic pollutants. However, this seems unlikely given that these moieties were directly reduced at the working electrode and that the reduced moieties can transfer electrons to DCPIP (this work) and to organic pollutants such as nitroaromatic compounds and chlorinated hydrocarbons.[19, 44] Second, it is conceivable that the increase in H-bond donor sites by reduction of quinones to hydroquinones was masked by the preferential sorption of water molecules to these sites. Water molecules are expected to strongly compete with the polar and bipolar pollutants for H-bond donating and accepting moieties. Yet, enhanced sorption of the polar and bipolar compounds over naphthalene (Figure **2b**) clearly demonstrated that HDA interactions were important for sorption of organic pollutants to LHA in

water. Comparable sorption of naphthalene to unreduced and reduced LHA shows that changes in the cohesive energy of LHA upon reduction, if they occurred, did not significantly affect organic pollutant sorption. Third, and the most likely explanation, reduction did not increase the H-bond donating capability and cohesive energy of LHA to an extent detectable by the sorption of the organic probe compounds. Reduction also did not result in a detectable increase in the anionic binding sites for paraquat. Comparable sorption of paraquat to unreduced and reduced LHA at pH 7 may be rationalized considering that reduced moieties formed during the reduction of LHA and other HA deprotonate at pH> 7.[16, 23, 45] At pH 9 and pH 11, however, the hydroquinones in LHA are expected to deprotonate,[14] but apparently this deprotonation did not result in a noticeable increase in paraquat sorption. It is possible that unreduced LHA contains a significant number of deprotonated hydroxy-substituted quinones, which, upon reduction, would not result in a strong increase in the overall phenolate concentrations, even at high pH. The presence of such moieties in LHA has recently been suggested.[22] Finally, if reduction resulted in changes of conformational structure of the LHA aggregates, these did not affect sorption of the probe compounds.

5.4. Environmental implications

This work on the effect of HA redox state on organic pollutant sorption has several implications. From a methodological perspective, this work demonstrates that direct electrochemical reduction of HA at glassy carbon electrodes in bulk electrolysis cells is a suitable method to generate large amounts of 'clean' reduced HA samples with well-defined redox states that can be directly used in follow-up experiments, such as sorption studies, as shown herein. Furthermore, this work demonstrates that the redox states of HA samples can readily be quantified by a spectrophotometric assay based on the reductive decolorization of the redox dye DCPIP. The assay is highly reproducible, simple, and allows for a high sample throughput. Reduction of DCPIP is directly quantified spectrophotometrically. This is an advantage over the commonly used Fe^{3+}-citrate assay to quantify HA redox states in which the formed Fe^{2+} needs to be complexed prior to spectrophotometric detection.

In the context of environmental fate and risk assessment, this work suggests that changes in the chemistry and the conformational structure of HA upon reduction do not significantly alter its properties as a sorbent for organic pollutants. Since LHA has one of the highest electron accepting capacities among the previously analyzed humic substances,[16] it is unlikely that reduction of other humic substances with similar or smaller electron accepting capacities than LHA significantly affects their sorbent properties. Changes in redox conditions in natural systems may alter organic pollutant sorption to NOM indirectly by affecting solution pH, microbial activity, and aqueous concentrations of metals. This work provides first evidence that organic pollutant sorption is not affected by redox-dependent interconversion of quinone and hydroquinone moieties in NOM. As a consequence, fate and transport models can employ redox-independent organic carbon partition coefficients for organic pollutants.

Acknowledgements

5.5. References

1. Niederer, C.; Goss, K. U.; Schwarzenbach, R. P., Sorption equilibrium of a wide spectrum of organic vapors in Leonardite humic acid: Experimental setup and experimental data. *Environmental Science & Technology* **2006,** *40*, 5368-5373.

2. Niederer, C.; Goss, K. U.; Schwarzenbach, R. P., Sorption equilibrium of a wide spectrum of organic vapors in Leonardite humic acid: Modeling of experimental data. *Environmental Science & Technology* **2006,** *40*, 5374-5379.

3. Niederer, C.; Schwarzenbach, R. P.; Goss, K. U., Elucidating differences in the sorption properties of 10 humic and fulvic acids for polar and nonpolar organic chemicals. *Environ Sci Technol* **2007,** *41*, 6711-7.

4. Bronner, G.; Goss, K. U., Predicting Sorption of Pesticides and Other Multifunctional Organic Chemicals to Soil Organic Carbon. *Environ Sci Technol* **2010**.

5. Bronner, G.; Goss, K. U., Sorption of Organic Chemicals to Soil Organic Matter: Influence of Soil Variability and pH Dependence. *Environ Sci Technol* **2010**.

6. Borisover, M.; Graber, E. R., Classifying NOM - Organic sorbate interactions using compound transfer from an inert solvent to the hydrated sorbent. *Environmental Science & Technology* **2003,** *37*, 5657-5664.

7. Pignatello, J. J.; Lu, Y. F.; LeBoeuf, E. J.; Huang, W. L.; Song, J. Z.; Xing, B. S., Nonlinear and competitive sorption of apolar compounds in black carbon-free natural organic materials. *Journal of Environmental Quality* **2006,** *35*, 1049-1059.

8. Liu, Z. F.; Lee, C., The role of organic matter in the sorption capacity of marine sediments. *Marine Chemistry* **2007,** *105*, 240-257.

9. Endo, S.; Grathwohl, P.; Haderlein, S. B.; Schmidt, T. C., Compound-specific factors influencing sorption nonlinearity in natural organic matter. *Environmental Science & Technology* **2008,** *42*, 5897-5903.

10. Endo, S.; Grathwohl, P.; Handerlein, S. B.; Schmidt, T. C., Characterization of Sorbent Properties of Soil Organic Matter and Carbonaceous Geosorbents Using n-Alkanes and Cycloalkanes as

Molecular Probes. *Environmental Science & Technology* **2009,** *43*, 393-400.

11. Nguyen, T. H.; Goss, K. U.; Ball, W. P., Polyparameter linear free energy relationships for estimating the equilibrium partition of organic compounds between water and the natural organic matter in soils and sediments. *Environ Sci Technol* **2005,** *39*, 913-24.

12. Richter, M. K.; Sander, M.; Krauss, M.; Christl, I.; Dahinden, M. G.; Schneider, M. K.; Schwarzenbach, R. P., Cation binding of antimicrobial sulfathiazole to leonardite humic acid. *Environ Sci Technol* **2009,** *43*, 6632-8.

13. Goss, K. U.; Schwarzenbach, R. P., Linear free energy relationships used to evaluate equilibrium partitioning of organic compounds. *Environmental Science & Technology* **2001,** *35*, 1-9.

14. Ritchie, J. D.; Perdue, E. M., Proton-binding study of standard and reference fulvic acids, humic acids, and natural organic matter. *Geochim. Cosmochim. Acta.* **2003,** *67*, 85-96.

15. http://www.ihss.gatech.edu/elements.html (Accessed 11. 9. 2011),

16. Aeschbacher, M.; Sander, M.; Schwarzenbach, R. P., Novel electrochemical approach to assess the redox properties of humic substances. *Environ. Sci. Technol.* **2010,** *44*, 87-93.

17. Ratasuk, N.; Nanny, M. A., Characterization and quantification of reversible redox sites in humic substances. *Environ. Sci. Technol.* **2007,** *41*, 7844-7850.

18. Scott, D. T.; McKnight, D. M.; Blunt-Harris, E. L.; Kolesar, S. E.; Lovley, D. R., Quinone moieties act as electron acceptors in the reduction of humic substances by humics-reducing microorganisms. *Environ. Sci. Technol.* **1998,** *32*, 2984-2989.

19. Dunnivant, F. M.; Schwarzenbach, R. P.; Macalady, D. L., Reduction of substituted nitrobenzenes in aqueous solutions containing natural organic matter *Environ. Sci. Technol.* **1992,** *26*, 2133-2141.

20. Nurmi, J. T.; Tratnyek, P. G., Electrochemical properties of natural organic matter (NOM), fractions of NOM, and model biogeochemical electron shuttles. *Environ. Sci. Technol.* **2002,** *36*, 617-624.

21. Senesi, N.; Chen, Y.; Schnitzer, M., Role of free radicals in oxidation and reduction of fulvic acid. *Soil. Biol. Biochem.* **1977,** *9*, 397-403.

22. Aeschbacher, M.; Vergari, D.; Schwarzenbach, R. P.; Sander, M., Electrochemical analysis of proton and electron transfer equilibria of the reducible moieties in humic acids. *Environmental Science & Technology* **2011,** *45*, 8385-8394.

23. Maurer, F.; Christl, I.; Kretzschmar, R., Reduction and reoxidation of humic acid: Influence on spectroscopic properties and proton binding. *Environ. Sci. Technol.* **2010,** *44*, 5787-5792.

24. Sutton, R.; Sposito, G., Molecular structure in soil humic substances: The new view. *Environmental Science & Technology* **2005,** *39*, 9009-9015.

25. Piccolo, A., The supramolecular structure of humic substances. *Soil Science* **2001,** *166*, 810-832.

26. Coates, J. D.; Chakraborty, R.; O'Connor, S. M.; Schmidt, C.; Thieme, J., The geochemical effects of microbial humic substances reduction. *Acta Hydrochimica Et Hydrobiologica* **2001,** *28*, 420-427.

27. Pfaender, F. K.; Kim, H. S.; Roper, J. C., Impacts of microbial redox conditions on the phase distribution of pyrene in soil-water systems. *Environmental Pollution* **2008,** *152*, 106-115.

28. Kim, H. S.; Lindsay, K. S.; Pfaender, F. K., Enhanced mobilization of field contaminated soil-bound PAHs to the aqueous phase under anaerobic conditions. *Water Air and Soil Pollution* **2008,** *189*, 135-147.

29. Pfaender, F. K.; Kim, H. S., Effects of microbially mediated redox conditions on PAH-soil interactions. *Environmental Science & Technology* **2005,** *39*, 9189-9196.

30. HunchakKariouk, K.; Schweitzer, L.; Suffet, I. H., Partitioning of 2,2',4,4'-tetrachlorobiphenyl by the dissolved organic matter in oxic and anoxic porewaters. *Environmental Science & Technology* **1997,** *31*, 639-645.

31. Pedersen, J. A.; Gabelich, C. J.; Lin, C. H.; Suffet, I. H., Aeration effects on the partitioning of a PCB to anoxic estuarine sediment pore water dissolved organic matter. *Environmental Science & Technology* **1999,** *33*, 1388-1397.

32. Popovic, V.; Pfendt, L. B.; Stefanovic, V. M., Analytical application of derivative spectrophotometry. *Journal of the Serbian Chemical Society* **2000,** *65*, 457-472.

33.   Armstrong, J. M., Molar extinction coefficient of 2,6-dichlorophenol indophenol. *Biochimica Et Biophysica Acta* **1964,** *86*, 194-&.

34.   Bauer, M.; Heitmann, T.; Macalady, D. L.; Blodau, C., Electron transfer capacities and reaction kinetics of peat dissolved organic matter. *Environ. Sci. Technol.* **2007,** *41*, 139-145.

35.   Blodau, C.; Bauer, M.; Regenspurg, S.; Macalady, D., Electron accepting capacity of dissolved organic matter as determined by reaction with metallic zinc. *Chemical Geology* **2009,** *260*, 186-195.

36.   Bauer, I.; Kappler, A., Rates and extent of reduction of Fe(III) compounds and O_2 by humic substances. *Environ. Sci. Technol.* **2009,** *43*, 4902-4908.

37.   Bauer, M.; Heitmann, T.; Macalady, D. L.; Blodau, C., Electron transfer capacities and reaction kinetics of peat dissolved organic matter. *Environmental Science & Technology* **2007,** *41*, 139-145.

38.   Zachara, J. M.; Ainsworth, C. C.; Cowan, C. E.; Thomas, B. L., Sorption of binary mixtures of aromatic nitrogen heterocyclic compounds on subsurface materials. *Environmental Science & Technology* **1987,** *21*, 397-402.

39.   Li, H.; Lee, L. S., Sorption and abiotic transformation of aniline and alpha-naphthylamine by surface soils. *Environmental Science & Technology* **1999,** *33*, 1864-1870.

40.   Nielsen, T.; Siigur, K.; Helweg, C.; Jorgensen, O.; Hansen, P. E.; Kirso, U., Sorption of polycyclic aromatic compounds to humic acid as studied by high-performance liquid chromatography. *Environmental Science & Technology* **1997,** *31*, 1102-1108.

41.   Sander, M.; Pignatello, J. J., Characterization of charcoal adsorption sites for aromatic compounds: insights drawn from single-solute and bi-solute competitive experiments. *Environ Sci Technol* **2005,** *39*, 1606-15.

42.   Abraham, M. H.; Chadha, H. S.; Whiting, G. S.; Mitchell, R. C., Hydrogen-Bonding. 32. An Analysis of Water-Octanol and Water-Alkane Partitioning and the Delta-Log-P Parameter of Seiler. *Journal of Pharmaceutical Sciences* **1994,** *83*, 1085-1100.

43.   Abraham, M. H.; Andonianhaftvan, J.; Whiting, G. S.; Leo, A.; Taft, R. S., Hydrogen bonding. 34. The factors that influence the solubility of gases and vapors in water at 298K, and a new method for its

determination. *Journal of the Chemical Society-Perkin Transactions 2* **1994**, 1777-1791.

44.   Kappler, A.; Haderlein, S. B., Natural organic matter as reductant for chlorinated aliphatic pollutants. *Environmental Science & Technology* **2003,** *37*, 2714-2719.

45.   Clark, W., *Oxidation-Reduction Potentials of Organic Systems*. Baltimore, 1960.

5.6. Supporting Information Chapter 5

Materials and Methods

Properties of Leonardite humic acid standard

Table **S1** provides selected chemical properties and the electron accepting capacity (EAC) of Leonardite Humic Acid Standard.

Preparation of organic pollutant solutions

Stock solutions of all nonionic organic pollutants were prepared in anoxic methanol inside the glovebox at concentrations of approximately 400 mM. The paraquat stock solution (20 mM) was prepared in anoxic H_2O inside the glovebox. The solutions used to fill the LHA-free dialysis half-cells were prepared by adding the required volume of the stock solutions into pH-buffered solutions, while keeping the final methanol content below 1% vol. For paraquat sorption experiments, which were conducted at lower LHA concentrations (i.e., 0.2 g/L), the pH-buffer solutions containing 0.1 M phosphate (pH 7), borate (pH 9), or carbonate (pH 11) and 0.1 M KCl were diluted 1:10 with water to lower the concentration of inorganic cations that could compete with paraquat for anionic sorption sites in LHA.

Initial concentrations of organic pollutants

One half-cell of each dialysis system was filled with a solution containing unreduced or reduced LHA. The second half-cell was filled with solutions containing one of the tested organic pollutants at initial concentrations, $C_{i,aq}^{0}$, specified in Table **S2**.

Table **S1.** Overview of the electron accepting capacity, elemental composition, numbers of acidic functional moieties, and titrated charge of Leonardite Humic Acid Standard.

Electron accepting capacity[a]	Elemental composition (ash corrected)[b]					Acidic functional groups[c]		Aromatic[b]	Aliphatic[b]	Titrated charge[d]		
E_h = -0.49V; pH 7	C	H	O	N	S	Carboxylic	Phenolic			pH 7	pH 9	pH 11
mmol$_{e-}$ g$_{LHA}$$^{-1}$	mmol g$_{LHA}$$^{-1}$					mmol g$_{LHA}$$^{-1}$		%	%	mmol g$_{LHA}$$^{-1}$	mmol g$_{LHA}$$^{-1}$	mmol g$_{LHA}$$^{-1}$
1.71±0.03	51.79	35.79	19.05	0.86	0.23	4.64	1.44	58	14	4.28	5.01	5.66

Sources: [a]from ref. 1 , [b]form ref. 2 , [c]from ref. 3 , [d]calculated with data from ref. 3

Table **S2**. Initial aqueous concentration, $C_{i,aq}^{0}$, of organic pollutants in the solutions filled into the LHA-free dialysis half-cells.

Compound	pH	Concentration in the filling solutions, $C_{i,aq}^{0}$ [μM]			
Naphthalene	7	28	102	152	303
2-Naphthol	7	30	101	312	1006
Quinoline	7	21	203	800	2071
Quinoline	9	19	201		1990
Acetophenone	7	34	198	771	3739
Paraquat	7		206		1539
Paraquat	9		205		1501
Paraquat	11		205		1535

Quantification of organic pollutant concentrations

Non-ionic organic pollutants. The nonionic organic pollutants were analyzed by HPLC using a Dionex system (Dionex, Olten, Switzerland) that consisted of a P680 pump, an automated sample injector (ASI-100), and a photodiode array detector (PDA-100). Chromatographic separation was achieved on a Supelcosil LC-18 reverse phase column (25 cm x 4.6 mm, particle size 5 μm, Supelco, Division of Fluka, Switzerland). Table **S3** shows the eluent mixtures and UV-visible detection wavelengths for the different compounds. The injection volumes were 30 μL and 10 μL for aqueous and ethyl acetate samples, respectively. Quantification of the pollutants was based on six-point calibration curves prepared from aqueous and ethyl acetate standards. Ethyl acetate standards were prepared by extracting aqueous concentration standards in 1:1 volumetric ratios, analogous to the extraction procedure for the LHA-containing samples.

Table **S3**. Elution conditions for HPLC measurements. Eluents were methanol (MeOH), water (H_2O), and 5 mM phosphate buffer pH 7 (PB). Detection wavelengths were adapted to yield linear signal responses to the pollutant concentrations.

Compound	Eluents	Volumetric ratio	Flow rate	Detection wavelength
naphthalene	MeOH/H$_2$O	70% / 30%	1 ml (min)$^{-1}$	220 nm
2-naphthol	MeOH/H$_2$O	60% / 40%	1 ml (min)$^{-1}$	225 nm/266 nm
quinoline	MeOH/PB	50% / 50%	1 ml (min)$^{-1}$	220 nm/266 nm
acetophenone	MeOH/H$_2$O	50% / 50%	1 ml (min)$^{-1}$	245 nm/230 nm

Paraquat concentrations in the LHA-free half-cells were quantified by collecting UV-visible spectra on a Varian Cary 100 Bio Spectrophotometer using 10 mm path length Quartz Suprasil® precision cells (Hellma, Basel, Switzerland). All spectra were referenced against absorbance of buffer solutions at the corresponding pH values. The LHA-free half-cells contained only minor amounts of LHA that had diffused across the dialysis membranes over the course of the sorption experiments. Absorption of UV-visible light by these small LHA concentrations distorted the absorption spectra of paraquat in the UV range. To avoid quantification artifacts, paraquat concentrations were determined by derivative spectrophotometry at 241 nm to reduce the effect of spectral background interferences.[4] Derivatives of the recorded spectra were calculated using Cary WinUV software. The first order derivative eliminated the LHA interference, given that the slope of the LHA spectra in the UV range was constant irrespective of the LHA concentration.

Spectrophotometric 2,6-dichlorophenol indophenol redox assay

The assay involved the following steps [1]: (i) Aliquots of 0 µL, 20 µL, 40 µL, and 80 µL of the reduced or 0 µL, 40 µL, 80 µL, and 150 µL of the unreduced LHA samples, respectively, were transferred into plastic cuvettes (Brand GMBH, Wertheim, Germany) containing 2 mL of an anoxic solution of oxidized DCPIP at 50 µM in buffers pH 7 and pH 9. At this concentration,

DCPIP was in excess to the number of electrons donated both by added unreduced and reduced LHA. (ii)The same volumes of LHA-containing solutions were spiked into reference cuvettes with 2 mL of pH-buffered solutions containing no DCPIP to correct for absorption of LHA at 603 nm. (iii) Cuvettes were capped, thoroughly mixed and, transferred to the spectrophotometer outside the glovebox. The UV-visible light absorbance of the DCPIP containing cuvettes was recorded versus the absorbance of the corresponding reference cuvettes containing only LHA on a Varian Cary 100 Bio Spectrophotometer from 800 to 400 nm. The concentration of oxidized DCPIP was quantified by the decrease in absorbance at λ= 603 nm from a linear six-point calibration for oxidized DCPIP (the molar extinction coefficient of DCPIP was ε_{DCPIP}= 20.6 mM^{-1} cm^{-1}). (iv) The quantified number of electrons transferred to DCPIP in the four cuvettes for one sample was plotted versus the mass of LHA added to the respective cuvettes. For each sample, the slope of the regression line corresponded to the final $n_{e-,DCPIP}$ value reported in the manuscript.

Diffusion kinetics

Table **S4**. Kinetics of diffusion through dialysis membranes. $C_{i,aq}^0$ is the initial aqueous concentration of the pollutants that was added to dialysis half-cell 1, half-cell 2 contained initially only buffer and no pollutants. C_1 and C_2 are the concentrations in the two cell half-cells after the given equilibration time. Equilibrium was attained within 6 days for the non-ionic contaminants as shown by the ratio C_2/C_1 close to unity. For the cationic paraquat equilibrium had been attained at the time points probed. While the dissolved fraction $(C_{i,1}+C_{i,2})/C_{i,aq}^0$ was close to one for quinoline and paraquat it was significantly below 1 for naphthalene and 2-naphthol due to sorption to the dialysis membrane. Sorption to the dialysis membrane is addressed in Table **S5**.

Compound	pH	t [d]	$C_{i,aq}^0$ [μM]	$\frac{1}{2}C_{i,aq}^0$ [μM]	$C_{i,1}$ [μM]	$C_{i,2}$ [μM]	$C_{i,2}/C_{i,1}$	$(C_{i,1}+C_{i,2})/C_{i,aq}^0$
Naphthalene	7	4	98.0	49.0	30.4	30.8	1.01	0.62
		6	98.0	49.0	29.4	28.9	0.98	0.60
		7	98.0	49.0	30.0	30.0	1.00	0.61
		11	98.0	49.0	27.5	27.8	1.01	0.56
Quinoline	7	6	102.7	51.3	49.3	49.5	1.00	0.96
		6	102.7	51.3	50.1	50.3	1.00	0.98
		8	102.7	51.3	48.2	48.5	1.01	0.94
		13	102.7	51.3	49.4	48.5	0.98	0.95
2-Naphthol	7	2	101.8	50.9	46.5	33.4	0.72	0.79
		6	101.8	50.9	36.0	35.7	0.99	0.70
		8	101.8	50.9	35.6	35.3	0.99	0.70
		13	101.8	50.9	35.2	35.0	0.99	0.70
Paraquat	7	9	206	103	100 ± 1	98 ± 1	0.98	0.96
	7	7	1539	770	778 ± 18	730 ± 14	0.94	0.98
	9	8	205	102	99 ± 2	97 ± 1	0.98	0.96
	9	8	1501	751	798 ± 22	753 ± 45	0.94	1.03
	11	8	205	103	105 ± 1	101 ± 1	0.96	1.01
	11	8	1535	767	751 ± 19	751 ± 9	1.00	0.98

Recovery experiments

Table **S5**. $C_{i,aq}^{0}$ is the initial aqueous concentration of the pollutants that was added to the LHA free half-cell. $C_{i,aq}$ and $C_{i,LHA\text{-}cell}$ are the pollutants concentrations in the LHA-free and in the LHA-containing half-cells, respectively, after equilibration. $C_{i,membrane}$ is the amount of substance in the membrane (extracted by MeOH) divided by the volume of one half-cell. The recovery corresponds to $100\%*(C_{i,aq} + C_{i,LHA\text{-}cell} + C_{i,membrane})/C_{i,aq}^{0}$.

Substance	Sample	$C_{i,aq}^{0}$ [μM]	$C_{i,aq}$ [μM]	$C_{i,LHA\text{-}cell}$ [μM]	$C_{i,membrane}$ [μM]	Recovery
Naphthalene	unred	102	24.2	38.2	35.7	97%
	red1	102	23.3	36.8	40.6	99%
	red2	102	22.4	35.4	35.8	92%
	red3	102	23.4	37.8	33.8	94%
Quinoline	unred 1	203	85.9	109.9	6.3	100%
	unred 2	203	86.1	114.9	9.8	104%
	unred 3	203	84.6	113.9	8.2	102%
	unred 4	203	84.6	111.0	7.7	100%
	red1	203	84.4	110.3	9.3	101%
	red2	203	84.6	111.1	7.1	100%
	red3	203	84.6	115.7	9.5	104%
	red4	203	84.6	114.6	7.4	102%
Acetophenone	unred 1	198	91.3	98.8	10.5	101%
	unred 2	198	90.7	99.0	7.5	100%
	unred 3	198	77.3	81.2	n.q.	n.q.
	red 1	198	88.6	95.7	8.4	97%
	red 2	198	90.2	97.5	10.4	100%
	red 3	198	89.4	93.3	n.q.	n.q.
	red 4	198	89.4	96.4	n.q.	n.q.
2-Naphthol	unred 1	101	28.0	35.9	24.8	88%
	unred 2	101	29.2	42.3	23.2	94%
	unred 3	101	29.6	37.9	22.6	89%
	red1	101	29.8	36.3	26.4	91%
	red2	101	29.7	34.5	27.6	91%
	red3	101	29.5	36.3	27.3	92%
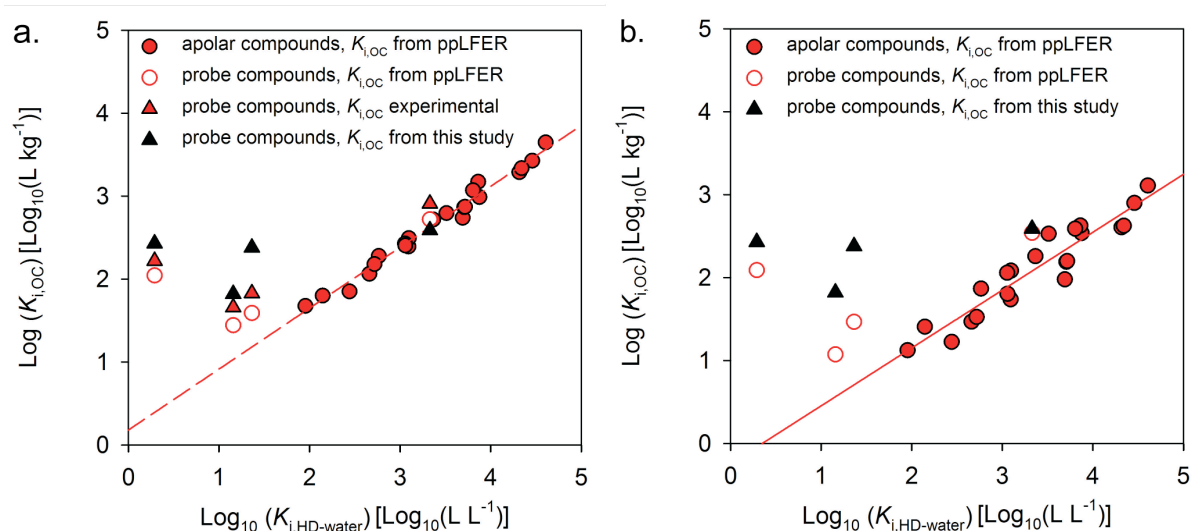
Figure **S1.** Log $K_{i,OC}$ values plotted versus Log $K_{i, HD-water}$ partitioning coefficients which were calculated from a poly-parameter linear free energy relationship (ppLFER) in ref.[5]. **a.** Log $K_{i,OC}$ values calculated from a ppLFER from ref. [6] for Leonardite humic acid for a diverse set of apolar compounds (closed circles) and for the probe compounds used in this study (open circles). The triangles represent measured Log $K_{i,OC}$ values. Red triangles: measured for LHA in refs.[6, 7] (value for 1-naphthol instead of 2-naphthol), black triangles: values measured in this study. **b.** Log $K_{i, OC}$ values calculated from a ppLFER from ref.[8] for Pahokee Peat for a diverse set of apolar compounds (closed circles) and for the probe compounds used in this study (open circles). The black triangles represent Log $K_{i, OC}$ values measured in this study. All substance descriptors used for the ppLFER calculations were from refs.[5, 9]

References

1. Aeschbacher, M.; Sander, M.; Schwarzenbach, R. P., Novel electrochemical approach to assess the redox properties of humic substances. *Environ. Sci. Technol.* **2010,** *44*, 87-93.

2. http://www.ihss.gatech.edu/elements.html (Accessed 11. 9. 2011),

3. Ritchie, J. D.; Perdue, E. M., Proton-binding study of standard and reference fulvic acids, humic acids, and natural organic matter. *Geochim. Cosmochim. Acta.* **2003,** *67*, 85-96.

4. Popovic, V.; Pfendt, L. B.; Stefanovic, V. M., Analytical application of derivative spectrophotometry. *Journal of the Serbian Chemical Society* **2000,** *65*, 457-472.

5. Abraham, M. H.; Chadha, H. S.; Whiting, G. S.; Mitchell, R. C., Hydrogen-Bonding. 32. An Analysis of Water-Octanol and Water-Alkane Partitioning and the Delta-Log-P Parameter of Seiler. *Journal of Pharmaceutical Sciences* **1994,** *83*, 1085-1100.

6. Niederer, C.; Goss, K. U.; Schwarzenbach, R. P., Sorption equilibrium of a wide spectrum of organic vapors in Leonardite humic acid: Modeling of experimental data. *Environmental Science & Technology* **2006,** *40*, 5374-5379.

7. Niederer, C.; Goss, K. U.; Schwarzenbach, R. P., Sorption equilibrium of a wide spectrum of organic vapors in Leonardite humic acid: Experimental setup and experimental data. *Environmental Science & Technology* **2006,** *40*, 5368-5373.

8. Bronner, G.; Goss, K. U., Predicting Sorption of Pesticides and Other Multifunctional Organic Chemicals to Soil Organic Carbon. *Environ Sci Technol* **2010**.

9. Abraham, M. H.; Andonianhaftvan, J.; Whiting, G. S.; Leo, A.; Taft, R. S., Hydrogen bonding. 34. The factors that influence the solubility of gases and vapors in water at 298K, and a new method for its determination. *Journal of the Chemical Society-Perkin Transactions 2* **1994**, 1777-1791.

Chapter 6

Conclusions and Outlook

6.1. Conclusions

This work advances both the methodological toolbox for investigating the redox reactions of HS and the fundamental understanding of the redox properties of humic substances (HS). The methodological work resulted in the development of a novel electrochemical approach to characterize the redox properties of humic substances. This approach was then applied to systematically characterize the redox properties of a diverse set of HS and natural organic matter (NOM) samples from different sources under both reducing and oxidizing conditions.

Methodological advancements

A novel electrochemical approach was developed that offers new possibilities for characterizing the redox properties of humic substances under both reducing and oxidizing conditions. The approach comprises three electrochemical methods.

(i)   *Direct electrochemical reduction* (DER) of HS at glassy carbon working electrodes in a bulk electrolysis cell allows generating large samples of reduced HS. This reduced HS is 'clean' because the electrons stem from chemically inert working electrodes and not, as in previous methods, from chemical reductants added to the HS. DER also has the advantage that the number of electrons transferred to the HS is continuously monitored by chronocoulometry, which allows generating HS with well-defined redox states. Coupling of DER to automated acid titration can be used to quantify the number of protons transferred to HS during the reduction.

(ii)   *Mediated electrochemical reduction* (MER) and *mediated electrochemical oxidation* (MEO) directly quantify the number of electrons transferred to and from small amounts of HS at a desired redox potential E_h and pH. Due to the sensitivity of MER and MEO, these techniques can also be used to determine the redox state of very small amounts of HS, for instance in aqueous environmental samples.

(iii)   In *Mediated potentiometry* small concentrations of redox mediators facilitate the attainment of redox equilibria between HS and redox electrodes

and likely also between different redox-active moieties in the HS. MP allows for stable and reproducible E_h measurements in HS solutions.

This novel electrochemical approach was then applied to characterize the electron accepting and donating properties of a diverse set of HS. The major results from this work are briefly summarized below.

Electron-accepting moieties in HS

The electron accepting capacities (EACs) of a diverse set of HS, including terrestrial and aquatic humic and fulvic acids, were linearly correlated with HS aromaticities (Chapter 2), suggesting that electron-accepting moieties are linked to aromatic structures in the HS. Electron transfer to Leonardite humic acid (LHA), which is derived from lignite, was largely reversibly over successive reduction O_2-reoxidation cycles (Chapter 2). This finding supports the role of HS as redox buffers by accepting electrons under reducing conditions and by donating the electrons upon re-aeration.

A characterization of the electron transfer equilibria of selected humic acids (HA) showed that HA act as redox buffers over a wide potential range. Accordingly modeling of the potential decrease during HS reduction revealed a wide distributions in the apparent standard reduction potentials of the reducible moieties in the HA (Chapter 3). The potential distributions of the reducible moieties allow, for the first time, assessing the free energy changes for electron transfer reactions to and from HS under reducing conditions. Electron transfer to the electron-accepting moieties in the HA was shown to be coupled to pH-dependent proton uptake. Consistently, the reduction potentials E_h of the tested HA decreased with increasing solution pH, as determined by mediated potentiometry.

Taken together, the findings are consistent with quinones as major electron accepting moieties in HS.

Electron-donating moieties in HS.

The work presented in chapter 4 is the first systematic assessment of the electron donating properties of a diverse set of HS and NOM. Electrochemical oxidation of an aquatic, a terrestrial, and a lignite-derived HA resulted only in a small increase in their electron accepting capacities, suggesting that oxidation of

the electron donating moieties in HA was largely irreversible. The electron donating capacities (EDCs) of all studied HS and NOM samples increased with increasing applied redox potential E_h and with increasing solution pH. All HS acted as electron donors under mildly oxidizing conditions. The continuous increase in the EDCs of three HAs with increasing E_h and pH suggests that the electron donating moieties in HS cover a wide range in one-electron standard reduction potentials and that the oxidation of these moieties is coupled to the release of protons. The EDCs were linearly correlated with the titrated phenol contents of the HS. These findings support phenolic electron donating moieties in HS. This work strongly suggests that HS can act as antioxidants in biogeochemical and pollutant redox reactions under oxic conditions.

Electron donating and electron accepting properties of HS.

A comparative analysis of a diverse set of 15 HS and NOM samples revealed clear patterns in the electron accepting capacities (EACs) and electron donating capacities (EACs) with HS origin and chemical composition. Relatively young HS formed from higher plant precursors in aquatic and mixed aquatic-terrestrial environments have comparatively high EDCs and low EACs. Conversely, older HS from terrestrial sources have comparatively low EDCs but higher EACs. These patterns indicate that abiotic and biotic oxidative processing of organic matter in the environment leads to a preferential loss of electron-donating polyphenolic moieties relative to the electron-accepting quinone moieties. The results support the hypothesis that the antioxidant properties of HS play a key role in the recalcitrance of HS in the environment [1].

6.2. Outlook

A direct outcome of this work is an improved understanding of the redox properties of humic substances, and, as a consequence, of the role of HS in biogeochemical and pollutant redox reactions. Beyond that, this work is expected to promote research directed towards characterizing the redox properties of other organic and inorganic phases in the environment. Some research areas to which this work is relevant are summarized.

Role of humic substances in microbial electron transfer reactions

It is well established that humic substances can act both as electron acceptors and as electron donors in microbial metabolism [2-5]. As of yet, the thermodynamics of electron transfer reactions between HS and microorganism are poorly investigated. For instance, it is unknown to which reduction potentials microbes may transfer electrons to HS. This information would advance our understanding of microbial electron transfer to environmental phases and of the follow-up reactions of microbially reduced HS, including the reductive dissolution of iron mineral phases [3, 6, 7]. Mediated electrochemical reduction and oxidation, in combination with mediated potentiometry would allow for direct electron balancing during microbial processes in laboratory

experiments and to link oxidation and reduction to changes in the reduction potential of the HS. This information cannot be provided by previous approaches to characterize the redox properties of HS. Furthermore, HS with defined redox states, generated by direct electrochemical reduction in bulk electrolysis cells, may be used in microbial growth experiments to assess the redox state to which microbial electron transfer to HS is possible for different electron donors. MEO and MER and mediated potentiometry may also be applied to humin and other forms of particulate organic matter. The amount of solid phase organic matter exceeds the amount of dissolved organic matter in many ecosystems. Recent work has demonstrated that particulate organic matter can act as electron acceptor in microbial respiration and as a reductant of iron oxide phases [8].

Electron balancing for redox reactions in organic-matter rich ecosystems

The high sensitivity of MER and MEO make it possible to directly analyze environmental NOM samples including aqueous samples and solid phase samples (e.g. from sediments and bogs). By analyzing both dissolved and particulate organic matter, the electrochemical approach would help to balance electron transfer reaction in these systems. This is particularly relevant for wetlands, peats, and bogs as it has been hypothesized that electron transfer to the organic matter in these systems greatly reduces methanogenesis [9]. Extending on work by Cervantes and coworkers [10], electrochemically reduced HS with different redox states may be added as electron acceptor to laboratory experiments. An increase in methanogenesis with increasing extent of electrochemical pre-reduction of HS would support the above hypothesis. The electrochemical approach may also be applied in field studies, for instance to monitor redox dynamics in wetlands with fluctuating water tables [11].

Role of HS in reductive and oxidative pollutant transformation reactions

While the effect of HS redox state on organic pollutant sorption is likely insignificant (Chapter 5), HS redox state is known to largely affect reductive and oxidative pollutant transformation reactions. Numerous studies have demonstrated that HS mediate the electron transfer from chemical bulk electron donors to organic pollutants. This approach is, however, not suited to study the

mechanism of electron transfer from HS to the organic pollutant. First, the chemical bulk electron donors and not the HS define the reduction potential in the studied systems. Second, many of the electron donors undergo irreversible side reactions with HS [12, 13]. Third, for most systems, changes in solution pH will affect the speciation of both the electron donor and the HS. Following up on the work of Kappler and Haderlein [14], direct electrochemical reduction can be used to prepare HS with well-defined redox states. These HS may then be reacted with organic pollutants as a function of pH (and hence E_h) to selectively assess the role and reactivity of HS as reductant for organic pollutants. Similarly, "clean" reduced HS may be used to revisit the reduction of inorganic pollutants, including arsenate and radionuclides.

Previous studies have demonstrated an inhibitory effect of HS on the indirect photochemical oxidation of organic pollutants. This effect was ascribed to electron donation from HS to oxidized pollutant radical intermediates, which reduced them back to the parent compound [15, 16]. This explanation is supported by this work, which systematically assessed the antioxidant properties of HS. Future studies would benefit from a combined photochemical and electrochemical approach that can relate differences in the inhibitory effects among HS to the differences in their EDCs. For a given HS, link the effect of solution pH on the inhibitory effect in photochemical oxidation can be compared to the pH dependence of the EDC. Optionally, the inhibitory effect of HS may be related to their phenol contents determined by potentiometric pH titrations.

Optical properties of HS

A number of recent studies suggest that the optical properties of HS arise from charge transfer complexes between hydroxy aromatic donor and quinoid or aromatic ketone acceptor moieties in the HS [17, 18]. As of yet, the relative importance of quinones and aromatic ketones as electron acceptors is still a matter of debate. Following up on previous work [17-19], direct electrochemical reduction may be employed to sequentially reduce HS of different origin, followed by measuring their optical properties. A gradual change in the optical properties with increasing extent of reduction and the extent of reversibility of the optical changes upon re-aeration of the samples would help to elucidate the

relative contribution of quinone moieties to the optical properties. A series of electrochemically reduced HS with well-defined redox states is valuable also to assess the effect of HS redox state to other spectroscopic properties of HS.

Reactive oxygen species formation during reductive cycling of HS

It is well established that reduced quinones (i.e. semiquinones or hydroquinones) can react with oxygen to produce hydrogen peroxide, H_2O_2 [20-23]. It is also conceivable that oxidation of reduced quinones in HS produces H_2O_2 in the environment, which may react with Fe(II) in a dark Fenton type reaction mechanism to form highly reactive hydroxyl radicals, OH• [24]. Hence redox cycling of HS at oxic-anoxic interfaces, which are ubiquitous in both terrestrial and aquatic systems, may result in high formation rates of OH•. This potential production pathway of OH• has not yet been recognized. If occurring, it would have far reaching consequences on the chemical reaction occurring at oxic-anoxic interfaces, including chemical alteration of the HS. To test for this formation pathway, the novel electrochemical approach can be used to reduce HS to well defined redox states, which are subsequently re-oxidized by O_2 in the presence of chemical probes selective to OH• [25].

Influence of origin and history on HS redox properties

This work provides evidence for pronounced and systematic effects of HS source material and age on the relative abundances of electron accepting and donating moieties in HS. Additional experiments are warranted to further investigate these effects. The hypothesis that polyphenols originating from higher plants are the precursors to electron donating moieties in HS may be tested by quantifying the EDCs of HS sampled along natural gradients of organic matter decomposition, such as samples from different depths of as soil profile or an estuary [26-28]. The preferential depletion of electron donating moieties during oxidative transformation of HS can be further investigated in the laboratory by quantifying the EDCs of samples obtained during time-series studies of plant material and humic acid degradation, for instance by white rot fungi [29, 30].

Removal of organic matter from drinking water

Chemical oxidants such as ozone or chlorine are added to drinking water for disinfection, pollutant degradation, decoloration and odor control [31]. Oxidant doses required for successful water treatment will likely depend on the electron donating capacity of the organic matter in the water. At present, however, drinking water treatment facilities lack suitable approaches to monitor the changes in the chemical oxidant demand of the incoming water in real time. Mediated electrochemical oxidation may allow doing so by constantly quantifying the electron donating capacities of the drinking water. The EDC measurements may also help to assess the potential of the water to form unwanted disinfection byproducts, as electron donating moieties in NOM are involved in this reaction [31-33].

Redox characterization of particulate organic and mineral phases

In addition to humic substances, other redox-active phases play a crucial role in biogeochemical redox processes and pollutant dynamics. Most of these phases are particulate and include black carbon [20, 34-36], clay minerals, iron oxides and hydroxides [37, 38], and manganese oxides. Most previous studies assessed the redox properties of these phases by determining its reactivity towards chemical probes, including organic pollutants such as nitroaromatics [39]. As of yet, methods to determine the reduction potentials, and the electron donating and accepting capacities of these phases are missing. In principle, the mediated electrochemical reduction and oxidation and the mediated potentiometry developed in this work are applicable also to characterize the redox properties of these particulate phases. In fact, these new electrochemical approaches have already been successfully applied to the redox characterization of iron bearing clay minerals [40].

6.3. References

1. Rimmer, D. L., Free radicals, antioxidants, and soil organic matter recalcitrance. *Eur J Soil Sci* **2006,** *57*, (2), 91-94.

2. Coates, J. D.; Ellis, D. J.; Blunt-Harris, E. L.; Gaw, C. V.; Roden, E. E.; Lovley, D. R., Recovery of humic-reducing bacteria from a diversity of environments. *Appl. Environ. Microbiol.* **1998,** *64*, (4), 1504-1509.

3. Lovley, D. R.; Coates, J. D.; Blunt-Harris, E. L.; Phillips, E. J. P.; Woodward, J. C., Humic substances as electron acceptors for microbial respiration. *Nature* **1996,** *382*, (6590), 445-448.

4. Lovley, D. R.; Fraga, J. L.; Coates, J. D.; Blunt-Harris, E. L., Humics as an electron donor for anaerobic respiration. *Environ Microbiol* **1999,** *1*, (1), 89-98.

5. Coates, J. D.; Cole, K. A.; Chakraborty, R.; O'Connor, S. M.; Achenbach, L. A., Diversity and ubiquity of bacteria capable of utilizing humic substances as electron donors for anaerobic respiration. *Appl. Environ. Microbiol.* **2002,** *68*, (5), 2445-2452.

6. Kappler, A.; Benz, M.; Schink, B.; Brune, A., Electron shuttling via humic acids in microbial iron(III) reduction in a freshwater sediment. *Fems Microbiol Ecol* **2004,** *47*, (1), 85-92.

7. Jiang, J.; Kappler, A., Kinetics of Microbial and Chemical Reduction of Humic Substances: Implications for Electron Shuttling. *Environ Sci Technol* **2008,** *42*, (10), 3563-3569.

8. Roden, E. E.; Kappler, A.; Bauer, I.; Jiang, J.; Paul, A.; Stoesser, R.; Konishi, H.; Xu, H. F., Extracellular electron transfer through microbial reduction of solid-phase humic substances. *Nat Geosci* **2010,** *3*, (6), 417-421.

9. Heitmann, T.; Goldhammer, T.; Beer, J.; Blodau, C., Electron transfer of dissolved organic matter and its potential significance for anaerobic respiration in a northern bog. *Glob. Change Biol.* **2007,** *13*, (8), 1771-1785.

10. Cervantes, F. J.; van der Velde, S.; Lettinga, G.; Field, J. A., Competition between methanogenesis and quinone respiration for ecologically important substrates in anaerobic consortia. *Fems Microbiol Ecol* **2000,** *34*, (2), 161-171.

11. Deppe, M.; McKnight, D. M.; Blodau, C., Effects of short-term drying and irrigation on electron flow in mesocosms of a northern bog and an alpine fen. *Environ Sci Technol* **2010,** *44*, (1), 80-6.

12. Perlinger, J. A.; Kalluri, V. M.; Venkatapathy, R.; Angst, W., Addition of hydrogen sulfide to juglone. *Environ Sci Technol* **2002,** *36*, (12), 2663-2669.

13. Blodau, C.; Heitmann, T., Oxidation and incorporation of hydrogen sulfide by dissolved organic matter. *Chem Geol* **2006,** *235*, (1-2), 12-20.

14. Kappler, A.; Haderlein, S. B., Natural organic matter as reductant for chlorinated aliphatic pollutants. *Environ Sci Technol* **2003,** *37*, (12), 2714-2719.

15. Wenk, J.; von Gunten, U.; Canonica, S., Effect of Dissolved Organic Matter on the Transformation of Contaminants Induced by Excited Triplet States and the Hydroxyl Radical. *Environ Sci Technol* **2011,** *45*, (4), 1334-1340.

16. Canonica, S.; Laubscher, H. U., Inhibitory effect of dissolved organic matter on triplet-induced oxidation of aquatic contaminants. *Photochem Photobiol Sci* **2008,** *7*, (5), 547-51.

17. Ma, J.; Del Vecchio, R.; Golanoski, K. S.; Boyle, E. S.; Blough, N. V., Optical properties of humic substances and CDOM: effects of borohydride reduction. *Environ Sci Technol* **2010,** *44*, (14), 5395-402.

18. Del Vecchio, R.; Blough, N. V., On the origin of the optical properties of humic substances. *Environ Sci Technol* **2004,** *38*, (14), 3885-3891.

19. Maurer, F.; Christl, I.; Kretzschmar, R., Reduction and reoxidation of humic acid: Influence on spectroscopic properties and proton binding. *Environ. Sci. Technol.* **2010,** *44*, (15), 5787-5792.

20. Garten, V. A.; Weiss, D. E., The Quinone Hydroquinone Character of Activated Carbon and Carbon Black. *Aust J Chem* **1955,** *8*, (1), 68-95.

21. Atherton, W.; Turner, H. A., The Formation of Hydrogen Peroxide during the Oxidation of Reduced Vat Dyes. *J Soc Dyers Colour* **1946,** *62*, (4), 108-114.

22. Squadrito, G. L.; Cueto, R.; Dellinger, B.; Pryor, W. A., Quinoid redox cycling as a mechanism for sustained free radical generation by inhaled airborne particulate matter. *Free Radical Bio Med* **2001,** *31*, (9), 1132-1138.

23. Chung, M. Y.; Lazaro, R. A.; Lim, D.; Jackson, J.; Lyon, J.; Rendulic, D.; Hasson, A. S., Aerosol-borne quinones and reactive oxygen species generation by particulate matter extracts. *Environ Sci Technol* **2006,** *40*, (16), 4880-6.

24. Zepp, R. G.; Faust, B. C.; Hoigne, J., Hydroxyl Radical Formation in Aqueous Reactions (Ph 3-8) of Iron(Ii) with Hydrogen-Peroxide - the Photo-Fenton Reaction. *Environ Sci Technol* **1992,** *26*, (2), 313-319.

25. Page, S. E.; Arnold, W. A.; McNeill, K., Terephthalate as a probe for photochemically generated hydroxyl radical. *Journal of Environmental Monitoring* **2010,** *12*, (9), 1658-1665.

26. Sleighter, R. L.; Hatcher, P. G., Molecular characterization of dissolved organic matter (DOM) along a river to ocean transect of the lower Chesapeake Bay by ultrahigh resolution electrospray ionization Fourier transform ion cyclotron resonance mass spectrometry. *Marine Chemistry* **2008,** *110*, (3-4), 140-152.

27. Mannino, A.; Harvey, H. R., Terrigenous dissolved organic matter along an estuarine gradient and its flux to the coastal ocean. *Org. Geochem.* **2000,** *31*, (12), 1611-1625.

28. Rimmer, D. L.; Smith, A. M., Antioxidants in soil organic matter and in associated plant materials. *Eur J Soil Sci* **2009,** *60*, (2), 170-175.

29. Matthiessen, A., *Determining the redox capacity of humic substances as a function of pH*. VCH: Weinheim, ALLEMAGNE, 1995; Vol. 84.

30. Grinhut, T.; Salame, T. M.; Chen, Y. N.; Hadar, Y., Involvement of ligninolytic enzymes and Fenton-like reaction in humic acid degradation by Trametes sp. *Appl Microbiol Biot* **2011,** *91*, (4), 1131-1140.

31. von Gunten, U., Ozonation of drinking water: Part I. Oxidation kinetics and product formation. *Water Res* **2003,** *37*, (7), 1443-1467.

32. von Gunten, U., Ozonation of drinking water: Part II. Disinfection and by-product formation in presence of bromide, iodide or chlorine. *Water Res* **2003,** *37*, (7), 1469-1487.

33. Norwood, D. L.; Christman, R. F.; Hatcher, P. G., Structural Characterization of Aquatic Humic Material .2. Phenolic Content and Its Relationship to Chlorination Mechanism in an Isolated Aquatic Fulvic-Acid. *Environ Sci Technol* **1987,** *21*, (8), 791-798.

34. Van der Zee, F. P.; Bisschops, I. A. E.; Lettinga, G.; Field, J. A., Activated carbon as an electron acceptor and redox mediator during the anaerobic biotransformation of azo dyes. *Environ Sci Technol* **2003,** *37*, (2), 402-408.

35. Jones, I. F.; Kaye, R. C., Polarography of Carbon Suspensions. *J Electroanal Chem* **1969,** *20*, (2), 213-&.

36. Oh, S. Y.; Chiu, P. C., Graphite- and soot-mediated reduction of 2,4-dinitrotoluene and hexahydro-1,3,5-trinitro-1,3,5-triazine. *Environ Sci Technol* **2009,** *43*, (18), 6983-8.

37. Gorski, C. A.; Nurmi, J. T.; Tratnyek, P. G.; Hofstetter, T. B.; Scherer, M. M., Redox behavior of magnetite: implications for contaminant reduction. *Environ Sci Technol* **2010,** *44*, (1), 55-60.

38. Tobler, N. B.; Hofstetter, T. B.; Straub, K. L.; Fontana, D.; Schwarzenbach, R. P., Iron-mediated microbial oxidation and abiotic reduction of organic contaminants under anoxic conditions. *Environ Sci Technol* **2007,** *41*, (22), 7765-72.

39. Neumann, A.; Hofstetter, T. B.; Lussi, M.; Cirpka, O. A.; Petit, S.; Schwarzenbach, R. P., Assessing the redox reactivity of structural iron in smectites using nitroaromatic compounds as kinetic probes. *Environ Sci Technol* **2008,** *42*, (22), 8381-7.

40. Gorski, C. A.; Sander, M.; Aeschbacher, M.; Hofstetter, T. B., Assessing the redox properties of iron-bearing clay minerals using homogeneous electrocatalysis. *Appl Geochem* **2011,** *26, Supplement*, (0), S191-S193.

Curriculum Vitae

Personal Data

Name:	Michael Aeschbacher
Date of Birth:	30th January 1982
Nationality:	Swiss
Citizen of:	Radelfingen BE

Education

2007 - present	Doctoral Studies at ETH Zurich, Department of Environmental Sciences, Institute of Bio-geochemistry and Pollutant Dynamics
2004 - 2007	Diploma Studies in Environmental Sciences, ETH Zurich
Jan/2004 - Jun/2004	Studies at the University of Edinburgh (UK) ERASMUS exchange program
2001	Maturität Typus C, Deutsches Gymnasium Biel

Working experience

2007 - present	Research assistant in the group of Prof. Dr. René Schwarzenbach
2007 - present	Teaching Assistant at the Department of Environmental Sciences, course "Case studies in environmental chemistry" by Dr. Thomas Hofstetter
Jan/2007 - Jun/2007	Diploma student in the group of Prof. Dr. René Schwarzenbach
Jun/2007 - Aug/2007	Mundo Dulce (Cl): Internship in the Department of Quality Control
Nov/2005-Mar/2006	Swiss Reinsurance Company (Swiss Re): Internship in the Department Risk Engineering Services
Mar/2005-Jun/2006	Teaching Assistant at the Department of Environmental Sciences in the class "Selected Chapters of Physical Chemistry" by Dr. Pierre Funck